2016

Role of Kruppel-like Factor 8 (KLF8) in Cancer and Cardiomyopathy

Satadru Lahiri
University of Central Florida

ROLE OF KRÜPPEL-LIKE FACTOR 8 (KLF8) IN CANCER AND CARDIOMYOPATHY

by

SATADRU K LAHIRI
B.Technology from Heritage Institute of Technology, Kolkata, India, 2009

A dissertation submitted in partial fulfillment of the requirements
for the degree of Doctor of Philosophy
in the Burnett School of Biomedical Sciences
in the College of Medicine
at the University of Central Florida
Orlando, Florida

Summer Term
2016

Major Professor: Jihe Zhao

ABSTRACT

Cancer and cardiovascular diseases are two most fatal diseases causing innumerable death each year. To understand the underlying mechanism of these two diseases is really critical to assess proper therapeutic approach. Krüppel-like factor 8 (KLF8) is a member of Krüppel like family transcription factors which was found to be upregulated in different types of cancers, primarily breast and ovarian cancer. No studies have elucidated role of KLF8 in cardiovascular diseases till date to our knowledge. KLF8 has been found to transcriptionally activate a host of downstream effectors like CyclinD1, EGFR, MMP9, EPSTI1, and CXCR4 to promote cell proliferation, cancer cell invasion and migration and transcriptionally represses E-cadherin to induce epithelial to mesenchymal transition and oncogenic transformation of cell in multiple cancers. Our studies identified a novel posttranslational modification of KLF8 essential for its role in promoting cancer cell migration and discovered a novel function of KLF8 in cardiomyopathy. In our first study, we identified Serine 48 as a novel phosphorylation site on KLF8. Pharmacological and genetic manipulations of various potential kinases further revealed ERK2 as the responsible kinase that phosphorylates KLF8 at S48. Functional studies indicated that this phosphorylation is crucial for protecting KLF8 protein from degradation in the nucleus and promoting cell migration and thereby identified this novel posttranslational modification critical for KLF8 mediated cancer progression. This finding is important in addition to already identified role of KLF8 in cancer which has been studied mostly in vitro and in xenograft model. To investigate KLF8 mediated tumorigenesis in a better physiologically relevant system, we

established the first KLF8 transgenic mouse model incorporated with Cre-loxP recombination in our second parallel study. As KLF8 has been found to be upregulated in multiple cancers, we first overexpressed KLF8 globally. While we found spontaneous mammary and testicular tumor in couple of these mice, strikingly almost 100% KLF8 global transgenic mice died much earlier with significantly enlarged heart compared to their littermate controls. We further characterized this disease as dilated cardiomyopathy by ultrasound echocardiograph. In depth study later on discovered KLF8 promoted systolic dysfunction leading to fatal dilated cardiomyopathy. Interestingly, cardiomyocyte specific KLF8 transgenic mice demonstrated these similar phenotypes further proposing an unknown function of KLF8 in cardiomyocytes. Cardiovascular disease PCR array subsequently identified possible KLF8 regulated gene targets including likes of STAT1, S100a8, and ATP2a2 as the cause of dilated cardiomyopathy in this mouse model. Overall, this study discovered a novel unknown role of KLF8 in dilated cardiomyopathy, one of the leading causes of death and further insight into the underlying mechanism will identify KLF8 as a strong therapeutic target in dilated cardiomyopathy alongside cancer.

Dedicated to

My late grandmother Bithi Roy

and my Parents & Brother

ACKNOWLEDGMENTS

First I want to thank UCF College of medicine for accepting me as a new PhD student. I sincerely want to thank Dr. Zhao and my lab members for their immense support in my research. Dr. Zhao was really supportive and patient with me all these years and helped me grow in research field. I can't thank him enough for his valuable advice on different aspects of research, critical thinking and shaping up future career goals. I am really grateful to him for this opportunity to work on these exciting projects. I also want to thank my committee members Dr. Parthasarathy, Dr. Siddiqi and Dr. Masternak for their support and encouragement throughout my PhD study. I am really fortunate to get their valuable insights on my projects. I am thankful to my previous committee members Dr. Altomare and Dr. Khaled. I am grateful to my wonderful co-lab members Lin Yu, Dr. Heng Lu and Dr. Debarati Mukherjee for the best lab environment ever possible. I want to thank Lin for taking care of everything in lab and making it so perfect to work. I am thankful to Heng and Debarati for all the discussion, valuable advices and help all these years. As a newcomer in lab, I learned most of the techniques from Heng and he introduced me to animal experiments. I am also thankful to previous lab members Ian Dalton, Justin Gray, Dr. Tianshu Li, Dr. Melissa Wason, Dr. Shen Chao and Dr. Liu Hu for their support. I am grateful to the BSBS and Vivarium staff for taking care of everything. I am lucky to have great friends both here and back home who encouraged me throughout my life. Finally I am grateful to my parents and my family as without their support I wouldn't be here today and nothing would have been possible. All my achievements and everything of these are dedicated to them.

TABLE OF CONTENTS

LIST OF FIGURES

LIST OF TABLES

LIST OF ABBREVIATIONS

Adipoq	Adiponectin
BLI	Bioluminescent Imaging
B-mode	Brightness mode (2D)
BW	Body weight
CA	Constitutive active
CDK5	Cyclin dependent kinase 5
Chx	Cyclohexamide
CIP	Calf-intestine phosphatase
CO	Cardiac output
CRM1	Exportin
CtBP	C terminal binding protein
EF	Ejection Fraction
EGFR	Epidermal growth factor receptor
EMT	Epithelial to mesenchymal transition
EPSTI1	Epithelial stromal interaction 1
ERK2	Extracellular signal-regulated kinases
FAK	Focal adhesion kinase
FS	Fractional shortening
GFP	Green fluorescence protein
GSK3	Glycogen synthase kinase 3
H&E	Hematoxylin and Eosin

HA	*Human influenza hemaglutinin*
HEK	Human embryonic kidney
HW	Heart weight
IACUC	institutional animal care and use committee
IHC	Immunohistochemistry
IRES	Internal ribosome entry site
IVISd	Intraventricular septum diameter at diastole
IVISs	Intraventricular septum diameter at systole
JNK	C-Jun N terminal kinase
KLF8	Krüppel-like factor 8
KLF8-aTg	KLF8 adipocyte specific transgenic mice
KLF8-gTg	KLF8 global transgenic mice
KLF8-hTg	KLF8 cardiomyocyte specific transgenic mice
KO	*Knock out*
LV	Left ventricle
LVIDd	Left ventricle inner diameter at diastole
LVIDs	Left ventricle inner diameter at systole
LVPWd	Left ventricular posterior wall thickness at diastole
LVPWs	Left ventricular posterior wall thickness at systole
LW	Lung weight
MEF	Mouse embryonic fibroblast
M-mode	Motion mode
MMP	Matrix metaloprotinase

Na3VO4	Sodium Orthovanadate
Nes	Nuclear exportation signal
PARP1	Poly(ADP-ribose) polymerase 1
PCAF	P300/CBP-associated factor
PKC	Protein kinase C
REP	Red fluorescence protein
Sumo	Small Ubiquitin-like Modifier
SV	Stroke volume
TG	Transgenic

CHAPTER 1: BACKGROUND

Krüppel-like factor 8 (KLF8)

Introduction

Kruppel like factor is a widely researched transcription regulator family critical in diverse diseases primarily in cancer [1, 2]. This family contains 17 members which share three highly conserved Cys2His2 zinc finger motifs as CACC GT box or GC-rich element DNA binding domain at their C-terminus. KLF family members have divergent role on their gene targets, whereas some of them act as only activator or repressors and others act as both. The first KLF protein KLF1 was identified as a mammalian homologue of Drosophila gene Kruppel which followed by discovery of newer members of this family. After its discovery, KLF8 was found to be widely expressed in different species. The locus of KLF8 was situated on X chromosome in human [3]. KLF8 protein was found to be expressed minimally in different tissues with the highest expression in kidney. In contrast, KLF8 expression was observed to be increased significantly in cancer tissues compared to normal tissues, which led to an array of research to investigate the unknown role of this protein in oncogenesis. Currently we have a better understanding of KLF8 structure, regulation and function in different cancers primarily breast and ovarian cancers. Till date, KLF8 has been identified to promote cancer progression[4], Epithelial to mesenchymal transition (EMT)[5], Metastasis [6] as a dual transcription factor with both activator and repressor role in regulating a host of critical genes like

CyclinD1[7], EPSTI[8], MMP9[4], MMP14[9], EGFR[10],CXCR4, E-Cadherin[5]. Overall, KLF8 has been established as an important EMT transcription factor promoting oncogenesis with an insight into the structure, post-translational modification, regulation and function. Current and future studies will lead to discovering unknown potential function and characteristics of this novel protein.

Structure of KLF8

Human KLF8 consists of 359 amino acid residues. As a transcription factor, it contains four critical domains including an N terminal repressor domain, a transcriptional activator domain, nuclear localization domain and C terminal DNA binding domain. KLF8 was first discovered as a transcriptional repressor of beta-globin[11]. The N terminal 86-90 position containing a five amino acid residue motif Proline-Valine-Aspartic acid-Leucine-Serine (PVDLS) was identified as the repression domain of KLF8[12]. KLF8 transcriptional repressor activity was found to depend on interaction of this PVDLS domain with C-terminal binding protein (CtBP), a transcriptional co-repressor protein. KLF8 shares this domain with some of the other KLF members like KLF3, KLF12 [13]. Except beta-globin and E-Cadherin, KLF8 activates most of its gene targets suggesting transcriptional activator as the predominant role of KLF8. In depth research has revealed that the glutamine residues Q118 and Q248 of KLF8 are critical for its transcriptional activator function as abolishing these sites hinder KLF8 mediated activation of its targets[14]. KLF8 nuclear localization is absolutely essential as its function which led to identifying Serine 165 and Lysine 171 as critical sites for KLF8

localization to nucleus[15]. While the exact role of these two sites on KLF8 nuclear localization remained mysterious, it was speculated that PKC phosphorylation on KLF8 S165 facilitates importin-beta binding through these sites leading to translocation of KLF8 to the nucleus, as both these site specific mutants and PKC inhibitor treatment prohibited KLF8 from localizing into nucleus, thereby inhibiting KLF8 mediated regulation of its downstream targets. Finally the three Zn finger motifs on C terminal of KLF8 triggers KLF8 binding to its target gene promoters. These DNA binding motif of KLF8 is conserved between different KLF family members. Truncation mutant of KLF8 without this motif inhibits KLF8 mediated downstream gene regulation by abolishing its binding to target gene promoters. The Zn finger domains of KLF8 also found to mediate KLF8 interaction with other protein. PARP1 was discovered to interact with KLF8 through this C terminal motif [16, 17]. In absence of this Zn finger domain, KLF8 and PARP1 interaction is diminished. PARP1 interaction to KLF8 was proved essential for KLF8 nuclear localization as it prevents KLF8 binding to nuclear exporting protein CRM1. In PARP1 null cells, KLF8 was mostly found to be localized in cytoplasm and had a very short half-life as in absence of this interaction; KLF8 is exported to cytoplasm by CRM1 and presumably degraded by proteasome complex affecting overall KLF8 function. PARP1/KLF8 interaction further recruits KLF8 to the DNA damage site which led to discovery of a novel function of KLF8 in DNA repair [1, 16, 18].

Post-Translational Modifications of KLF8

Post translational modification of a protein is critical for its physiological expression and functions. Most of the KLF members undergo diverse post-translational modifications regulating their function in both positive and negative manners [1]. Our protein of interest is no exception of it. Till date, KLF8 has been identified to be regulated by various post-translational modifications including sumoylation[19], acetylation[14], ubiquitination, parylation[17] and phosphorylation. KLF8 was first found to be sumoylated at Lysine 67 residue by Sumo-1, Sumo-2 and Sumo-3; primarily Sumo-1. KLF8 interacted with the PIAS family of SUMO E3 ligases PIAS1, PIASy, and PIASxα which triggers KLF8 sumoylation[19]. CtBP binding to the PVDLS domain recruits E2 and E3 ligases to KLF8 to enhance KLF8 sumoylation. Sumoylation of KLF8 delimits KLF8 transcriptional activity as desumoylation increased both KLF8 mediated transcriptional activation and repression[20]. In contrast, sumoylation of KLF8 was critical for PARP1 mediated KLF8 recruitment to DNA repair sites. Overall this limiting role of KLF8 sumoylation suggested that in normal physiological condition, KLF8 is sumoylated when it is not required but it goes through desumoylation to regulate downstream targets when needed. Further research also identified that KLF8 gets acetylated at Lysine93, Lysine95 and Lysine67 by histone acetyltransferase P300 and PCAF co-activators [14]. Interestingly as K67 was mediated by both sumoylation and acetylation, an intra-regulatory role of these two post transcriptional modifications on KLF8 was discovered. KLF8 acetylation at K93 and K95 inhibits sumoylation of KLF8 by inhibiting CtBP binding to the PVDLS repression domain which revealed the reason

behind enhance in KLF8 mediated gene expression during acetylation. Further studies unveiled that a perfect balance between sumoylation and acetylation of KLF8 is necessary for its function as acetylation promotes KLF8 transcriptional regulator function whereas sumoylation limits the uncontrolled gene regulation by this protein[20]. This is extremely critical in context of cancer where KLF8 activates various gene targets to enhance cancer progression and metastasis. KLF8 has been identified to go through parylation mediated by PARP1 interaction [17]. Parylation of KLF8 facilitates its nuclear localization by inhibiting CRM1 binding. In absence of parylation, KLF8 was localized in cytoplasm with a high ubiquitination state. Current research is undergoing in order to identify specific ubiquitination site of KLF8. KLF8 phosphorylation has not been studied in that proportions like the other post-translational modifications mentioned. KLF8 S165 was speculated to be phosphorylated by PKC to mediate its nuclear localization [15]. KLF8 recruitment to the DNA damage site was predicted to somehow depend on KLF8 Serine 80 phosphorylation by PKC. One part of our current study addresses and discovers a novel phosphorylation site of KLF8 critical for its protein stability and function.

KLF8 signaling link to Cancer

Since its discovery, KLF8 has been established as a critical transcription factor in cancer as it regulates an array of important genes like CyclinD1[7],MMP9[4], MMP14[9], E-Cadherin[5], KLF4[11], EPSTI1[8], EGFR[10] and CXCR4, thereby playing essential

roles in diverse cellular processes including cell proliferation, oncogenic transformation, EMT, invasion, migration and metastasis. KLF8 was found to be upregulated in different types of human cancers including breast, ovarian, pancreatic, liver, brain, gastric and renal cancers. Previous research have shed light on KLF8 regulation by upstream genes in the cancer tissues and furthermore downstream targets regulated by KLF8 for a better understanding of the functional link of KLF8 in cancer. KLF8 acts as a downstream effector of FAK, which promotes cell proliferation, migration mediated by integrin signaling [7, 21]. Further studies in ovarian cancer cells demonstrated that FAK-PI3K/AKT axis activates SP1 transcription factor which binds directly to KLF8 gene promoter in upregulating its expression [21]. An inter-regulatory signaling loop was identified among KLF8, KLF3 and KLF1, while KLF1 directly activates KLF8 and KLF3 represses KLF8 expression [13]. A recent study identified KLF8 upregulation by Wnt in liver cancer cells [22]. Overall understanding the factors behind KLF8 upregulation in cancers led the research towards finding downstream effectors of KLF8 to investigate the KLF8 mediated signaling axis in cancer. The FAK/KLF8 signaling cascade identified CyclinD1 as a direct target of KLF8. KLF8 upregulates CyclinD1 by binding directly to GT box of its promoter and enhance cell cycle progression in ovarian cancer cells leading to tumorigenesis [7]. KLF8 regulation of CyclinD1 was found to play a partial role in KLF8 mediated oncogenic transformation of NIH3T3 cells. Ectopic expression of KLF8 induced transforming phenotype in these cells including serum independent growth, loss of contact inhibition between cells and change in cell morphology[23]. Inhibition of KLF8 also reduced Src mediated oncogenic transformation which establishes a synergistic role of both these FAK downstream proteins in promoting

cancer. KLF8 could also induce tumorigenesis as it represses tumor suppressor KLF4 by binding to its promoter. KLF8 was found to promote EMT by transcriptionally repress epithelial cells marker E-cadherin [5]. EMT is a critical step which facilitates benign cancer epithelial cell to divide and migrate on their own to become more malignant cancer cells and thereby enhances metastasis and cancer related death. Along with Snail, Twist, Zeb; KLF8 also has been established as an independent EMT inducing transcription factor[24]. KLF8 downregulates E-cadherin in transforming epithelial cells to more fibroblast like mesenchymal cells and enhance their survival in circulation by inhibiting anoikis-cell detachment from extracellular matrix mediated apoptosis method[5]. KLF8 also upregulates MMP9 and MMP14 directly in promoting breast cancer cell invasion, migration and overall metastasis as MMPs facilitates breakage of extracellular matrix[4, 9]. KLF8 knockdown in lung metastatic breast cancer cells inhibited breast tumor formation and lung metastasis in xenograft and tail vein nude mouse models and were rescued by overexpressing the downstream gene targets. KLF8 activates a novel protein EPSTI1 in order to promote breast cancer invasion and metastasis [8]. KLF8 role as dual transcription factor was evident in an interesting study identifying that KLF8 mediates breast cancer malignancy through EGFR by transcriptionally activating it directly and transcriptionally repressing miR141, an inhibitory microRNA of EGFR in a KLF8/EGFR/miR141 axis[10]. A recent study identified G protein coupled receptor CXCR4 as a direct target of KLF8. Novel role of KLF8 in transendothelial migration was discovered by this study as CXCR4 upregulation by KLF8 promoted transendo-migration and overall metastasis in breast cancer cells. A novel link between KLF8 and cancer stem cells has been established by a current study

which demonstrated that KLF8 induces tumorigenic mammary stem cells by upregulating miR146a[25]. Although KLF8 has been studied primarily in breast and ovarian cancers, various new studies are exploring its role in other cancers like renal, gastric, liver and brain cancers as KLF8 was first identified to have elevated expression level in all these cancer types. Silencing KLF8 in renal carcinoma cells induced apoptosis and inhibited cancer cell invasion in vitro and xenograft models [26]. KLF8 knockdown in gastric cancer cells showed less tumorigenesis in xenograft model by inhibiting KLF8 mediated upregulation of CyclinD1, BCL-2 and downregulation of P27 and Bax[27, 28]. Lentivirus base KLF8 knockdown also demonstrated reduced SGC-7901 gastric cancer cell proliferation and invasion [29, 30]. Another study in gastric cancer cells identified TGF-beta as the upstream activator of KLF8/E-Cadherin link in promoting EMT in these cells [31]. A comprehensive study with 154 human gastric cancer patients revealed that high expression of KLF8 is significantly correlated with gastric cancer progression and poor prognosis suggesting KLF8 can be used as a therapeutic target or biomarker for this disease[32]. In human hepatocellular carcinomas (HCC), the aberrant overexpression of KLF8 was correlated with the metastatic potential, post-surgical recurrence of the HCC tumors and poor survival studied in more than 300 patient cases[33]. KLF8 promotes proliferation and invasion and inhibits apoptosis through upregulation of cyclin D1, MMP2, BCLxL, E to N –Cadherin switch and transcriptional repression of caspases 3 and 9 in these cells. Current studies have suggested a novel role of KLF8 in mediating Wnt to β-catenin signaling to activate the transcription of c-Myc, cyclin D1 and Axin1 in enhancing HCC cell proliferation [22]. An early study in U-251MG human glioblastoma cells demonstrated evident dependence of

KLF8 expression on FAK activity and correlation with the increase/decrease of cyclin D1/p27 in the context of cell cycle progression[34]. Subsequently, a recent study showed that these glioblastoma cells can go through apoptosis by silencing KLF8 [34, 35]. A novel interaction between KLF8 and androgen receptor has been recently discovered to be critical for prostate cancer cell proliferation [36]. KLF8 role in colorectal cancer has been demonstrated by KLF8 mediated direct activation of FHL2 which results in induction of EMT and metastasis of this cancer [6]. Inhibiting MEK/ERK pathway reduced KLF8 and tumorigenesis in colorectal cancer cells [37]. MiR-135a was identified as an inhibitory micro RNA of KLF8 which decreases lung cancer progression by downregulating KLF8 expression [38]. KLF8 was also found to be critical for bladder cancer proliferation and migration[39]. In addition, one study showed that KLF8 is an important regulator of oral cancer cell as knockdown of KLF8 in CAL27 oral cancer cells inhibits proliferation of these cells [40]. In another study with human pancreatic cancer tissue, KLF8 high expression was observed to correlate with poor prognosis of the disease[41]. Growing importance of KLF8 in different types of cancer was further evident from couple of recent studies about KLF8 inhibition leading to decrease in cell proliferation and invasion potential of Saos-2 osteosarcoma cells[42] and SUNE1-5-8F nasopharyngeal carcinoma cells[43] both in vitro and xenograft models. Overall KLF8 has been observed to have critical role in oncogenesis in various cancer types and ongoing studies will provide better understanding of any other unknown function of KLF8 in cancer in establishing KLF8 as a possible therapeutic target in cancer treatments.

KLF8 in other diseases

Although primary functions of KLF8 have been primarily explored in cancer till date, few studies suggest a widespread scope of KLF8 involvement in other diseases. A novel developmental role of KLF8 was established by a study where they observed KLF8 to be downregulated during preeclampsia, which is a pregnancy disorder [44]. KLF8 was found to be expressed in the trophoblast layer, the outer layer of blastocyst in the first trimester. This study demonstrated that hypoxia-reoxygenation downregulates KLF8/MMP9 signaling axis inhibiting trophoblast invasion which reveals that KLF8 can act as a novel oxygen tension sensor in pathogenesis of preeclampsia[45]. Further studies are required to get insight of the mechanistic approach. Recently KLF8 expression in brain has been characterized. In zebrafish model, it has been demonstrated that KLF8 regulates P53 and met expression to maintain neuronal progenitor cells which is critical for zebrafish cerebellar development[46]. KLF8 was found to be down regulated in advanced stages of Alzheimer's disease. In depth study identified KLF8 mediated activation of Wnt-beta catenin signaling inhibited NF-kB signaling as beta-catenin prevents NF-kB to translocate to nucleus. This KLF8 mediated indirect downregulation of NF-kB leads to decrease in amyloid precursor protein (APP) and Tau expression and overall decrease in Taupathy in Alzheimer's disease. Overall this study established a novel inhibitory role on Alzheimer's disease progression [47]. A novel signaling link was discovered in adipogenesis where KLF8 was demonstrated to transcriptionally activate peroxisome proliferator-activated receptor γ (PPARγ) and CCAAT/enhancer-binding protein α (C/EBPα) directly in order to promote adipocyte

differentiation[48]. Taken together, involvement of KLF8 in diverse diseases beside cancer is being studied in order to evaluate significance of this novel protein in a myriad of physiological disorder [48].

Figure

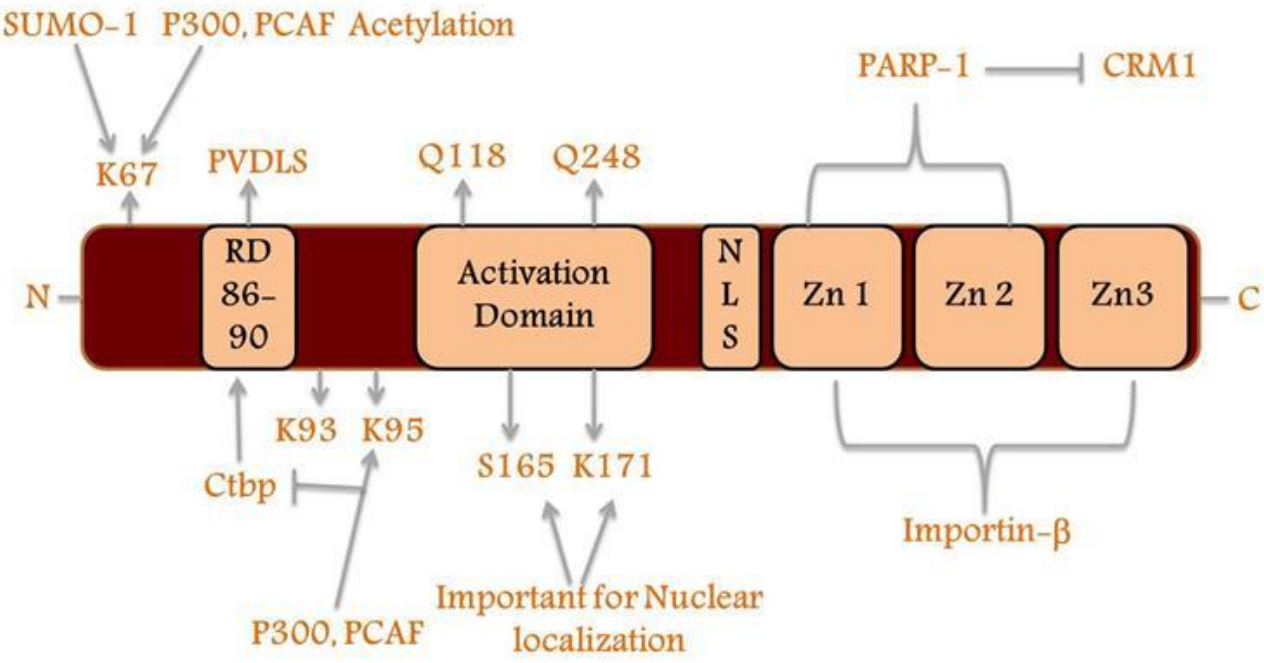

Figure 1. Schematic structure of KLF8 protein and its post-translational modifications [2]

KLF8 interacts with the transcriptional co-repressor C-terminal binding protein (CtBP) through its repression domain (RD or PVDLS motif), with the transcriptional co-activators P300 and PCAF histone acetyl-transferases through its activation domain (AD centered on Q118/Q248), with target DNA GT-box sequence via the three C2H2 zinc-finger (ZnF) motifs. KLF8 also binds to importin through its nuclear localization signal sequences and PARP-1 at the ZnF region to regulate its nuclear localization. The acetylation sites and sumoylation site of KLF8 are also shown.

Genetically Engineered Mouse Models

Introduction

Genetically engineered mouse model is an important tool in in vivo research [49-51]. In 1974, Rudolf Jaenisch first invented genetic modified mouse by inserting a DNA virus into early embryo [52, 53]. Since then, the research area of genetically modified mice has been advanced impressively in establishing new methods of incorporating transgene into mice and knocking out critical genes from mouse genome[54-57]. Mouse organs and tissues mostly mimic human tissues and with these engineered mice, there has been a significant improvement in assessing critical role of various genes in diverse diseases in a best physiological condition[58]. Compared to xenograft nude mouse models, these engineered mice have intact immune systems to provide physiological relevance to the human context [59, 60]. Additionally, mice can be housed in a large number and a litter of mice have a large number of homogenous mice to provide proper controls to study [61, 62]. Genetically engineered mice can be of different types, primarily transgenic and knock out mice. In transgenic mice the human gene of interest is incorporated into mouse genome under a strong promoter to study its role in relevant diseases[63]. In contrast, a knock out model replaces the functional gene of interest with a non-functional gene mutant by homologous recombination to investigate the function of that particular gene. A relevant example is a transgenic mouse model for an oncogene and a knockout mouse model for a tumor suppressor gene where both of

them will be studied to explore tumorigenesis. The discovery of the Cre-loxP and FLP-FRT based recombination has advance field further by providing an ideal platform for tissue specific gene overexpression and knockout. This techniques in contrast to primitive models, helps us to study effect of our gene of interest in specifically the target tissue [64-68]. Advance techniques also include gene expression under tamoxifen induced promoter, which developed a system where providing tamoxifen through mouse drinking water can turn on the gene expression and it depletes out in absence of this drug[69]. Overall the genetically engineered mouse models provide a mammalian system to test our in vitro, xenograft model derived hypothesis in vivo. It has been found by different studies that micro environment is critical for different diseases. In context of cancer, tumorigenesis and angiogenesis depends greatly on interaction with the surrounding stroma and immune cells [70, 71]. Compared to a heterogeneous human population, where various adaptive factors like genetic background, environmental effect, and lifestyle can regulate progression of a disease, in a much simple homogenous mouse model, these variable conditions can be kept constant to study the specific function of a gene of interest in that disease progression. Finally, the genetically engineered mouse models for diverse diseases provide a more physiologically relevant in vivo tool to study efficacy of therapeutic drugs before pre-clinical trials in humans.

Establishing KLF8 transgenic mouse model

KLF8, an important transcription factor has been found to promote cancer progression and metastasis[2]. All of these studies have been performed in cell culture and xenograft nude mouse models. To investigate role of KLF8 in oncogenesis in a more physiologically relevant system, we started constructing the first novel KLF8 transgenic mouse model for spontaneous tumorigenesis study. Other transgenic mouse models for mostly studied oncogenes like Myc, Ras, Her2 has developed spontaneous mammary, lung tumor formation and it was observed that these transgenic mouse models mimic human cancers[72-77]. As there are no studies till date exploring role of KLF8 in a KLF8 transgenic model, in the other part of our study we started establishing this novel transgenic model. To construct any transgenic model, we require a transgene cassette with the gene of interest. As a mammalian expression promoter, we utilized a synthetic promoter named CAG where C stands for cytomegalovirus early enhancement element (CMV)[78-80], A stands for the promoter followed by the first exon and intron of chicken beta actin gene and G stands for the splice acceptor of the rabbit beta-globin gene. As KLF8 was primarily studied in breast and ovarian cancers, we decided to establish a transgenic model equipped with Cre-LoxP system to explore role of KLF8 independently in different tissues. The overall scheme of KLF8 transgenic mouse construction is described in details in the methods section of Chapter 3. Briefly the transgene plasmid contained a HA tagged human KLF8 cDNA followed by A GFP-Luciferase fused cDNA (GL) under CAG promoter. A RFP gene with STOP codon flanked by the loxP sites was inserted upstream of KLF8 sequence. The STOP codon

prevented KLF8 expression in the founder mice while only Cre recombination can release the RFP-STOP cassette and induce HA tagged KLF8 expression followed by GL. As KLF8 has been found to have critical role in different cancers, we first constructed global KLF8 transgenic mice with aberrant overexpression of KLF8 in all tissues to explore spontaneous tumorigenesis, although our primary aim was to induce KLF8 expression in mammary tissue by recombination with mammary specific Cre mice. Interestingly, the KLF8 global transgenic mice, both male and female started dying much earlier compared to the littermate controls without any trace of tumorigenesis. While investigating further by necropsy of these mice, we found an exciting novel cardiac phenotype promoted by KLF8 in these mice. KLF8 global transgenic mice were observed to have severe dilation of heart which caused the higher mortality rate in them. A string of in depth studies described in chapter 3 revealed an unknown novel role of KLF8 in cardiomyopathy, further establishing the importance of genetically engineered mouse models in discovering unknown potential of individual genes in a better physiological context.

Advantage of our mouse model

The primary advantage of our genetically engineered KLF8 transgenic mouse model is incorporating the transgene with a Cre-LoxP system. Both Cre recombinase and loxP sequence were first isolated from bacteriophage P1 and implied in engineered mouse models. Cre recombinase identifies and binds to the LoxP sequences to form a dimer

[67, 81-83]. In this system, a transgene is inserted with two loxP sites. The position of the loxP sites on the transgene depends on the expected gene expression. In transgenic mouse models, generally a reporter protein followed by a STOP codon is inserted in between two loxP sites, upstream of the gene of interest whereas in knockout model, the gene of interest designed between the loxP sites. The mechanism behind Cre-LoxP based recombination relies on Cre recombinase binding to both loxP sites forming a tetramer and excising the DNA flanked by loxP sites. In case of transgenic models, Cre recombination will excise the STOP codon flanked by LoxP in order to promote expression of gene of interest, whereas in KO model, the gene of interest will be excised as it is flanked by loxP sites to delete it from the genome. The best use of Cre-LoxP based method is inducing tissue specific expression. The founder mice with loxP flanked transgene in their genome are known as floxed mice. Cre mice are designed with Cre transgene under various tissue specific promoters. Myh6-Cre [84] mouse facilitates Cre expression specifically in cardiomyocytes as the Cre transgene is placed under a Myh6 promoter which is expressed predominantly in cardiomyocytes. The founder floxed mice can be crossed with diverse tissue specific Cre mice to induce transgene overexpression or knock out by promoting Cre mediated recombination in those tissues. In our transgenic mouse model, floxed KLF8 can be crossed with any different tissue specific Cre mice to excise the loxP flanked RFP-STOP cassette and facilitating KLF8 overexpression in that specific tissue. We used EIIA-Cre [85] mice to develop global KLF8 transgenic mice, as EIIA promoter expresses Cre in germline distributing it in all different tissues. Later on we also used Myh6-Cre [84] to construct cardiomyocyte specific KLF8 transgenic mice, Adipoq-Cre[86] to construct adipocyte

specific KLF8 transgenic mice and MMTV-Cre[87] to construct mammary epithelial cell specific KLF8 transgenic mice. This system in our founder floxed mice provides a huge platform to study role of KLF8 in any different tissues, thereby establishing a great potential of this KLF8 genetically engineered mouse model in exploring role of KLF8 beyond cancer and other diseases. The advantage of the reporter genes is to visualize the Cre base d recombination and transgene expression both qualitatively and quantitatively. As our transgene contains a loxP flanked RFP gene and GFP-Luciferase downstream of KLF8, Cre recombination mediated KLF8 overexpression can be evaluated by an evident RFP to GFP-Luciferase switch which was visualized in vitro by fluorescence imaging, luminescence an in vivo by Bio Luminescence Imaging and Bio Fluorescence imaging. This system provides a great tool for investigating efficacy of the Cre-loxP system of the transgene, tissue specific transgene expression and further genotyping the transgenic mice. Taken together, we have established the first KLF8 transgenic mouse model which will have a significant impact on research of KLF8 and beyond.

KLF8 knockout mouse model

To assess the critical role of KLF8 in vivo, we also started constructing a KLF8 knock out mouse model. The KLF8 KO mouse model, also equipped with Cre-LoxP based system is being maintained by Dr. Heng Lu in our lab. The Floxed KO mouse has been constructed by replacing endogenous mouse KLF8 gene with LoxP flanked KLF8 gene by homologous recombination. Cre recombination will delete the KLF8 gene by excising

it between the loxP sites to provide KLF8 KO model in different tissues. We are currently studying KLF8-KO mouse model in different tissues like global, cardiomyocyte, and adipocyte. Both global and cardiomyocyte specific KLF8 KO mice had the reverse cardiac phenotype, observed in transgenic mice which thereby strengthen our hypothesis regarding the novel role of KLF8 in cardiomyopathy. Global KLF8 KO mice further showed increased abdominal fat mass which suggests a notion about KLF8 involvement in adipocyte differentiation. Ongoing studies will provide a better understanding about it. Thus, we currently have both KLF8 transgenic and KO models with different tissue specific distribution potential, presenting us a critical tool for addressing the unexplored roles of KLF8 in vivo.

Cardiomyopathy

Introduction

Cardiomyopathy in simple definition is cardiac muscle disease. It describes a large spectrum of diseases related to heart muscle. Cardiomyopathy is the leading cause of death[88]. According to Framingham heart study, 1 out of 5 of us has high risk of having heart disease during our life span [89-91]. American Heart Association defined cardiomyopathy as “Cardiomyopathies are a heterogeneous group of diseases of the myocardium associated with mechanical and/or electrical dysfunction that usually (but

not invariably) exhibit inappropriate ventricular hypertrophy or dilatation and are due to a variety of causes that frequently are genetic. Cardiomyopathies either is confined to the heart or is part of generalized systemic disorders, which may lead to cardiovascular death or progressive heart failure-related disability" [92]. A broad array of factors has been elucidated to be critical for different cardiomyopathies which made classification and prognosis of a specific cardiomyopathy much more critical. American Heart Association divided cardiomyopathy into two broad groups which further have different subgroups [93, 94]. Primary cardiomyopathy affects the heart alone and secondary cardiomyopathy affects the heart due to disease in other tissues systemically. Incidence of the primary cardiomyopathy is much more prevalent and causes progressive or sudden cardiac arrest[95]. Further this primary cardiomyopathy is classified into four groups; dilated cardiomyopathy (DCM), Hypertrophic cardiomyopathy (HCM), Restrictive cardiomyopathy and Arrhythmogenic Right Ventricular cardiomyopathy (ARVC) based on pathophysiology and characteristics. All these four groups can be further subtyped into several groups based on the underlying cause of the disease. Disease to primary characteristic phenotype illustrates dilated cardiomyopathy with enlarged heart, hypertrophic cardiomyopathy with thickening of heart muscle, restrictive cardiomyopathy with stiff heart muscle and arrhythmogenic right ventricular cardiomyopathy with abnormal electrical force transmission[96]. Overall this section of the background will elaborate on these four types of cardiomyopathy with most emphasis on dilated cardiomyopathy including its causes and treatments.

Dilated Cardiomyopathy (DCM)

Introduction

Dilated cardiomyopathy is defined by enlargement of heart with systolic dysfunction. This type of cardiomyopathy initiates from stretching of heart muscle leading to the dilation of left ventricle [97, 98]. Dilated cardiomyopathy occurs primarily between 30 to 60 years of age with more prevalence in men[97]. Patients diagnosed with this disease show distinct systolic dysfunction. Systolic dysfunction is characterized by decreased contractile efficiency of cardiac muscle[99]. Overall this disease results in increased myocardial mass and volume. Ischemic cardiomyopathy which is defined as the heart disease caused by coronary artery disease primarily artery blockage, culminates into similar phenotype as dilated cardiomyopathy which makes the diagnosis of this disease critical [100]. Dilated cardiomyopathy is an irreversible disease of cardiac muscle cells whereas ischemic cardiomyopathy occurs due to lack of blood flow and oxygen influx due to artery blockage and can be reversed by treating the coronary artery disease. Dilated cardiomyopathy is a progressive disorder as the dilation of left ventricle due to stretching of cardiac muscle, further enhances dilation of right ventricle and overall heart which leads to deterioration of cardiac function and severe heart failure[92]. The primary symptoms associated with this disease are shortness of breath and fatigue. Taken together, dilated cardiomyopathy is a non-ischemic cardiomyopathy with systolic dysfunction. Decreased pumping efficacy of the left ventricle further causes fluid accumulation in lung, which is known as cardiogenic pulmonary edema.

Characteristic

The most predominant characteristic of dilated cardiomyopathy is impaired systolic function[101]. Echocardiography is one of the critical measures to diagnose this disease. Echocardiograph of patients suffering from dilated cardiomyopathy demonstrates increase in left ventricle end systolic and diastolic diameter. Further decrease in ejection fraction and fractional shortening indicate the onset of this disease [102-104]. In human, ejection fraction less than 45% and fractional shortening less than 25% generally diagnose dilated cardiomyopathy[105]. Based on underlying cause, dilated cardiomyopathy can be sub grouped into three types including familial dilated cardiomyopathy (FDCM), idiopathic dilated cardiomyopathy (iDCM) and other dilated cardiomyopathy. Genetically inherited forms of dilated cardiomyopathy are known as familial DCM which contributes to 30% of this disease occurrence [106-108]. Idiopathic dilated cardiomyopathy is defined as DCM with unknown underlying cause[109]. Other dilated cardiomyopathy includes peripartum cardiomyopathy[110], valvular cardiomyopathy, alcoholic cardiomyopathy[111], toxic cardiomyopathy[112] and tachycardia induced cardiomyopathy[113]. Hearts of patients diagnosed with this disease show prominent myocardial fibrosis [114, 115]. Cardiomyocyte cells are observed to be elongated with the nucleus spread along their width [116]. Decreased contractile efficiency in these cardiomyocytes links to the systolic dysfunction characteristic of this disease. In addition, large number of these cardiomyocytes goes through apoptosis and gets replaced by fibrous tissue leading to myocardial fibrosis. Overall dilated cardiomyopathy is a progressive heart failure associated with systolic

dysfunction which promotes ventricle chamber enlargement further leading to irreversible myocardial infarction.

Pathophysiology

The underlying mechanism of dilated cardiomyopathy is not clearly understood which defines most of its occurrences as idiopathic cardiomyopathy. Familial cardiomyopathy which is involved in approximately thirty percent of this disease is genetically inherited [108, 117-120]. The cause of genetic dilated cardiomyopathy is being explored and till date several critical gene mutations have been identified in patient's heart with this disease[118]. Most of these mutants are inherited in an autosomal dominant pattern and leads to dilated cardiomyopathy. Family history is one of the critical factors of diagnosis of this disease due to increased understanding of the genetic complexity. Sarcomere is the basic unit of striated muscle cells consisting of two major proteins myosin and actin, the first forming the thick filaments and later forming the thin filaments of the muscle fibers. Actin binding to the globular head of myosin mediates myocardial contraction. Stimulation by axon potential promotes a calcium induced calcium release from the sarcoplasmic reticulum of cardiac muscle cells. Calcium ions bind to the tropomyosin (cardiac troponin) and change its structural conformation to expose the actin binding sites on myosin, leading to contraction of these cells. Most of the sarcomere genes have been identified to be mutated in dilated cardiomyopathy and contractile dysfunction [121-125]. These mutants were also characterized as dominant negative mutants of these sarcomere genes affecting both the force generation and force transmission in context of cardiomyocyte contraction. Genes associated with dilated

cardiomyopathy includes Cardiac actin[126], Desmin[127], δ-Sarcoglycan[128], β-Myosin heavy chain[129], Cardiac troponin T[130], α-Tropomyosin[131], Metavinculin[132], Myosin-binding protein C[133], Muscle LIM protein[134], α-Actinin-2[134], α-Myosin heavy chain[135], SUR2A[136], Lamin A/C[137], Phospholamban[138], Cypher[139] etc. Mouse models with these gene mutants knock in demonstrated severe dilated cardiomyopathy. Dominant negative mutation in β-Myosin heavy chain and Cardiac troponin T diminishes actin myosin binding further decreasing force generation and contractile potential of muscle cells. Additionally ablation of structural proteins like α-Actinin-2, δ-Sarcoglycan inhibits actin binding to the extracellular matrix, thereby sacrificing the transmission of contractile force between cardiomyocytes. Mutation in phospholamban, a sarcoplasmic reticulum calcium regulator further abolishes calcium induced calcium release and contraction [138]. All of these sarcomere, Z disc and cytoskeleton associated genes regulate cardiomyocyte contraction. Familial mutation in these proteins overall ablates cardiomyocyte contraction efficacy leading to lower ejection fraction and fractional shortening. In order to increase its systolic function, heart undergoes a remodeling process and tends to increase its size to accumulate more amount of blood in the left ventricle, thereby leading to dilated cardiomyopathy. One of the other primary causes of dilated cardiomyopathy is myocarditis which is promoted by viral agents mediated cleavage of a cytoskeleton protein dystrophin leading to loss of cardiomyocyte integrity [140]. Peripartum cardiomyopathy develops in the last trimester of pregnancy[110]. Valvular cardiomyopathy develops due to increase in cardiac work load due to valve dysfunction. Further, abnormal alcohol consumption also leads to alcoholic cardiomyopathy[50].

Advance researches are being focused to explore the underlying genetic complexity behind incidence of different types of dilated cardiomyopathy.

Current Treatments

Genetic counseling is the primary line of treatment to evaluate the history of dilated cardiomyopathy. Family history of this disease suggests genetic cardiomyopathy. Echocardiograph and MRI are used primarily to diagnose systolic dysfunction and dilated cardiomyopathy. Once the disease has been observed to be progressed, the early pharmacological treatments include ACE inhibitors, diuretics and beta inhibitors which improve the ejection fraction and systolic function of heart[141]. Angiotensin-converting-enzyme inhibitor (ACE inhibitor) is a drug generally used to treat hypertension. It helps cardiomyocyte cells survive with less oxygen in a more stressful condition. Diuretics prevent dilated cardiomyopathy associated pulmonary edema. Combined treatments of ACE inhibitor and diuretics delay disease progression of dilated cardiomyopathy. Beta blockers like bisoprolol, metaprolol decreases the risk of sudden cardiac death of patients with dilated cardiomyopathy. One study with 25 mg spironolactone significantly diminished the risk of sudden death by 30% in human patients with EF less than 35%, thereby further clarified the efficacy of beta blockers[142]. After the disease has progressed to further critical stages with evident enlargement of left ventricle, cardiac resynchronization therapy with biventricular pacing is used to treat systolic dysfunction and worsening of the disease. Currently the only treatment for late stage of dilated cardiomyopathy is orthotopic heart transplantation.

Left ventricular assist device is used to maintain the heart condition during waiting time for organ availability. In some cases, where organ transplant is not possible, left ventricular assist device is critical for improvement of quality of life.

Hypertrophic Cardiomyopathy (HCM)

Hypertrophic cardiomyopathy is characterized by increase in ventricle wall thickness without any occurrence of coronary artery disease. This is the most prevalent cardiomyopathies with a high incidence of 1 in 500 individuals all over the word. Genetic cause behind this disease is much better understood in comparison with dilated cardiomyopathy [143-146]. The primary two genes which are predominantly observed to be mutated in patients with hypertrophic cardiomyopathy are beta-myosin heavy chain and myosin-binding protein C[147]. Various autosomal dominant mutants of these two genes have been found to be involved in the onset of seventy percent of this disease. Till date, almost five hundred mutations have been discovered from 13 different genes [148]. In this disease, cardiomyocyte hypertrophy increases the cell size as more sarcomere units are added. Overall this leads to thickening of ventricle walls, primarily in left ventricle. Thickening of the heart walls and intraventricular septum further mediates narrowing of the ventricle chambers. Echocardiography is the first measure to assess the progression of this disease. Patients diagnosed with hypertrophic cardiomyopathy demonstrate increased left ventricle posterior wall and intraventricular

septum thickness. In some incidents, hypertrophic cardiomyopathy develops into dilated cardiomyopathy [146, 149].

Restrictive Cardiomyopathy

Restrictive Cardiomyopathy is associated with restricted cardiac filling of heart leading to decrease in diastolic volume and diastolic dysfunction. Prognosis of this type of cardiomyopathy is very difficult as it doesn't show change in ventricle or wall size as other two types of cardiomyopathy. Patients with this disease don't show any systolic function abnormality. In some incidents, later stage of the disease can impair systolic function. Restrictive cardiomyopathy can be idiopathic or associated with diseases like amyloidosis and endomyocardial disease with hypereosinophilia. Recently in depth studies revealed that restrictive cardiomyopathy is also associated with sarcomeric gene mutations in some cases [150]. Discovery of genetic background of this type of cardiomyopathy has been proven critical in proper diagnosis and prediction of restrictive cardiomyopathy. This disease first effect the left ventricle relaxation which further distributes to the right ventricle causing congestive heart failure [151, 152].

Arrhythmogenic Right Ventricular Cardiomyopathy (ARVC)

Arrhythmogenic Right Ventricular Cardiomyopathy (ARVC), also known as Arrythmogenic Right Ventricle Dysplasia (ARVD) is a nonischemic heart disorder.

Cardiomyocytes are linked together by a protein complex known as desmosome and this interconnection between cardiomyocyte is essential in maintaining a healthy systolic function. The primary cause behind ARVC has been established to be mutation in a desmosome protein desmin[153]. Progression of this disease starts from apoptotic death of myocyte and fatty tissue infiltration in myocardium of primarily right ventricle. At this stage, this disease is still in concealed phase as it doesn't show any defect in right ventricle yet like thinning of right ventricle posterior wall. Further the fibro-fatty tissue replaces right ventricular myocardium leading to thinning of wall and irregular cardiac rhythm which can be measured by echocardiograph and EKG. Previously it was believed that ARVC initiates in right ventricle and during later stages it spreads into left ventricle to become biventricular cardiac disorder. Few studies elucidated recently that the detrimental effect on left ventricle happens from the onset of the disease. Overall symptom of this disease is abnormal heart rhythm, palpitation, shortness of breath. Current treatment includes implantable cardioverter defibrillator (ICD) implantation which reverses irregular cardiac rhythms by providing electrical shock to heart. In extreme cases, patients with disease go through heart transplant surgery [154].

CHAPTER 2: ERK2 PHOSPHORYLATES KRÜPPEL-LIKE FACTOR 8 PROTEIN AT SERINE 48 TO MAINTAIN ITS STABILITY

Am J Cancer Res. 2016 May 1;6(5):910-23

Abstract

Krüppel-like factor 8 (KLF8) plays important roles in cancer and is strictly regulated by various post-translational modifications such as sumoylation, acetylation, ubiquitylation and PARylation. Here we report a novel phosphorylation of KLF8 by ERK2 responsible and critical for the stability of KLF8 protein. The full-length KLF8 protein displays a doublet in SDS-PAGE gel. The upper band of the doublet, however, disappeared when the N-terminal 50 amino acids were deleted. In its full-length the upper band disappeared upon phosphatase treatment or mutation of the serine 48 (S48) to alanine whereas the lower band was lost when the S48 was mutated to aspartic acid that mimics phosphorylated S48. These results suggest that S48 phosphorylation is responsible for the motility up-shift of KLF8 protein. Pharmacological and genetic manipulations of various potential kinases identified ERK2 as the likely one that phosphorylates KLF8 at S48. Functional studies indicated that this phosphorylation is crucial for protecting KLF8 protein from degradation in the nucleus and promoting cell migration. Taken together, this study identifies a novel mechanism of phosphorylation critical for KLF8 protein stabilization and function.

Introduction

Krüppel-like factor 8 (KLF8), a member of Krüppel-like transcription factor family, is upregulated and plays important roles in various cancer types [2, 4, 6, 9, 21-23, 27, 37, 155]. KLF8 functions as a dual transcriptional factor and has been shown to repress or activate a variety of cancer-related genes such as E-cadherin [5], KLF4 [19], cyclin D1 [7, 23], epidermal growth factor receptor (EGFR) [37], MMP9 and MMP14 [4, 9] and epithelial-stromal interaction 1 [27]. In addition to regulating cancer-promoting processes including transformation [23], epithelial to mesenchymal transition [5] and metastasis [4, 9, 27, 37], KLF8 also plays a role for DNA repair [16], adipogenesis [48] and Alzheimer's disease [47]. Indeed, KLF8 is emerging as a critical factor for diverse diseases [2].

Post-translational modification (PTM) is one of the most important protein regulatory mechanisms. Previous studies showed that KLF8 undergoes sumoylation at lysine 67 [19], acetylation at lysine 93 and lysine 95, and potential phosphorylation at serine 165 and serine 80 [16, 19, 20]. The sumoylation, acetylation and their crosstalk play an important role in KLF8 function [19, 20]. The serines 165 and 80 of KLF8 are critical for its nuclear localization and function such as DNA repair [15, 16]. Interestingly, previous study with KLF8 truncation mutants revealed that the doublet of KLF8 protein became a single band when $\geq$ 50 amino acids were deleted from the N-terminus [15], suggesting that a PTM in this deleted region is responsible for the mobility shift and doublet

formation. However, none of the PTM sites on KLF8 described above is located within this region. It has been mysterious how the mobility shift occurs and whether it has any impact on the function of KLF8.

In this study, we provide strong evidence that mobility shift of KLF8 protein is due to the phosphorylation at serine 48 by ERK2 and this phosphorylation is essential for maintaining the stability and function of KLF8 protein in the nucleus.

Materials and methods

Antibodies and Reagents

Primary antibodies used for western blotting include mouse monoclonal to HA-probe (F-7) (sc-7392) (1:3000), mouse monoclonal to β-actin (C4) (sc-47778) (1:4000), Mouse monoclonal for c-Myc (9E10) (Sc-40) (1:2000), mouse monoclonal to pERK (E-4) (Sc-7383) (1:2000) and rabbit polyclonal to ERK (c-16) (Sc-93) (1:2000) (Santa Cruz Biotechnology, Inc., Dallas, TX, USA). Secondary antibodies were horse radish peroxidase conjugated donkey anti-mouse (715-035-150) and donkey anti-rabbit IgG (711-035-152) (both 1:5000. Jackson ImmunoResearch laboratories, West Grove, PA, USA). Antibody used for co-immunoprecipitation was Anti-HA mouse monoclonal (IP0010) Immunoprecipitation Kit (Sigma-Aldrich, St. Louis, MO, USA). MEK inhibitor

PD98059 (513000) and U0126 (662005) as well as the inhibitor of protein synthesis cycloheximide were from Calbiochem (San Diego, CA, USA). Glycogen synthase kinase 3 (GSK3) inhibitor SB216763 (S1075) was from Selleckbiochem (Boston, MA, USA). cyclin-dependent kinase 5 (CDK5) inhibitor Roscovitine (557360) was from Milipore (Billerica, MA, USA). c-Jun N-terminal kinase I (JNKI) inhibitor BI 78D3 (Cat. No. 3314) and JNKII inhibitor AEG 3482 (Cat. No. 2651) were from Tocris (Ellisville, MO, USA). All the inhibitors were reconstituted with DMSO. The alkaline phosphatase calf intestinal phosphatase(CIP. M0290) were purchased from New England Biolabs (Ipswich, MA, USA).

Plasmid construction

The mammalian expression vectors pKH3 (HA-tagged), pHAN (Myc-tagged), pKH3-KLF8, pKH3-KLF8-dN50, pHAN-KLF8 and pHAN-KLF8-dN50 were previously described [14]. KLF8 deletion and point mutants were constructed by site-directed mutagenesis PCR [156] using the pKH3-KLF8 vector as the template. We used the primer pKH3-F paired with mutant-R and primer mutant-F paired with pKH3-R for the mutagenesis PCR and the pKH3-F and pKH3-R primer pair for overlapping PCR. The mutant fragments were digested with HindIII and EcoRI to clone into pKH3 vector between the sate sites. To construct lentiviral vectors pLVPZ-KLF8-S48A and pLVZP-KLF8-S48D, we PCR-amplified the HA-KLF8-S48A and HA-KLF8-S48D fragments from pKH3-KLF8-S48A and pKH3-KLF8-S48D plasmids. These fragments were digested

with Pst1/Not1 and inserted into the lentiviral vector pLVPZ [9]. All the constructs were verified by DNA sequencing. The human ERK2 cDNA was amplified using ERK2-SmaI-F and ERK2-ClaI-R primers. This amplified fragment was digested with SmaI/ClaI and cloned into pHAN vector between the same sites. The ERK2 dominant-negative (K54R in which the ATP binding activity is disabled [157, 158]) and constitutively active (ERK2-CA, an ERK2 double mutant consisting of R67S that promotes ERK2 autophosphorylation and D321N that inhibits ERK2 phosphatase binding [158-160]) mutants were constructed by site-directed mutagenesis similarly. See Table 1 for sequences of all the primers and oligonucleotides used.

Cell culture, cell line generation and transfection

The HEK293 [156, 161, 162] and MCF-7 [5, 23] cell lines were described previously. These cells were maintained in DMEM with 10% fetal bovine serum (FBS) and proper antibiotic supplements. MCF7 stable cells expressing HA-KLF8 (MCF7-K8) and its mutant S48A (MCF7-K8-S48A) and S48D (MCF7-K8-S48D) were generated by infecting the MCF7 cells with lentiviruses derived from the corresponding lentiviral vectors followed by puromycin selection. Selected cells were maintained in DMEM supplemented with 10% FBS and puromycin. GSK3$\beta^{-/-}$ and GSK3$\alpha^{-/-}$ and matched wild-type mouse embryonic fibroblasts (MEFs) were kind gifts from Dr. Jim Woodgett of Lunenfeld-Tanenbaum Research Institute [163]. These cells were maintained in DMEM plus 10% FBS. Transfections were done using Lipofectamine 2000 (Invitrogen, Grand Island, NY, USA).

Phosphatase treatment

After 36 - 48 h of transfection, cells were washed with ice-cold phosphate-buffered saline, lysed with NP-40 buffer containing protease inhibitor cocktail (1 mM PMSF, 0.2 IU/ml approtini and 20 □g/ml leupeptin) for 30 minutes at 4°C and centrifuged (12,000 rpm, 10 min, 4°C) to obtain the cell lysate. A aliquot of 20 □g lysate was treated with 30 units of CIP in 40 □l reaction with NEBuffer 3 for 2 h at 37°C followed by SDS-PAGE and western blotting. Untreated lysate and lysate treated with CIP plus its inhibitor sodium orthovanadate (20 mM) were included as controls.

Western blotting and co-immunoprecipitation (Co-IP)

These assays were done as previously described [5, 16]. Cells and antibodies used were described above. Western blots were quantified using Image Lab 3.0 (Bio-Rad, Hercules, CA) as previously described [16]

Protein lifespan assay

Cycloheximide (CHX) chase assay was performed essentially as previously described [16]. The HA-KLF8 and its mutant proteins overexpressed either transiently in HEK293 cells or stably in the MCF7 cell lines described above were treated with 50 ng/ml of CHX. In some experiment, the MEK inhibitor U0126 was included in the medium at 10

□M for 30 minutes prior to addition of CHX and at 3 □M during the CHX chase period of time. Lysates were collected at different time points for western blotting.

Cell migration assays

MCF7, MCF7-K8, MCF7-K8-S48A and MCF7-K8-S48D cells were seeded in a 12-well plate and grown to confluent state. Would closure (24 h) and Boyden Chamber (20 h) migrations were performed and analyzed quantitatively as previously described [5].

Statistical Analysis

At least three observations per group were conducted. Data are presented as mean ± the standard deviation. Unpaired, paired or single sample Student's *t*-test with the Bonferroni correction for the multiple comparisons was applied as appropriate. Statistical significance was determined using the alpha level of 0.05.

Results

Mobility shift of KLF8 is due to phosphorylation among its N-terminal 50 amino acids

The full-length wild-type KLF8 protein migrates as a doublet on SDS-PAGE and deletion of 50 or more amino acids from the N-terminus changes the doublet into a single band [15] regardless of the epitope types attached (Figure 2A). Since the known PTMs of KLF8 do not have evident effect on the mobility shift [14-17, 19, 20] and protein phosphorylation most frequently causes protein mobility up-shift [164, 165], we sought to determine if phosphorylation plays a role for the KLF8's mobility shift observed. We treated the cell lysates containing epitope-tagged KLF8 protein with calf intestine phosphatase (CIP) that removes phosphate group from phosphorylated serine, threonine or tyrosine. The result clearly showed that CIP treatment significantly reduced, if not abolished, the upper band of the doublet irrespective of the tag types (Figure 1B, compare middle to left lane). This is specific to the catalytic activity of CIP in that the loss of the upper band was prevented with the CIP inhibitor sodium orthovanadate (Na_3VO_4) [166] (Figure 2B, lane 3). Taken together, these results strongly suggest that phosphorylation of a residue among the N-terminal 50 amino acids is responsible for the mobility shift of KLF8 protein.

Phosphorylation of KLF8 at the serine 48 is responsible for the mobility up-shift

To determine the phosphorylation site, we first constructed small deletion mutants of KLF8 by deleting 10 amino acids at a time from the N-terminal 50 amino acid region (Figure 3A). Deletion of either the residues 31-40 or 41-50 resulted in a loss of the upper band, whereas other deletions did not affect the mobility (Figure 3B). This result suggested that the phosphorylated residue of KLF8 is somewhere between the amino acids 30 and 50. To identify the exact amino acid(s) that is phosphorylated, we mutated all the serine, threonine and tyrosine residues in the 31-50 region to alanine individually to prevent phosphorylation. We found that only the S48A mutant migrated as a single band with mobility identical to the lower band of the doublet (Figure 3C), whereas the S48D mutant, where the serine was mutated to aspartic acid to mimic the phosphorylated serine [167, 168], migrated as a single band with mobility identical to the upper band of the doublet (Figure 3D). Thus, KLF8 is likely phosphorylated at S48, which is responsible for the mobility up-shift. Phylogenic analysis showed that the S48 residue is highly conserved across the species (Figure 3E). Taken together, these results provided strong evidence that the S48 can be phosphorylated which is potentially of functional importance for KLF8.

The amino acid 31-40 region plays a regulatory role for the phosphorylation of KLF8 at S48

The loss of the upper band from the d31-40 mutant protein (Figure 3B) is not due to failure to be phosphorylated within this deleted region in that mutation of the serine 31, the only potential phosphorylation residue, to alanine did not alter the mobility of the protein (Figure 3C). This result suggested that, while this region does not contain a phosphorylation site, it might play a role in facilitating the phosphorylation at S48. We then made two smaller deletion mutants of KLF8, i.e., d31-35 and d36-40 and found that interestingly, the d31-35 mutant showed mostly the upper band whereas the d36-40 mutant migrated as only the lower band (Figure 4A). This result suggested that the amino acid 31-35 and 36-40 regions might respectively regulate the phosphorylation at S48 negatively and positively. Indeed, both phosphatase treatment and a second S48A mutation brought the d31-35 mutant protein to the lower band position, while the S48D-d31-35 mutant protein remained in the upper band position regardless of the phosphatase treatment (Figure 4B). We then mutated each residue to alanine in this region individually or in combination and found that only the R33A/R35A mutant showed a migration pattern closest to the d31-35 mutant (Figure 4C). This result suggested that this R-X-R motif at 33-35 position might be the one that mediates the negative effect on the phosphorylation at S48. To determine the core residue or motif among 36-40 residues, we similarly mutated each individual residue in this region to alanine. Isoleucine residue at position 40 was also mutated to arginine given that isoleucine and alanine share similar amino acid structure. All the single point-mutants migrated as a

doublet similar to the wild-type KLF8. Because proline actively participates in protein folding to maintain protein tertiary structure, we constructed a P37A/P38A mutant of KLF8. It has been also reported that D-X-X-E motif is important for binding to metal ions [169] and proteins such as focal adhesion kinase [170]. Hence, we made a D36A/E39A mutant also to obstruct this motif. Interestingly, the D36A/E39A double mutant migrated as the lower band only whereas the P37A/P38A mutation did not alter the mobility (Figure 4D). These results suggested that the D-X-X-E motif at 36-39 positions mediates the positive effect on the phosphorylation at S48. Taken together, the amino acid 31-40 region appears to play an important counteracting role to balance a proper level of phosphorylation of KLF8 at S48 through mechanisms to be determined (Figure 4E).

ERK2 phosphorylates KLF8 at S48

We then sought to determine the protein kinase responsible for the phosphorylation of KLF8 at S48. We first attempted to predict potential kinase(s) for the S48 site using the online application programs including NetPhosK [171] (http://www.cbs.dtu.dk/services/NetPhosK/), PhosphoNet (http://www.phosphonet.ca/) and Kinasephos (http://kinasephos.mbc.nctu.edu.tw/). The GSK3, CDK5, ERK and JNK stood out as the potential kinase candidates with GSK3□ having the highest predicted score. Next, we treated the HEK293 cells overexpressing HA-KLF8 with specific inhibitors of these kinases. Only the MEK1/2 inhibitor treatment showed less KLF8

phosphorylation compared to DMSO treatment (Figure 5A). As the GSK3 inhibitor used was for both GSK3α and GSK3β, we transfected KLF8 into GSK3α knockout (GSK3$\alpha^{-/-}$) and GSK3β knockout (GSK3$\beta^{-/-}$) mouse embryonic fibroblast (MEF) cells [163]. KLF8 protein mobility remained unchanged in these knockout cells as in the wild-type MEF cells (Figure 5B), thereby, excluding GSK3s. These results indicated that the MEK-ERK pathway might play a role in the phosphorylation of KLF8 at S48.

To determine cancer relevance of the aforementioned results, we generated MCF7 cell lines stably overexpressing the wild-type KLF8 (MCF7-K8) and the S48A mutant (MCF7-K8-S48A), respectively. Treating the MCF7-K8 cells with the MEK inhibitors, PD98059 or U0126, caused a dramatic reduction in the phosphorylation of KLF8 that is well correlated with the decrease in the phosphorylation of ERKs (Figure 5C-5F). This result suggested that MEK(s) or/and ERK(s) could be responsible for the phosphorylation of KLF8 in the breast cancer cells. Since the above described computer programs predicted ERK(s) rather than MEKs as a potential KLF8 kinase, and the phosphorylation of ERK2 appeared to be inhibited more than ERK1 did by the MEK inhibitors in the cells (Figure 5C-5F), we next tested the potential phosphorylation of KLF8 by ERK2. Overexpression of ERK2 increased the phosphorylation of KLF8 whereas its kinase dead, dominant negative mutant (ERK2-K54R) decreased the phosphorylation of KLF8 (Figure 5G). By contrast, the S48A mutant of KLF8 did not show any phosphorylated upper band upon ERK2 overexpression (Figure 5G). These results strongly suggested that ERK2 could phosphorylate KLF8 at S48. This notion was further supported by the co-IP assay that detected an interaction between ERK2

and KLF8 in the cells (Figure 5H). In addition, EGF stimulation of ERKs clearly increased the phosphorylation of KLF8, which was blocked by the ERK2 dominant negative mutant (Figure 4I). Furthermore, overexpression of the constitutively active mutant (ERK2-CA) prevented inhibition of the phosphorylation of KLF8 by the MEK inhibitor U0126 (Figure 5J). Taken together, these results identified ERK2 as the kinase likely responsible for the phosphorylation of KLF8 at the S48 site.

Phosphorylation of KLF8 at S48 maintains the stability of KLF8 protein

The phosphorylation of KLF8 appears to correlate with the total levels of KLF8 (Figure 5A and 5J), suggesting a potential protection of KLF8 protein from degradation by the phosphorylation at the S48 site. Indeed, both the phosphorylation-defective mutants, KLF8-S48A and KLF8-d41-50, expressed at a significant lower level than the wild-type KLF8 did (Figure 6A). We performed protein chase assays in transient transfected HEK 293 cells and found out that the wild-type KLF8 and the S48A mutant have the longest and shortest life-span, respectively (Figure 6B and 6C). Unexpectedly yet interestingly, the S48D and d31-35 mutants did not show a prolonged life over the wild-type KLF8 although the d36-40 mutant, like the S48A mutant, showed a shortened lifespan compared to the wild-type KLF8 (Figure 6B and 6C). Taken together, these results suggested that the phosphorylation at S48 is critical for maintaining the stability of KLF8 protein.

Phosphorylated KLF8 acts as a mask to protect the overall stability of KLF8 protein

In the MCF7 stable cell lines, we obtained stability patterns for the wild-type KLF8 and the S48A mutant similar to what was observed in the HEK293 cells (Figure 7A and 7B). Surprisingly, the unphosphorylated form (lower band) of the wild-type KLF8 stayed more stable than the phosphorylated form (upper band) (Figure 7B). These results raised an interesting possibility that the phosphorylation of KLF8 at S48 helps maintain the overall KLF8 protein levels by protecting the unphosphorylated form of KLF8 from degradation. This notion was further supported by the result showing that the lower band of KLF8 was degraded faster in the cells treated with the MEK inhibitor than that in the mock treated cells (Figure 7C and 7D). Therefore, the phosphorylated KLF8 may sacrifice itself to protect the unphosphorylated form of it.

KLF8 requires the phosphorylation at the S48 site to promote cell migration

Lastly, we attempted to see if the phosphorylation of KLF8 at the S48 site plays a role for any known cellular function of KLF8. We performed two independent migration assays both of which demonstrated that the S48A, but not the S48D, mutant lost the capacity to promote the MCF7 cell migration (Figure 8). This result suggested that the phosphorylation of KLF8 at the S48 site by ERK2 is critical for KLF8 function.

Discussion

This study identified the serine 48 as a novel phosphorylation site on KLF8 responsible for its mobility shift and ERK2 as a novel kinase for the phosphorylation of KLF8 at this site. Based on the results of the study, we propose a model of mechanism of action (Figure 9) in which ERK2 phosphorylation of KLF8 at the serine 48 site gears the degradation of KLF8 protein from the unphosphorylated towards phosphorylated form of the protein to protect the stability of unphosphorylated form. The unphosphorylated form may be the primary functional form of KLF8. In addition, the phosphorylation at the serine 48 is critically balanced by N-terminal region of residues 31-40 where the regions of 31-15 and 36-40 have a negative and positive effect, respectively via unknown mechanisms.

In support of this study, it was reported that ERK2 phosphorylates c-Myc at serine 62 to increase the stability of c-Myc protein [172], and blocking this phosphorylation by inhibiting ERK2 leads to a marked decrease in the c-Myc protein level and tumor malignancy [173]. In addition to KLF8, other KLF family members such as KLF5 [174], KLF3 [175] and KLF2 [176] are also regulated by phosphorylation. Indeed, it has been reported that ERK2 phosphorylated KLF2 protein is more sensitive to proteasomal degradation [176], and ERK phosphorylation of KLF4 at serine 123 results in inhibition of KLF4's function [48]. Another recent report showed that ERK inhibitor treatment decreased KLF8 expression and the ERK-KLF8 pathway might play a role in

chemoresistance of colorectal cancer cells [37]. Our results provide mechanistic interpretation of this report. Our recent work has revealed that KLF8 upregulates EGFR in breast cancer cells [37]. Given that EGF stimulation enhances the ERK2-dependent phosphorylation of KLF8 (see Figure 5I), it is possible that a potential positive feedback loop of KLF8 to EGFR to ERK to KLF8 exists.

We showed that both the constitutively phosphorylation-mimicking and unphosphorylated mutants of KLF8 protein have a shortened lifespan compared to the total wild-type KLF8 (Figure 6). However, the phosphorylated form (upper band) of wild-type KLF8 has a much shorter lifespan than its unphosphorylated counterpart (lower band) (Figure 7). These seemingly paradoxical observations suggest a protective role of the phosphorylated form for the stability of the unphosphorylated form that might be the functional form of KLF8 in the nucleus.

How the amino acid 31-40 region regulates the phosphorylation of KLF8 at the serine 48 site remains to be determined. The R-X-R motif located in the 33-35 region has been shown to play an essential role in protein-protein interaction [177], endoplasmic reticulum (ER) retention of protein [178], and phosphatase binding [179]. This motif was first identified as an ER retention motif [180, 181]. Proteins with this motif tend to show high ER retention and less ER to Golgi transport [182, 183]. The positively charged arginine (R) residues can interact with other negatively charged residues to regulate

protein tertiary structure [184]. This motif is also involved in co-factor binding [182]. Interestingly, two reports suggested that F-X-X-R-X-R motif is the binding site of the phosphatase PP1 [179, 185]. It will be interesting to test if the KLF8's ^{30}ASVRNR^{35} motif plays a docking role for PP1 or PP1-like phosphatases. The D-X-X-E in the 36-39 region, unlike R-X-R motif, had a positive influence on the phosphorylation of KLF8. D-X-X-E motif was first found on β-integrin cytoplasmic tail critical for focal adhesion kinase binding [170]. Recent studies have also demonstrated the binding of D-X-X-E motif to the metal ion of magnesium, manganese or calcium [169, 186, 187]. Calcium has been shown to activate ERK through adynyl cyclase [188]. Therefore, it is possible that the ^{36}DPPEI^{40} motif might play a role in metal binding required for the phosphorylation of KLF8 at the serine 48 site by ERK2.

Previous report showed that poly (ADP-ribose) polymerase 1 binds to KLF8 to promote its nuclear retention and prevent nuclear export and subsequent degradation of KLF8 protein in the cytoplasm [17]. Interestingly, the KLF8 S48A mutant is localized in the nucleus and the phosphorylation of KLF8 at serine 48 does not play any role in poly (ADP-ribose) polymerase 1 binding (data not shown). Therefore, it is likely that the stability of KLF8 protein is regulated in both the cytoplasm and nucleus via distinct molecular mechanisms. Additionally, cross talks between different PTM types KLF8 have been reported. For instance, a switch between acetylation and sumoylation of KLF8 was found to be critical for its transcriptional activity [20]. Whether or not the

phosphorylation of KLF8 at the serine 48 site plays a role for other PTM types is another interesting topic of future study.

Physiologically critical yet pathologically important proteins such as proto-oncogenic and tumor suppressor proteins are tightly regulated to maintain their expression and function within the physiological window. Loss of the regulatory balance is a major cause of diseases. Both the S48 site of KLF8 and the function of ERK2 are well conserved across species. PTMs such as protein phosphorylation are among the most important protein regulatory mechanisms. These lines of evidence underscore the pathological importance of the ERK2-dependent phosphorylation of KLF8 at the serine 48 site discovered in this study.

Figures

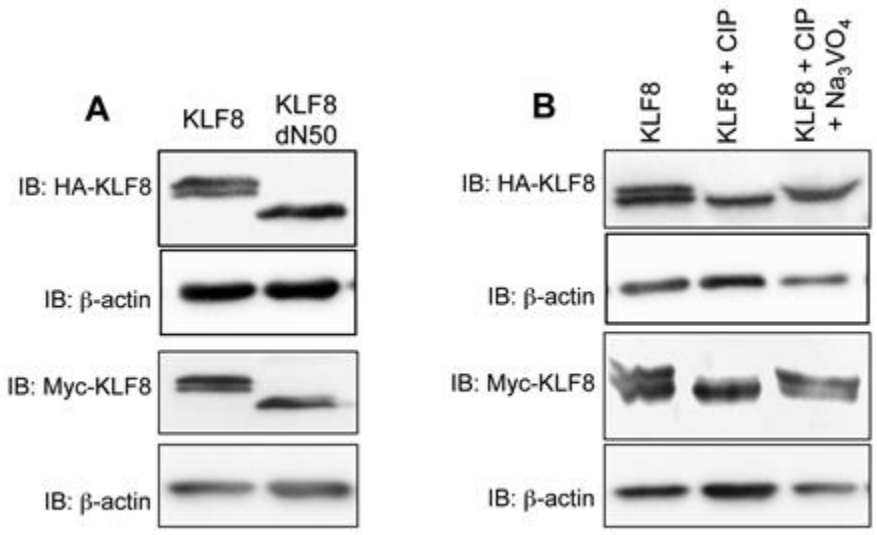

Figure 2. Mobility shift of KLF8 is due to phosphorylation in its N-terminal 50 amino acid residues.

(*A*) The N-terminal region of 50 residues is required for maintaining the doublet of KLF8 protein on SDS-PAGE gels. HA-KLF8, HA-KLF8-dN50, Myc-KLF8 or Myc-KLF8-dN50 was transfected into HEK293 cells. Whole cell lysates were collected after 48 hours and processed for western blotting with anti-HA (1:3000) or anti-Myc (1:2000) antibody with anti-□-actin as loading control. (*B*) Treatment with alkaline phosphatase abolished the upper band of the KLF8 doublet. HA-KLF8 or Myc-KLF8 was oeverexpressed in HEK293 cells. Lysates prepared from the cells were treated with CIP without or with its inhibitor sodium orthovanadate (Na_3VO_4) as described in the Experimental Procedures and processed for western blotting as described above.

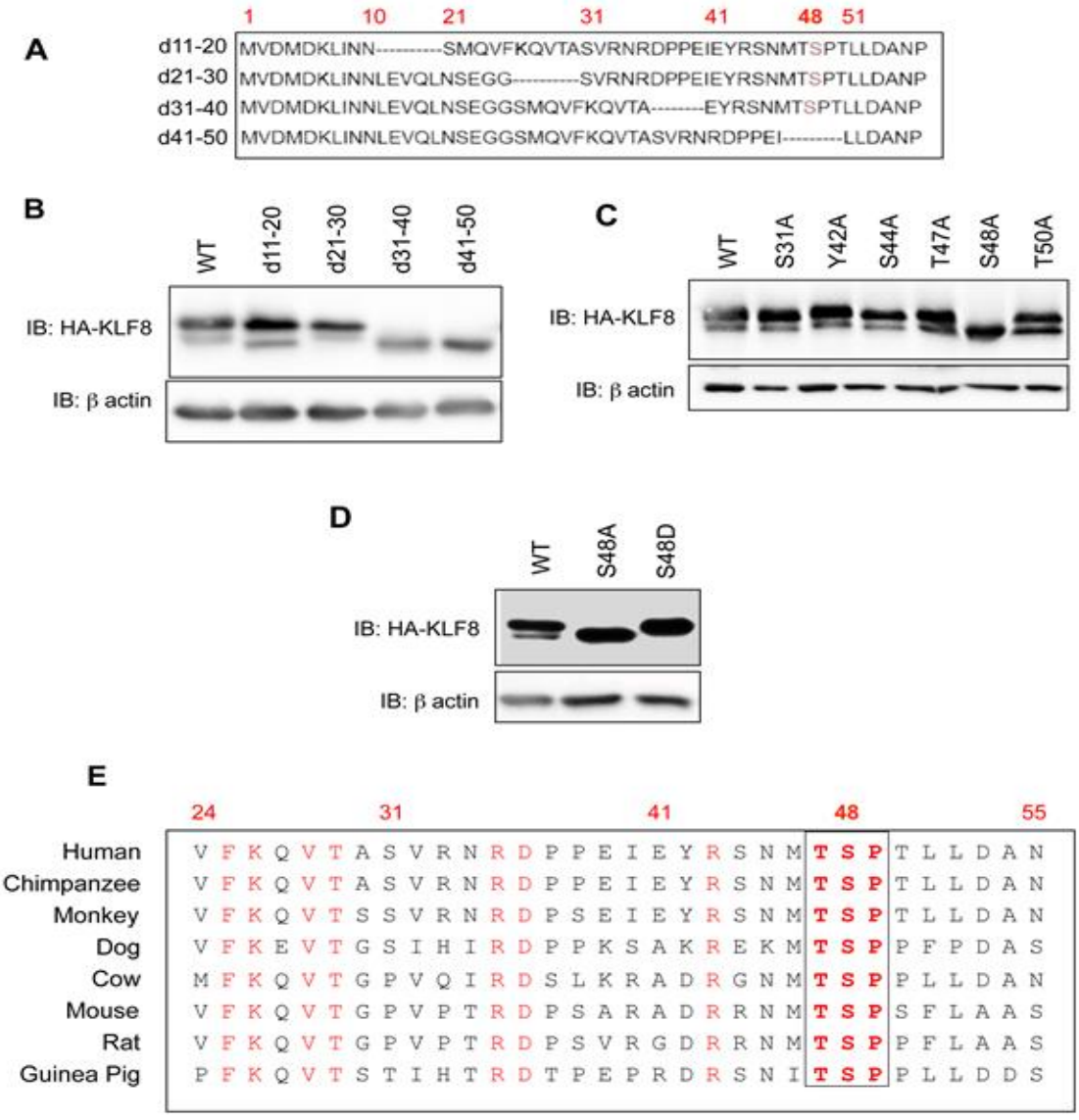

Figure 3. Phosphorylation of KLF8 at the serine 48 (S48) is responsible for the up-shift of KLF8 mobility.

(*A, B*) Both KLF8 31-40 and 41-50 aa regions are essential for the phosphorylation (mobility upshift) of KLF8. Indicated small deletion mutants of KLF8 (*A*) were overexpessed for western blotting (*B*). (*C, D*) The mobility up-shift of KLF8 is due to the phosphorylation at the S48. All the potential phosphorylated residues including serine, threonine and tyrosine residues in the area of residues 31-50 were mutated to alanine and their band patterns were analyzed by overexpression and western blotting (*C*). Only the S48A mutant showed a single (lower) band. (*D*) Mutation of S48 to Aspartate results in the upper band only. The phosphorylation-mimicking mutant S48D was overexpressed for western blotting. (*E*) The S48 site of KLF8 is conserved across the species. Sequence homology was analyzed using the NCBI multiple sequence alignment.

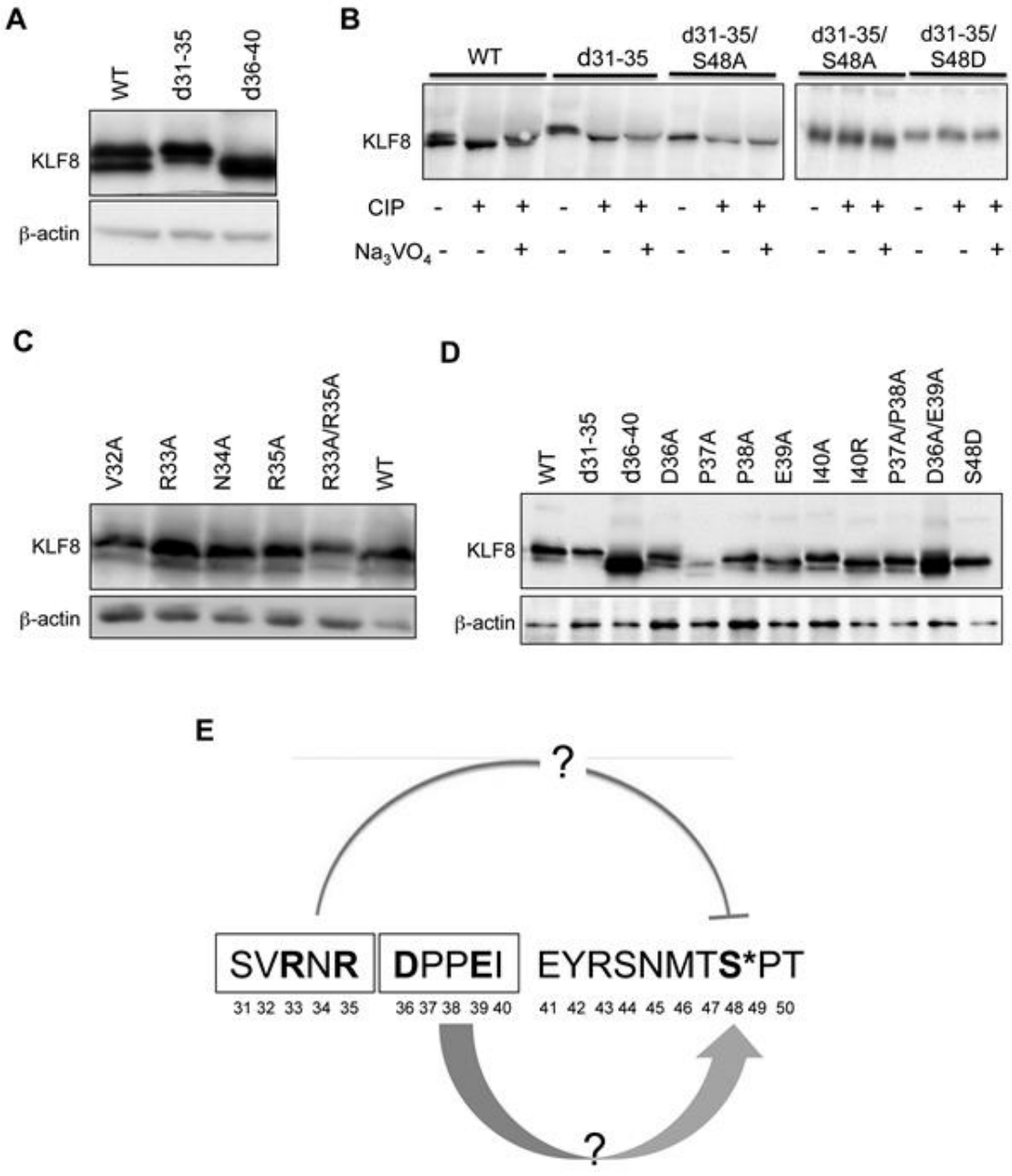

Figure 4. The region of residues 31 - 40 plays an essential regulatory role in the phosphorylation of KLF8 at the S48 site.

The R-X-R motif in ^{31}SVRNR^{35} of KLF8 plays an inhibitory role in the phosphorylation of KLF8 at the S48 (*A-C*) whereas the D-X-X-E motif in ^{36}DPPEI^{40} of KLF8 has a positive effect on it (*D*). Indicated KLF8 mutants were overexpressed and lysates were prepared with or without CIP treatment in the presence or absence of the CIP inhibitor for western blotting. (*E*) The counteracting role of the R-X-R and D-X-X-E motifs was illustrated.

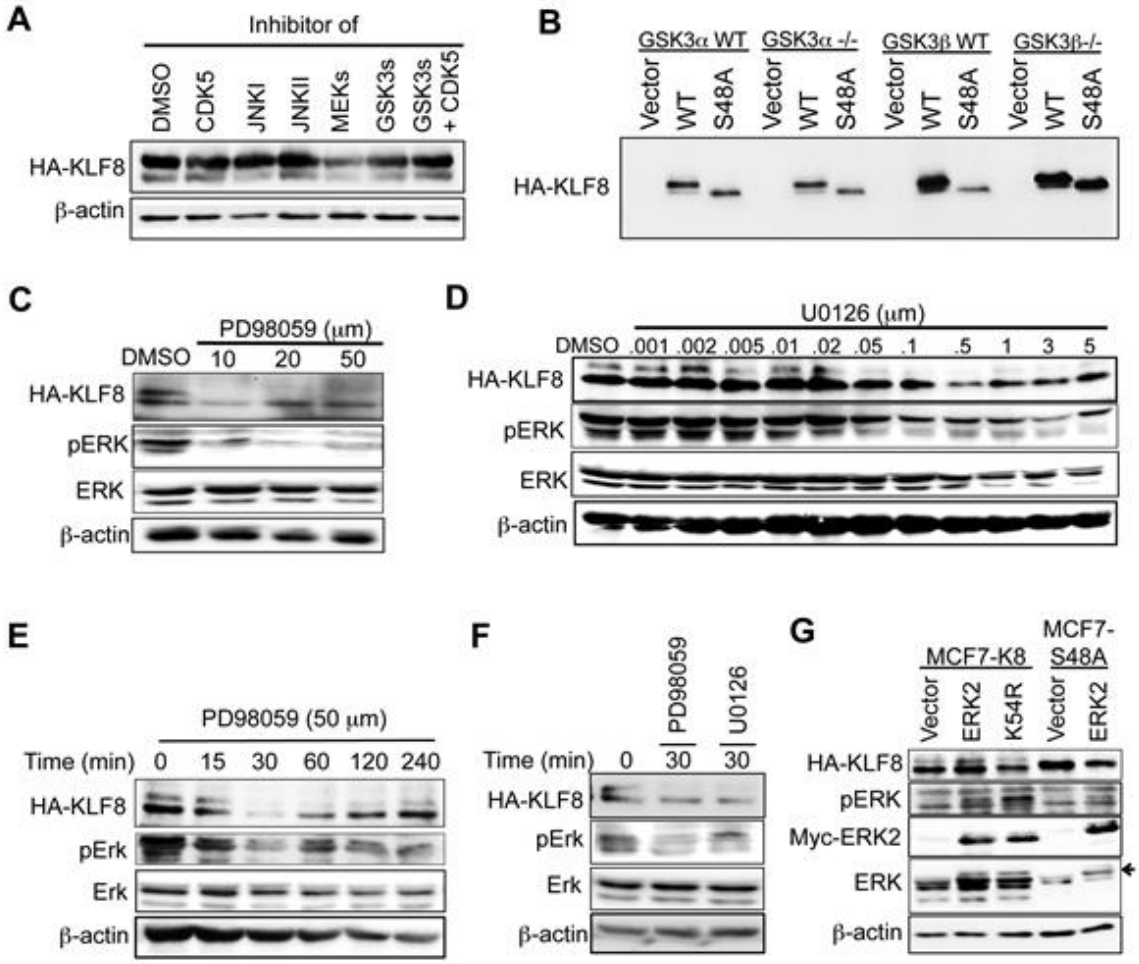
A
Inhibitor of
DMSO
CDK5
JNKI
JNKII
MEKs
GSK3s
GSK3s + CDK5
HA-KLF8
β-actin
B
GSK3α WT
GSK3α -/-
GSK3β WT
GSK3β-/-
Vector
WT
S48A
HA-KLF8
C
PD98059 (μm)
DMSO
10
20
50
HA-KLF8
pERK
ERK
β-actin
D
U0126 (μm)
DMSO .001 .002 .005 .01 .02 .05 .1 .5 1 3 5
HA-KLF8
pERK
ERK
β-actin
E
PD98059 (50 μm)
Time (min) 0 15 30 60 120 240
HA-KLF8
pErk
Erk
β-actin
F
PD98059
U0126
Time (min) 0 30 30
HA-KLF8
pErk
Erk
β-actin
G
MCF7-K8
MCF7-S48A
Vector
ERK2
K54R
Vector
ERK2
HA-KLF8
pERK
Myc-ERK2
ERK
β-actin

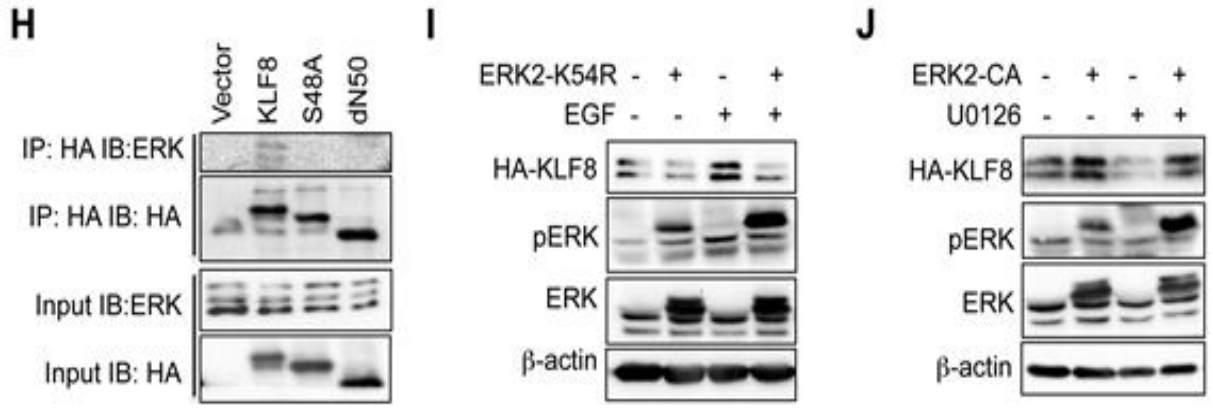

Figure 5. ERK2 is the kinase responsible for the phosphorylation of KLF8 at the S48 site.

(*A*) Inhibition of MEKs, but not JNKs, GSK3s or CDK5, leads to a decrease in the phosphorylation of KLF8. HEK293 cells overexpressing KLF8 were treated with indicated inhibitors for 4 h. Cell lysates were prepared for western blotting. (*B*) Knockout of GSK3s does not affect mobility of KLF8 protein. Wild-type KLF8 (WT), its S48A mutant or vector control was overexpressed in the indicated cells for 48 h. Cell lysates were prepared for western blotting. (*C-F*) Dose- and time-dependent inhibition of phosphorylation of KLF8 by MEK inhibitors. The MCF7-K8 cells at ~80% confluent growth were treated with PD98059 or U0126 as indicated, cell lysates were processed for western blotting for the band patterns of KLF8. Total ERK, pERK and □-actin were included as controls. For the dose-dependent study the treatment time was 4 hours. In (F) 50 □M PD98059 and 5 □M U0126 were used respectively. (*G*) The catalytic activity of ERK2 is the phosphorylation of KLF8 at the S48 site. Myc-tagged ERK2 or its dominant-negative mutant K54R was overexpressed in the MCF7-K8 or MCF-K8S48A cells. Lysates were prepared after 48 hours for western blotting. (*H*) ERK2 interacts with KLF8 in an S48-dependent manner. Indicated KLF8, its mutant or vector control was overexpressed in HEK293 cells and precipitated with anti-HA antibody from cell lysates prepared after 48 hours. Co-precipitated ERKs were analyzed by western blotting. (*I*) ERK2 activity is required for EGF-stimulated phosphorylation of KLF8. The MCF7-K8 cells were transfected with dominant-negative ERK2 mutant K54R plasmid or vector alone. After 36 h, the cells were serum-starved for 16 h and then treated with 50 ng/ml EGF or DMSO. Cell lysates were collected after 30 minutes for western blotting. (*J*) ERK2 activity is sufficient for the phosphorylation of KLF8. The MCF7-K8 cells were transfected with the ERK2 constitutive active mutant (ERK2-CA). After 36 h, the cells were treated with U0126 (5 □m) for 30 minutes. Cell lysates were then prepared for western blotting.

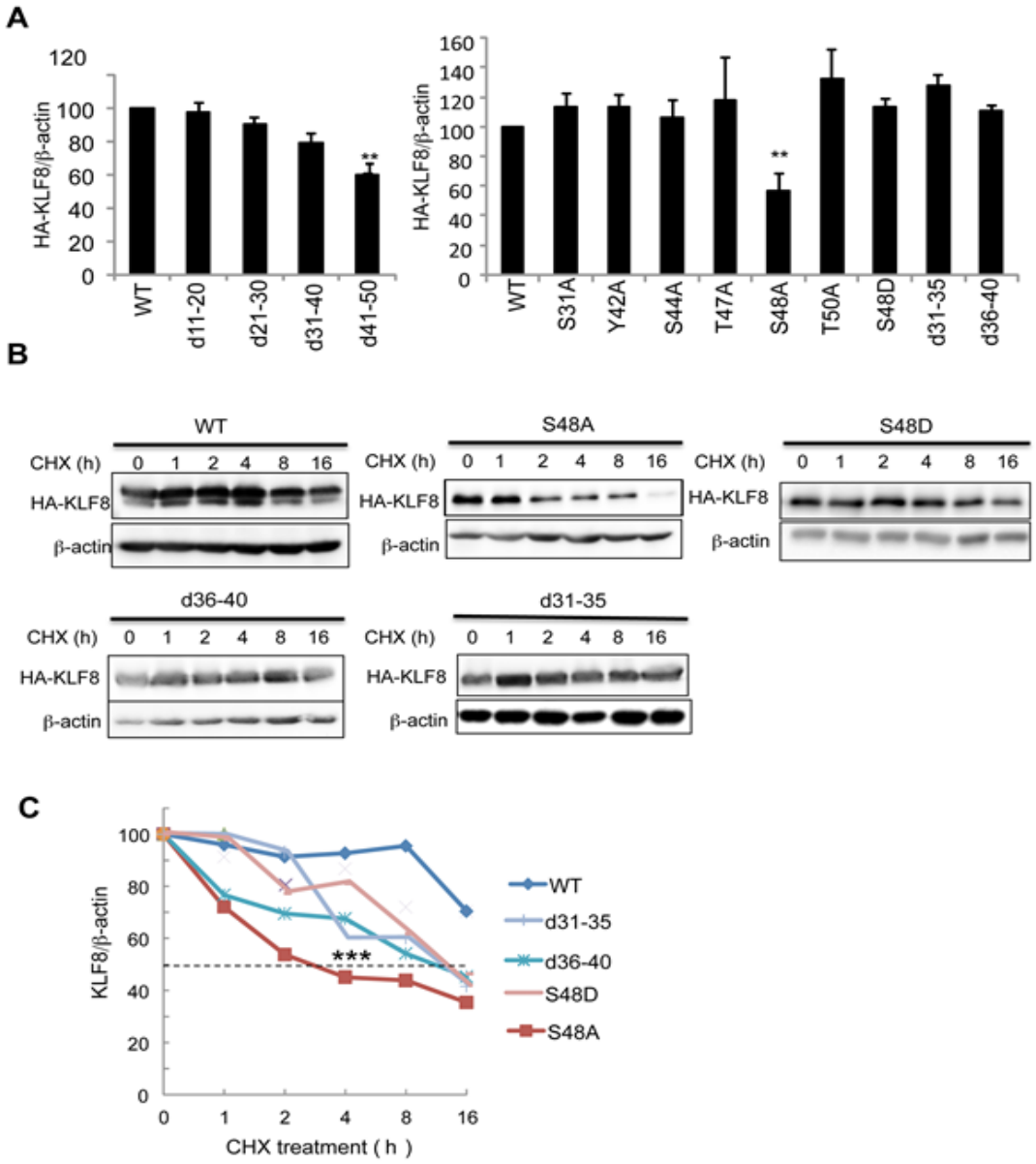

Figure 6. Phosphorylation of KLF8 at the S48 site is critical for KLF8 stability.

(A)The unphosphorylated KLF8 mutant proteins express at a decreased level. Indicated HA-tagged KLF8 and its mutants were overexpressed in HEK293 cells for 48 h prior to preparation of cell lysates for western blotting with HA and □-actin antibodies and quantification of protein expression. (*B, C*) The unphosphorylated KLF8 mutant proteins have a shortened lifespan. Indicated HA-KLF8 and its mutants were overexpressed in HEK293 cells for 36 h. CHX drug was then added and cell lysates were collected at eh indicated time points for western blotting and protein quantification.

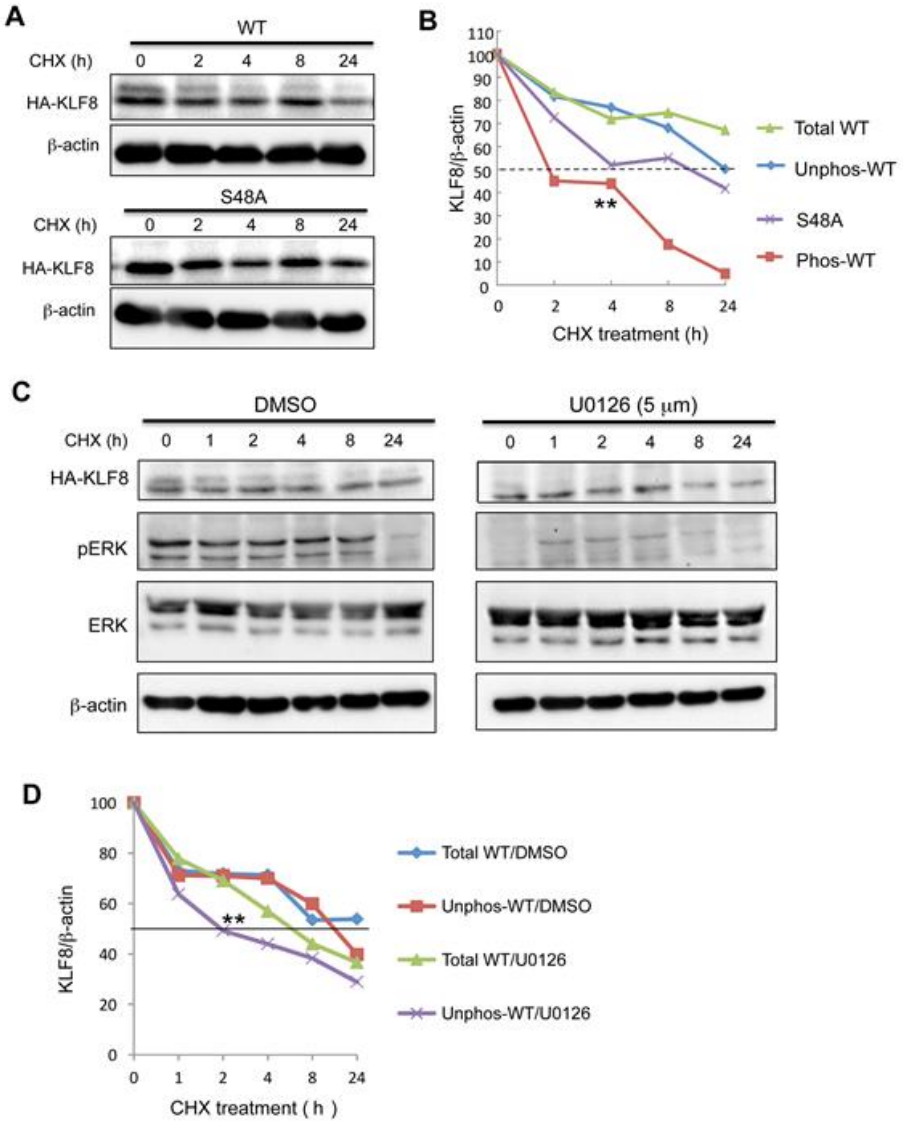

Figure 7. The phosphorylated form of KLF8 acts as a mask to protect the overall stability of KLF8 protein.

(*A, B*) The phosphorylated form of KLF8 protein degrades to protect the unphosphorylated form. The MCF7-K8 and MCF7-K8-S48 cells were subjected to CHX chase assay as described above. The upper and lower bands of the wild-type KLF8 were quantified separately and compared to total expression of the wild-type KLF8 as well as the S48A mutant protein. (*C, D*) The lifespan of the unphosphorylated form of KLF8 protein decreases in the absence of the phosphorylated form. The CHX chase assay was carried out similarly except that the MCF7-K8 cells were treated with the MEK inhibitor U0126 inhibitor before and during the chase assay as described in the Experimental Procedures.

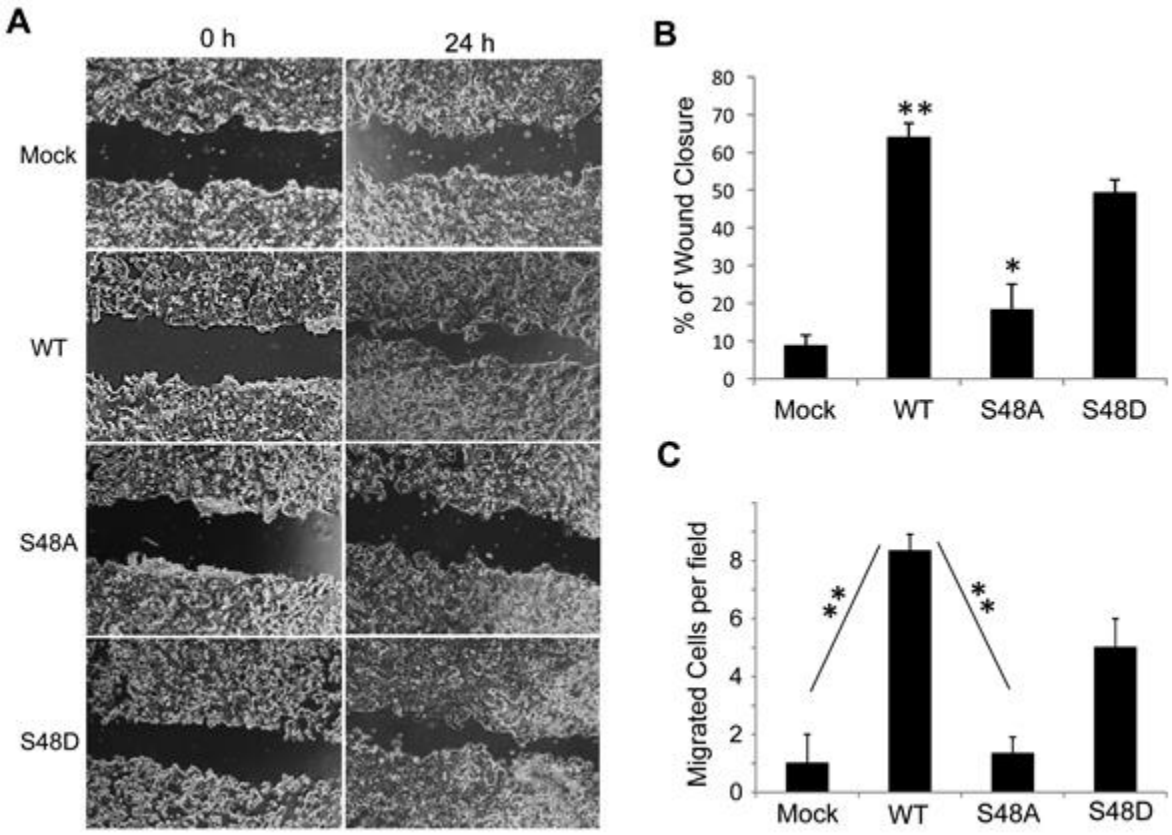

Figure 8. The phosphorylation at the S48 is essential for KLF8 to promote cell migration

The MCF7-K8 (WT), MCF7-K8-S48A, MCF7-K8-S48D alongside the mock control cells were grown and subject to wound closure (*A, B*) as well as Boyden chamber (C) migration assays as described in the Experimental Procedures.

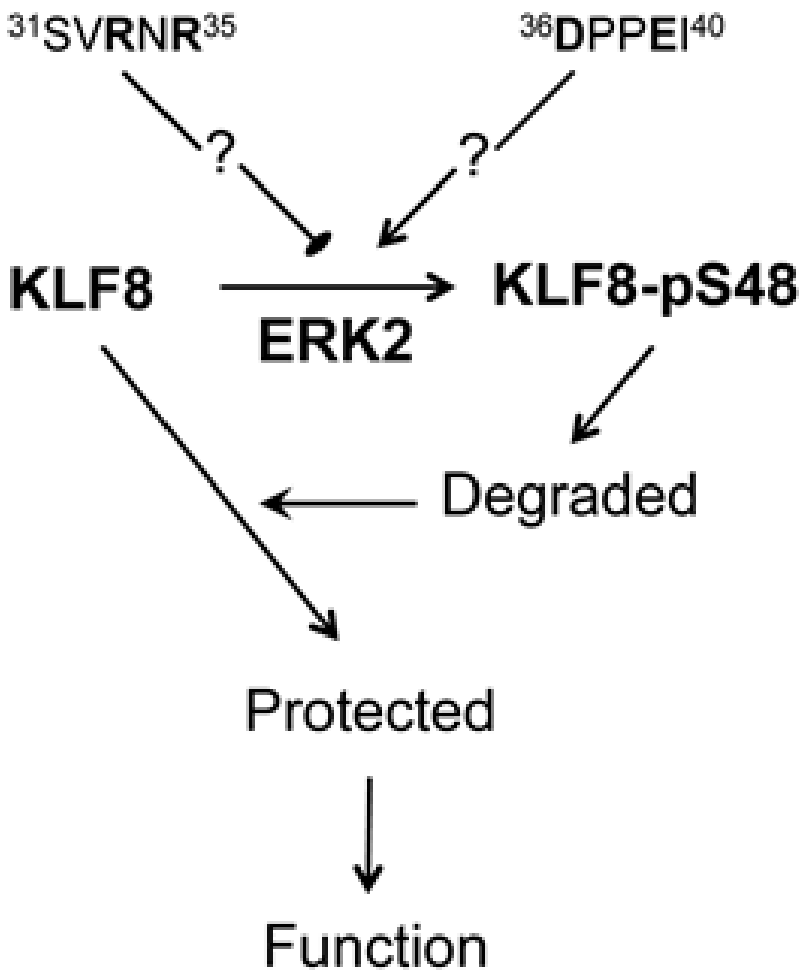

Figure 9. Proposed model of the mechanism of action

ERK2 phosphorylate KLF8 at the S48 site. This phosphorylation distracts KLF8 degradation of unknown mechanism away from the unphosphorylated form towards the phosphorylated form of the protein, resulting in an increase in overall stability of the KLF8 protein. On the other hand, the ERK2 phosphorylation of KLF8 is balanced by two potential counteracting mechanisms of regulation mediated by the inhibitory R-N-R motif and the supporting D-P-P-E motif.

Table 1. Sequences of primers and oligonucleotides used

Primer name	Primer sequence (5' – 3')
pKH3-F	CCC AAG CTT CTG CAG GTC G
pKH3-R	GGA CAA ACC ACA ACT AGA ATG CAG
KLF8 d11-20-R	CCT GCA T TG AGT TGT T TA TGA GTT TAT CC
KLF8 d11-20-F	AAC AAC TCA ATG CAG GTA TTC AAG C
KLF8 d21-30-R	CGA ACA GAG CCA CCT TCT GAA TTA AGT T
KLF8 d21-30-F	AGG TGG CTC TGT TCG GAA CAG AGA TC
KLF8 d31-40-R	CTG TAT TCA GCA GTG ACC TGC TTG AAT A
KLF8 d31-40-F	TCA CTG CTG AAT ACA GAA GTA ATA TGA CT
KLF8 d41-50-R	ATC CAG GAG TAT CTC AGG GGG ATC TCT
KLF8 d41-50-F	TGA GAT ACT CCT GGA TGC CAA CCC CAT
KLF8 S31A-R	CCG AAC AGC AGC AGT GAC CTG
KLF8 S31A-F	ACT GCT GCT GTT CGG AAC AGA GAT C
KLF8 Y42A-R	ACT TCT GGC TTC TAT CTC AGG G
KLF8 Y42A-F	ATA GAA GCC AGA AGT AAT ATG ACT TCT CC
KLF8 S44A-R	CAT ATT AGC TCT GTA TTC TAT CTC AGG G
KLF8 S44A-F	TAC AGA GCT AAT ATG ACT TCT CCA ACA
KLF8 T47A-R	TGG AGA AGC CAT ATT ACT TCT GTA TTC
KLF8 T47A-F	AAT ATG GCT TCT CCA ACA CTC CTG
KLF8 S48A-R	TGT TGG AGC AGT CAT ATT ACT TCT
KLF8 S48A-F	ATG ACT GCT CCA ACA CTC CTG GAT

Primer name	Primer sequence (5’ – 3’)
KLF8 T50A-R	CAG GAG TGC TGG AGA AGT CAT ATT
KLF8 T50A-F	TCT CCA GCA CTC CTG GAT GCC
KLF8 S48D-R	TGT TGG ATC AGT CAT ATT ACT TCT GTA
KLF8 S48D-F	ATG ACT GAT CCA ACA CTC CTG GAT
KLF8 d31-35-F	ACT GCT GAT CCC CCT GAG ATA GAA
KLF8 d31-35-R	AGG GGG ATC AGC AGT GAC CTG CTT
KLF8 d36-40-F	CGG A CGG AAC AGA GAA TAC AGA AGT AAT ATG AC AGA
KLF8 d36-40-R	TCT GTA TTC TCT GTT CCG AAC AGA AGC
KLF8 P37A-R	TAT CTC AGG GGC ATC TCT GTT CCG
KLF8 P37A-F	AGA GAT GCC CCT GAG ATA GAA TAC
KLF8 P38A-R	TAT CTC AGC GGG ATC TCT GTT CCG
KLF8 P38A-F	AGA GAT CCC GCT GAG ATA GAA TAC
KLF8 P37/38A-R	TAT CTC AGC GGC ATC TCT GTT CCG
KLF8 P37/38A-F	AGA GAT GCC GCT GAG ATA GAA TAC
KLF8 D36A-R	AGG GGG AGC TCT GTT CCG AAC AGA
KLF8 D36A-F	AAC AGA GCT CCC CCT GAG ATA GAA
KLF8 E39A-R	TTC TAT CGC AGG GGG ATC TCT GTT
KLF8 E39A-F	TCC CCC TGC GAT AGA ATA CAG AAG
KLF8 D36/E39A-R	TTC TAT CGC AGG GGG AGC TCT GTT
KLF8 D36/E39A-F	AAC AGA GCT CCC CCT GCG ATA GAA

Primer name	Primer sequence (5’ – 3’)
KLF8 I40A-R	GTA TTC TGC CTC AGG GGG ATC TCT
KLF8 I40A-F	CCT GAG GCA GAA TAC AGA AGT AAT
KLF8 I40R-R	GTA TTC TCT CTC AGG GGG ATC TCT
KLF8 I40R-F	CCT GAG AGA GAA TAC AGA AGT AAT
ERK2-SmaI-F	TTT CCC GGG AGC AGC TGC GGC GGC GGC GGG CGC
ERK2-ClaI-R	CCC ATC GAT TTA AGA TCT GTA TCC TGG CTG GAA TC
ERK2 K54R-F	GCT ATC AGG AAA ATC AGC CCC TTT
ERK2 K54R-R	GAT TTT CCT GAT AGC TAC TCG AAC
ERK2 R67S-F	TGC CAG AGC ACC CTG AGG GAG ATA
ERK2 R67S-R	CAG GGT GCT CTG GCA GTA GGT CTG
ERK2 D321N-F	CCG AGT AAC GAG CCC ATC GCC GAA
ERK2 D321N-R	GGG CTC GTT ACT CGG GTC GTA ATA

CHAPTER 3: KLF8 PROMOTES SYSTOLIC DYSFUNCTION THAT LEADS TO SEVERE DILATED CARDIOMYOPATHY IN KLF8 TRANSGENIC MOUSE MODEL

Abstract

Krüppel-like factor 8 (KLF8) is highly expressed in several types of human cancers. Our previous studies have demonstrated that KLF8 as a dual transcription factor promotes tumor formation and metastasis by up- or down-regulating several transcriptional targets including cyclin D1, MMPs, EGFR, EPSTI1 CXCR4, KLF4, E-cadherin, microRNA-146a and microRNA-141. KLF8 has also been reported to play a critical role in DNA repair, adipogenesis, preeclampsia, zebrafish development and Alzheimer's disease. KLF8's role in cancer has been studied primarily *in vitro* and in xenograft mouse models. To better understand KLF8's function *in vivo* in a physiologically relevant context, we generated conditional KLF8 transgenic mouse model to investigate role of KLF8 in spontaneous tumorigenesis. Surprisingly, global induction of expression of the transgene caused postnatal early death of all the mice with significantly enlarged heart. Further timespan ultrasound echocardiograph studies revealed that KLF8 induces systolic dysfunction from as early as one month of age that leads to fatal dilated cardiomyopathy causing early death. Excitingly cardiomyocyte specific induction of KLF8 expression demonstrated identical phenotypes, thereby suggesting that KLF8 overexpression in cardiomyocyte leads to dilated cardiomyopathy. Studies on the

underlying molecular mechanisms are in progress including identifying KLF8 regulated mRNA and miRNA targets in cardiomyocyte to reveal the mechanism behind KLF8 mediated cardiomyopathy. Overall this study identifies a novel role of KLF8 in cardiomyopathy, one of the leading causes of cardiac death and provides insight into the responsible mechanism that will advance the cardiac research field to invent new therapeutics for this deadly disease.

Introduction

Kruppel like factor 8 is a dual transcription factor critical for cell cycle regulation, oncogenic transformation, cancer cell invasion, migration and metastasis in different types of cancer[2, 4, 5, 7, 21, 23]. Other than cancer its involvement in other cellular functions like DNA repair[16], developmental role in preeclampsia[44, 45], Alzheimer's disease[47], adipogenesis[48], cerebellar development in zebrafish[46] have been recently elucidated. Most of the studies with KLF8 have been carried out in vitro and xenograft models, whereas its function in vivo in a better physiological context remains unexplored. As KLF8 is known to actively promote different cancer progression [4, 6, 27, 39, 189, 190], it is absolutely critical to assess its role in vivo to establish KLF8 as a therapeutic target for cancer and other relevant diseases. Genetically engineered mouse model is the most important tool to evaluate function of a gene in vivo [52, 56, 61, 191]. Currently the only KLF8 genetically engineered mice available is a KLF3/KLF8

double knock out mice where KLF8 is knocked out by gene trap method[192]. This study demonstrated these double knockout mice were embryonic lethal with decreased expression of beta-globin without further mechanistic approach which limits us to understand the role of KLF8 in vivo in different tissues clearly. To explore KLF8 function in vivo, we constructed a conditional KLF8 transgenic mouse model induced by Cre-loxP recombination as KLF8 is found in elevated level in different cancers. This is the first transgenic mouse model of KLF8 to our knowledge and provides a better tool in understanding role of KLF8 in vivo. As being equipped with a Cre-loxP system, these model also present immense potential of exploring KLF8 function in different tissues specifically. We also constructed the first Cre based KLF8 knock out mouse model to study its role in parallel.

Our primary aim was to investigate KLF8 mediated spontaneous tumorigenesis in these mice as KLF8 has been implied mostly in different cancers including breast, ovarian, gastric, liver, renal, glioma, osteosarcoma, oral, nasopharyngeal carcinoma, bladder, prostate and bladder cancer[2]. In view of this widespread role of KLF8 in various cancers, before evaluating mammary specific KLF8 transgenic mice, we decided to construct KLF8 global transgenic mice to initiate KLF8 overexpression in germ line distributing to all different tissues. The first striking observation was significant higher postnatal death in the KLF8 global transgenic mice. Necropsy of these mice revealed increased heart size which later proved to be dilated cardiomyopathy in presence of KLF8 overexpression and thus discovering a novel role of KLF8 in cardiac function. In parallel, the reverse cardiac phenotype was observed in the KLF8 KO mice,

thereby suggesting a critical role of KLF8 in cardiac tissue. Overall this study gives mechanistic insight into an unknown novel role of KLF8 in dilated cardiomyopathy.

Cardiomyopathy, the primary disease of heart muscle is a leading cause of heart failure and death[193]. It can happen in spite of any age, condition and background. Severe cardiomyopathy causes irreversible damage to heart which further aggravates the disease. There are mainly three subtype of cardiomyopathy; dilated cardiomyopathy [97, 194, 195], hypertrophic cardiomyopathy [145, 146] and restrictive cardiomyopathy[151, 196] while the first two have been studied the most due to their high occurrence. Hypertrophic cardiomyopathy is the leading cause behind sudden cardiac arrest. In this type of cardiomyopathy, size of heart muscle cells cardiomyocytes enlarge in width as sarcomeres are added widthwise, enhancing increase in heart posterior wall and intraventricular septum thickness. Thickening of wall in hypertrophic cardiomyopathy causes abnormal filling of left ventricle and diastolic dysfunction which leads to increase in blood pressure, cardiac stiffening and sudden cardiac arrest [143, 145, 146, 197, 198]. In contrast dilated cardiomyopathy causes increase in the ventricle size. Dilation of heart generally initiates from left ventricle and spreads out to atria and right ventricle during severity. The stretch in heart muscles causes the enlargement of the left ventricle leading to dysfunction in pumping out blood throughout body. Severity of this cardiomyopathy is directly proportional to decrease in cardiac output and finally leads to death [97, 117]. The underlying mechanism behind dilated cardiomyopathy is not clearly understood till date. Both inheritance of a genetic signature or effect of environment like stress, alcohol, toxin, diabetes can lead to dilated cardiomyopathy

[108]. Current treatments are limited to beta-blocker, ACE inhibitor, ARB, and diuretics drug based prevention of further heart dilation and heart transplant in extreme conditions. Further mechanistic studies are necessary to get an insight on the molecular mechanism behind this disease to find a better therapeutic target in cure of heart failure.

In this current study we established the first KLF8 transgenic mouse model and further exploring these mice, we demonstrated a novel role of KLF8 in dilated cardiomyopathy. We also identified KLF8 overexpression in cardiomyocytes, initiates systolic dysfunction leading to severe dilated cardiomyopathy in transgenic mouse models. Ongoing studies are focused to discovering the KLF8 mediated signaling link causing this cardiomyopathy in molecular level.

Materials & Methods

KLF8 transgene plasmid construction

pTraffic plasmid was obtained from Dr. Lydia Matesic (University of South Carolina).dEGFP-F and dEGFP-R primers were used to delete the eGFP gene from this plasmid. TGL-F and R primer were used to amplify TGL coding sequence from SFG-nesTGL vector. THE TGL sequence was cloned into pTraffic vector after deleting EGFP to construct pTraffic-nesTGL vector. pTraffic-nesTGL vector was digested by AscI and ClaI as a host plasmid and pKH3-KLF8 plasmid was digested with SalI and ClaI to release HA tagged KLF8. Both the AscI site on the vector and Sal1 site were blunted by klenow enzyme treatment. Later on we also deleted the T sequence to get pTraffic-KLF8-nGL transgenic construct. The nes sequence exports GFP and luciferase to cytoplasm to negate any interference on KLF8 function. The luciferase expression provides us a non-invasive quantitative tool to visualize transgene expression in vivo. There is a secondary ribosome binding site, IRES after KLF8 to initiate protein translation under the same transcript. Overall, pTraffic-KLF8-Gl (KLF8 transgene) plasmid has been constructed to promote KLF8 overexpression. For tissue specific expression loxP flanked STOP codon has been incorporated upstream of KLF8. The plasmid consists of a CAG promoter, a combination of the cytomegalovirus (CMV) early enhancer element and chicken beta-actin promoter. This promoter is used for high gene expression in mammalian cell. The CAG promoter is followed by a loxP-dsRed2-STOP-

loxP cassette. This cassette is followed by human KLF8 cDNA tagged with 3 HA tags in the N terminal. After the KLF8, there is IRES (Secondary ribosome binding site) and a fused GFP and Luciferase cDNA. This circular plasmid was digested with SspI and SfiI restriction endonucleases to cleave the SV40-Amp region. The SV40-Amp region is not required for transgenic DNA microinjection. So the digestion gives rise to a 10.5 kbp linear fragment which will be used to generate transgenic mouse line.

Transfection, Fluorescence Microscopy and Luciferase activity

Transfection was performed in HEK293 and MEF cells as with lipofectamine 2000 reagents as mentioned before. After 48 hrs of transfection, cells were observed under fluorescent microscope in both RFP and GFP channels. Luciferase assay was performed as described before.

Construction of KLF8 transgenic mouse models

The linearized KLF8 transgene pTg-K8-GL(Fig. S1) was injected directly into the pronucleus of a newly fertilized mouse (B6 strain) egg to generate floxed KLF8 transgenic by University of Michigan, transgenic mouse facility. We optimized a taqman real time PCR method to detect 0.01 copy no of plasmid DNA in a pool of WT mouse genomic DNA. Plasmid DNA was mixed in different copy no ratio with WT mouse genomic DNA and qPCR was done with pTgK8 primer and R2 value of 0.98

demonstrated the efficacy of this protocol. After we identified the B65-Floxed-KLF8 Tg mice; we crossed 4 separate founders with homozygous FVB/N-TgN(EIIa-Cre)C5379Lmgd (Jackson lab stock 003314 ; This line carries a Cre transgene under the control of the adenovirus EIIa promoter that targets expression of Cre recombinase to the early mouse embryo) mice. The offsprings were of mixed FVB.B65 background including the Cre control and KLF8-gTg mice.

Genotyping

We collected genomic DNA (Promega genomic DNA extraction kit; A1120), RNA (Trizol) and Protein (SDS sample buffer) from mice tails using liquid nitrogen based homogenization. Genomic DNA was used for PCR with LoxP-F (5'-AGG ACT ACA CCA TCG TGG AGC-3'), pTg-K8-F (5'-TTC GGC TTC TGG CGT GTG ACC-3') and pTg-K8-R (5'-TGG CAT CCA GGA GTG TTG GAG-3') primers. These primers are designed to detect the KLF8 transgene. Lox-P forward primer and pTg-K8 reverse primer will give rise to an amplification of 601 bp without Cre recombination and there will be no amplification after Cre recombination as this forward primer is designed on the loxP flanked site, which will be excised by Cre. The pTg-K8 forward and reverse primer will give rise to an amplification of 1393 bp fragment without Cre and 400 bp after Cre recombination. Genotyping was done by genomic DNA PCR with pTg-K8 F, pTg-K8-R primer, RT PCR for RFP (RFP-RT-F 5'-GTC ATC ACC GAG TTC ATG CG-3'; RFP-RT-R 5'-ACC TTG GAG CCG TAC TGG AA), GFP (eGFP-RT-F 5'-TGA ACT TCA AGA

TCC GCC ACA-3'; eGFP-RT-R 5'-TTC TCG TTG GGG TCT TTG CT-3'), HA-K8 (HA-F 5'-tccagattacgctggatcc-3', HA-K8-R 5'-ttggcatccaggagtgttg-3') primers. Western blot was also done with tail lysates for HA-KLF8, GFP and RFP expression. For tissue specific KLF8 expressing mice, tail genomic DNA was used in PCR with pTg-K8-F/R primer and Cre-F/R primer to evaluate presence of transgene and Cre in tail DNA. Mice having both were characterized as positive transgenic mice, whereas the other three possibilities will produce floxed control, cre control and WT control mice.

Bio-Luminescence Imaging

The mice were anaesthetized using isoflurane and injected intraperitoneally with D-Luciferin in phosphate buffer (30 mg/kg mouse weight). D-Luciferin solution is light sensitive and kept in -20C for long term storage. It should be aliquoted to prevent freeze-thaw cycles. Mice hair was removed from the area of interest. We applied eye ointment to the mouse eyes to protect them from UV light during imaging. Luminescence and GFP channel fluorescence were imaged by IVIS50 to investigate efficacy of transgene expression in vivo.

Ultrasound Echocardiograph and hemodynamic analysis

The Visual Sonics VEVO 2100 echocardiography machine is turned on along with the oxygen generator to ensure the oxygen supply. The ultrasound gel warmer is turned on

before to pre-warm the gel. Mouse handling pad is warmed and maintained in 37c throughout the procedure. Mice are anesthetized with isoflurane (1-2%). The anesthetized mouse is secured to an animal handling platform in supine position with its nose covered by a cone with constant supply of 1-2% isoflurane to maintain anesthesia. Mouse paws are secured to the electrode pads with conductive gel (SIGNAGEL® Electrode Gel – Parkers Laboratories) to asses ECG. A rectal probe is also used to overall ensure 37c body temperature and respiration rate for physiological assessment during imaging. Depilatory (hair removing) crème is applied on the mouse chest and upper abdomen area for couple of minutes. All hair in those areas is removed by sterilized cotton buds and further cleaned to remove any trace of remaining hair. Pre-warmed ultrasound gel (Aquasonic clear ultrasound gel – parker Laboratories) is applied on the mouse chest and cotton buds are used to get rid of the bubbles. 40 MHz transducer (ultrasound probe) of the Visual Sonics VEVO 2100 echocardiography machine is moved gently on the mouse chest with gentle pressure to find the long axis view of LV. VEVO 2100 machine is used to record both B mode and M mode images of the left ventricle in long axis region and then the probe is rotated to obtain the parasternal short axis view of LV. The M mode images are used for further measurements. After recording all the images, the mouse is cleaned with a sterilized wipe and returned to its cage. The cage is kept on a heating pad to help the mouse regain consciousness. The mouse is monitored following days to ensure no side effects of this procedure. M mode images were analyzed by VEVO 2.1 software.

Organ collection and preparation

Different organs were collected after necropsy of mice. Collected organs were stored in formalin solution in 4C after PBS wash. Different organs were paraffin processed overnight by paraffin in Leica processor. After embedding into tissue blocks, these organs were sectioned @ 7um size of tissue which was utilized further for different staining.

H&E and Masson's Trichrome Staining

Paraffin processed tissue slides were baked @ 65° C for 20 minutes to melt paraffin. Dehydration procedure was done by treatment with Xylene twice for 10 minutes, 100% EtOH twice for 5 minutes each, 95% ethanol for 5 mins followed by 15 dips in 70% ethanol and 50% ethanol. After air drying, the slides were stained with filtered Mayers Hematoxylin for 3 mins followed by a treatment with 0.2% NH4OH for 30 sec-1min depends on the required blue color intensity. The slides were rinsed in cool running ddH2O for 5 minutes and stained with Eosin (0.5% in 95%EtOH) 12 times. These slides are quickly rinsed and rehydrated by treatment with 50% EtOH 10 times, 70% EtOH 10 times, 95% EtOH for 30 seconds and equilibrate in 100% EtOH for 1 minute. Permount

solution was used to mount the slides after final xylene wash. Masson's trichrome staining was done with sigma HT-15 kit and following the manufacturer protocol.

qPCR and Western Blot

Trizol was used to isolate both RNA and protein from different mouse organs after liquid nitrogen based homogenization. Thermo fisher maxima 1st strand synthesis kit was used to reverse transcribes mRNA and qPCR was performed with Sybr green in ABI7900 HT equipment. Both qPCR and western blot was done according to our previously published protocols.

Immunohistostaining

Paraffin embedded tissue were used for immunohistostaining. The detailed procedure is described previously[199]. HA antibody was used 1:200 ratio.

Cardiovascular disease mRNA and miRNA PCR array

KLF8-hTg mice hearts were collected along with floxed control mice. Similar position of the left ventricle was extracted and stored in -80C to protect RNA integrity. Liquid nitrogen was utilized to homogenize the heart tissues, and mRNA was isolated by trizol based method whereas micro RNAs were isolated by miReasy kit. Both mRNA and

miRNA were reverse transcribed using their respective reverse transcriptase kit from qiagen to negate genomic DNA contamination. A master mix was prepared with SyBr green, cDNA and water and 20 ul of this was added into each well of one array plate (SA biosciences PAMM-174Z and MIMM-113Z). The result was analyzed by SA bioscience software.

Isolation of primary cardiomyocytes

5 days old mice were sacrificed after confirming transgene expression by BLI. Heart was quickly extracted and cleaned with HBSS buffer. Primary cardiomyocyte was isolated using Pierce primary cardiomyocyte isolation kit (Thermofischer 88281). Spontaneous beating of cardiomyocytes was observed after 7 days of culture.

Results

Construction of Global KLF8 Transgenic Mice

To investigate KLF8 role in vivo, we started generating KLF8 transgenic mice. Although our primary aim was to identify mammary tumor formation mediated by KLF8, we first made global KLF8 transgenic mice to assess the role of KLF8 in any other potential diseases. In order to generate the transgenic mice, we first constructed pTraffic-KLF8-GL plasmid with HA tagged KLF8 transgene under a CAG promoter [78, 79], a combination of the cytomegalovirus (CMV) early enhancer element and chicken beta-actin promoter. The plasmid mapping includes a CAG promoter followed by a loxP-dsRed2-STOP-loxP cassette upstream of N terminal 3 HA tagged human KLF8, IRES (Secondary ribosome binding site) and a fused GFP-Luciferase gene (Fig 10A). Cre-loxp mediated recombination will promote HA tagged KLF8 expression and a RFP to GFP-Luciferase switch by excising the loxp-flanked RFP and STOP codon. To validate the efficacy of this transgene in vitro, the linearized plasmid was transfected into 293FT cells with and without Cre recombinase expressing plasmid co-transfection. Expectedly, Cre mediated recombination showed an evident RFP to GFP switch by fluorescence microscopy (Fig 10B); induction in HA-KLF8, GFP expression in western blot (Fig 10C) and increased luminescence activity (Fig 10D) in 293 and MEF (Data not shown) cells. After confirming the plasmid efficacy, linearized pTg-KLF8-GL plasmid was injected directly into the pronucleus of a newly fertilized mouse (B6 strain) egg by University of Michigan, transgenic mouse facility. We designed a standardized genotyping protocol to

genotype these founder floxed mice. To increase the efficacy of this test, transgenic plamid was mixed with wild type mouse genomic DNA in different copy numbers starting from as low as 0.1 copy. Two different primers were used to investigate if low copy no of transgene when masked in genomic DNA, can be detected. Genomic DNA PCR could identify till 1 copy no of transgene (Fig. 11A-C). To further make this genotyping test more productive, we decided to use taqman qPCR assay as it uses a third specific probe alongside two primers. We used this taqman qPCR to perform the similar experiment and excitingly this method was observed to be able to detect till 0.01 copy no of transgene (Fig 11E). We plotted all this different copy no of transgene CT values in a standard curve which came out to be very significant with a R^2 value of 0.97 (Fig 11F). Upon receiving the offspring mice from University of Michigan transgenic facility, we genotyped these mice by our standardized taqman real time PCR to identify the positive mice which harbored the loxp-flanked transgene (Fig 12A-B). We also used genomic DNA PCR from tail snip DNA to detect the presence of the transgene (Fig 12 C), RFP expression in tail snips by fluorescence microscopy (Fig 12D) and western blot to detect RFP expression (Data not shown). The founder mice with loxp-flanked transgene were named as B65-Floxed-KLF8-Tg. We backcrossed two of the founder lines (one with high transgene copy no and one with medium transgene copy no) with FVB WT mice to obtain pure FVB strain floxed-KLF8 mice which would be more relevant for breast cancer studies. We decided to over express KLF8 globally primarily to investigate role of KLF8 in promoting oncogenesis in various tissues as KLF8 have been implicated in a large array of cancer types. To induce KLF8 transgene expression globally, we crossed 4 separate founder B65-Floxed-KLF8-Tg mice with homozygous

FVB/N-TgN(EIIa-Cre)C5379Lmgd (Jackson lab stock 003314 ; This line carries a Cre transgene under the control of the adenovirus EIIa promoter that targets expression of Cre recombinase to the early mouse embryo) mice[85] (Fig 14A). The offsprings were of mixed FVB.B65 background including the Cre control and transgenic mice with global KLF8 expression (FVB.B65-KLF8-gTg). The KLF8-gTg mice were genotyped by Bioluminescence Imaging, genomic DNA PCR (Fig 15) for the transgene, real time PCR for RFP, GFP, HA-KLF8 expression and western blot for HA-KLF8 expression. KLF8-gTg mice showed high luminescence compared to Cre control in whole body BLI (Fig. 14B). Organ specific BLI (Fig. 14C) demonstrated distribution of KLF8 transgene expression globally in all tissues including heart, lung, liver, muscle, brain and kidney. Real time PCR with universal KLF8 primer showed increase in KLF8 expression in different tissues of KLF8-gTg mice compared to littermate Cre controls (Fig 14D). Further overexpression of KLF8 and GFP in KLF8-gTg mice heart was confirmed by western blot (Fig 14E). Overall these result demonstrated successful construction of global KLF8 transgenic mice (KLF8-gTg) which was used further in this study to investigate any potential unknown function of KLF8 in vivo.

KLF8 global transgenic mice (KLF8-gTg) showed increased heart size and decreased survival rate

In order to identify any critical phenotypical differences, KLF8-gTg mice were observed against the littermate Cre control mice. KLF8-gTg mice and its littermate controls were in mixed background (B65-Floxed-KLF8 X FVB-EIIA-Cre). We observed that KLF8-gTg mice started dying from a very early age (5 months) with hair loss and lethargic

condition. Overall survival analysis of these mice by Kaplan-Meier plot revealed that KLF8-gTg mice had significantly lower survival (higher mortality) rate compared to the littermate controls with a Z score of 7.32 (Fig 16A). Interestingly, all of the transgenic mice died by 16-20 months of age much earlier than the littermate control mice. This higher mortality rate was observed in both transgenic male and female mice whereas in male mice it was slightly higher than the female mice (Fig 16B). To unveil the cause of this sudden death of KLF8-gTg mice, we performed necropsy and strikingly found these mice having enlarged hearts compared to their littermate controls (Fig 16C-D). Most of the transgenic mice with enlarged heart were also observed to have increased lung size (Fig 16C-E). Almost all KLF8-gTg mice died early showed this striking cardiac phenotype (Fig 17). As the heart phenotype seemed to be the likely cause of the sudden death in transgenic mice, we also observed decrease in transgenic mice body weight compared to littermate controls (Fig 16F) which reasserts the lean phenotype observed of these mice in BLI (Fig 18). We also observed other tissues in KLF8-gTg mice and compared whole mount organ and tissue morphology with its negative littermate controls. We didn't find any significant phenotype in KLF8-gTg mice brain, lung, liver, spleen, muscle etc (Fig 19 A,C-G). Further necropsy demonstrated that KLF8-gTg mice had significantly lower fat mass in gonadal depots attached to the epididymis and testes in males and the uterus and ovaries in females compared to the negative controls (Fig 19B,I and Fig 20A-C), which uncovered the mystery behind the decrease in transgenic mouse body weight. H&E staining of the abdominal white adipose tissue showed that the KLF8-gTg mice had significantly smaller adipocyte cells (Fig 20D) suggesting these mice might develop lipoatrophy. KLF8-gTg mice didn't show

any significant difference in food intake compared to the littermate controls (Fig 20E), which excluded any effect of food consumption difference on the body weight change phenotype. Along with white adipose tissue difference, we also observed less brown adipose tissue in the KLF8-gTg mice (Fig 21A-B). As the cardiac phenotype was most likely the cause of early death in transgenic mice, we confirmed KLF8 overexpression in transgenic mice heart tissue (Fig 16G). Overall, we discovered two novel phenotypes in the global KLF8 transgenic mice causing early death. Further mechanistic studies are required to establish if the decrease in fat mass phenotype is a consequence of the cardiac phenotype or an unrelated novel phenotype observed in these KLF8-gTg mice.

Global expression of KLF8 induces dilated cardiomyopathy in transgenic mice

As previous results suggested the cardiac phenotype to be possible cause of early death in global KLF8 transgenic mice, we stained the mice hearts with masson's trichrome staining to investigate cardiac fibrosis which is a positive indicator of heart failure. KLF8-gTg mice was found to have significantly increased cardiac fibrosis, predominantly in the ventricular walls (Fig 22A-B) compared to the Cre littermate controls which further validated heart failure as the reason behind the higher mortality rate in these transgenic mice. Fig 23 demonstrates representative images of increased myocardial fibrosis in KLF8-gTg mice. Moreover significant increased heart failure associated marker genes; b-MHC, ANP and BNP expression in KLF8-gTg mice hearts (Fig 22C-E) suggested global overexpression of KLF8 induces cardiomyopathy in

transgenic mice. To characterize the cardiomyopathy observed in these transgenic mice, hemodynamic analysis was performed by ultrasound echocardiography starting at 10 months of age. B mode images from ultrasound echocardiograph clearly showed increase of left ventricular cavity size in KLF8-gTg mice (Data not shown). Hemodynamic analysis from the M mode results (Table 2) revealed that KLF8 global transgenic mice had significant increase in left ventricle inner diameter both at systole and diastole (Fig 22F-H). In addition, the KLF8-gTg mice also showed significant decrease in left ventricular function with sharp decline in ejection fraction and fractional shortening (Fig 22I,J). We didn't observe any significant change in KLF8-gTg mice intraventricular septum and left ventricular posterior wall diameter which excludes the possibility of hypertrophic cardiomyopathy. Overall the ultrasound echocardiograph results revealed that KLF8-gTg mice have significant dilation in left ventricle cavity and decrease in left ventricular function which is a characteristic of dilated cardiomyopathy. The dilated cardiomyopathy disease progressed aggressively in KLF8-gTg mice as we observed significant increase in LV diameter at systole and diastole and severe deterioration in ejection fraction and fractional shortening after 3 months from the first ultrasound echocardiograph. Negative control littermate didn't show any significant difference in cardiac parameters in this duration (Fig 24-25). We also did Tunel assay to assess apoptotic cardiomyocyte to investigate the cardiac injury by this disease in KLF8-gTg mice. Results from this experiment clearly showed increased cardiomyocyte apoptosis in KLF8-gTg mice hearts compared to negative control mice (Fig 26). We sub grouped the KLF8-gTg mice into medium and high KLF8 expressing mice based on their transgene expression (Data not shown) to investigate dose dependent effect on

KLF8 on dilated cardiomyopathy in these transgenic mice. Strikingly, the KLF8-gTg mice with high transgene expression showed more severe left ventricular dilation and cardiac dysfunction compared to the medium KLF8 expressing mice group (Fig 27A-D, Table 3). This strong positive correlation between KLF8 expression and cardiac dysfunction strengthen our hypothesis that KLF8 promotes dilated cardiomyopathy causing early death in transgenic mice in both male and female.

KLF8 induces systolic dysfunction which leads to dilated cardiomyopathy in KLF8 global transgenic mice

Dilated cardiomyopathy is associated with both systolic and diastolic dysfunction. Systolic dysfunction is defined as decrease in myocardial contractility whereas diastolic dysfunction is characterized by abnormal filling of left ventricle. The previous echocardiograph of the KLF8-gTg mice started from 9 months of age showing increase in left ventricular inner diameter both at systole and diastole limiting our knowledge about the underlying cause of this KLF8 induced dilated cardiomyopathy. To investigate the progression of the disease, we started time point hemodynamic analysis with KLF8-gTg mice from one month of age. As our B65-Floxed-KLF8 mice were being backcrossed with FVB WT mice to construct pure strain of FVB.B65-Floxed-KLF8-Tg mice, the second group of KLF8-gTg mice constructed was of FVB background. Interestingly, ultrasound echocardiograph showed increase in left ventricular diameter only at systole and associated decrease in ejection fraction, fractional shortening in KLF8-gTg mice from 1 month of age whereas, no change was observed in left

ventricular diastolic diameter at that early age (Fig 28A-E). Strikingly, increase in diastolic diameter and dilation of left ventricle in transgenic mice were observed from 3 months of age with further deterioration in left ventricular dysfunction causing early death in these mice. Overall this result revealed that KLF8 promotes systolic dysfunction characterized by increase in left ventricular systolic diameter and decline in fractional shortening first at a very early age (from 1 month) which eventually leads to severe dilation of heart identifying systolic dysfunction as the mediator of this KLF8 induced dilated cardiomyopathy. Interestingly, FVB background mice started dying earlier compared to FVB.B65 mixed background mice but independent of strain background, the KLF8-gTg mice died much earlier compared to the negative Cre control mice (Fig. 29), which reasserts this novel cardiac phenotype induced by KLF8. Both these strain of mice demonstrated similar cardiac and fat phenotypes (Fig. 30A-B). These results were further used to interpret the increase in lung size phenotype observed in KLF8-gTg mice (Fig. 16C) as probable pulmonary edema which is a known associated phenotype with systolic dysfunction. Based on these findings, we hypothesized that KLF8 might be critical for myocardial contractile function as overexpression of KLF8 causes systolic dysfunction (contractile dysfunction) culminating into fatal dilated cardiomyopathy.

Construction of cardiomyocyte specific KLF8 transgenic mice

Previously in this study we have discovered KLF8 overexpression globally stimulates systolic dysfunction leading to severe dilated cardiomyopathy in transgenic mice. As KLF8 was overexpressed globally in the KLF8-gTg mice, it is difficult to interpret the functional link of KLF8 to this disease in molecular basis. To address the unknown molecular mechanism behind KLF8 mediated cardiomyopathy, we started constructing cardiomyocyte specific KLF8 transgenic mice as cardiomyocyte is the foremost cells in making up cardiac muscle. To construct these mice, FVB-B6-floxed-KLF8 (7th generation) mice were crossed with cardiomyocyte specific B6-FVB-Tg-Myh6-Cre [5]. The offsprings were of FVB.B65 mixed strain and consisted four different groups including KLF8 cardiomyocyte specific transgenic mice named as KLF8-hTg, floxed control, Cre control and WT control mice (Fig. 31A). Genomic DNA was isolated from mice tails and we did PCR with pTg-K8-F and pTg-K8-R primer to investigate the transgene incorporation into genome and with Cre-F and Cre-R to investigate presence of Cre transgene. Heart specific transgene expression in the KLF8-hTg mice was validated by Bio luminescence Imaging (Fig 31B). Further qPCR with universal KLF8 primer confirmed in transgenic mice, KLF8 was specifically overexpressed in heart tissue whereas in other tissue like fat; KLF8 overexpression was not observed (Fig. 31C). Phenotypic characteristics of these KLF8-hTg mice were studied alongside different negative littermate control mice. The first noticeable difference identified was higher mortality rate of cardiomyocyte specific KLF8 transgenic mice (Fig. 31D). As we didn't see any significant difference in mortality rate of the floxed, cre and WT control

mice; those were clubbed together and compared against the mortality rate of positive KLF8-hTg mice. Overall, successful construction of cardiomyocyte specific KLF8 transgenic mice showed similar early postnatal death as observed in global KLF8 transgenic mice suggesting the phenotype observed in KLF8-gTg mice might be caused by KLF8 overexpression in cardiomyocytes.

KLF8-hTg mice phenocopy KLF8-gTg mice with systolic dysfunctional progression to dilated cardiomyopathy:

As we already observed the similar trend in mortality rate in cardiomyocyte specific KLF8 transgenic mice, we started investigating if the cause behind it corroborates with the same of global transgenic mice. Necropsy demonstrated KLF8-hTg mice had larger heart size compared to all the control littermate (Fig. 32A,C and Fig 33B). We used the floxed control mice heart image as the representative negative control in this figure. Furthermore KLF8-hTg mice hearts had significantly elevated level of myocardial fibrosis (Fig. 32A,B and Fig 34) reasserting myocardial infarction in these mice. It was finally validated by the increase of heart failure marker genes ANP and BNP in KLF8-hTg mice hearts. Hemodynamic analysis interestingly unveils that the cardiomyocyte specific KLF8 transgenic mice also have severe dilation of left ventricle (Fig. 32E) with increased systolic and diastolic LV inner diameter and decreased ejection fraction, fractional shortening; cumulatively pointing to dilated cardiomyopathy in these mice. Time point echocardiograph results revealed that KLF8 overexpression in cardiomyocyte promotes systolic dysfunction at a very early age as we observed

significant increase only in systolic LV diameter in transgenic mice from 1 month of age. Eventually the KLF8-hTg mice LV became dilated as they aged with further severe systolic dysfunction (Table 4 and Fig. 32F-I). To test if this novel KLF8 induced phenotype is specific to its expression in cardiomyocyte, we constructed adipocyte specific KLF8 transgenic mice by crossing FVB-B6-floxed-KLF8 (8th generation) with C57BL/6J;FVB/NJ-Adipoq-Cre mice (Fig. 35A). Genomic DNA PCR and BLI validated adipose specific KLF8 overexpression in the KLF8-aTg mice (Fig. 35B). However KLF8-aTg mice didn't show any change in mortality compared to different control groups (Data not shown). Further hemodynamic analyses with these transgenic mice also didn't show any decline in left ventricular function (Fig. 35C). Additionally, KLF8-hTg mice had significantly lower ejection faction compared to KLF8-aTg mice at the same 2 months of age (Fig 35D) which strengthen our hypothesis that KLF8 overexpression specifically in cardiomyocyte induces this novel cardiac phenotype. As we found the fat phenotype in KLF8-gTg mice, we wanted to investigate if KLF8-hTg mice also have detrimental fat accumulation effect. Interestingly, cardiomyocyte specific overexpression of KLF8 didn't demonstrate the decrease in mouse body weight, fat mass and adipocyte cell size, taking food consumption into account (Fig 36A-D) which suggests that the fat phenotype observed in global transgenic mice was probably not a direct consequence of the cardiomyopathy. Some of the KLF8-hTg mice had lower body weight compared to their respective littermate controls but overall it was not significant. Further studies with KLF8-aTg mice will give us insight about the underlying mechanism of KLF8 induced lipoatrophy.

Cardiovascular disease mRNA and miRNA PCR array to identify KLF8 regulated target genes and miRNAs in context of Cardiomyopathy

As KLF8 is a known transcription factor, we hypothesized that KLF8 mediated regulation of some critical genes lead to systolic dysfunction and dilated cardiomyopathy. In view of increasing importance of micro RNAs in cardiomyopathy and as KLF8 also has been shown to transcriptionally activate miR-146a and transcriptionally repress miR-14, we decided to identify KLF8 regulated miRNAs in parallel to mRNAs in dilated cardiomyopathy. Both mRNAs and miRNAs were isolated from 3 pairs of KLF8-hTg mice heart left ventricles along with floxed littermate controls. The most critical consideration was to select the mouse samples in an optimized age. In order to negate out the dilated cardiomyopathy consequence gene signature, we decided to use the mice with already decreased cardiac function (EF) but without evident dilation of heart because change in heart size can significantly change the gene expression signature. Cardiovascular disease mRNA and miRNA PCR array (Fig. 37) was used to identify KLF8 regulated mRNA and miRNA targets respectively in KLF8-hTg hearts from an array of 84 critical genes for various cardiomyocyte function. The most significant regulated genes and micro RNAs with a P value less than 0.01 were further validated by qPCR with specific primers. As KLF8 is a dual transcription factor, we did find both upregulation and downregulation of some critical genes. The most upregulated target of KLF8 includes Nppa, Col1a1, Col3a1, S100a8 and Stat1 whereas downregulated genes include ATP2a2 and Anxa4 (Fig 38A-C). These gene target regulation will be evaluated in early stage to onset of dilated cardiomyopathy in KLF8-

hTg mice, which will identify the most probable KLF8 signaling axis as a cause of this disease. We also did miRNA PCR array to identify possible micro RNA targets of KLF8 in the onset of cardiomyopathy. miR-122 was the most downregulated miRNA whereas miR-208b was the most upregulated miRNA found in these transgenic mice heart (Fig 39A-C).

Potential KLF8 mediated upregulation of STAT1 in KLF8-hTg primary cardiomyocytes

To asses KLF8 mediated regulation of downstream targets; we isolated primary cardiomyocytes from 5 days old KLF8-hTg mice and their floxed littermate controls (Fig 40). Our primary observation regarding these cells showed that KLF8-hTg mice cardiomyocytes had slower contraction compared to floxed control (data not shown). Further electrophysiological experiments will unveil this mystery from these cells. In order to investigate KLF8 mediated target gene regulation in these cells, we first explored STAT1 expression. Interestingly STAT1 was upregulated both at mRNA and protein level in these cells along with KLF8 expression (Fig. 41A-B). We also found increase in heart failure marker Nppa or ANP expression in KLF8-hTg mice cardiomyocytes indicating possible onset of systolic dysfunction as earlier than 1 month of age. To confirm KLF8 mediated STAT1 upregulation, we transiently transfected KLF8 in 293FT cells which showed significant upregulation of STAT1 mRNA expression (Fig. 41C). Further luciferase-promoter assay along with CHIP and BOP assay will be done to investigate direct KLF8 mediated upregulation of STAT1 in the onset of this disease.

Discussion

Comprehensively, this novel study with KLF8 transgenic mouse model revealed a novel cardiac function of KLF8. KLF8 global transgenic mice had much higher mortal rate compared to negative mice. The cause of death was evaluated as heart failure and the transgenic mice had severe dilated hearts. Further cardiac hemodynamic analysis characterized this disease as dilated cardiomyopathy with severe reduction in cardiac output leading to death in transgenic mice. Time point hemodynamic analysis revealed that KLF8 promotes systolic dysfunction as early as 4 weeks of age and that leads to severe fatal dilated cardiomyopathy. As the first part of our study was performed in a KLF8 transgenic mouse model where KLF8 is overexpressed in all tissues, we decided to express it tissue specifically to explore more in depth role of KLF8 in cardiomyopathy. Cardiomyocyte specific KLF8 overexpression led to the similar cardiac phenotype as observed in global transgenic mice, unveiling KLF8 mediated gene regulation specifically in cardiomyocytes induces this disease. In contrast we didn't observe the cardiac phenotype in adipocyte specific mice, thereby strengthening our hypothesis about a novel KLF8 mediated signaling axis as potential cause of systolic dysfunction and dilated cardiomyopathy.

Role of KLF8 in cardiac tissue has not been elucidated before in our knowledge and this is the first report about a critical novel role of this cancer promoting gene. Kruppel like family members have been implied before in cardiomyopathy, specifically KLF4 [200], KLF11 and KLF15 [201, 202]. One study with KLF4 showed that KLF8

expression is elevated in cardiomyocytes of angiotensin induced mouse cardiomyopathy model which stands to reason after this study where we found KLF8 overexpression causes cardiomyopathy[203]. We also compared KLF8 mRNA expression from NCBI GEO profile database, which clearly demonstrated higher expression of KLF8 in patient samples with dilated cardiomyopathy. Both global and cardiomyocyte specific mice showed the similar cardiac phenotype, which led us to believe KLF8 expression in cardiomyocytes as the cause of cardiomyopathy. We confirmed this notion when adipocyte specific mice didn't show any cardiac phenotype.

In depth hemodynamic analysis of cardiac function from an early age of mice demonstrated that KLF8 expression in cardiomyocytes leads to systolic dysfunction as earliest which later on culminates into severe dilated cardiomyopathy. Systolic dysfunction is abnormal pumping function in heart which initiates from contractile dysfunction of cardiomyocytes [204, 205]. It has been well established that, reduction in cardiomyocytes contractile potential deteriorates cardiac function. As heart cannot pump enough blood throughout body which is characterized by decrease in ejection fraction and fractional shortening, it goes through remodeling and tends to dilate to contain more blood in the left ventricles which predominantly forms dilated cardiomyopathy. Abrupt changes in gene signature are critical in cardiomyocyte contraction. Innumerable studies have shown that mutation associated with the cardiomyocyte sarcomere genes have direct relevance to pathogenesis of this disease [121, 122, 206-208]. Cardiomyocyte contraction is a calcium dependent method, where the myosin and actin bands slide against each other to initiate contraction using a

mechanism unique to cardiac muscle called calcium-induced calcium release. After receiving the stimuli, calcium influx in cardiomyocytes induces more calcium from sarcoplasmic reticulum to cytoplasm. In a relaxed state, cardiac troponin binds to the actin binding site of myosin and calcium binding to this protein removes it from that site leading actin-myosin binding and initiation of contraction. Different studies with transgenic, knockout models of these sarcomere genes proved them to be critical for cardiac contraction and cardiomyopathy. In our mRNA PCR array we identified ATP2a2, sarco/endoplasmic reticulum Ca2+-ATPase pump as a negatively regulated target of KLF8. This calcium pump is critical in storing calcium ions in sarcoplasmic reticulum and knock out model of this gene has been demonstrated to induce cardiomyopathy [209, 210]. In our model, KLF8 might transcriptionally repress ATP2a2 and therefore promotes contractile dysfunction by depleting the calcium ions from cardiomyocytes. We are currently identifying potential KLF8 regulated targets and cumulatively it will help us to elucidate an overall KLF8 mediated gene regulation in cardiomyopathy.

One of the most significantly upregulated target found from mRNA array was STAT1. Isolated primary cardiomyocytes from KLF8-hTg mice showed increase in STAT1 expression at both mRNA and protein level. Further experiments are needed to explore KLF8 mediated upregulation of STAT1. STAT1 has been elucidated in ischemia induced cardiac injury. STAT1 has been found to be upregulated in ischemic cardiomyopathy [211-213]. Later on it was found that STAT1 activate both intrinsic and extrinsic cardiomyocyte apoptotic pathways by activating Caspase-1 and FADD respectively [214, 215]. It was found that STAT1 knockout can protect mice from

ischemic cardiac injury [211, 216]. Correlated with these findings, it has been also found Caspase-1 transgenic mice develop heart failure [217, 218]. Overall cardiomyocyte loss due to apoptosis has huge impact in cardiomyopathy [219-221]. We observed increased apoptosis in KLF8-gTg mice heart (Fig 26) which helps us to form a hypothesis that KLF8 mediated upregulation of STAT1 promotes to cardiomyocyte apoptosis further leading to systolic dysfunction and dilated cardiomyopathy. Overall our proposed schematic model (Fig 42) shows that KLF8 over expression in cardiomyocyte upregulates and downregulates several critical mRNA and miRNA targets. Two of the most potentially important target genes are STAT1 and ATP2a2. KLF8 mediated upregulation of STAT1 can lead to cardiomyocyte apoptosis, further promoting systolic dysfunction and dilated cardiomyopathy. KLF8 mediated downregulation of ATP2a2 can potentially lead to decrease in cardiomyocyte contractility and systolic dysfunction

We also observed a novel fat phenotype in the global KLF8 transgenic mice. KLF8-gTg mice had significantly less body weight and abdominal fat accumulation, predominantly close to the reproductive organs. H&E staining revealed those KLF8-gTg mice had significantly smaller adipocyte cell size. This novel fat phenotype was not evident in cardiomyocyte specific KLF8 transgenic mice which led us to believe that cardiac expression of KLF8 may not be responsible for this fat phenotype and it can be induced by an independent KLF8 mediated regulation in a different tissue. We observed the reverse phenotype in KLF8 global KO mice where fat mass was significantly increased. In view of these result, we decided to construct adipocyte specific KLF8 transgenic mice to investigate if the fat phenotype observed is a consequence of KLF8

expression in adipocytes. Both global and adipocyte specific KLF8 transgenic mice demonstrated significant decrease in glucose tolerance which might be a key to this unknown phenotype. Currently both these adipocyte specific transgenic and knock out mice being studied to discover any novel function of KLF8 in adipose tissue.

Overall this study establishes the first KLF8 transgenic mouse model and discovers a novel role of KLF8 in cardiomyopathy. In future, the signaling link of KLF8 to onset of this cardiomyopathy will be explored. We currently are validating some KLF8 regulated critical mRNA and miRNA targets which will be studied for functional significance in context of KLF8 in this transgenic mouse tissue and primary cardiomyocytes obtained from these mice. KLF8 KO mice study in parallel will present a great insight into the importance of KLF8 in cardiac tissue. Taken together this findings not only discovers a novel unknown role of KLF8, it provides an outstanding tool to study role of KLF8 in different diseases. Most available transgenic mouse models for cardiomyopathy are induced by angiotensin and TAC surgery whereas our KLF8 cardiomyocyte specific transgenic mouse model presents a spontaneous dilated cardiomyopathy disease model which can be of immense potential for drug testing and therapeutic research in successful advancement of this cardiovascular field.

Figures

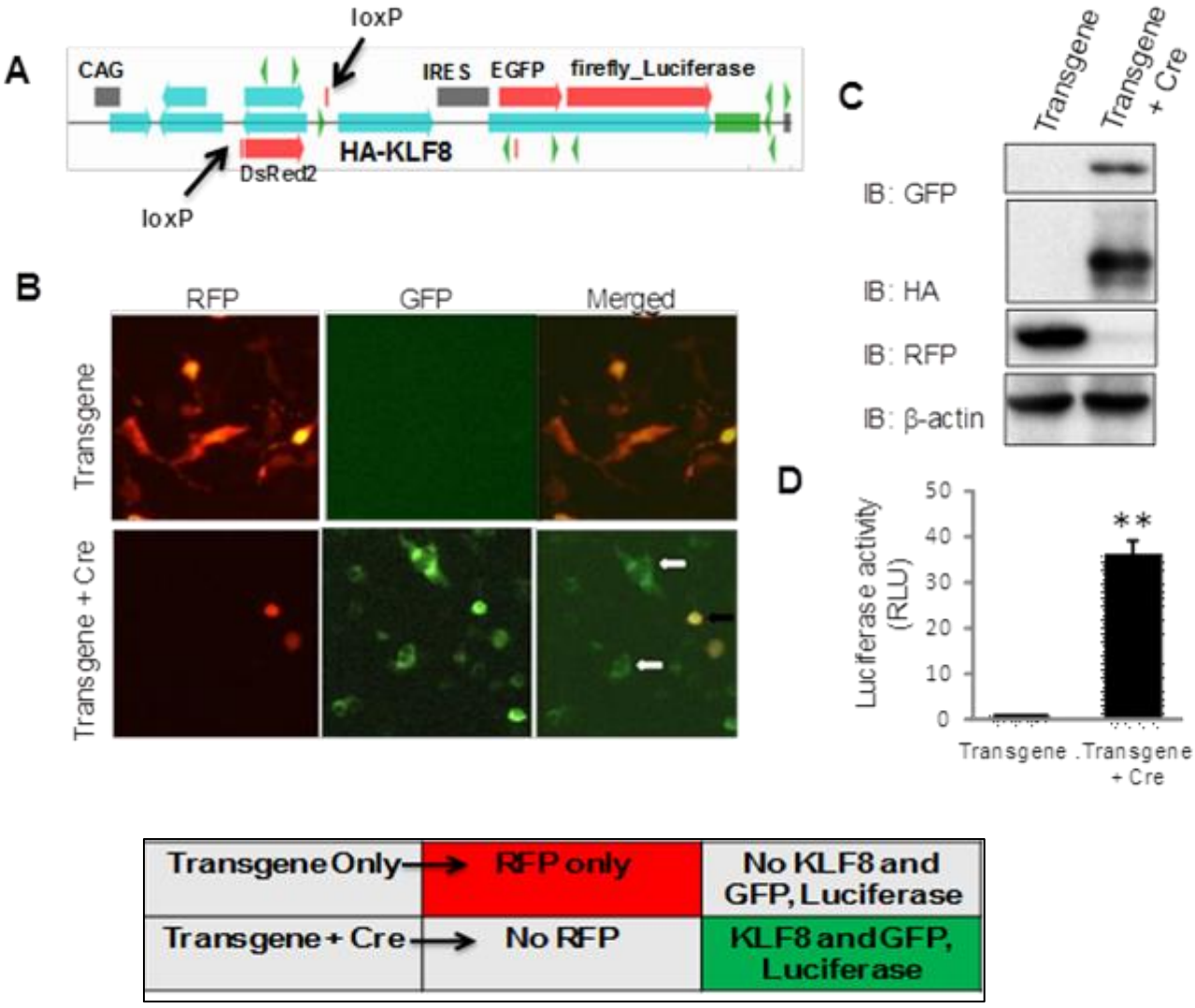

Figure 10. Validating KLF8 Transgene expression in vitro

(A) pTraffic-KLF8-Gl (KLF8 transgene) plasmid has been constructed to promote KLF8 overexpression. (B-D)The liberated linear transgene after digestion with Ssp1, Sfi1 were transfected in 293 FT (human kidney cells) with lipofectamine 2000 (invitrogen). Co-transfection was also done with Cre (HA-Cre). The Cre vector used is pKH3-Cre which expresses HA tagged Cre (42KD). Fluorescent microscopy (B) showed RFP to GFP switch after Cre recombination. Western blot (C) with anti GFP (sc-9996; 1:1000), anti-HA (SC-7392; 1:3000), anti-RFP (ab34771; 1:4000) and anti-beta-actin antibody (**; 1:4000) confirmed Cre recombination induce HA-KLF8 expression and RFP to GFP switch. Luciferase assay result (D) also validated this result.

*, P<0.05; **, P<0.01; ***, P<0.001.

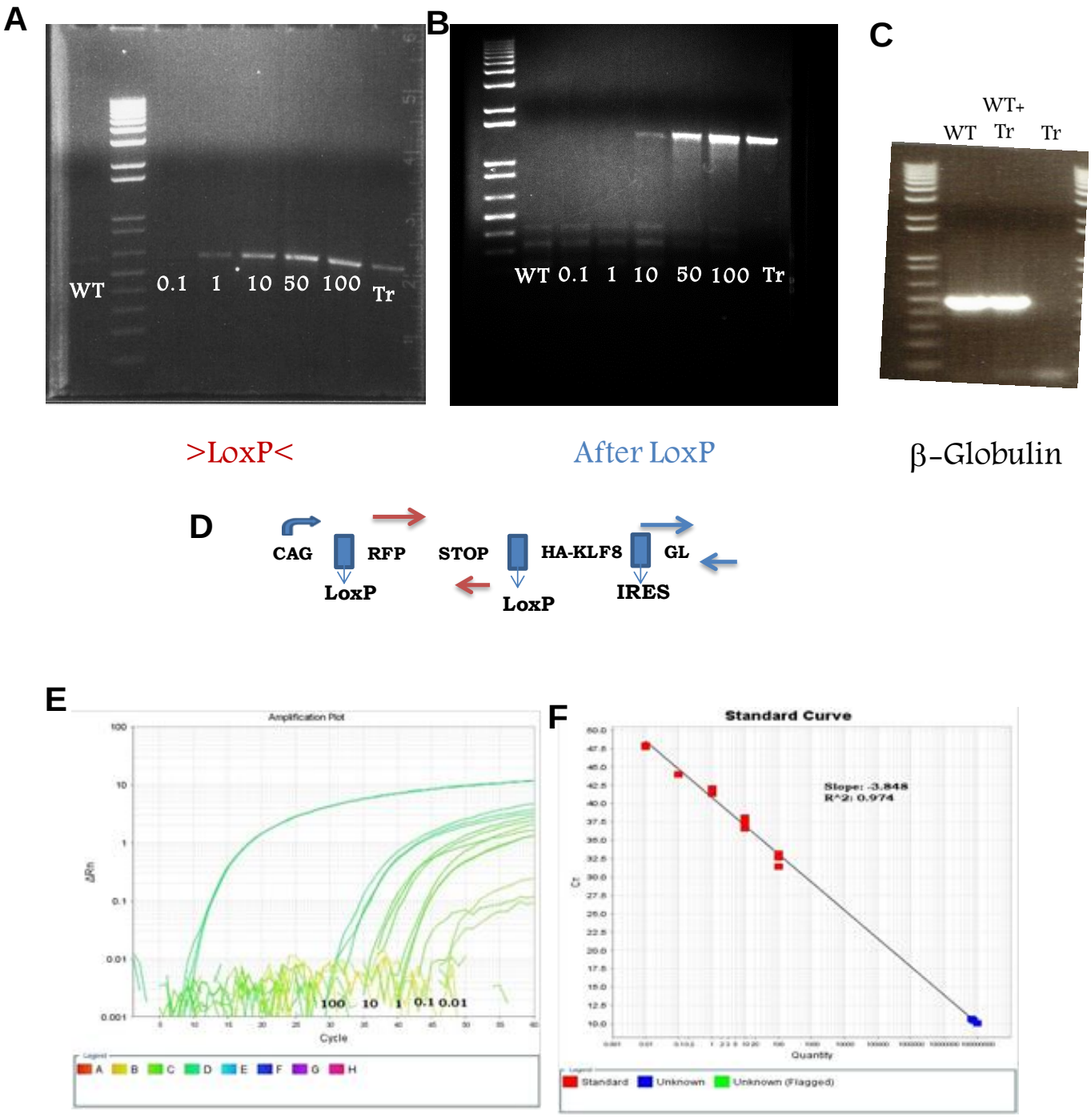

Figure 11. Validation of Genotyping efficiency to detect low copy no of transgene

After validating in vitro, the transgene was sent to the University of Michigan transgenic facility to construct the transgenic mice. To genotype the positive floxed-KLF8 mice, we had to design a genotyping assay. (A-C) Genomic DNA PCR with two different primers. WT is wildtype genomic DNA. Corresponding copy no of transgenic plasmids were

mixed with WT genomic DNA in order to test the efficacy of this test. B-globulin confirmed same amount of WT DNA. (D) Schematics of two sets of genotyping primers. LoxP primers (red arrow) will detect amplification inside the loxP flanked sequence. After loxP primer (blue arrow) will detect the transgene after the loxP sites. (E) These primers and corresponding probes were used for taqman qPCR to standardize this assay. (F) Standard curve based on different copy no of transgene detection gave a R^2 value of 0.97 which is very significant. We further used this standardized taqman qPCR assay to detect the founder B65-Floxed-KLF8Tg mice.

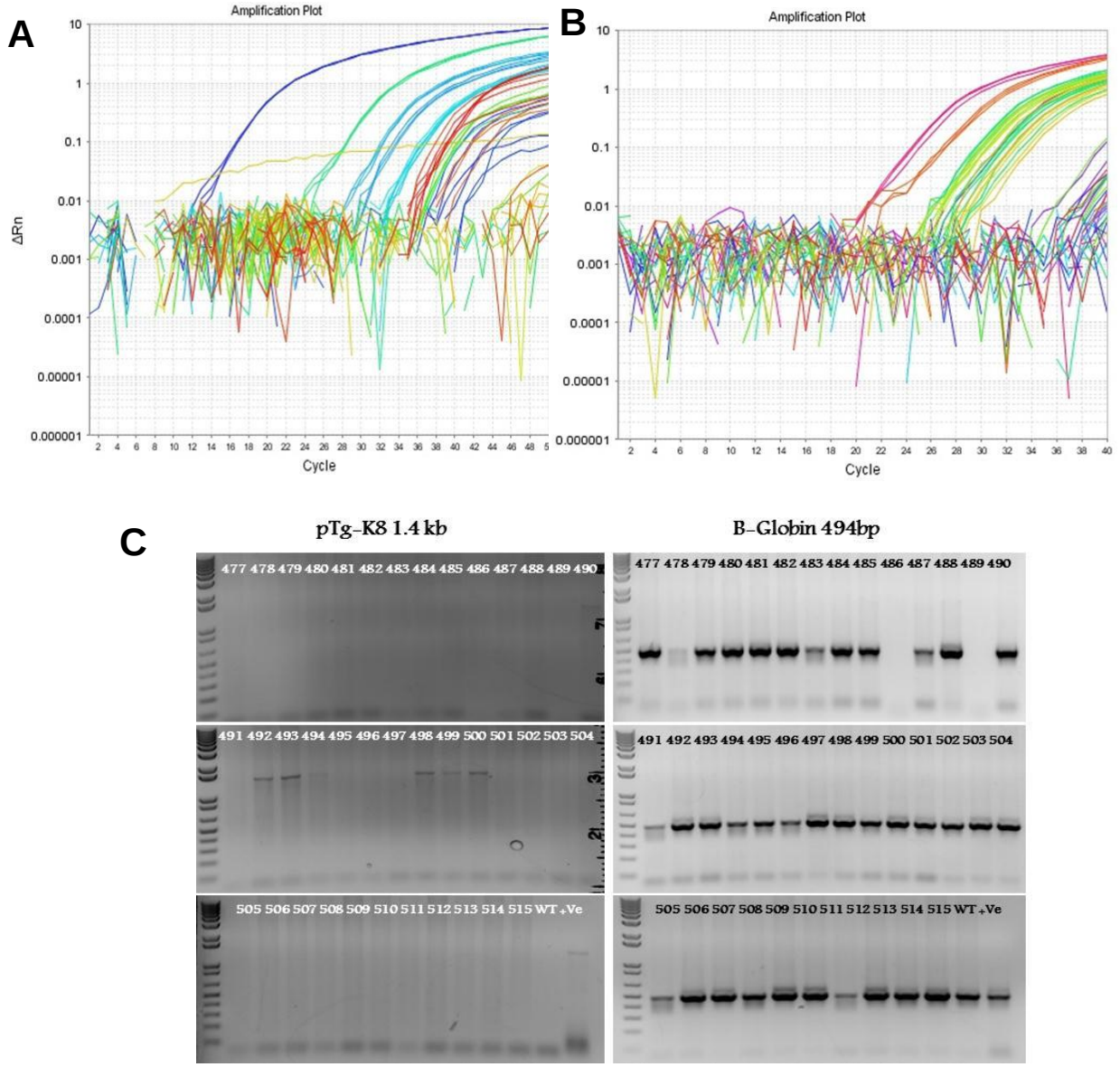

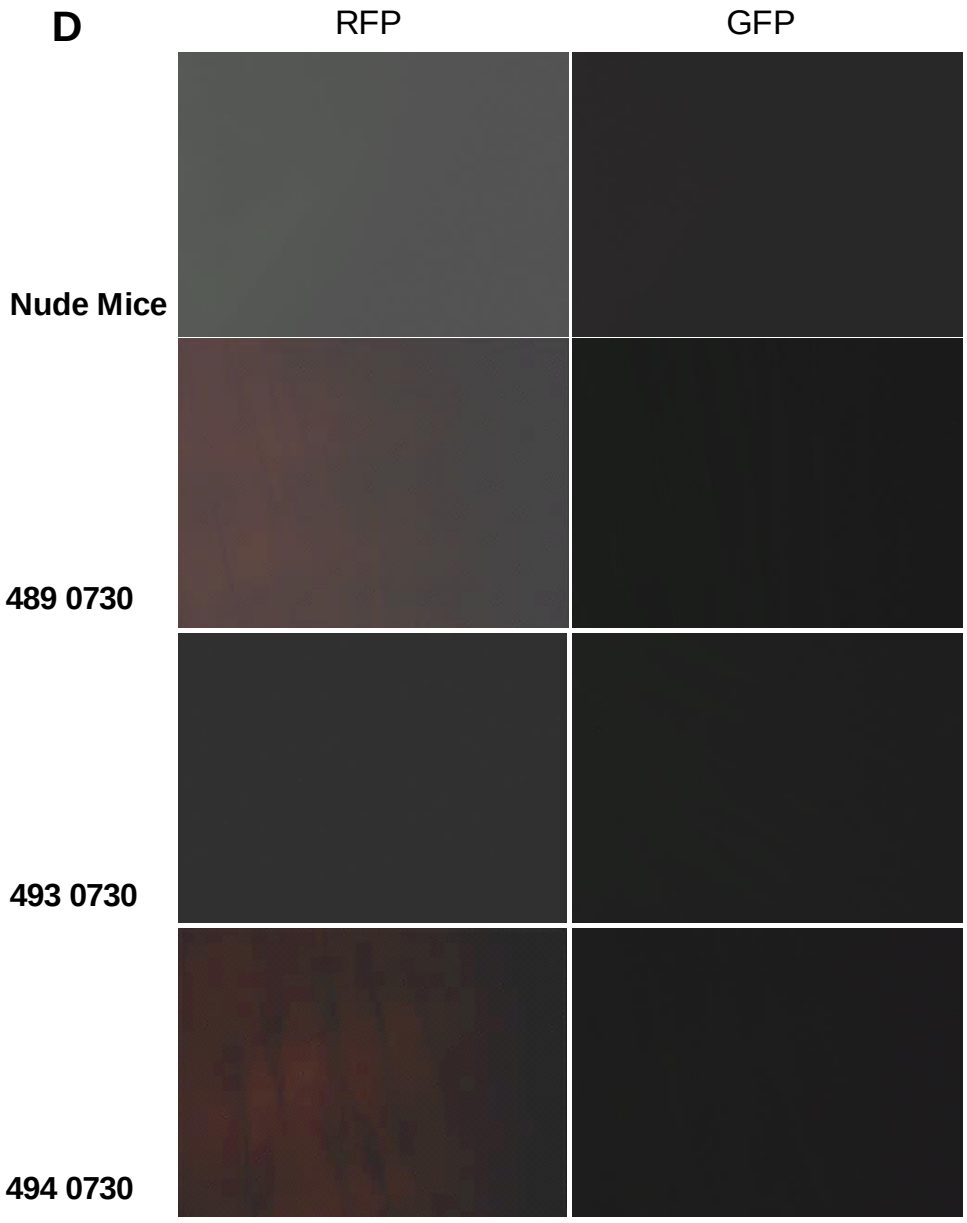

Figure 12. Genotyping to identify founder B65-floxed-KLF8 mice

(A-B) Taqman qPCR genotyping standardized assay was used to identify B65-floxed-KLF8-Tg mice. Positive amplification indicated positive founder mice. (C) Genotyping was also confirmed by genomic DNA PCR (pTg-K8 primer-1.4 kb amplification). B-globin was used to confirm genomic DNA integrity.(D) As the floxed mice have RFP expression, we also confirmed RFP expression from tail snips by fluorescence microscopy (489 and 494 are positive and other two are negative). We also did RT-PCR and western blot further to validate RFP expression (Data not shown).

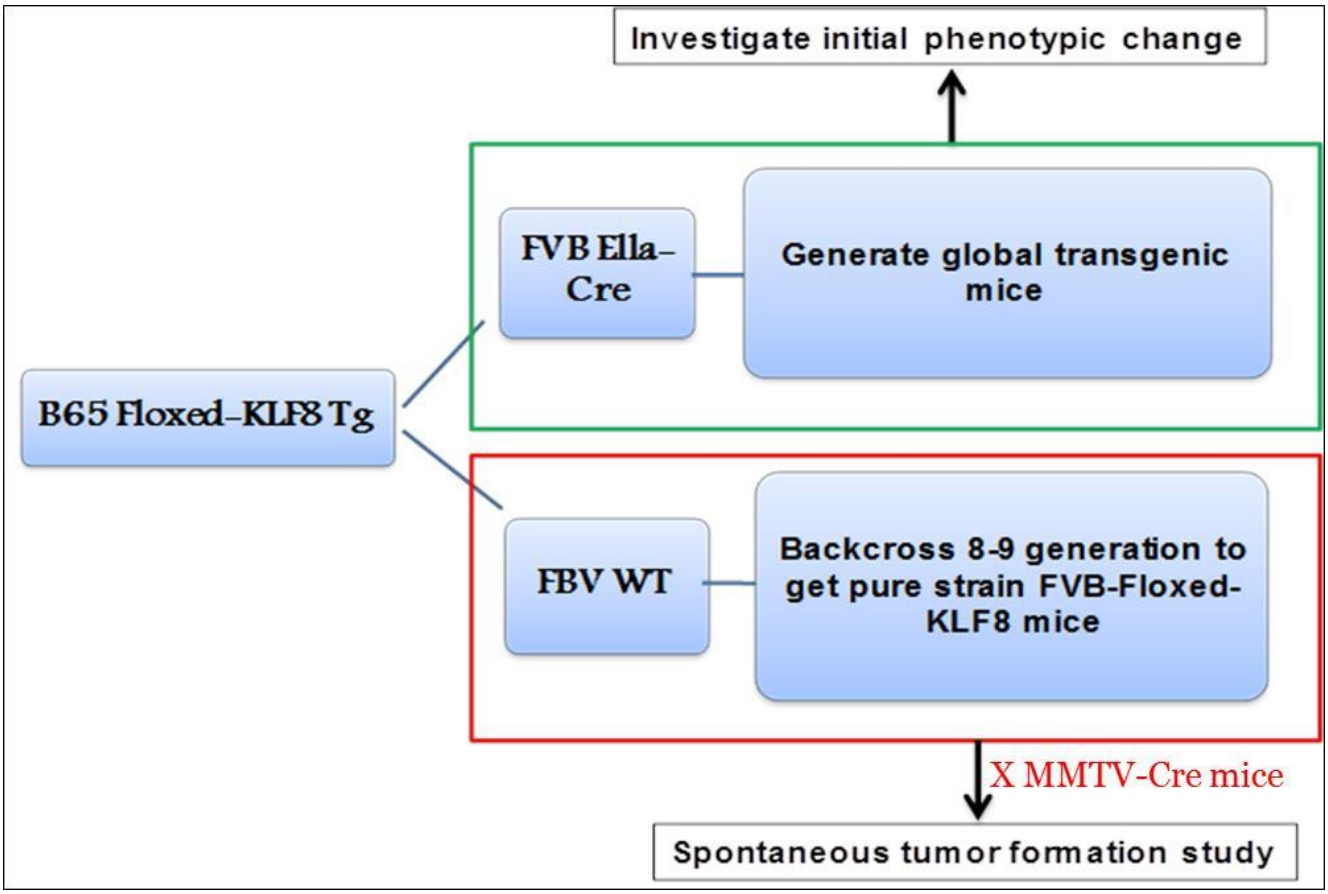

Figure 13. Schematic of transgenic mice breeding

B65-Floxed-KLF8Tg mice were backcrossed with FVB WT mice to get pure FVB strain of mice. Currently we have backcrossed 11th generation FVB-floxed-KLF8Tg mice. We also crossed B65-Floxed-KLF8Tg with FVB-EIIA-Cre mice to obtain global KLF8 transgenic mice (KLF8-gTg) which were observed for initial phenotypic changes due to KLF8 overexpression globally.

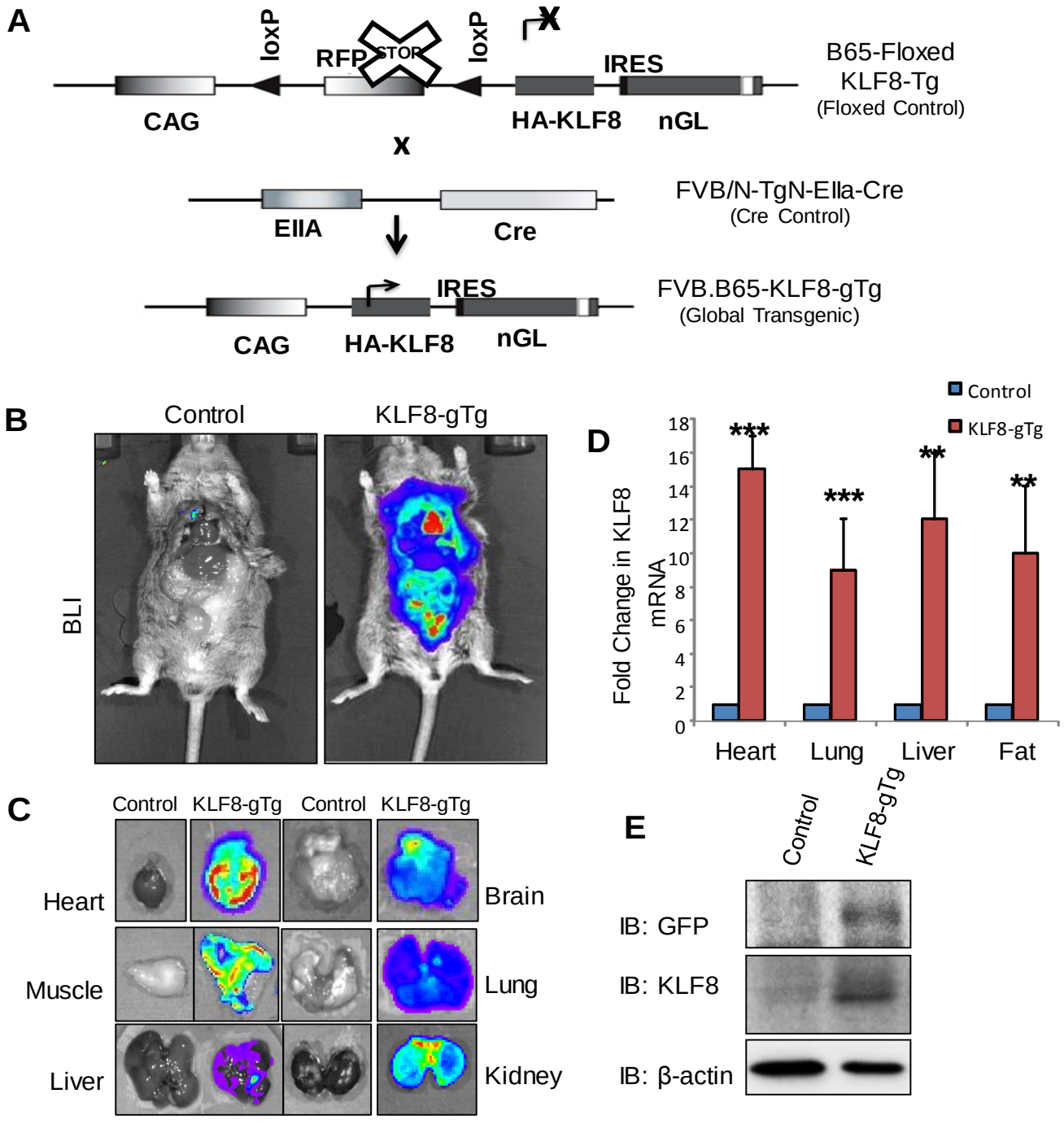

Figure 14. Construction of Global KLF8 Transgenic Mice

(A) Schematic model of Global KLF8 transgenic mice construction. After we identified the B65-Floxed-KLF8 Tg mice; we crossed 4 separate founders with homozygous FVB/N-TgN(EIIa-Cre)C5379Lmgd (Jackson lab stock 003314 ; This line carries a Cre transgene under the control of the adenovirus EIIa promoter that targets expression of

Cre recombinase to the early mouse embryo) mice. The offsprings were of mixed FVB.B65 background including the Cre control and KLF8-gTg mice. (B-C) Bioluminescence Imaging showed positive luciferase signal in KLF8-gTg compared to control (B). Organ specific BLI (C) showed distribution of transgene expression in all tissues. (D) KLF8-gTg mice have high expression of KLF8 mRNA compared to control mice. QPCR was done for KLF8 mRNA expression (n=10) using universal KLF8 primer (E) KLF8-gTg showed increased KLF8 and GFP protein expression. Western blot with anti GFP (sc-9996; 1:1000), anti-KLF8 (8477; 1:1000), anti-RFP anti beta-actin antibody (**; 1:4000) showed increased KLF8 expression in KLF8-gTg mice hearts.

*, P<0.05; **, P<0.01; ***, P<0.001.

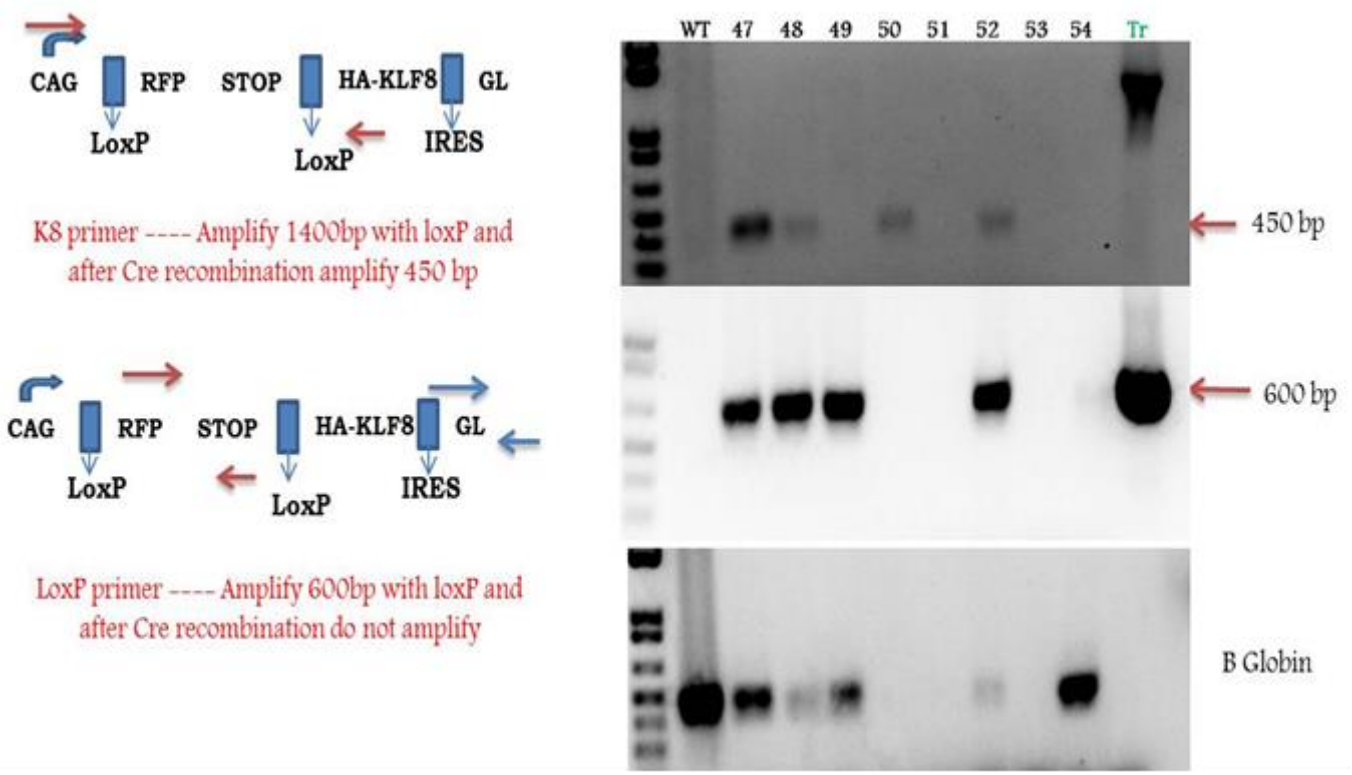

Figure 15. Genotyping KLF8-gTg mice

KLF8-gTg mice were identified by genomic DNA PCR with two different primers on the transgene. B-globin was used for genomic DNA integrity. We also did RT-PCR and western blot with RFP, GFP and HA to validate the mice genotyping. As the EII-Cre mice were homozygous and our floxed-KLF8 mice were heterozygous, the offspring were wither KLF8-gTg or Cre control mice.

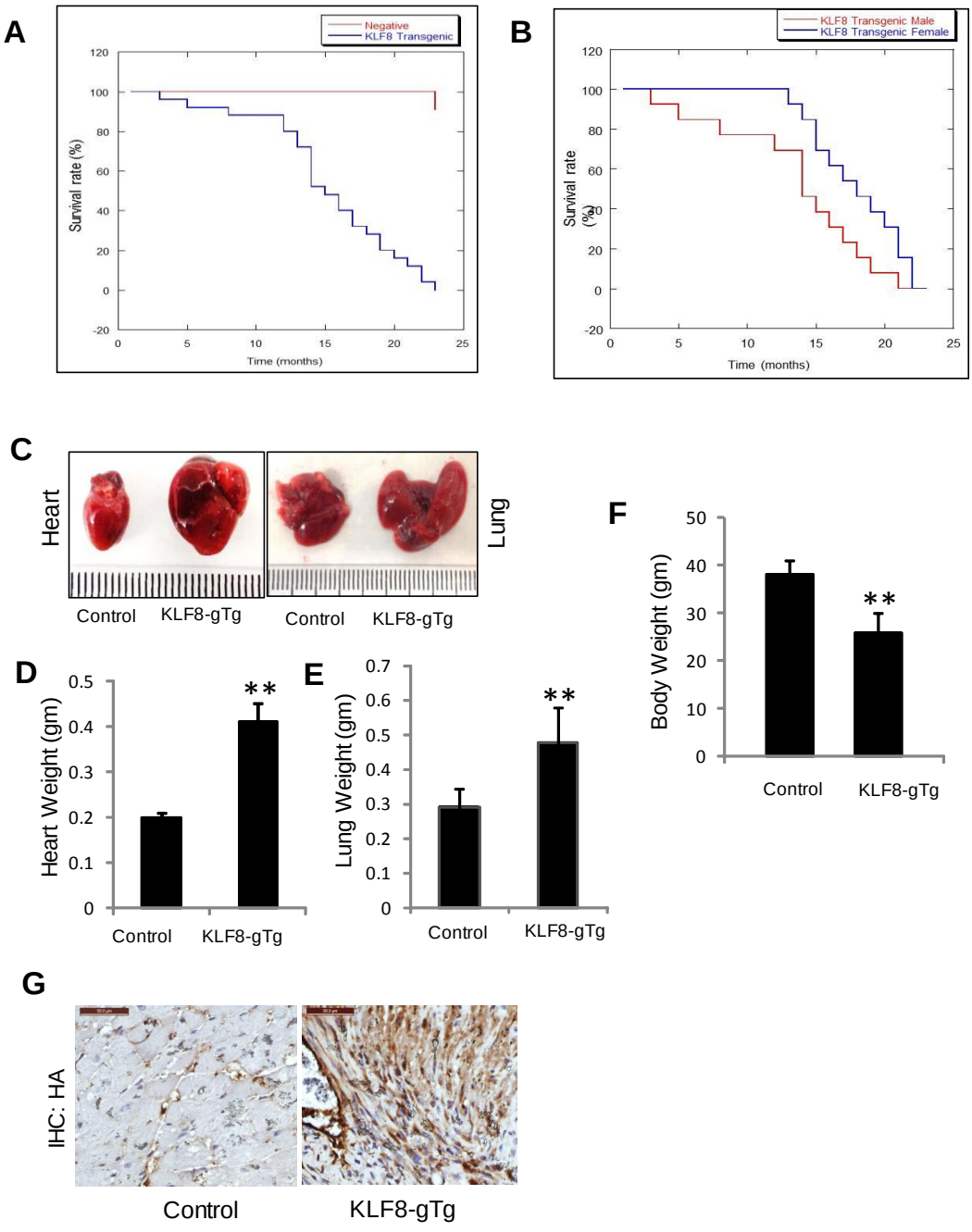

Figure 16. KLF8 global transgenic mice showed increased heart size and decreased survival rate.

(A-B) KLF8 global transgenic mice have significantly lower survival rate. KLF8-gTg mice started dyeing from 4 months of age. We calculated the survival rate of both KLF8-gTg mice (n=26) and control mice (n=23) and plotted in Kaplan-Meier survival plot (A) which showed that KLF8-gTg mice has significantly lower survival rate. We also compared survival rate of KLF8-gTg male (n=13) and female (n=13) which showed that the male

mice had lower survival rate. (C-E) KLF8-gTg mice showed significantly increased heart and lung size. KLF8-gTg mice heart was collected along with its littermate control mice. Both heart and lung were washed in PBS and imaged longitudinally. KLF8-gTg mice showed increased heart and lung size compared to negative control (C). Both heart weight (D) and lung weight (E) were significantly increased in KLF8-gTg mice (n=12). This increase in heart and lung was observed in both male and female mice. (F) KLF8-gTg mice showed less body weight. Both KLF8-gTg and control mice were weighed before euthanasia and KLF8-gTg mice body weight was significantly less compared to control mice (n=12). (g) KLF8-gTg mice heart has positive HA-KLF8 expression. These heart sections were used for IHC staining with anti-HA (Sc-7392; 1:200) antibody.

*, P<0.05; **, P<0.01; ***, P<0.001.

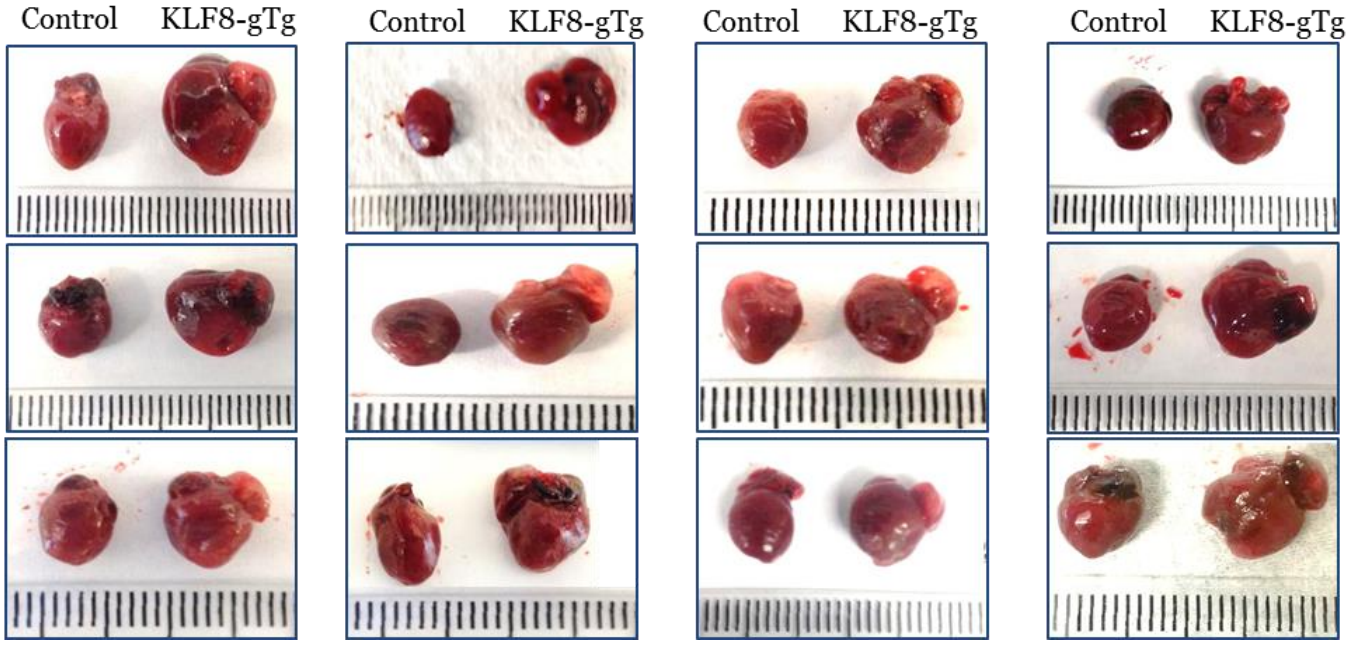

Figure 17. KLF8-gTg mice heart samples

KLF8-gTg mice showed enlarged heart compared to negative Cre control mice. These mice are of different ages (Ranging from 5 months to 15 months). All the KLF8-gTg mice hearts are aligned with its control littermate Cre control mice hearts.

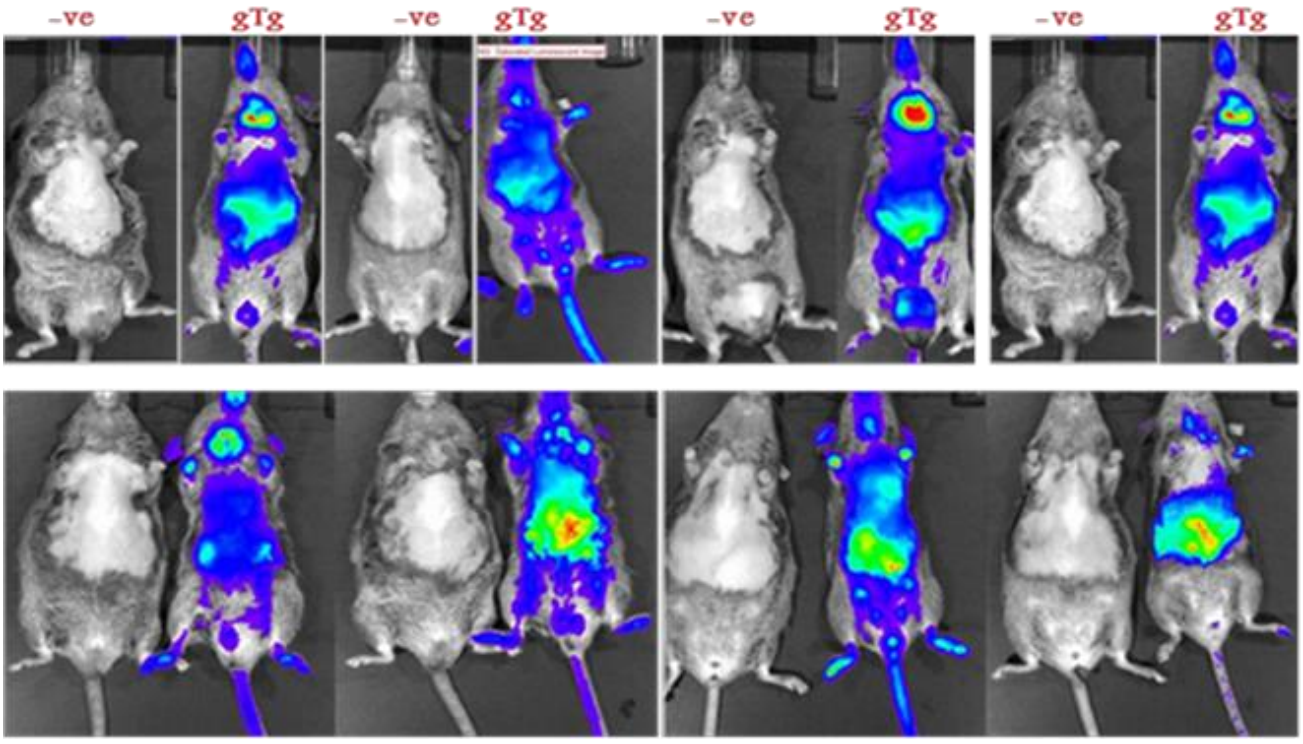

Figure 18. KLF8-gTg mice shows a lean characteristic in BLI

Bioluminescence Imaging revealed a lean phenotype in the KLF8-gTg mice compared to its littermate Cre control mice.

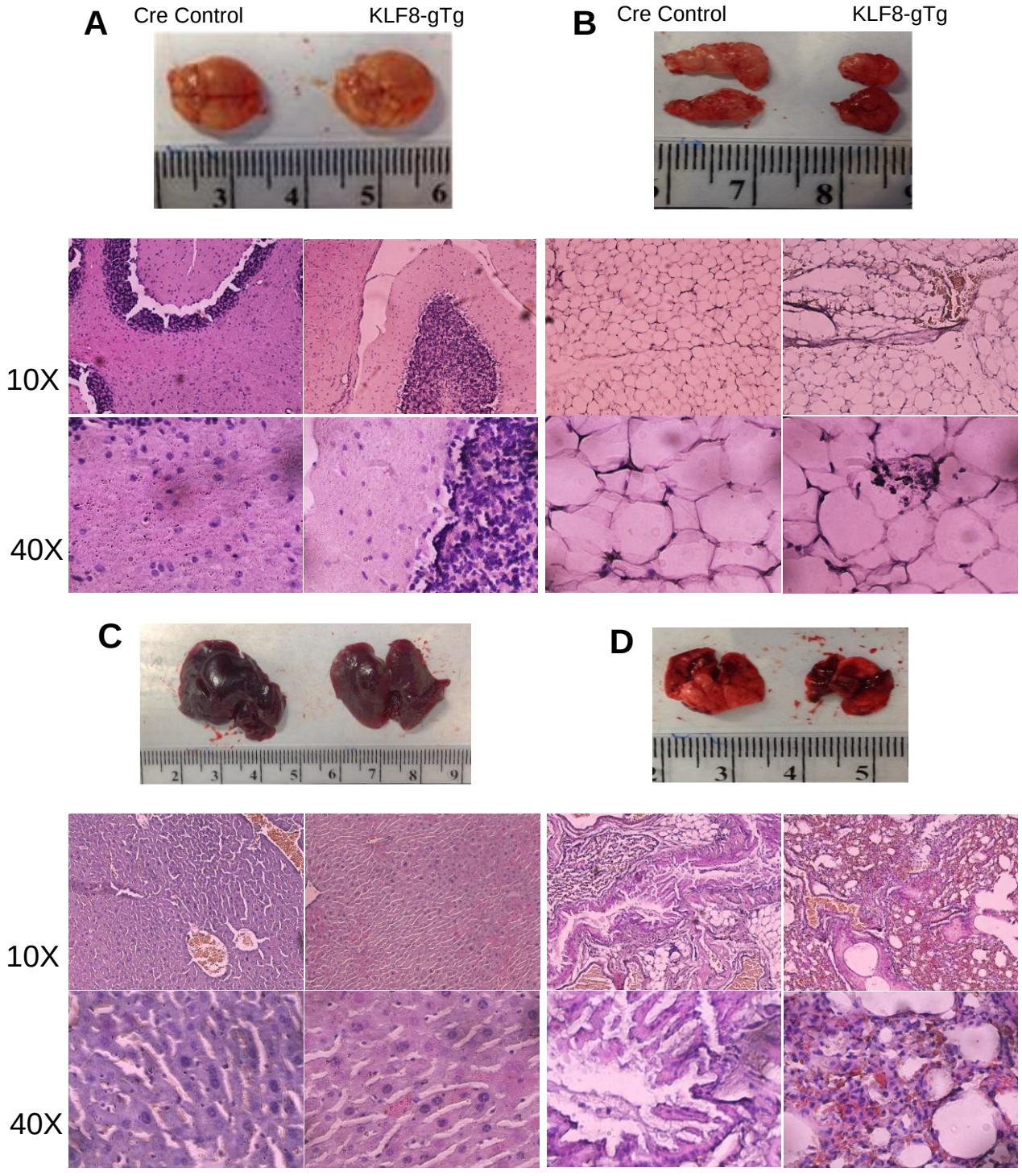
A
Cre Control
KLF8-gTg
B
Cre Control
KLF8-gTg
10X
40X
C
D
10X
40X

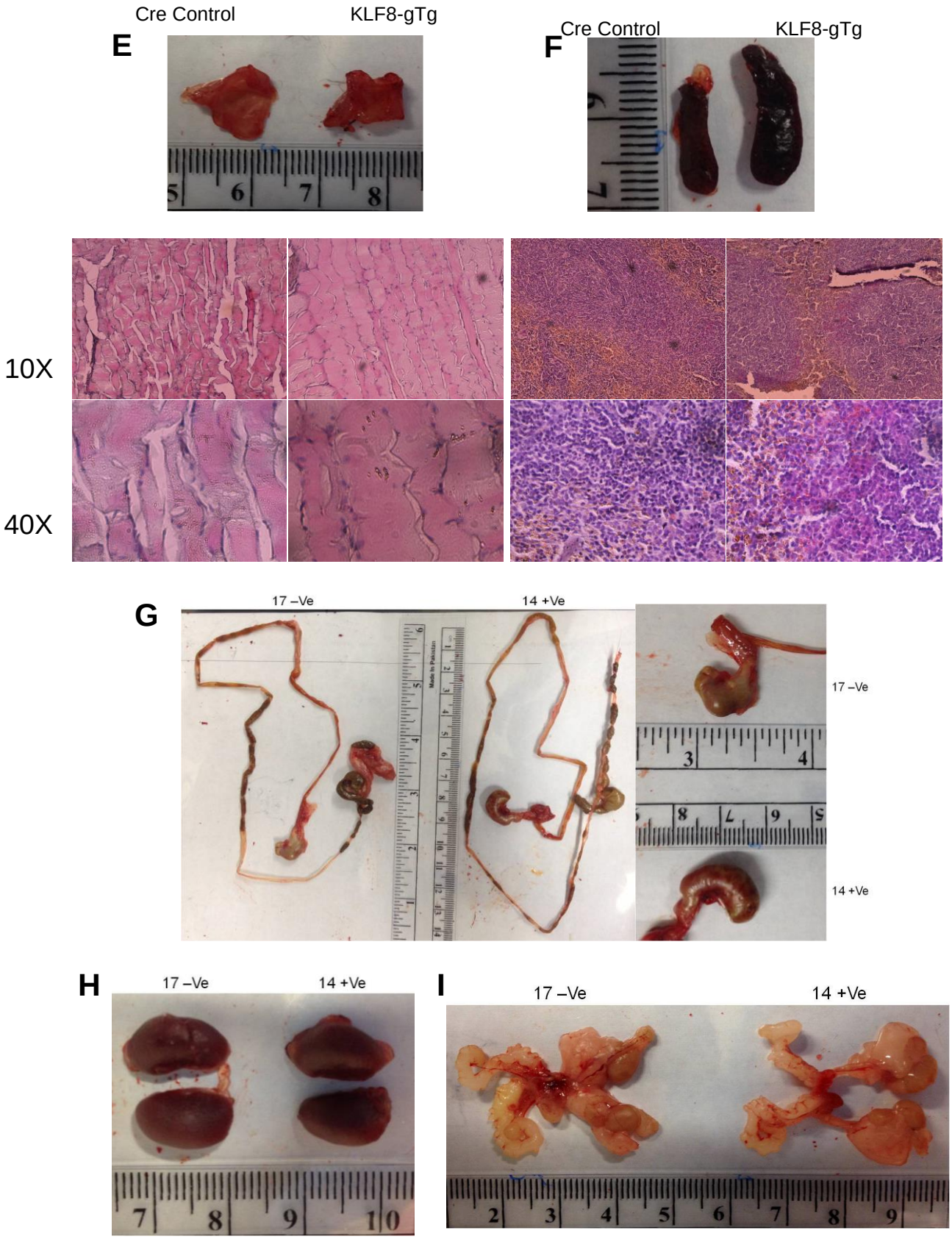
Cre Control
KLF8-gTg
E
F
Cre Control
KLF8-gTg
10X
40X
G
17 –Ve
14 +Ve
17 –Ve
14 +Ve
H
17 –Ve
14 +Ve
I
17 –Ve
14 +Ve

Figure 19. Investigating KLF8-gTg mouse different tissues for any phenotypic characteristics

Various tissues of KLF8-gTg mice were compared with its littermate negative control mice tissues for any evident phenotypes. We also did H&E staining to investigate any microscopic differences in tissue morphology. We didn't see any evident phenotypes or morphological differences in KLF8-gTg mice Brain (A), Liver (C), Lung (D), Muscle (E), Spleen (F), Intestine/stomach (G), Kidney (H). KLF8-gTg mice abdominal fat (B) and reproductive fat (I) was less compared to the negative control.

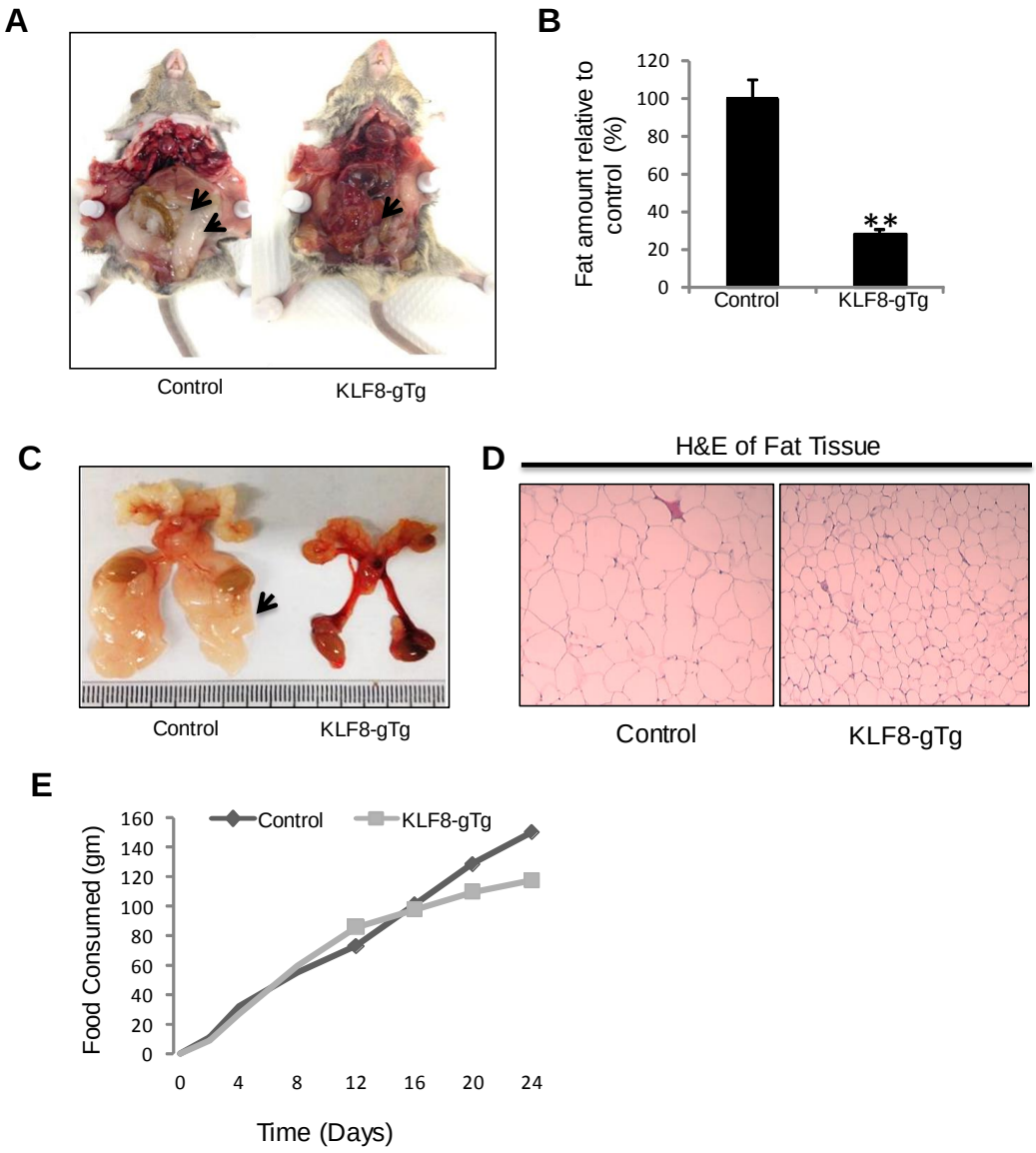

Figure 20. KLF8 global transgenic mice showed less accumulation of Fat.

(A-C) KLF8-gTg mice showed decreased body weight compared to control. KLF8-gTg mice had very little abdominal (A) and reproductive (C) fat (indicated by black arrow) compared to littermate control. KLF8 transgenic mice almost had 70-80% decreased fat amount compared to negative control mice (B; n=12). (D) H&E staining of Fat sections showed that KLF8 transgenic mice reproductive fat had much decreased adipocyte cell size compared to control mice. (E) 4 months old transgenic and control mice (n=2) were housed in individual cages with same amount of food. We measured the food intake each 4 days (Food shredded by mice were also taken into consideration). After 24 day experiment the food intake was plotted against time and the food consumption plot didn't show much difference between KLF8-gTg and control mice.

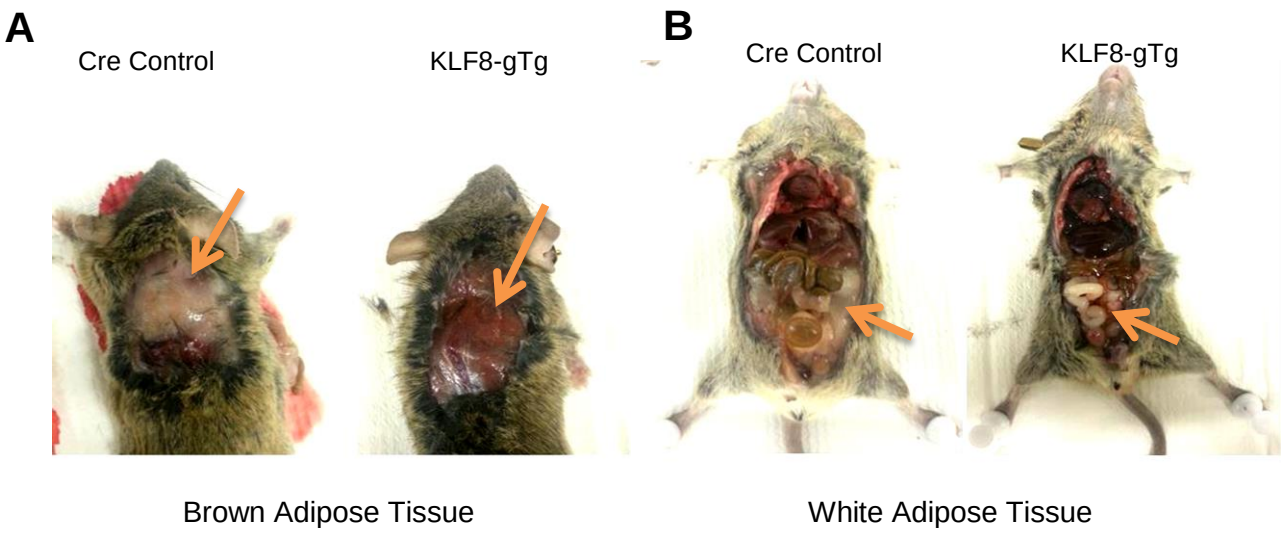

Figure 21. KLF8-gTg mice showed decrease in both brown and white adipose tissue.

(A) We observed significant decreased brown adipose tissue (back of neck) mass and (B) white adipose tissue (both abdominal and reproductive) mass in KLF8-gTg mice compared to Cre control littermates.

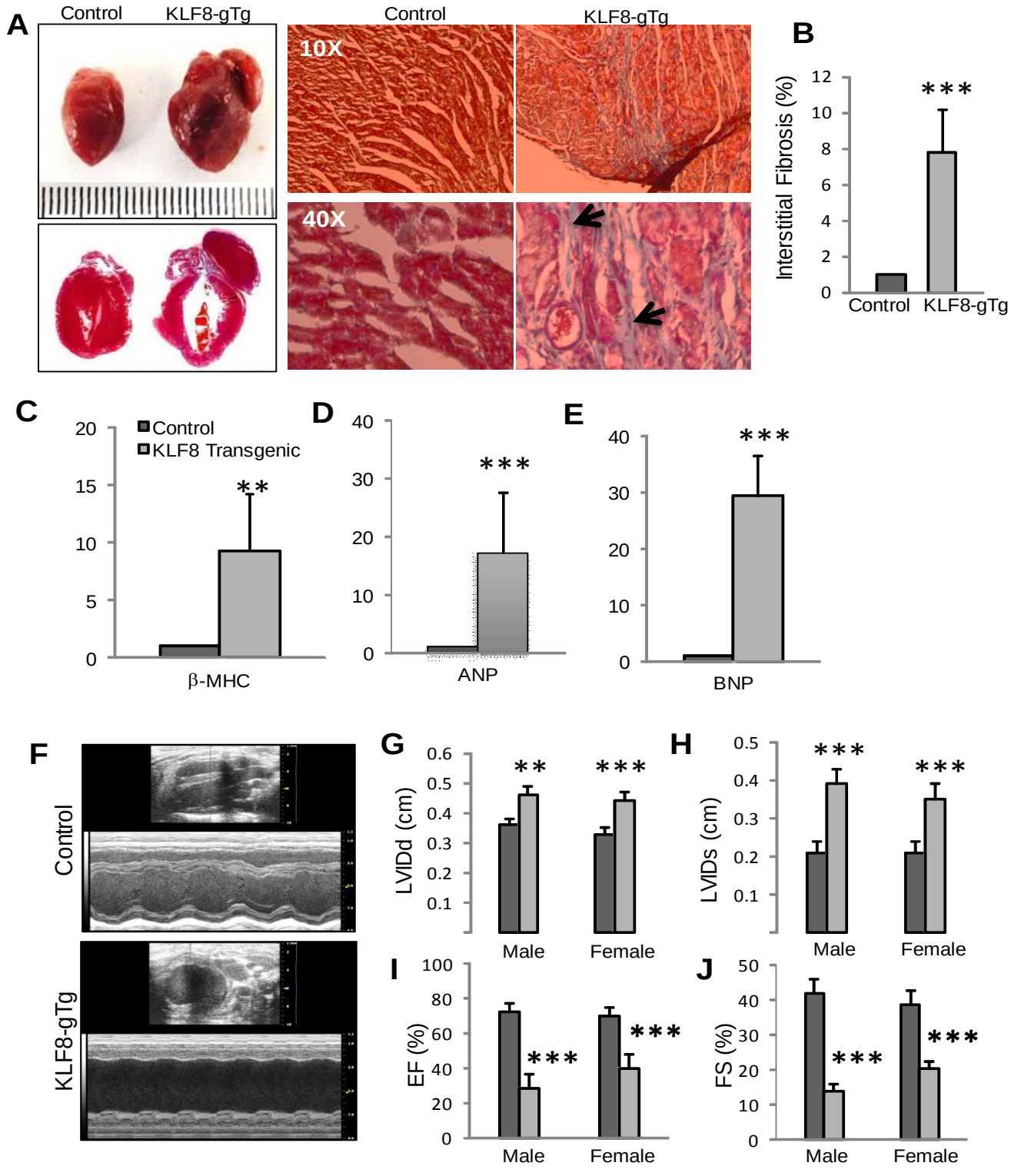

Figure 22. Global expression of KLF8 induces dilated cardiomyopathy in transgenic mice

(A-B) KLF8-gTg mice showed increased myocardial fibrosis (light blue color; indicated by black arrow heads) (A). Cardiac fibrotic area (light blue) was analyzed with image J software (n=8) and plotted (B). Quantification showed that KLF8-gTg showed significantly increased interstitial fibrosis. (C-E) KLF8-gTg mice heart had increased expression of heart failure markers. KLF8-gTg and control mice hearts RNA were collected and used for qPCR with mouse beta-MHC (C), ANP (D) and BNP (E) primers (n=8). All these heart failure markers showed increased expression in transgenic heart compared to control heart RNA. (F-J) Hemodynamic analysis showed KLF8 induces dilated cardiomyopathy in transgenic mice. Ultrasound echocardiograph was done with KLF8-gTg and control mice (n=20 each group) to measure cardiac function. All M mode pictures were measured with ultrasonic software and tabulated. Table 1 showed that both KLF8-gTg male and females showed significant increased LVIDd (G), LVIDs (H) and decreased EF (I) and FS (J) whereas there was no significant change in ventricular wall and intraventricular septum.

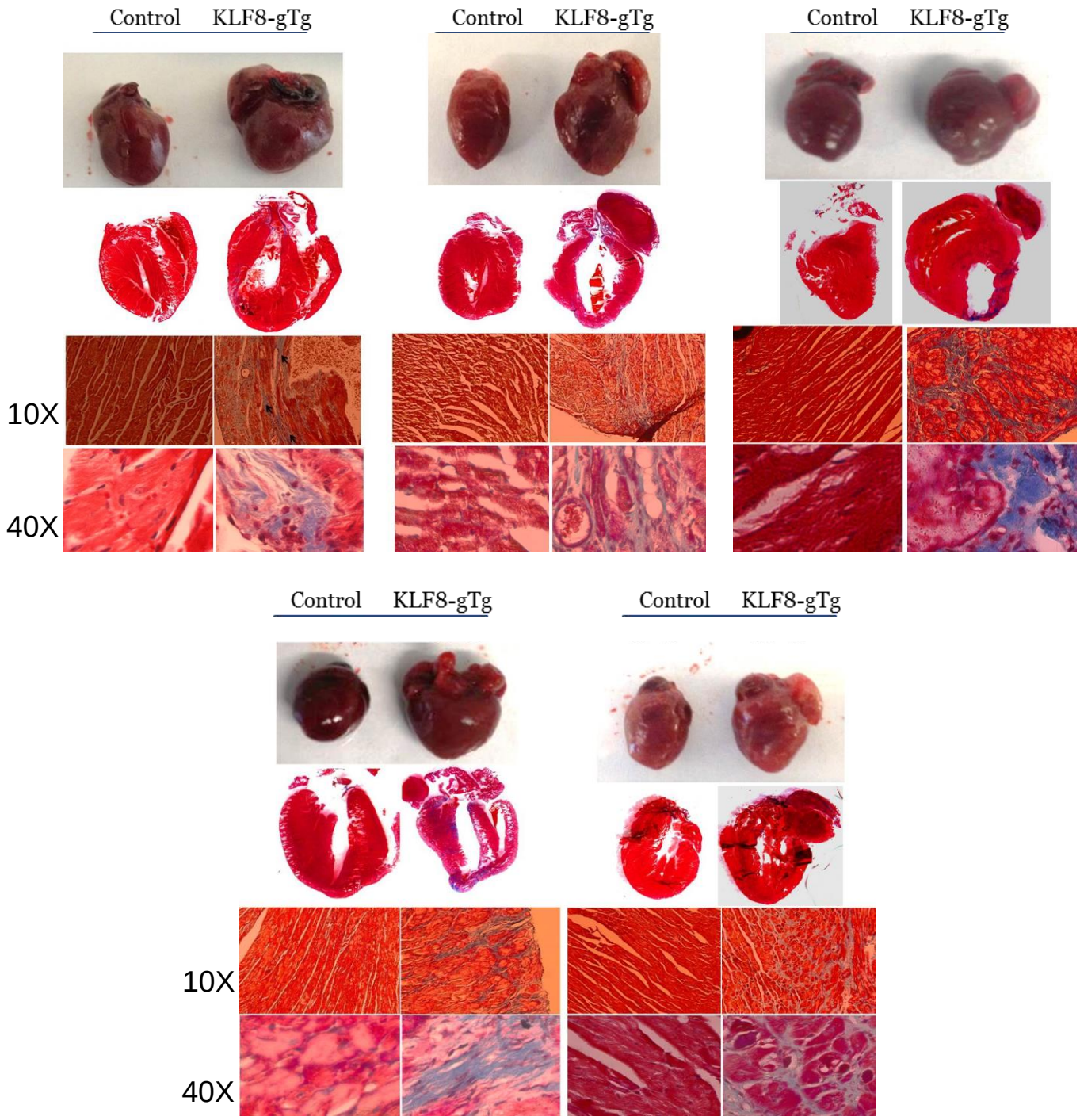

Figure 23. Trichrome staining of KLF8-gTg mouse hearts along with littermate controls

Masson's trichrome staining of 5 pairs of mixed background KLF8-gTg mice hearts along with negative littermate control. All of them showed increased myocardial fibrosis in KLF8-gTg mice hearts.

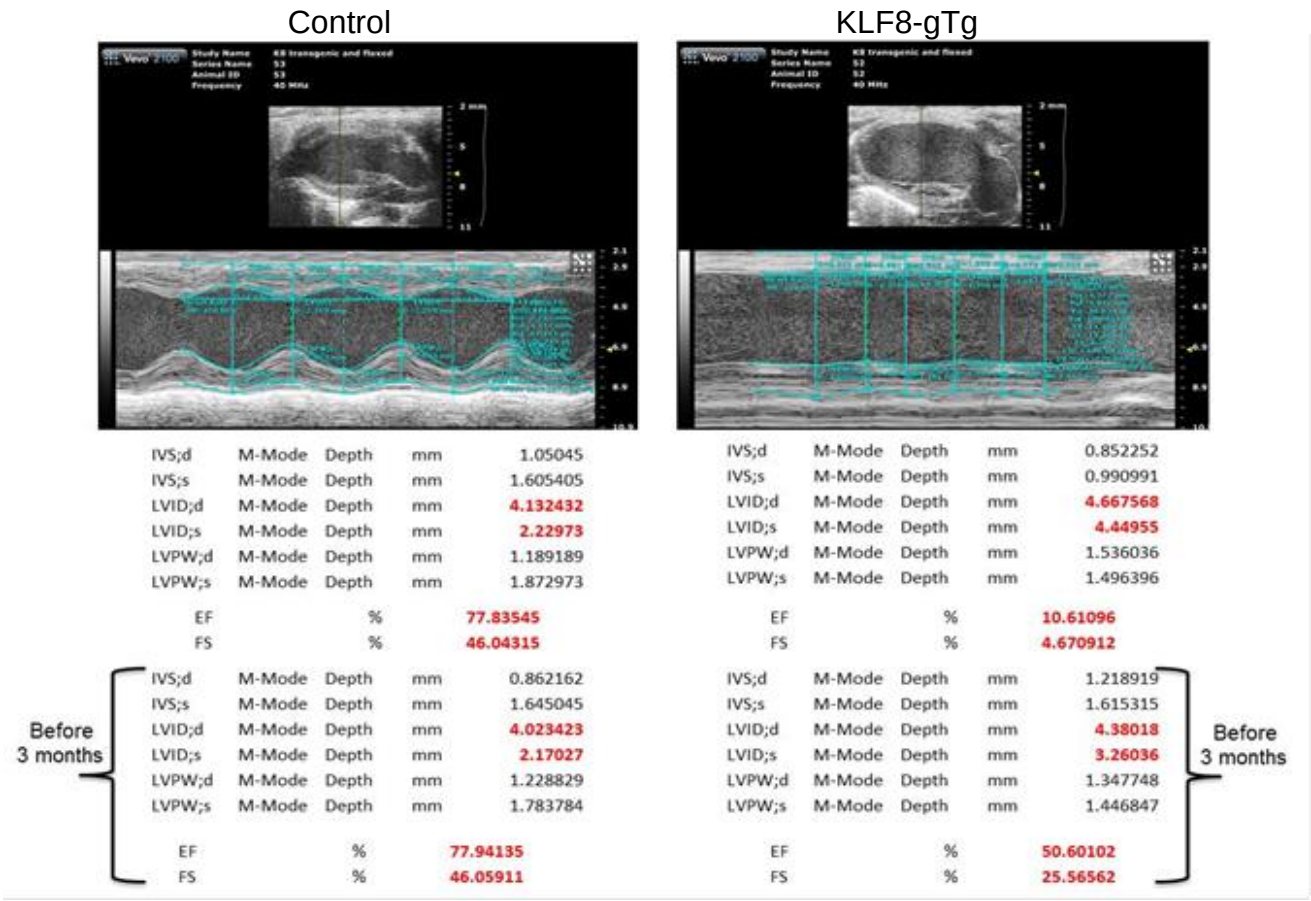

Figure 24. Severe deterioration in progressive cardiomyopathy in KLF8-gTg mice

One pair of KLF8-gTg mouse and its control negative littermate hemodynamics are shown above to indicate the severity of this cardiomyopathy. The top data table is of 14 months while the bottom one is of 11 months of age. The Ejection fraction (EF) of KLF8-gTg deteriorates from 50% to 10% in these 3 months while the negative littermate didn't show any change. Corresponding systolic LV diameter increased severely in KLF8-gTg mice in 3 months and its heart became further dilated which is indicated by increase in diastolic LV diameter. The images shown above are of 14 months of age which clearly showed that KLF8-gTg mice had severely impaired systole.

Table 2. Hemodynamic analysis of KLF8 global transgenic mice cardiac function

	LVIDd (cm)	LVIDs (cm)	LVPWd (cm)	LVPWs (cm)	IVS,d (cm)	IVS,s (cm)	LV volume d (ul)	LV Volume s (ul)	EF (%)	FS(%)
KLF8-gTg Male (11)	**0.46± 0.03**	**0.39± 0.04**	0.12 ± 0.01	0.13 ± 0.02	0.10± 0.008	0.12 ± 0.01	**99.9 ± 17**	**73.02 ± 17**	**28.5± 6**	**14± 4**
Cre control male (11)	**0.36± 0.02** **P = 0.0037**	**0.21± 0.03** **P = 0.00085**	0.13 ± 0.003 P= 0.30	0.15 ± 0.01 P= 0.15	0.09 ± 0.01 P= 0.32	0.15 ± 0.006 P= 0.08	**59.2 ± 7** **P= 0.02**	**15.82 ± 5** **P= 0.004**	**72 ± 2** **P = 0.00011**	**42.1± 2** **P = 0.00007**
Floxed male (8)	**0.35± 0.01** **P = 0.013**	**0.25± 0.02** **P = 0.009**	0.15 ± 0.02 P= 0.13	0.16 ± 0.02 P= 0.14	0.11± 0.008 P= 0.24	0.15 ± 0.01 P= 0.08	**53.2 ± 6** **P= 0.02**	**23.8 ± 5** **P= 0.02**	**62 ± 5** **P = 0.007**	**31± 3** **P = 0.008**
KLF8-gTg Female (9)	**0.44± 0.02**	**0.35 ± 0.02**	0.11 ± 0.05	0.12 ± 0.004	0.1 ± 0.003	0.13 ± 0.007	**88.2 ± 9**	**54.8 ± 10**	**40 ± 5**	**20.3± 3** **P = 0.002**
Cre control female (9)	**0.33± 0.01** **P= 0.0001**	**0.21± 0.01** **P = 0.0001**	0.12± 0.006 P= 0.36	0.13 ± 0.006 P= 0.63	0.09± 0.004 P = 0.48	0.15 ± 0.002 P= 0.01	**44.4 ± 5** **P= 0.0005**	**13.6 ± 2** **P= 0.001**	**70± 3** **P= 0.00009**	**38.6 ± 3** **P = 0.0002**
Floxed Female (5)	**0.31± 0.01** **P= 0.00006**	**0.22± 0.02** **P = 0.0003**	0.14± 0.02 P= 0.28	0.15 ± 0.02 P= 0.32	0.11± 0.01 P = 0.51	0.13 ± 0.01 P= 0.8	**37.5 ± 2.5** **P= 0.00016**	**16 ± 1** **P= 0.002**	**59± 6** **P= 0.0003**	**31± 1** **P = 0.008**

Hemodynamic analysis was done with 10 month old mice. Numbers are mean6SEM. LV, left ventricle; IVSd, intraventricular septum diastolic; LVIDd, left ventricle inner diameter diastolic; LVPWd, left ventricle posterior wall diastolic; %EF, percentage of ejection fraction, %FS, Fractional shortening.

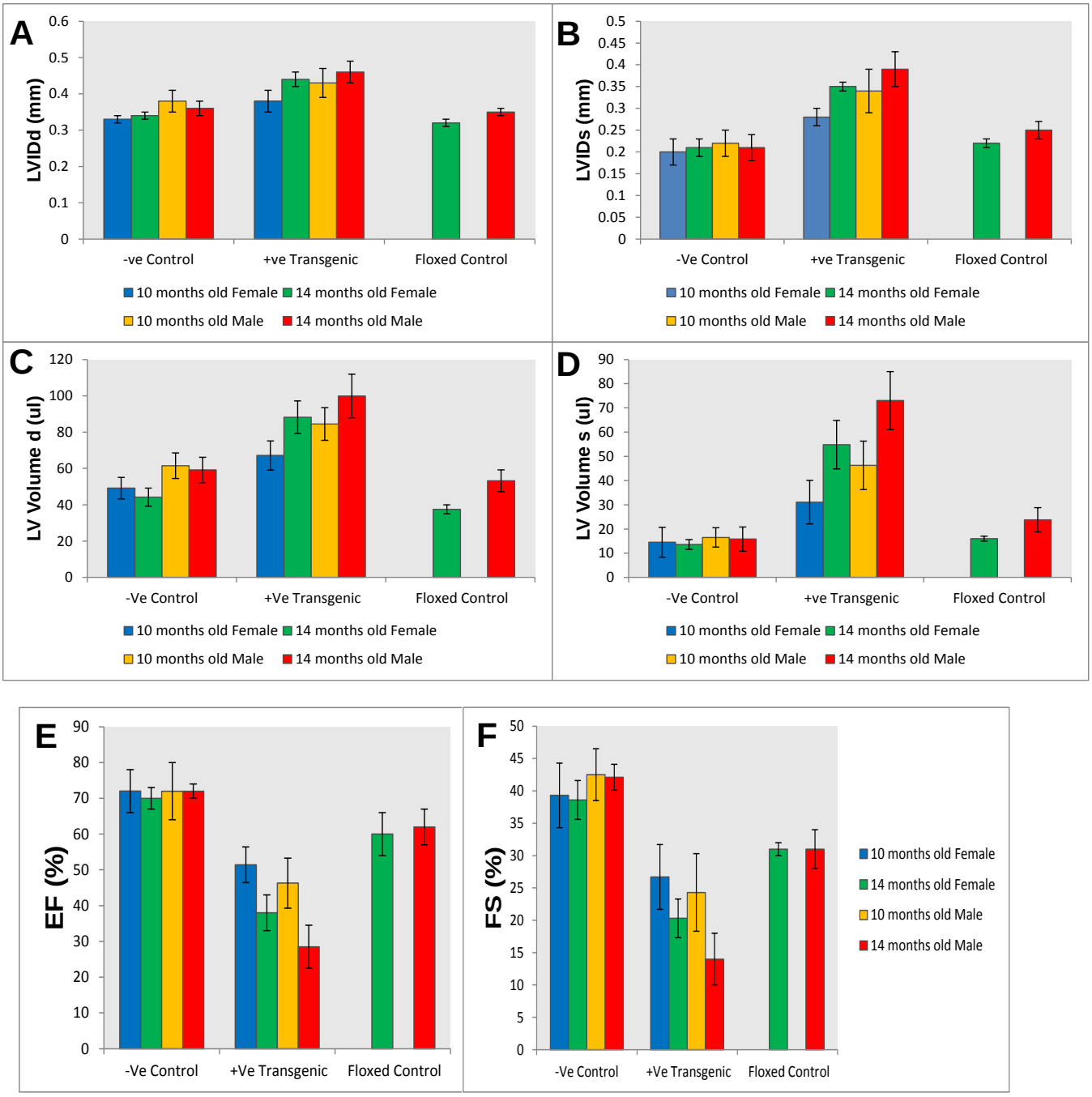

Figure 25. Hemodynamic analysis of adult KLF8 global transgenic mice cardiac function

Both adult male and female KLF8-gTg mice showed significant increase in LV diameter in diastole (A), LV diameter in systole (B), LV volume in diastole (C) and LV volume in systole (D). These parameters were further increased after 4 months in KLF8-gTg mice whereas both negative control (Cre control and floxed control) didn't show much difference. Further KLF8-gTg mice also showed significantly decreased ejection fraction

(EF) and fractional shortening (FS) compared to negative controls. Both EF and FS was severely deteriorated in KLF8-gTg mice while we didn't observe much change in the controls.

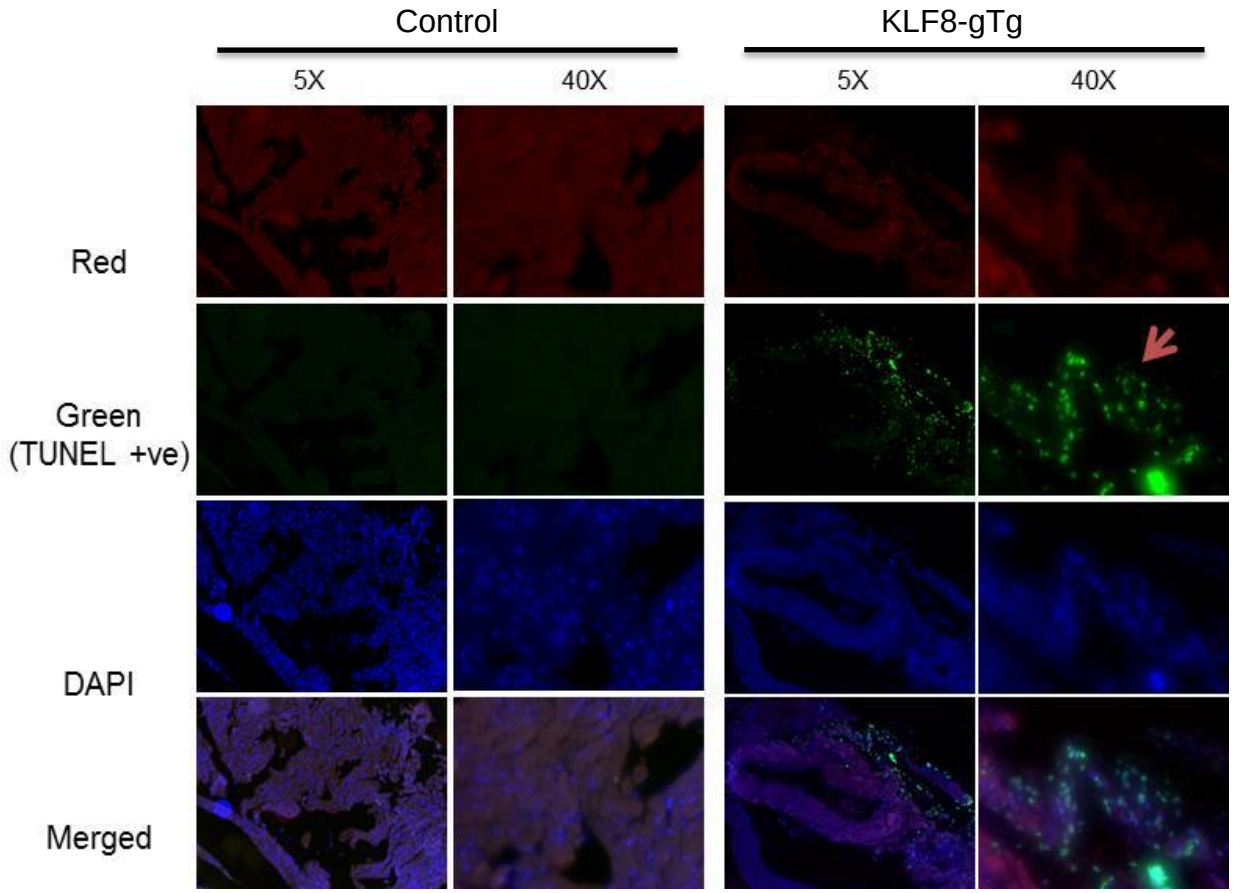

Figure 26. KLF8-gTg mice showed more apoptosis in heart

Tunnel staining was done with mouse heart tissue samples. KLF8-gTg mice heart clearly showed much more apoptosis (green) compared to the negative control mice heart. Red channel was used to negate the auto fluorescence. Tunel assay was done with Deadend Flurometric Tunel system (Promega G3250)

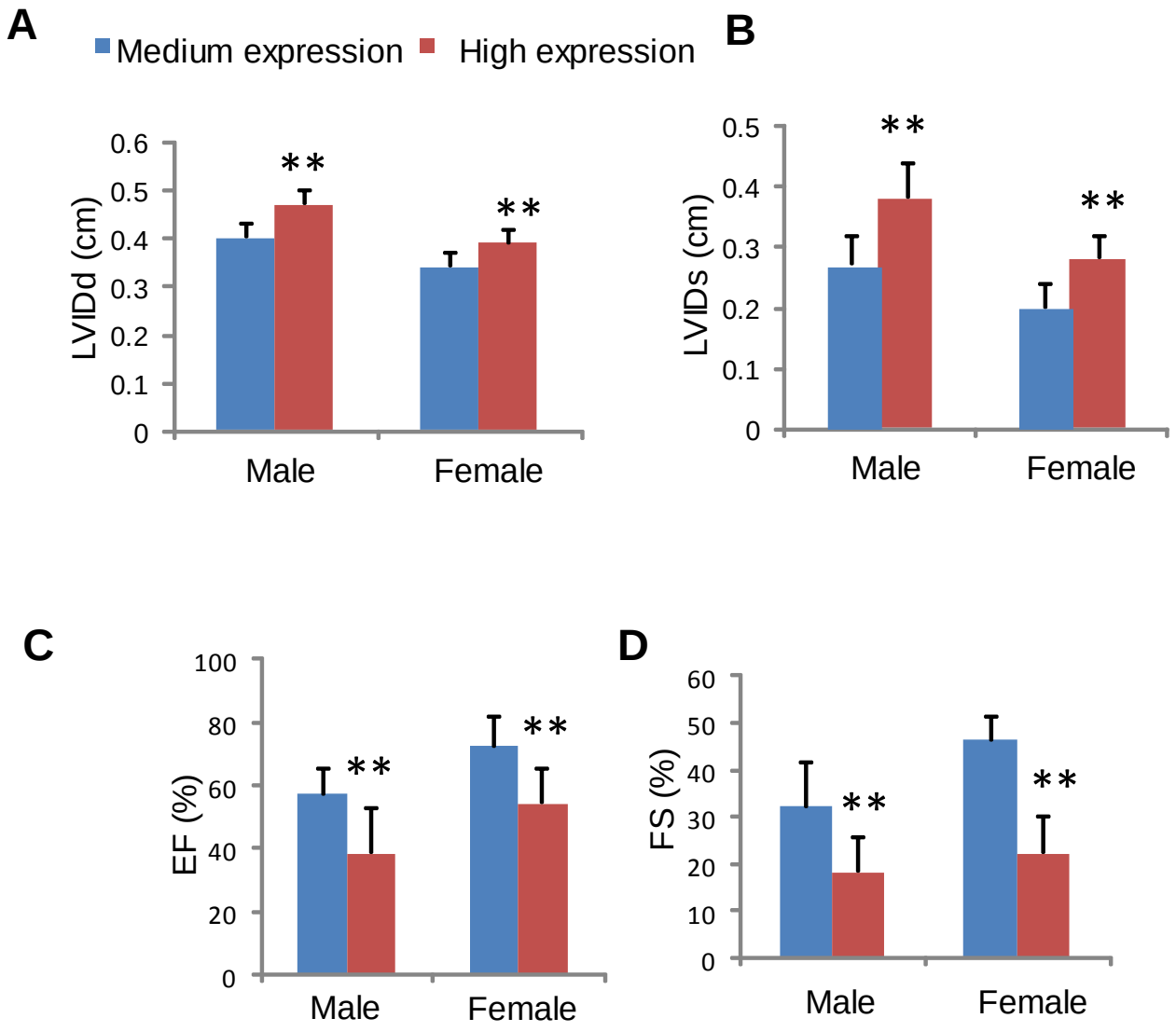

Figure 27. Higher expression of KLF8 transgene correlates with the severity of cardiac dysfunction

(A-D) KLF8 high expression mice showed significantly increased LV diameter at both systole and diastole and decreased EF and FS. We grouped the mice based on transgene expression (BLI data not shown).

Table 3.Hemodynamic analysis based on KLF8 transgene expression

	LVIDd (cm)	LVIDs (cm)	EF (%)	FS (%)
High Expression Male (5)	**0.47 ± 0.03**	**0.38 ± 0.06**	**38.33 ± 14.5**	**18.58 ± 7.7**
Low Expression male (5)	**0.4 ± 0.03**	**0.27 ± 0.05**	**57.73 ± 8.3**	**32.065 ± 9.6**
	P = 0.005	**P = 0.009**	**P = 0.02**	**P = 0.02**
High Expression Female (6)	**0.39 ± 0.03**	**0.28 ± 0.04**	**54.3 ± 11**	**22.37± 8.9**
Low expression female (5)	**0.34 ± 0.03**	**0.2 ± 0.04**	**72.02 ± 10**	**46.33 ± 5.5**
	P= 0.01	**P = 0.0047**	**P= 0.0026**	**P = 0.002**

Numbers are mean6SEM. LV, left ventricle; IVSd, intraventricular septum diastolic; LVIDd, left ventricle inner diameter diastolic; LVPWd, left ventricle posterior wall diastolic; %EF, percentage of ejection fraction, %FS, Fractional shortening.

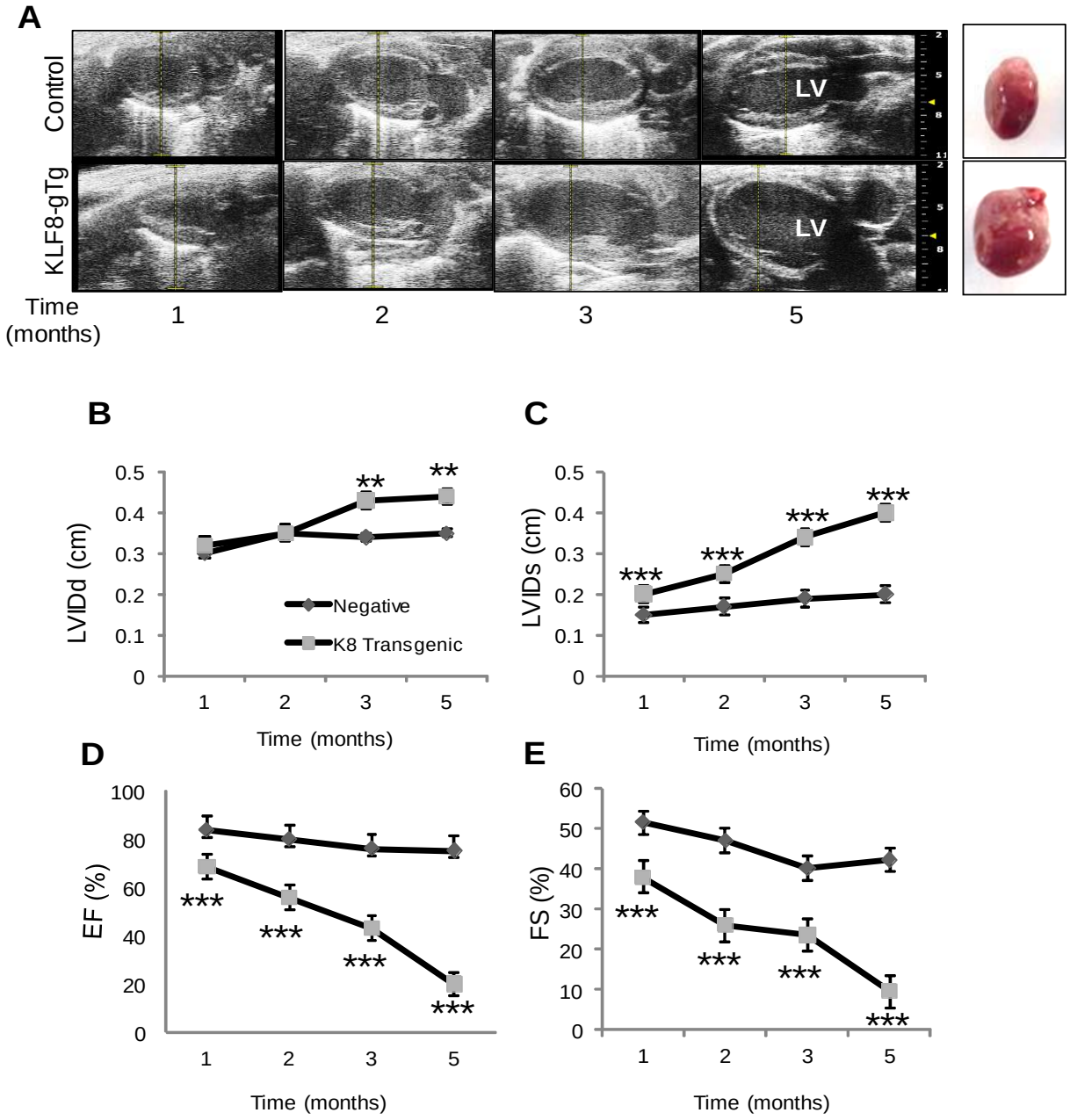

Figure 28. KLF8 induces systolic dysfunction which leads to dilated cardiomyopathy in KLF8 global transgenic mice.

Time point hemodynamic analysis showed that heart size in transgenic mice increases from 3 months of age (A). (We use FVB-K8-gTg mice which had lower survival rate compared to the mixed control). (B-E) shows that KLF8 promote increase in LV systolic diameter which leads to decrease in EF, FS at 1 month of age. Time point analysis showed further deterioration of cardiac function in transgenic mice which leads to dilated cardiomyopathy.

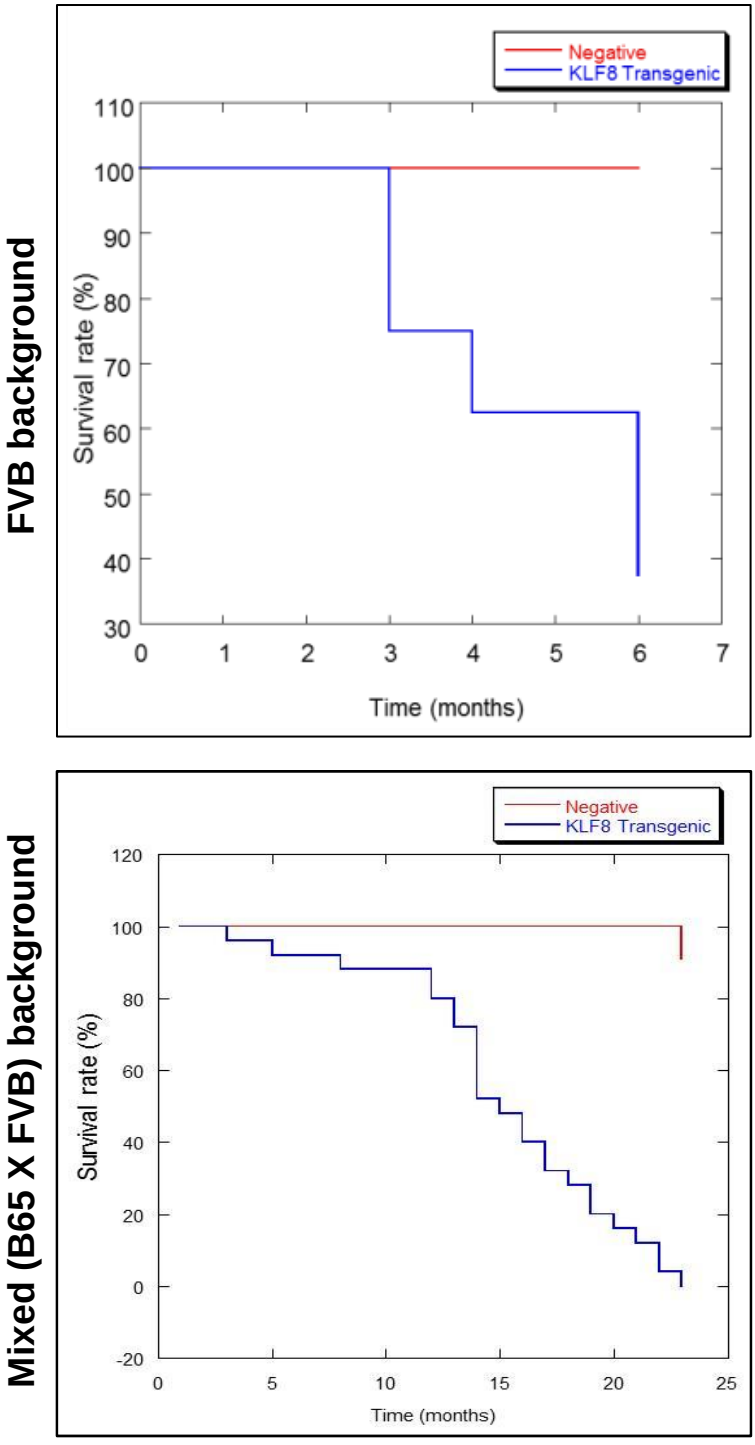

Figure 29. Survival rate of Different strain background of KLF8-gTg mice

Both FVB and mixed background KLF8-gTg had lower survival rate compared to their respective negative controls.

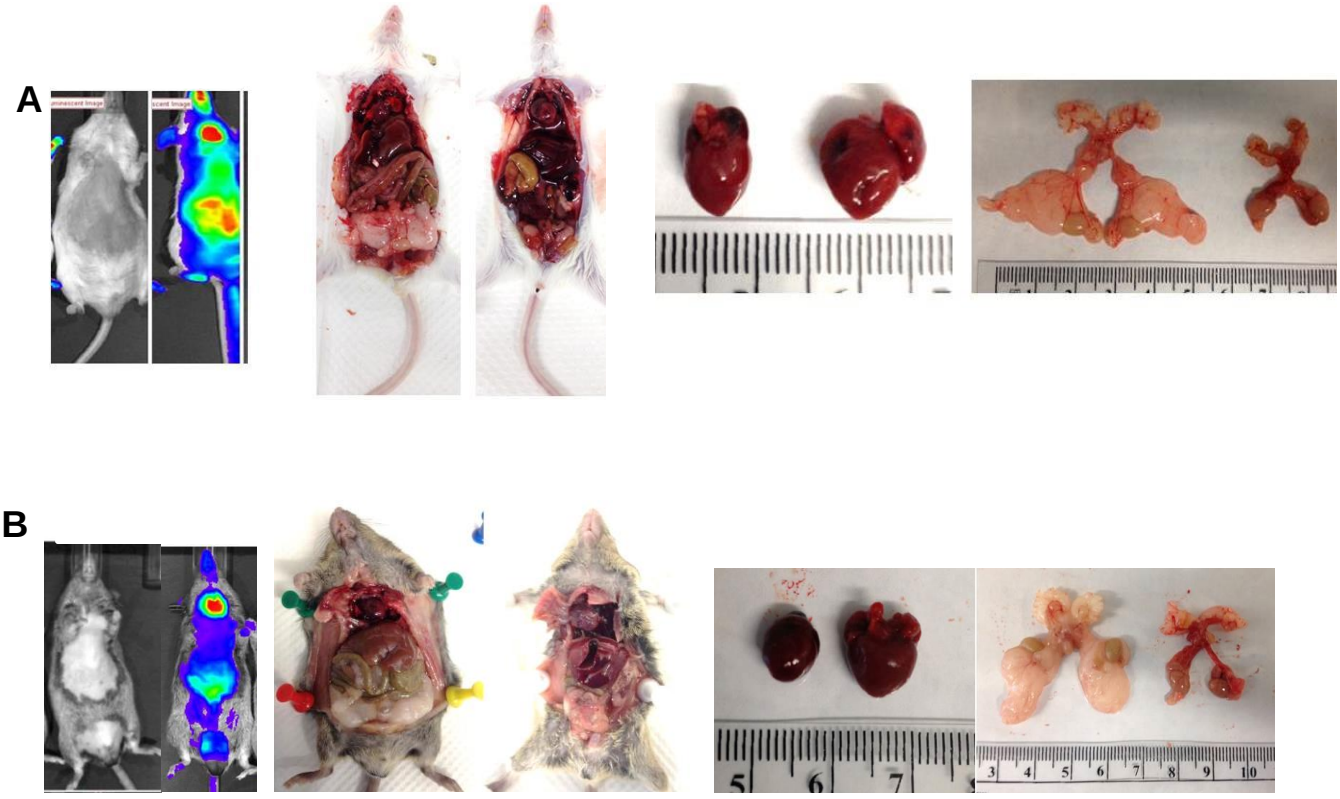

Figure 30. Cardiac phenotype is observed independent of mouse strain background

Overall our study we used two different strains of KLF8-gTg mice. Both FVB background mice (A) and mixed background KLF8-gTg mice (B) showed lean phenotype, enlarged heart and less fat phenotypes.

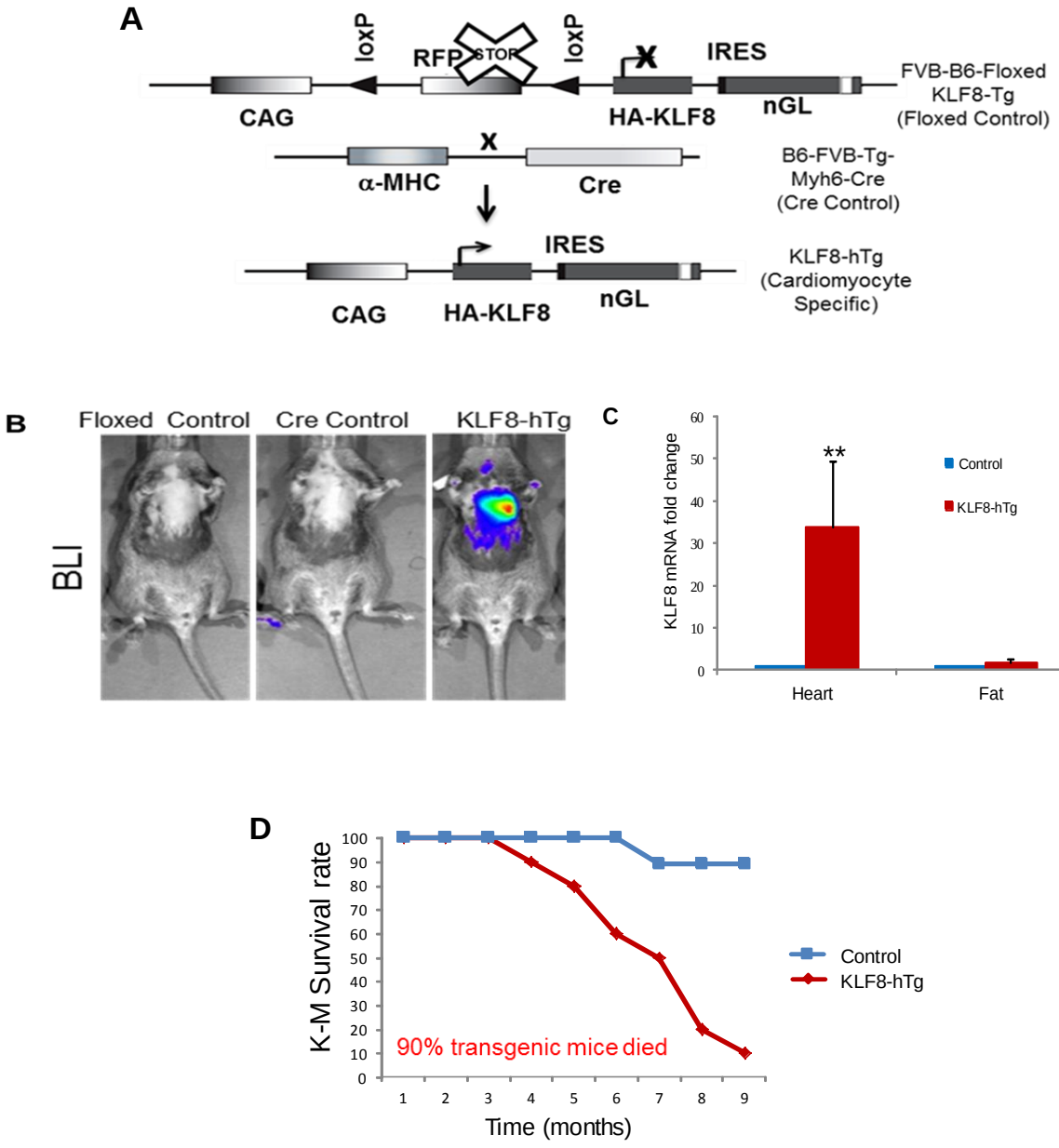

Figure 31. Construction of cardiomyocyte specific KLF8 transgenic mice

(A) Construction of cardiomyocyte specific KLF8 transgenic mice (KLF8-hTg): FVB-B6-floxed-KLF8 (7th generation) mice were crossed with B6-FVB-Tg-Myh6-Cre mice. We got 4 different off springs including KLF8-hTg, floxed control, Cre control and WT control mice. (B) KLF8-hTg mice showed heart specific transgene expression: We did BLI with KLF8-hTg mice along with the littermate controls and the KLF8-hTg mice showed heart specific luciferase expression. The control littermates did not show any luminescence. (C) Confirm KLF8 mRNA overexpression specific to heart tissue of KLF8-hTg mice compared to fat tissue of these mice. RNA from both KLF8-hTg mice heart and fat were

isolated along with floxed control mice. qPCR was done using universal KLF8 primer (detects both human and mouse KLF8) to investigate KLF8 expression in these tissues. (D) Survival rate of KLF8-hTg mice is much lower compared to control mice (none of the 3 control group mice died as early as the KLF8-hTg mice, so we pooled all the control mice in a single negative control mice group and plotted against KLF8-hTg mice.

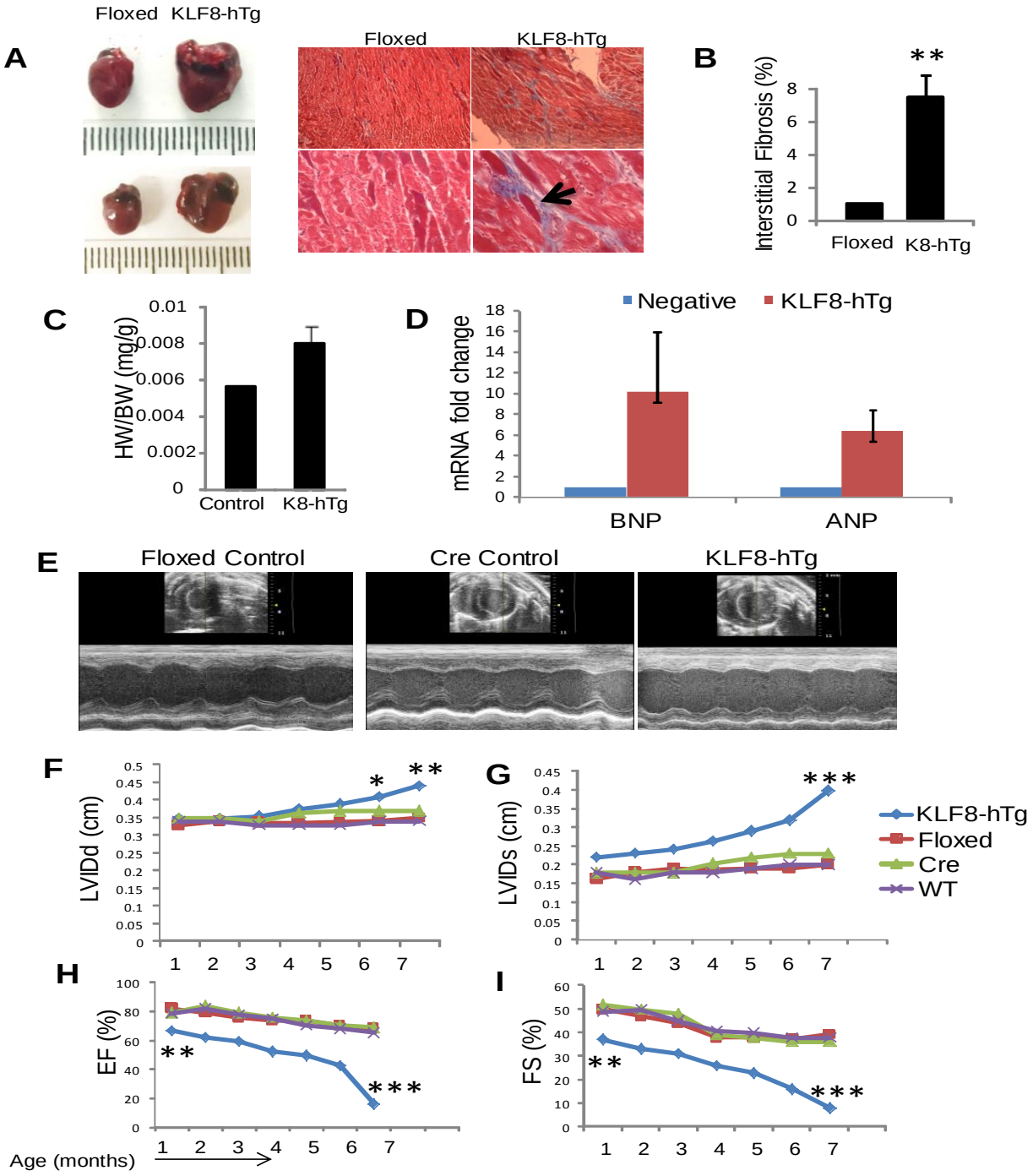

Figure 32. Cardiomyocyte specific over-expression of KLF8 induces systolic dysfunction leading to dilated cardiomyopathy

(A-B) KLF8-hTg mice showed increased heart size and cardiac fibrosis. Heart size (A) and weight (C) was significantly higher in KLF8-hTg compared to all three control. We used floxed control mice here as representative figure. We used these heart sections to do mason's trichrome staining to check collagen deposition in cardiac tissue (light blue color; indicated by black arrow heads). KLF8-hTg mice showed positive cardiac fibrosis compared to control mice heart (A). Cardiac fibrotic area (light blue) was analyzed with image J software (n=6) and plotted (B). Increase in heart failure markers ANP and BNP were also observed in KLF8-hTg mice hearts (D). KLF8-hTg mice along with its control littermates were used for ultrasound to investigate heart function. Ultrasound result showed cardiac expression of KLF8 leads to increased LVIDs and decreased EF, FS in KLF8-hTg mice. (E-I) Cardiomyocyte specific expression of KLF8 also induce systolic dysfunction: Time point haemodynamic analysis of KLF8-hTg along with its control littermates showed that KLF8-hTg mice hearts have increased LVIDs and decreased EF,FS. Heart function in KLF8-hTg mice deteriorates faster compared to negative controls. We have not yet seen significant change in heart LVIDd but these mice are still studied each month to investigate if this systolic dysfunction leads to dilated cardiomyopathy. We use FVB-K8-gTg mice which had lower survival rate compared to the mixed control). (F-I) shows that KLF8 promote increase in LV systolic diameter which leads to decrease in EF, FS at 1 month of age. Time point analysis showed further deterioration of cardiac function in transgenic mice which leads to dilated cardiomyopathy.

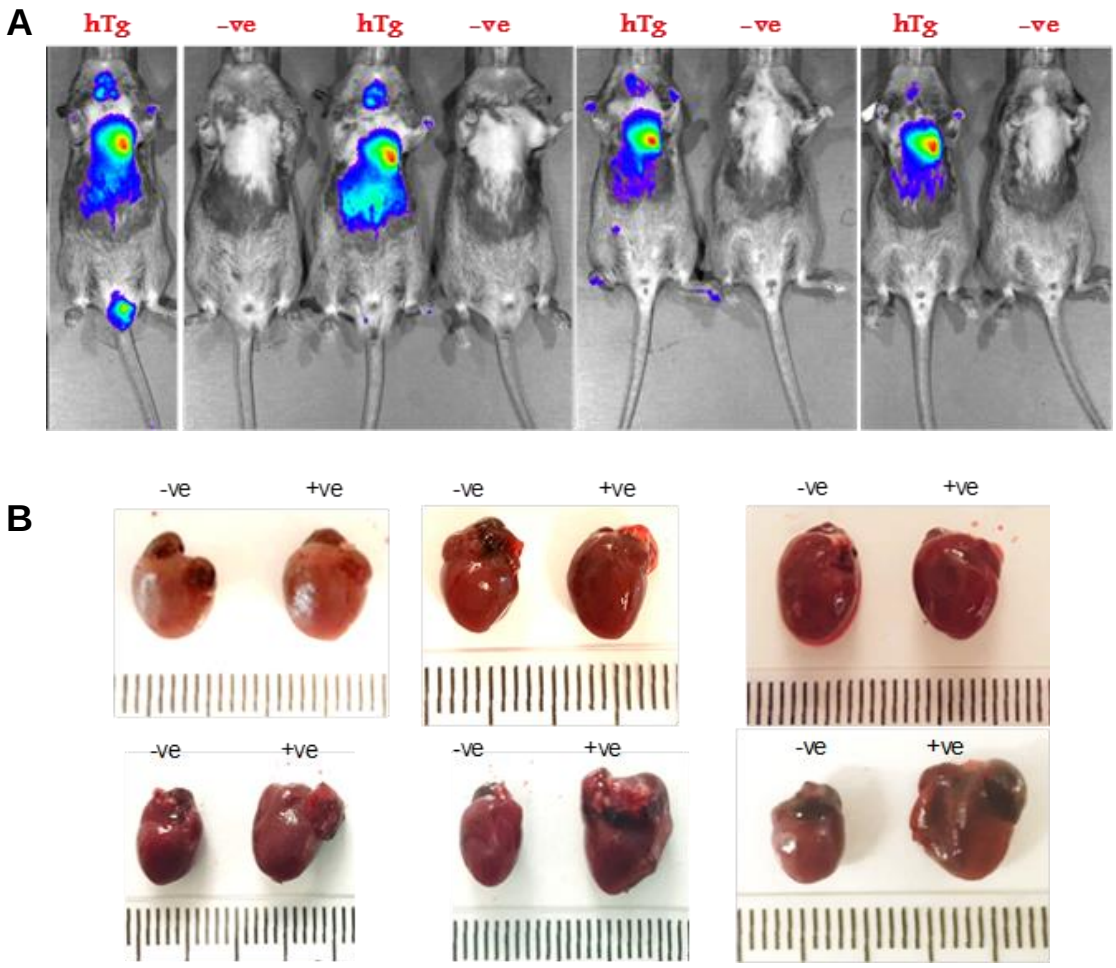

Figure 33. Cardiomyocyte specific KLF8 transgenic mice heart samples

(A) Cardiomyocyte specific KLF8 transgenic mice (KLF8-hTg) didn't show very clear lean phenotype in BLI. (B) KLF8-hTg mice had enlarged heart compared to their negative controls (Negative controls include floxed control, cre control and WT control). The hearts on the top row were collected before heart became dilated for PCR array study.

Table 4. Hemodynamic analysis of Cardiomyocyte specific KLF8 transgenic mice

	LVIDd (cm)	LVIDs (cm)	LVPWd (cm)	LVPWs (cm)	IVS,d (cm)	IVS,s (cm)	EF (%)	FS (%)
KLF8-hTg(9)	0.35 ± 0.03	0.23 ± 0.03	0.1± 0.018	0.12 ± 0.002	0.09 ± 0.01	0.128 ± 0.01	62 ± 5.3	33 ± 5
Floxed Control (5)	0.34 ± 0.02 P = 0.78	0.18 ± 0.01 P = 0.01	0.12 ± 0.008 P= 0.09	0.15± 0.01 P= 0.06	0.096 ± 0.02 P= 0.51	0.15 ± 0.01 P= 0.09	79 ± 3.1 P = 0.001	47 ± 3.6 P = 0.0002
Cre Control (2)	0.35 ± 0.02 P = 0.7	0.18 ± 0.007 P = 0.001	0.13 ± 0.002 P= 0.01	0.16 ± 0.001 P= 0.09	0.087 ± 0.04 P= 0.7	0.15 ± 0.01 P= 0.25	84 ± 4 P = 0.01	53 ± 5.5 P = 0.01
WT Control (3)	0.34 ± 0.04 P = 0.7	0.16 ± 0.02 P = 0.01	0.11 ± 0.03 P= 0.87	0.14 ± 0.02 P= 0.24	0.086± 0.004 P= 0.48	0.133 ± 0.01 P= 0.69	82 ± 6.5 P = 0.01	50 ± 6 P = 0.001

Hemodynamic analysis was done from 1 month old mice. This table demonstrated 3 months old mice data. Numbers are mean6SEM. LV, left ventricle; IVSd, intraventricular septum diastolic; LVIDd, left ventricle inner diameter diastolic; LVPWd, left ventricle posterior wall diastolic; %EF, percentage of ejection fraction, %FS, Fractional shortening.

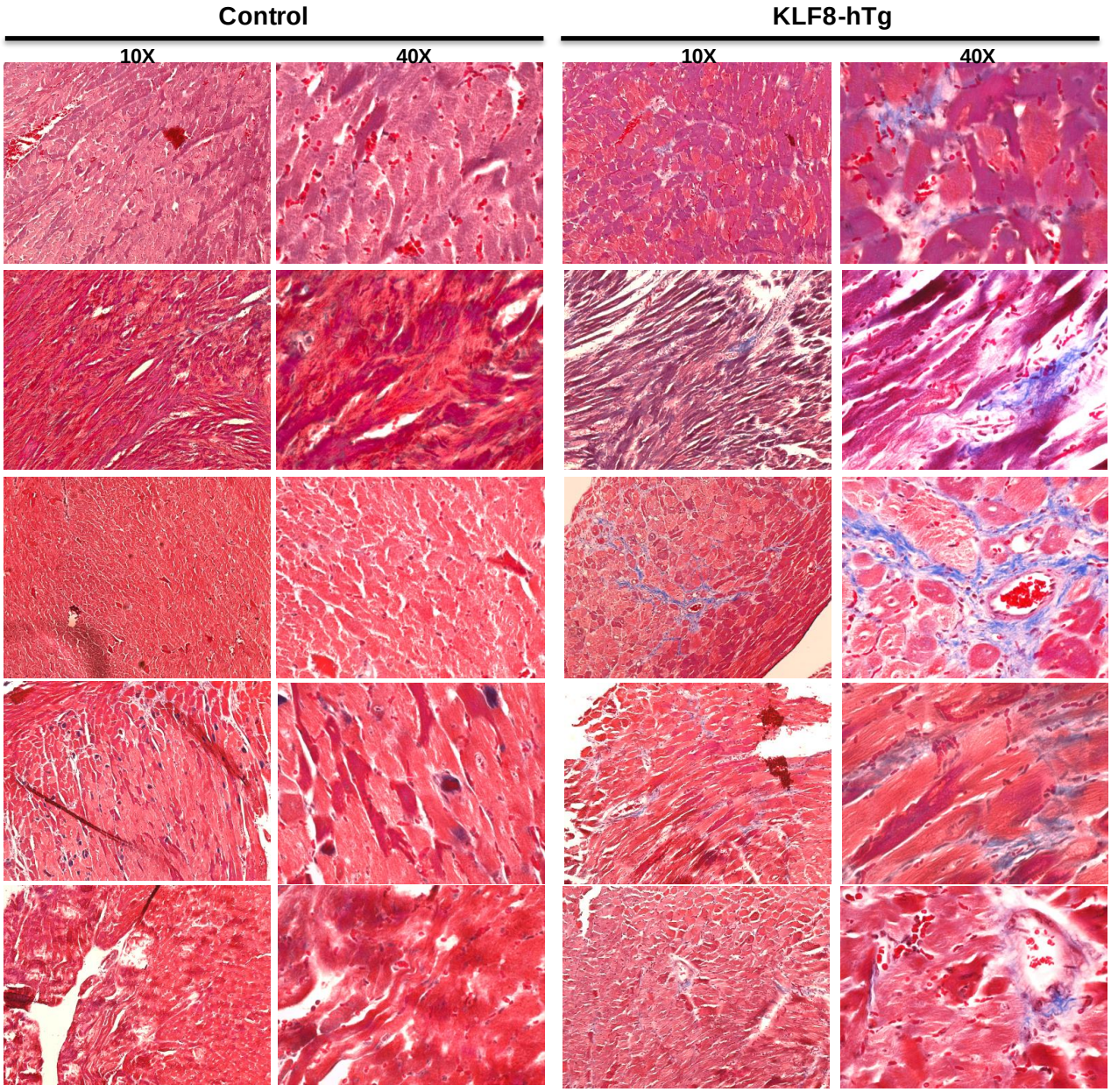

Figure 34. KLF8-hTg mice hearts showed much increased myocardial fibrosis

Representative images of KLF8-hTg mice hearts' masson's trichrome staining revealed significantly higher myocardial fibrosis (primarily in the ventricular area) in positive mice compared to negative controls (Light blue color indicates fibrosis).

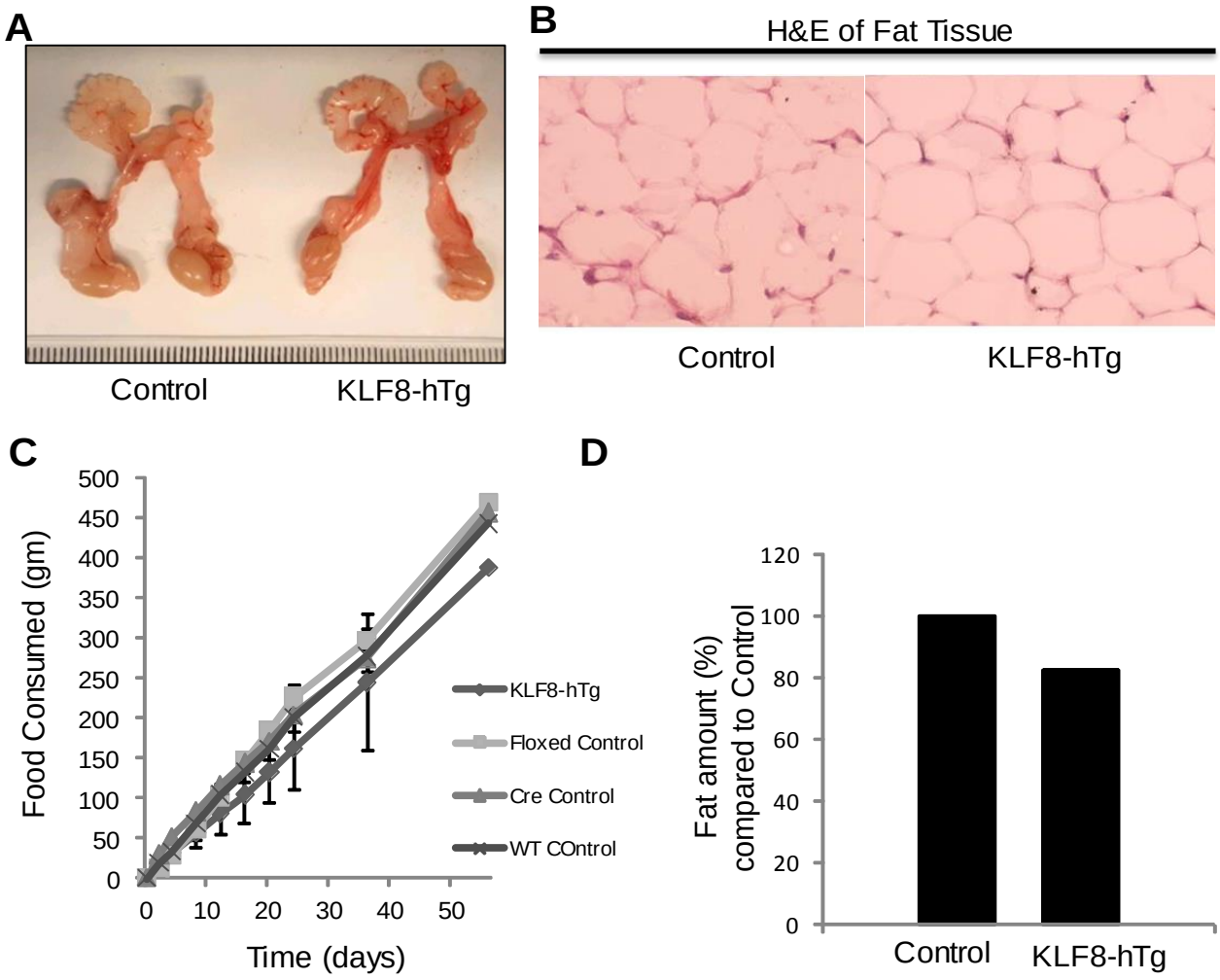

Figure 35. Cardiomyocyte specific KLF8 transgenic mice didn't show significant difference in the fat phenotype.

(A-B) KLF8-hTg mice didn't show significant decrease in fat volume and adipocyte cell size. (C-D) We performed food consumption test with these mice (n=3) and the results demonstrated no significant change in food uptake which would have excluded food consumption difference as a cause for any fat phenotype observed.

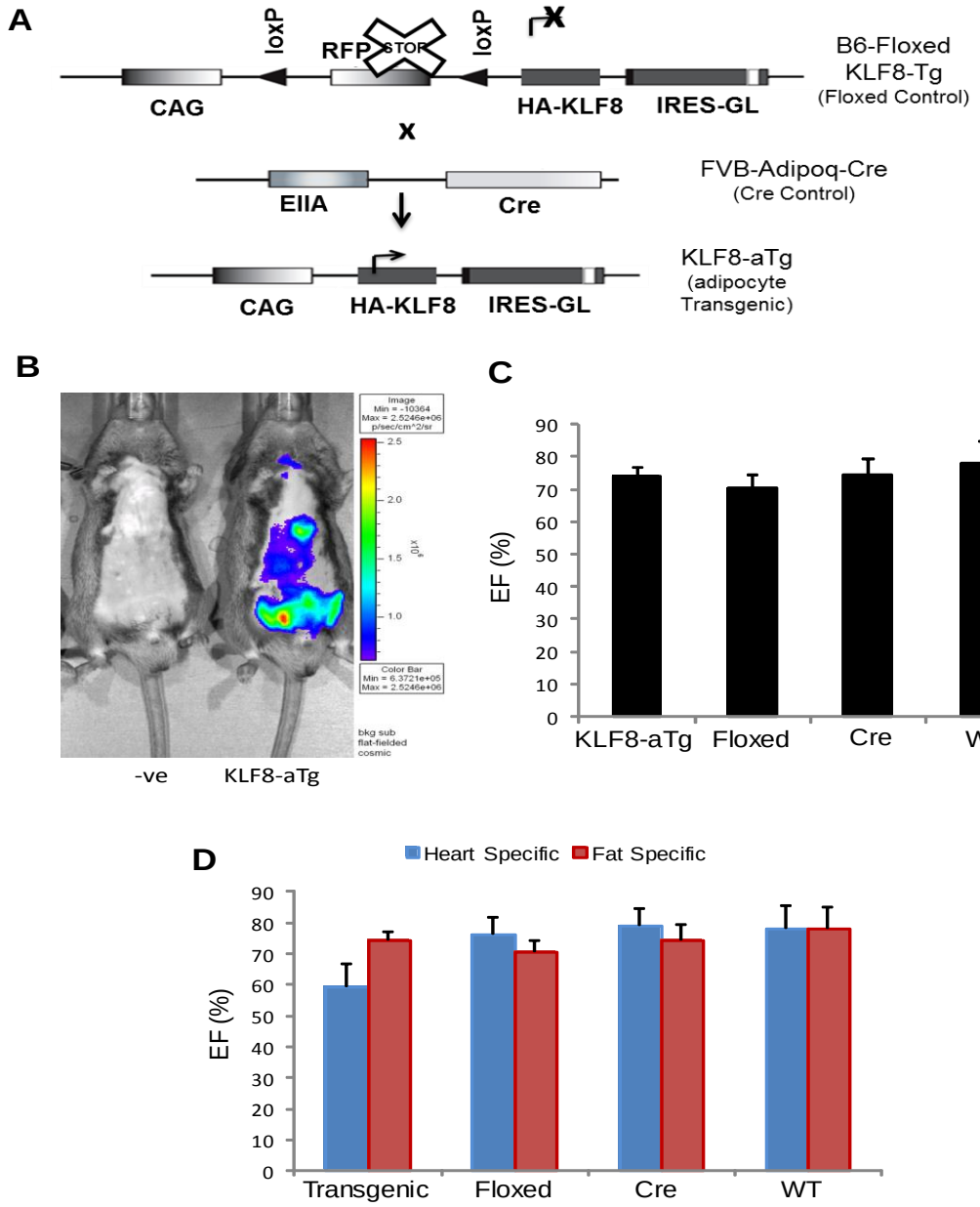

Figure 36. Adipocyte specific KLF8 overexpression didn't show cardiomyopathy

(A) Construction of adipocyte specific KLF8 transgenic mice (KLF8-hTg): FVB-B6-floxed-KLF8 (8^{th} generation) mice were crossed with C57BL/6J;FVB/NJ-Adipoq-Cre mice. We got 4 different offsprings including KLF8-hTg, floxed control, Cre control and WT control mice. (B) BLI identified abdominal fat specific luminescence in the KLF8-aTg mice compared to the negative control. (C) Ultrasound with KLF8-aTg mice along with its control didn't show any significant change in cardiac function in transgenic mice. (D) We compared cardiac function of 2 months old KLF8-aTg and KLF8-hTg mice which revealed significant cardiac dysfunction in KLF8-hTg mice.

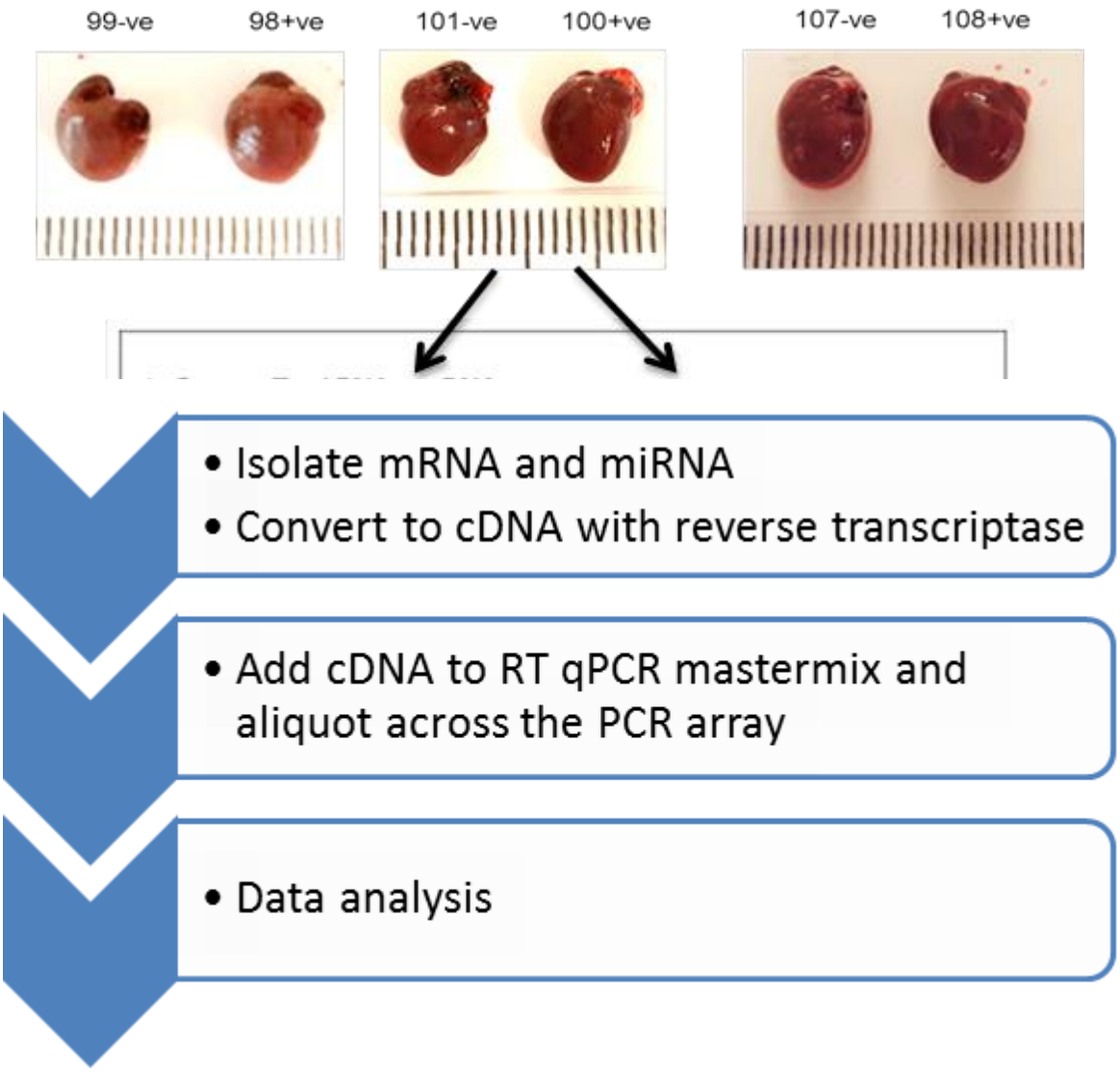

Figure 37. Schematic diagram of cardiovascular mRNA and miRNA PCR array (SABioscience)

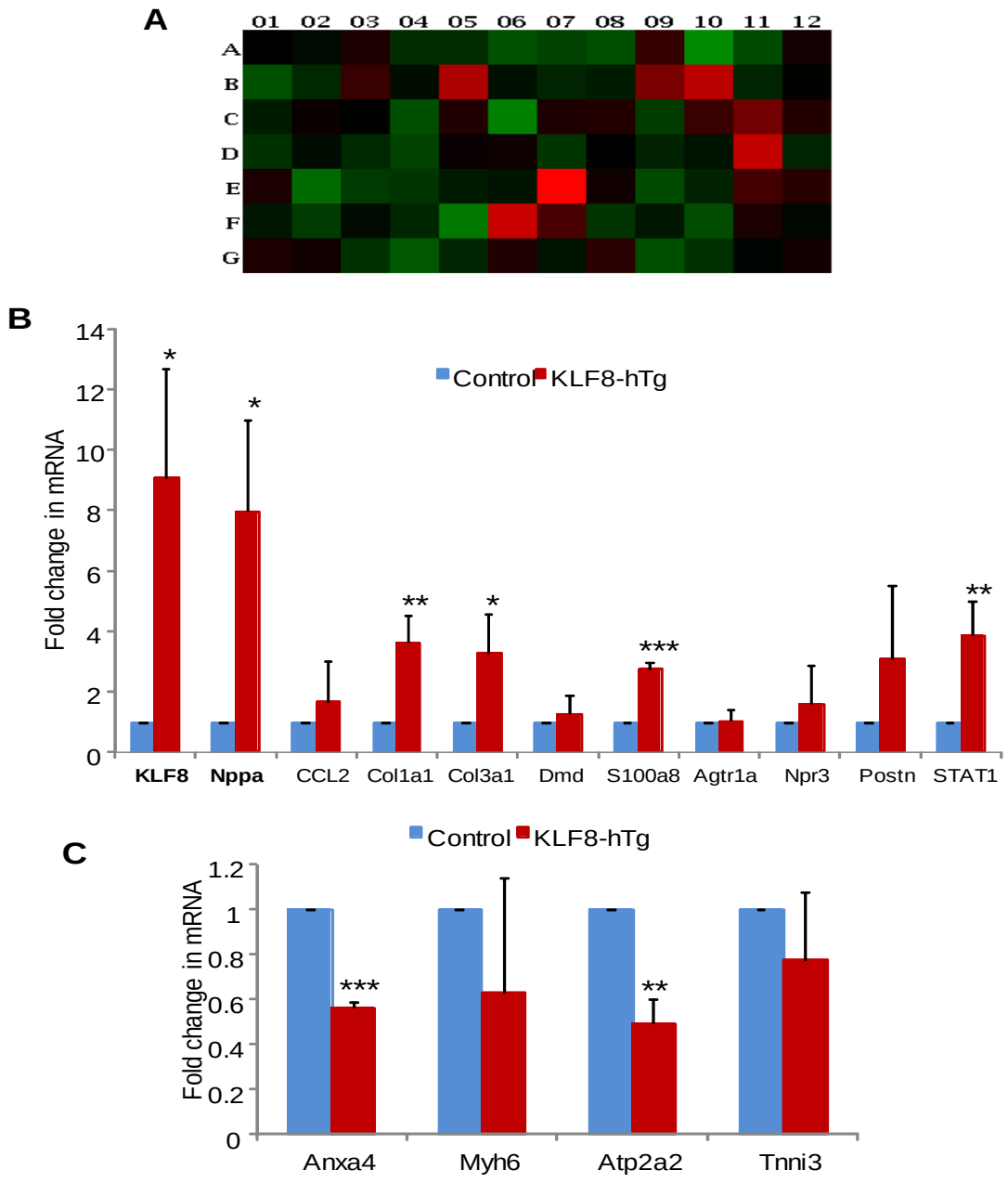

Figure 38. Cardiovascular disease mRNA PCR array

(A) Heat map of cardiovascular disease mRNA PCR array (N=3). qPCR to validate KLF8 upregulated (B) and downregulated (C) mRNA targets in cardiomyopathy.

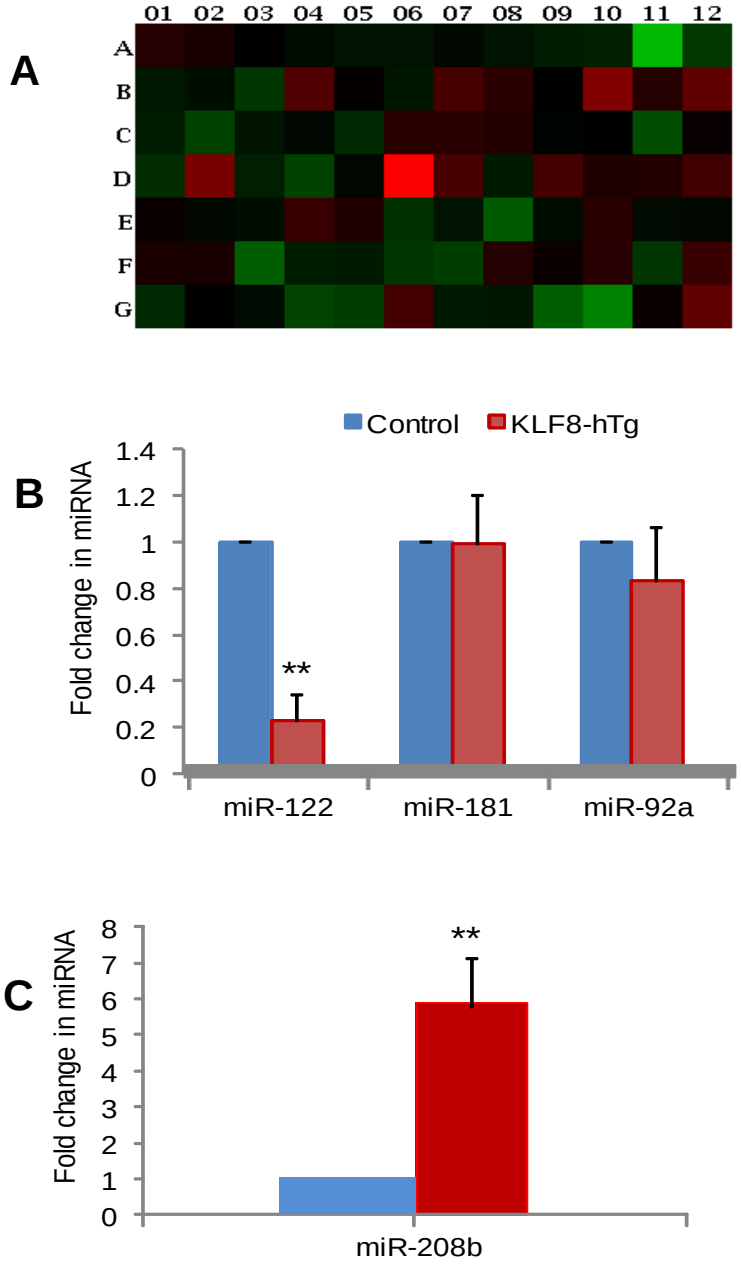

Figure 39. Cardiovascular disease miRNA PCR array

(A) Heat map of cardiovascular disease miRNA PCR array (N=3). qPCR to validate KLF8 upregulated (B) and downregulated (C) miRNA targets in cardiomyopathy.

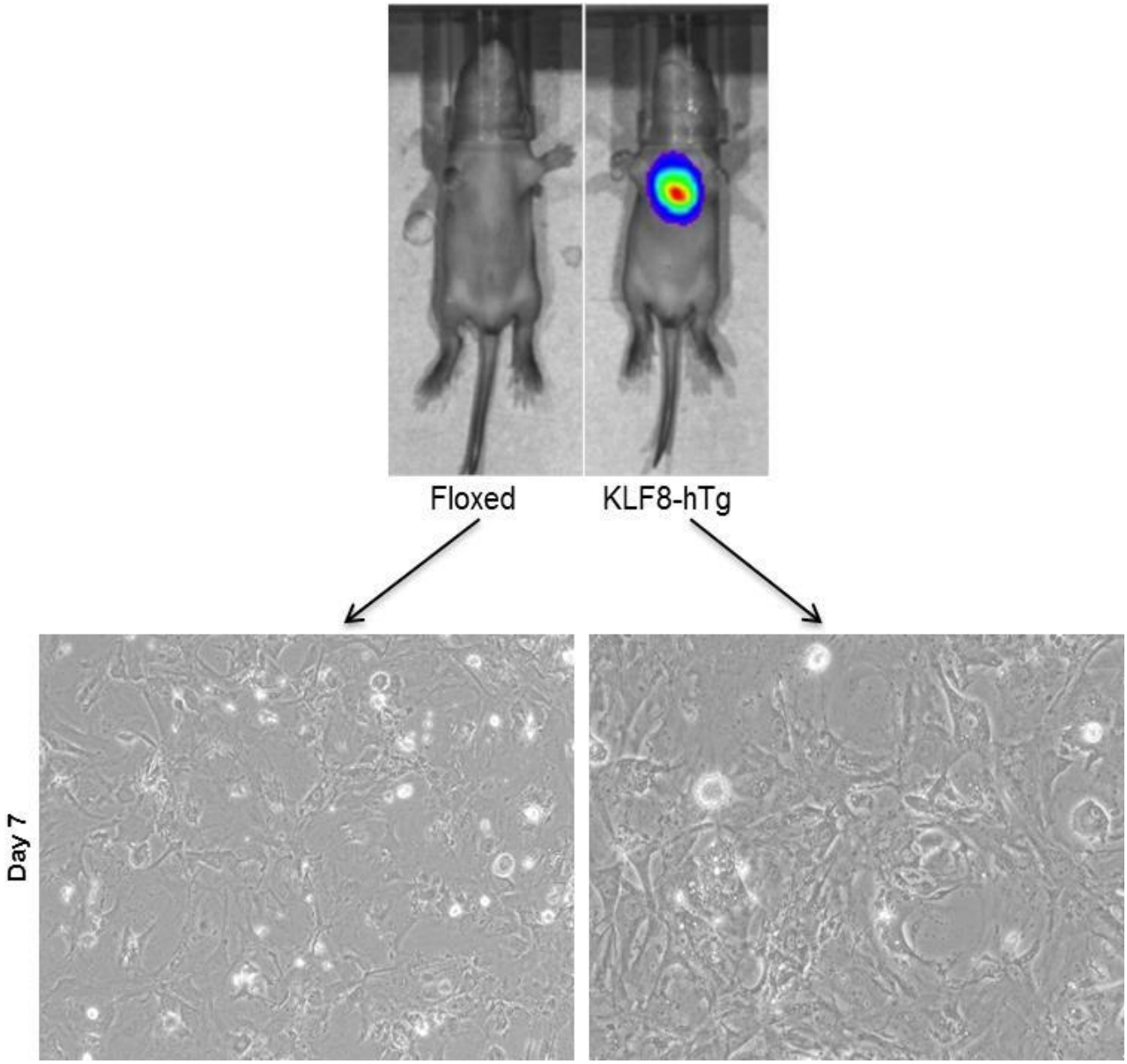

Figure 40. Isolation of primary cardiomyocytes

Primary cardiomyocyte was isolated and cultured from 5 days old KLF8-hTg mice and their littermate controls using Pierce™ Primary Cardiomyocyte Isolation Kit.

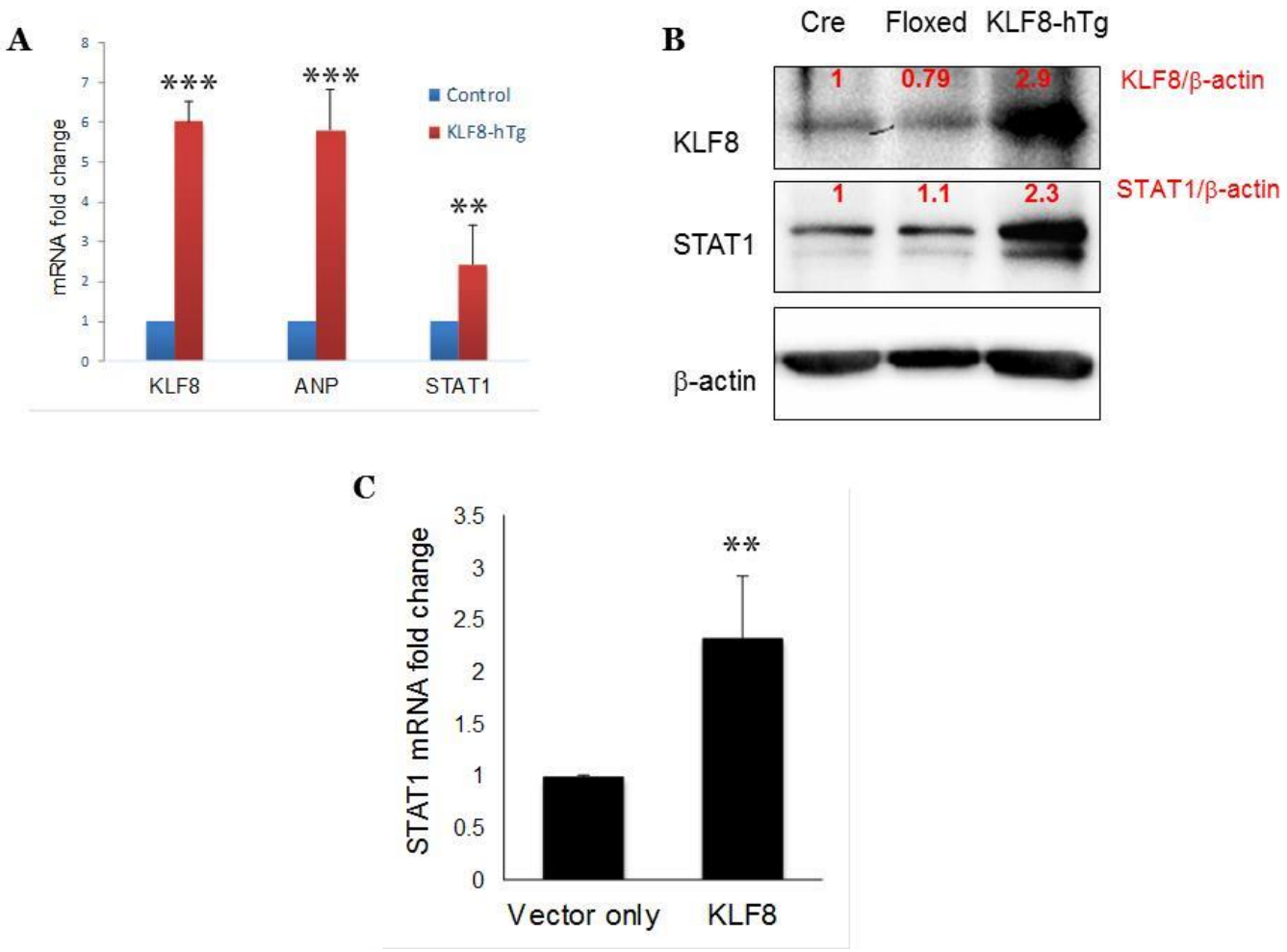

Figure 41. STAT1 upregulation in isolated primary cardiomyocytes from KLF8-hTg mice

(A) Validating mRNA fold increase in KLF8, ANP and STAT1 in KLF8-hTg cardiomyocytes compared to floxed control. (B) Western blot showed increase in both KLF8 and STAT1 expression in KLF8-hTg mouse cardiomyocytes. (C) KLF8 transient transfection in 293FT cells further induced increase in STAT1 expression suggesting KLF8 mediated upregulation of STAT1.

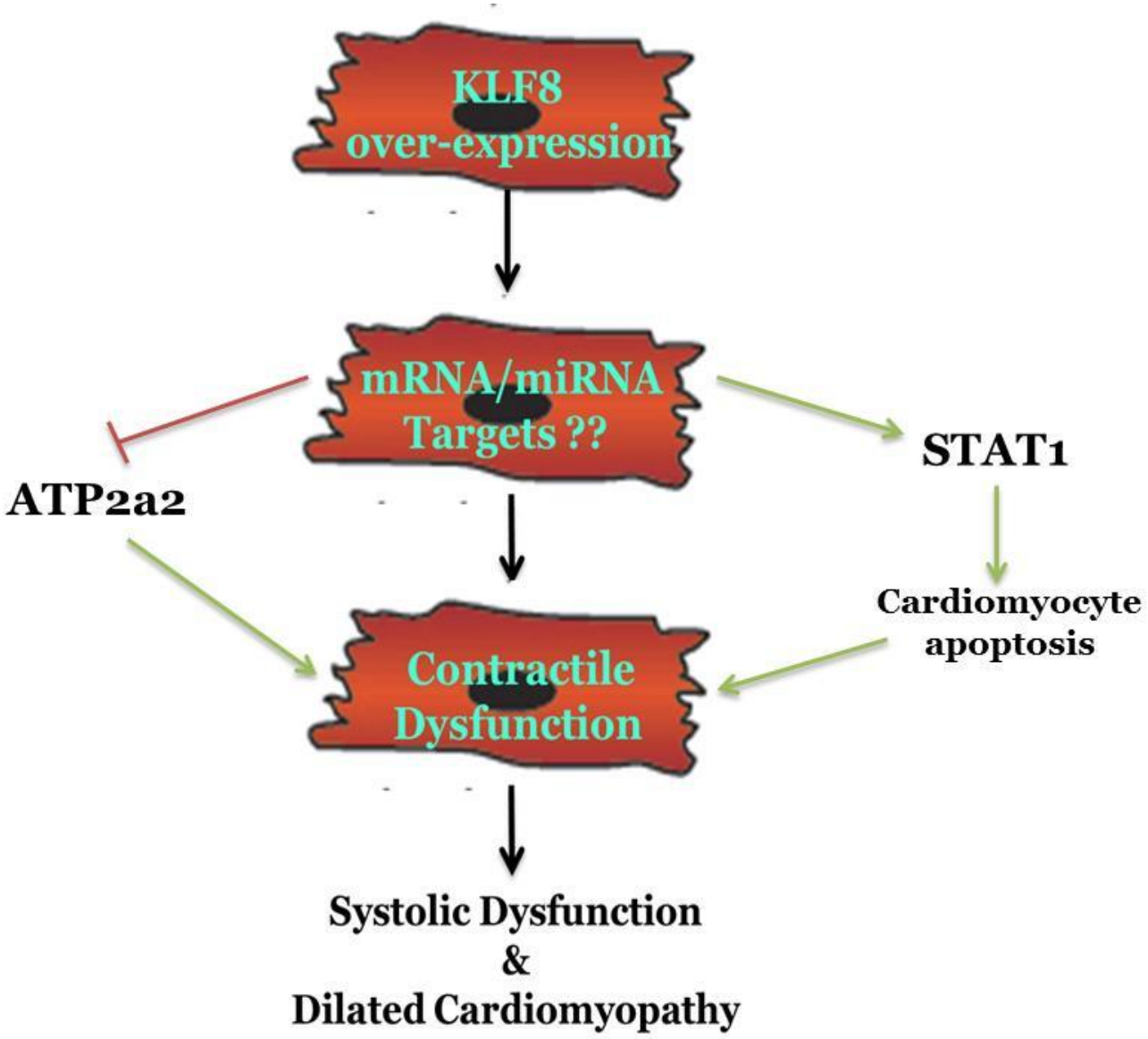

Figure 42. Proposed schematic model of KLF8 mediated dilated cardiomyopathy

KLF8 over expression in cardiomyocyte upregulates and downregulates several critical mRNA and miRNA targets. Two of the most potentially important target gene are STAT1 and ATP2a2. KLF8 mediated upregulation of STAT1 can lead to cardiomyocyte apoptosis, further promoting systolic dysfunction and dilated cardiomyopathy. KLF8 mediated downregulation of ATP2a2 can potentially lead to decrease in cardiomyocyte contractility and systolic dysfunction.

CHAPTER 4: CONCLUSION

Overall my work addresses two novel characteristic of KLF8. KLF8, a dual transcription factor have been implicated in promoting different cancer progressions. Both independent studies in parallel provide unexplored KLF8 behavior and function. One of these studies identifies a novel post-translational modification of KLF8 in context of cancer while the other discovers a novel unknown function in KLF8 in cardiomyopathy, thereby implying the increasing physiological importance of this protein. We constructed the first KLF8 transgenic model which is not only essential for this current study but also provides an outstanding tool in both KLF8 and cardiovascular research field.

Various post-translational modifications including sumoylation, acetylation, parylation have been found to regulate KLF8 function, localization and expression. We discovered a novel phosphorylation of KLF8 at serine 48 to add in the KLF8 post-translational modification paradigm. ERK2 was identified as the responsible kinase in phosphorylating KLF8 at this novel site. Further studies revealed that ERK2 phosphorylation of KLF8 is critical for its protein stability and involvement in cancer cell migration. In absence of Serine 48 phosphorylation, KLF8 had much shorter half-life and potential for promoting cancer cell migration in vitro. Taken together, this study not only discovers the novel site on KLF8 but also links ERK2 to KLF8 in order to establish

as a downstream effector of MAP kinase pathway. Inter regulatory role between different post-translational modification of a same protein has found to be critical for their physiological function. In view of KLF8, sumoylation and acetylation act against each other to regulate transcriptional regulator function of KLF8. In one of the KLF8 mutants (d31-35) with hyper phosphorylation state, we observed an evident change in KLF8 sumoylation pattern which suggests that this novel phosphorylation site of KLF8 might be critical for the other post-translational modification. This study also provides critical future directions by revealing few novel sites of KLF8 like P37, P38, E39, I40 mutants which affect KLF8 motility and expression pattern. We also discovered two interesting motifs on KLF8 N terminal 31-35 and 36-40 region, which have intraregulatory role on phosphorylation at Serine 48. While the first motif negatively regulates S48 phosphorylation, the second one activates it which suggests potential protein phosphatase binding to KLF8 to the first motif and ERK2 binds to the second motif. Investigating the mechanism of these motifs can potentially discover novel interacting partners, structure, functions of KLF8 advancing our understanding on KLF8 further. Finally this study suggests a novel nuclear degradation mechanism of KLF8 which is more relevant as KLF8 localization in nucleus is critical for its function. Post-translational modifications have been implicated to regulate a protein function by various studies. KLF8 S48 phosphorylation was also proved to be essential in KLF8 mediated cancer cell migration. Taken together, we identified a novel phosphorylation site of KLF8 critical for its stability, ERK2 as the upstream kinase and a novel ERK2-KLF8 signaling axis linking to KLF8 mediated breast cancer cell migration providing a great potential for future research on KLF8 as an oncogene.

KLF8 involvement in cancer has been studied in vitro and xenograft model so far. To investigate role of KLF8 in a better physiologically relevant context, we constructed the first novel KLF8 transgenic mice. As mentioned before, being equipped with Cre-loxp, these transgenic mice provide great potential to study tissue specific function of KLF8. We also constructed a KLF8 KO mouse model which is not elucidated in this study. Our KLF8 transgenic mice with KLF8 expression globally started dying much earlier compared to control mice and later on dilated cardiomyopathy was identified as the potential cause of this higher mortality. Cardiomyocyte specific KLF8 transgenic mice unveiled that the systolic dysfunction and dilated cardiomyopathy phenotype is an effect of KLF8 overexpression in cardiomyocytes. No studies to our knowledge, have demonstrated any involvement of KLF8 in cardiac tissue till date which makes these finding extremely novel and exciting. This further implies the significance of exploring a protein's function in genetically engineered mouse model.

Diverse studies demonstrated that Kruppel like factors shared some critical function. Since discovering this novel function of KLF8 in cardiomyopathy in KLF8 transgenic mouse model, we wanted to review the literature to evaluate transgenic or knock out mouse models of other KLF members to investigate the involvement of this family genes in cardiomyopathy. Krüppel-like Factor 2 (KLF2), also known as lung Krüppel-like Factor (LKLF) is involved in lung development, T-Cell viability and adipogenesis.KLF2 ko mice were embryonic lethal and died at embryonic 12.5 to 14.5 days due to severe intra-embryonic and intra-amniotic hemorrhaging[222]. It was found

that KLF2 is an important factor for blood vessel formation as lack of KLF2 led to thin blood vessel wall and thin arteries. Vascular smooth muscle cells in the aortae from the LKLF-/- animals displayed a cuboidal morphology and failed to organize into a compact tunica media [223]. As KLF2-/- mice were embryonic lethal, not much post-natal application of these mice are available. Cell specific knock out of KLF2 showed delayed lung development, defective T cells and defective adipocyte differentiation [224-227]. Myeloid cell specific KLF2 inactivation increases Atherosclerosis in hypercholesterolemic mice[228, 229]. KLF3 originally termed Basic Krüppel-like Factor (BKLF) acts mainly as a transcriptional repressor. KlF3 knockout mice have less white adipose tissue, and their fat pads contain smaller and fewer cells[230]. Overexpression of Klf3 inhibits adipocytic differentiation of 3T3-L1 cells in vitro[230]. Krüppel-like Factor 4 (KLF4), also known as gut enriched Krüppel-like Factor (GKLF) is a tumor suppressor in colon cancer. It also plays important role in regulating adipogenesis. KLF4 has been proved to be a critical factor in inducing pluoripotent stem cells along with other known factors like Sox2, nanog[231]. In vitro studies have suggested that Klf4 plays an important role in skin cell proliferation and/or differentiation [232]. Mice homozygous for a null mutation in Klf4 die within 15 hours of birth and show selective perturbation of late-stage differentiation structures in the epidermis. Klf4–/– mice possessed a defective epidermal barrier which was the cause of death [233]. Klf4−/− mice also show abnormal differentiation of goblet cells but not colonocytes or enteroendocrine cells in the colon. These mice also showed altered expression of goblet cell marker Muc2 [234]. Expression of Kruppel-like factor KLF4 in mouse hair follicle stem cells contributes to cutaneous wound healing[235]. Induction of KLF4 in basal keratinocytes blocks the

proliferation−differentiation switch and initiates squamous epithelial dysplasia [232]. Endothelial Kruppel-like factor 4 protects against atherothrombosis in mice. By in vivo EC-specific KLF4 overexpression it was found that KLF4 induced an antiadhesive, antithrombotic state [236]. Krüppel-like Factor 5 (KLF5), also known as intestinal enriched Krüppel-like Factor (IKLF) is involved in intestinal homeostasis, cardiac remodeling, lung maturation, adipogenesis. It has been also shown to be involved in breast and prostate cancer. KLF5 knockout mouse was embryonic lethal at E8.5 days [237]. Heterozygous and tissue specific knock out of KLF5 showed reduced cardiac fibrosis and hypertrophy in response to stress [238]. It also showed deficiencies in white adipose tissue formation, defective lung morphogenesis [239, 240]. Other studies showed that the TIEG−/− knock-out mouse developed features of cardiac hypertrophy including asymmetric septal hypertrophy, an increase in ventricular size at age 16 months, an increase (214%) in mouse heart/weight body weight ratio TIEG−/−, and an increase in wall thickness in TIEG−/− mice of (1.85 ± 0.21 mm), compared to the control (1.13 ± 0.15 mm, $P < 0.04$). Masson Trichrome staining demonstrated evidence of myocyte disarray and myofibroblast fibrosis[241]. KLF10-/- mice showed increased skin tumor formation and acts as a tumor suppressor[242]. KLF11 also known as TIEG2 (transforming growth factor β (TGF-β)-inducible gene) plays important role in cardiac hypertrophy. It also plays tumor suppressor role in pancreatic cancer. Cardiac-specific KLF11 transgenic mice do not show any difference from their littermates at baseline. However, cardiac-specific KLF11 overexpression protects mice from TAC-induced cardiac hypertrophy[243]. KLF11 knockout mice showed normal development and life span. One recent study showed that KLF11 knockout mice (Klf11−/−) showed

decreased Mono Amine Oxidase A (MAO A) mRNA expression and catalytic activity, which supports the substantial role of KLF11 in the up-regulation of MAO A[244]. Interestingly, the differences in MAO A expression were readily amplified after dexamethasone exposure. KLF13 is involved in cardiac development, T-cell and B-cell development. Krüppel-like factor 15 also known as KKLF (kidney-enriched Krüppel-like factor) is a regulator of cardiac hypertrophy. It also plays important role in gluconeogenesis. Overexpression of KLF15 transcription factor in adipocytes of mice results in down-regulation of SCD1 protein expression in adipocytes and consequent enhancement of glucose-induced insulin secretion [245]. KLF15/A mice are transgenic mice specifically overexpressing transcription factor KLF15 (Kruppel-like factor 15) in skeletal muscle. This strain expresses full-length cDNA encoding mouse KLF15 under the control of human α actin promoter. This strain doesn't show specific phenotype, but it's suggested that KLF15 may increase GLUT4 expression level [246, 247]. KLF15-null mice are viable but, in response to pressure overload, develop an eccentric form of cardiac hypertrophy characterized by increased heart weight, exaggerated expression of hypertrophic genes, left ventricular cavity dilatation with increased myocyte size, and reduced left ventricular systolic function[248]. KLF15-/- liver and skeletal muscle show markedly reduced mRNA expression of amino acid-degrading enzymes. Furthermore, the enzymatic activity of alanine aminotransferase (ALT), which converts the critical gluconeogenic amino acid alanine into pyruvate, is decreased in KLF15-/- hepatocytes. This leads to hypoglycemia in KLF15-/- mice [249, 250]. One recent study showed that KLF15 plays an important role in cardiac lipid metabolism[251].

We are currently investigating KLF8 regulated mRNA and miRNA targets in the onset of dilated cardiomyopathy in transgenic mice. We are also characterizing adipocyte specific KLF8 transgenic mice to evaluate KLF8 mediated decrease in white adipose tissue accumulation. In addition, we constructed KLF8 mammary specific transgenic mouse by crossing FVB-floxed-KLF8 with FVB-MMTV-Cre mouse. These mice are being observed for mammary tumorigenesis to asses KLF8 role in breast cancer in vivo. KLF8 KO mice model for these different tissues are also maintained providing an ideal platform to evaluate critical role of KLF8 in diverse diseases. Currently identified mRNA targets of KLF8 from KLF8-hTg hearts include Nppa, Stat1, S100a8, Col1a1, Col3a1, ATP2a2 and Anxa4. Some of these targets might be indirectly regulated by KLF8. Nppa or natriuretic peptide A is a heart muscle secreted hormone which is responsible for controlling blood pressure by clearing fat and other metabolites from circulation. Nppa or ANP is a known biomarker for cardiovascular diseases and it is upregulated during heart failure [252, 253]. Nppa upregulation in KLF8-hTg mice can be the response of systolic dysfunction but we will validate if there is any direct KLF8 mediated regulation of Nppa in these mice which might contribute to the cardiac phenotype. Signal transducers and activators of transcription (STAT1) is one of the other important upregulated targets in these mice hearts. STAT1 has been found to be overexpressed in cardiomyocytes during ischemic injury [214, 215]. These studies further demonstrated that STAT1 activates pro-apoptotic factor caspase 1 to promote cardiomyocyte apoptosis. We also observed increased cardiomyocyte apoptosis in KLF8-gTg hearts. KLF8 might activate this apoptotic pathway through caspase 1 by

upregulating STAT1 expression in cardiomyocytes. STAT1 inhibitors have been used to prevent cardiac hypertrophy [212, 216]. STAT-1 has been also found to be involved in mediating myocardial fibrosis [254, 255]. Col1a1 and Col3a1 genes are critical for collagen synthesis during cardiac remodeling and fibrosis [256]. S100 calcium-binding protein A8 (S100A8) is a protein, also known as calgranulin A is a calcium binding protein. There has not been much research about this protein in dilated cardiomyopathy. Although one study recently showed that S100a8 exasperate post-ischemic heart failure by activating both MAP kinase and NF-kB pathway [257]. KLF8 has been previously identified to activate EGFR/ERK and NF-kB signaling pathway. This link through KLF8 mediated upregulation of S100a8 might prove critical for cardiomyopathy. KLF8-hTg mice heart mRNA PCR array found ATP2a2 and Anxa4 as the downregulated targets. ATP2a2 or Serc2a2 has been discussed before in chapter 3 discussions. Anxa4 or Annexin 4A is a calcium dependent phospholipid binding protein. It is critical for cardiomyocyte contraction. One study showed that Annexin 4 is upregulated in failing heart [258]. We have to investigate further to interpret this result.

KLF8-gTg mice showed a very prominent fat phenotype other than the predominant cardiac phenotype. KLF8-gTg mice had significantly less epididymis and reproductive white adipose fat compared to littermate control. White adipose tissue cells were much smaller in size in KLF8-gTg mice. We didn’t observe this phenotype in KLF8-hTg mice as evident as KLF8-gTg. This result suggested a different KLF8 mediated signaling cascade regulating this fat phenotype. Our hypothesis was further strengthened when we observed KLf8-Ko mice showing excessively increased white fat

compared to their littermate controls (data not shown). We started constructing adipocyte specific KLf8 transgenic mice (KLF8-aTg) to decipher this mystery. This part of research is still in progress. We didn't observe body weight change in these mice yet. We sacrificed one pair of KLF8-aTg mice of 4 months of age. After necropsy, we observed little reduction in primarily brown adipose tissue (Fig 43). H&E staining didn't show much difference in white and brown adipose tissue morphology between KLF8-aTg and its littermate floxed control mice (Fig 44). To unveil the metabolism of KLF8-gTg mice, we performed glucose and insulin tolerance test with KLF8-gTg mice. Interestingly, our preliminary results showed significant increase in glucose and insulin tolerance in KLF8-gTg mice compared to its littermate controls (Fig 45 A-B) further linking to the reduced fat phenotype. We also performed these experiments with KLF8-hTg mice to investigate if cardiomyocyte expression of KLF8 has any role to play in metabolism although we didn't see any evident phenotype. Surprisingly, we observed a similar increased glucose and insulin tolerance trend in KLF8-hTg mice (Fig 45 C-D) which further suggests that KLF8 expression in cardiomyocytes might have a partial role to play in this fat phenotype and there might be a novel systemic role of KLF8 in initiating both these cardiac and fat phenotypes. Excitingly KLF8 global KO had decreased glucose tolerance and increased insulin resistance which is a potential prediabetes condition (data not shown). Overall it also proposes that KLF8 might have a protective role in diabetes and KLF8-gTg mice might develop obesity and diabetes later than control mice in a high fat diet induced experiment. Further investigation in this regard have immense potential of discovering a novel unknown role of KLF8 in adipogenesis.

Our primary aim was to study tumorigenesis in KLF8 transgenic mice as KLF8 function has been mostly researched in different cancers. Our KLF8-gTg mice were dying much earlier because of dilated cardiomyopathy and possibly masked any possible tumorigenesis as spontaneous tumorigenesis takes a long time to develop. Excitingly two pairs of KLF8-gTg mice which were alive till 8 months of age demonstrated tumor like structure. One of the KLF8-gTg mice developed testicular tumor and other one developed mammary hyperplasia. Both of these tumor-like tissues were positive for ki-67 staining. To study tumorigenesis mediated by KLF8 in a greater extent, we developed first mammary specific KLF8 transgenic mice by crossing FVB-floxed-KLF8 and FVB-MMTV-Cre mice. Currently these mice are kept under observation for any potential mammary tumorigenesis. As KLF8 role in cancer has been elucidated in different tissues, our floxed KLF8 mice can be crossed with various tissue specific Cre mice to identify KLF8 role in multiple cancer and other unknown diseases.

Finally, this work has extended the knowledge on KLF8 in cancer and cardiovascular research to great measures. Identification of ERK2 mediated KLF8 phosphorylation proposed a new feedback loop including KLF8/EGFR/ERK2/KLF8-p which might be critical for KLF8 mediated tumorigenesis and metastasis. Further, this project identifies various critical amino acids for KLF8 structure which later can reveal novel regulation of KLf8. We established the first KLF8 transgenic and knock out mouse model in a Cre-loxP induced system which will be a great asset to dissecting KLF8 function in different diseases. Our work on KLF8 in cardiomyopathy is the first literature on KLF8 involvement in heart failure and future research exploring the underlying

mechanism will give rise to novel KLF8 mediated signaling cascades in onset of fatal dilated cardiomyopathy. Future goal will be to inhibit KLF8 with small molecule inhibitors in order to prevent progression of this disease. Overall, this work will establish KLF8 as a novel therapeutic target of both cardiomyopathy and cancer, two most deadly diseases in our time.

Figures

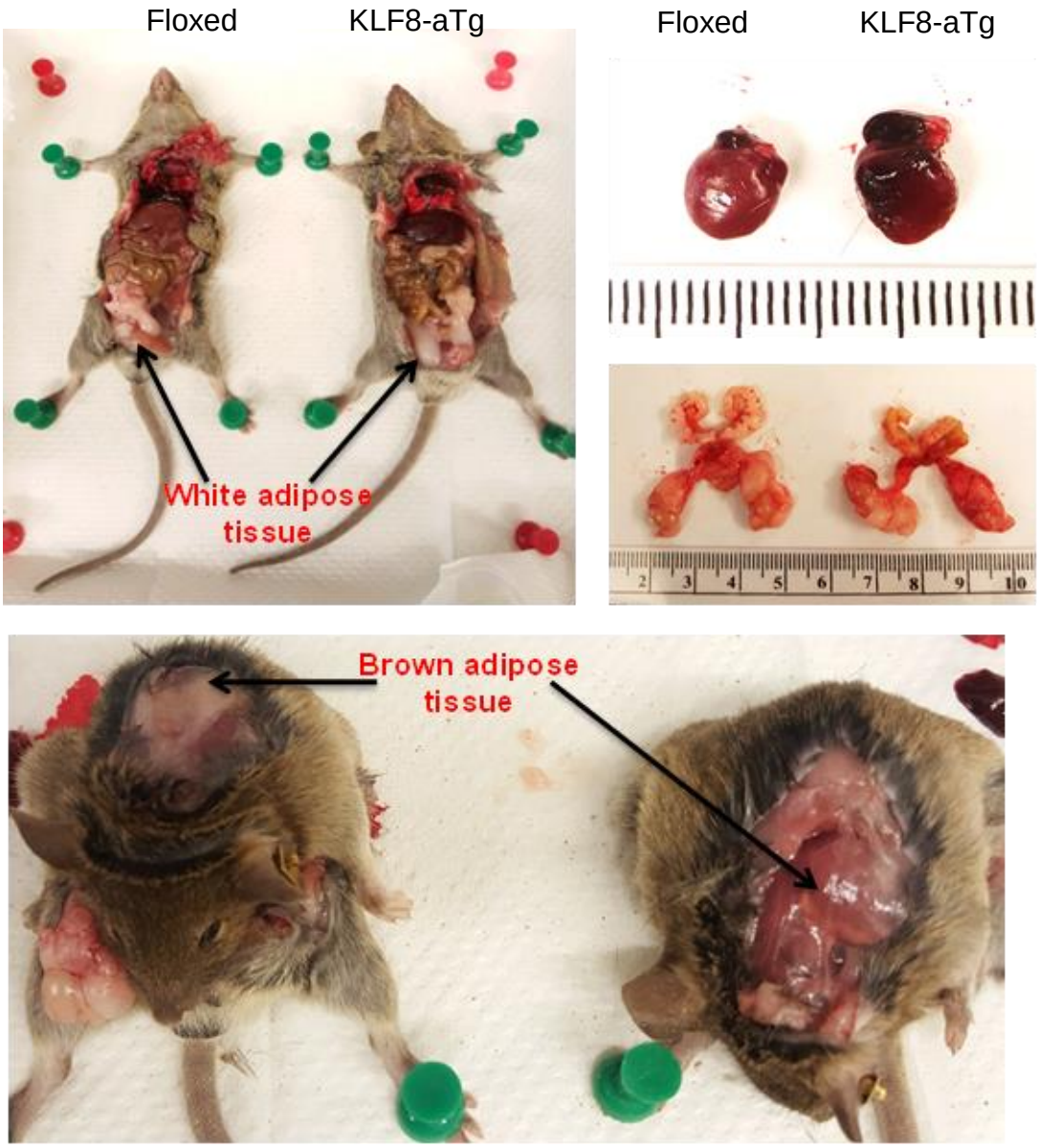

Figure 43. KLF8-aTg mice necropsy

KLF8-aTg mice of 4 months of age were sacrificed along with floxed control mice. We didn't observed significant change in white adipose tissue (both abdominal and reproductive fat). We observed a slight decrease in brown fat volume. These mice are currently under observation for any phenotypic change.

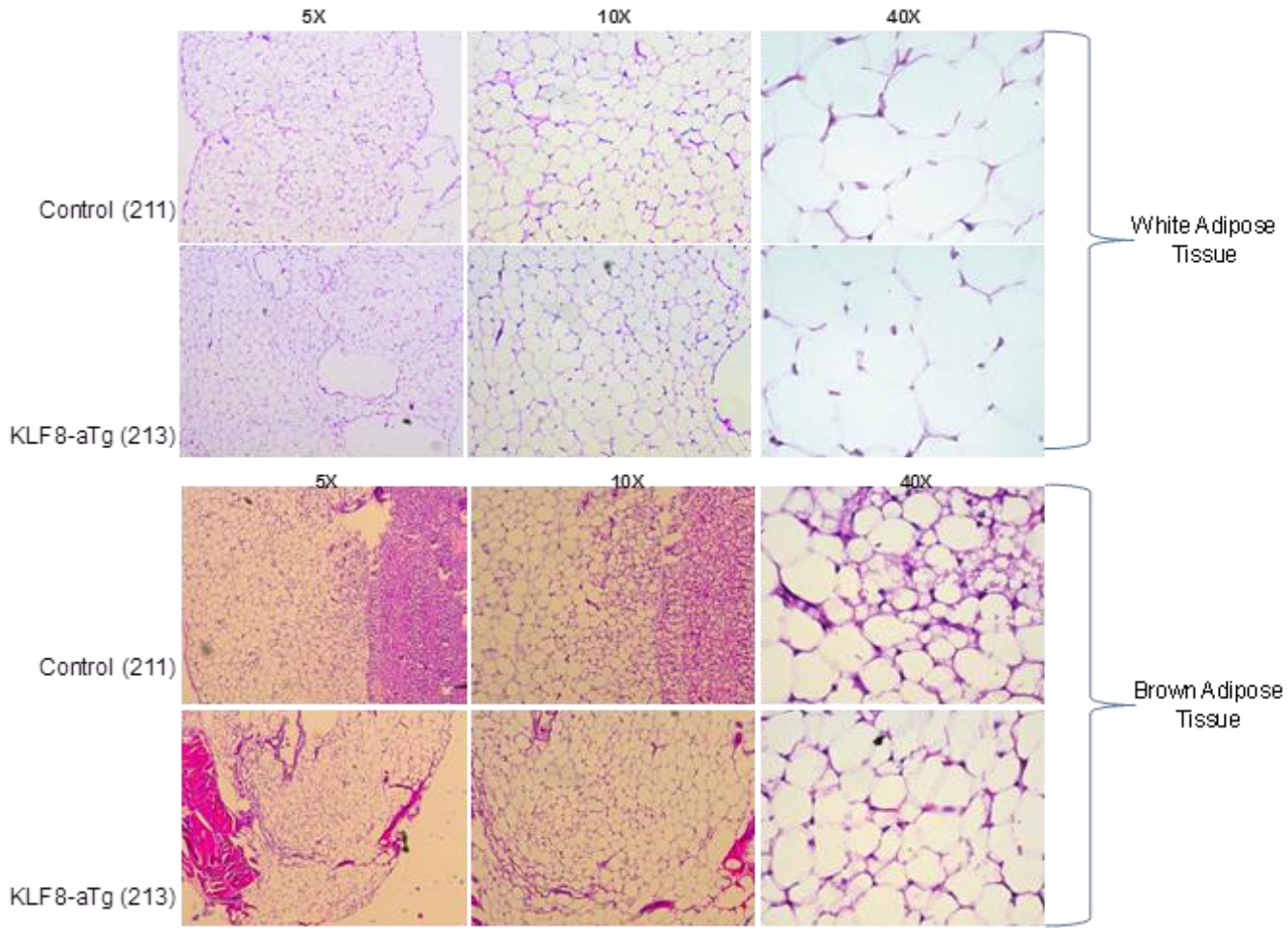

Figure 44. H&E staining of KLF8-aTg mice adipose tissues

We didn't observe any change in KLF8-aTg mice white adipocyte and brown adipocyte cell size and no compared to floxed mice.

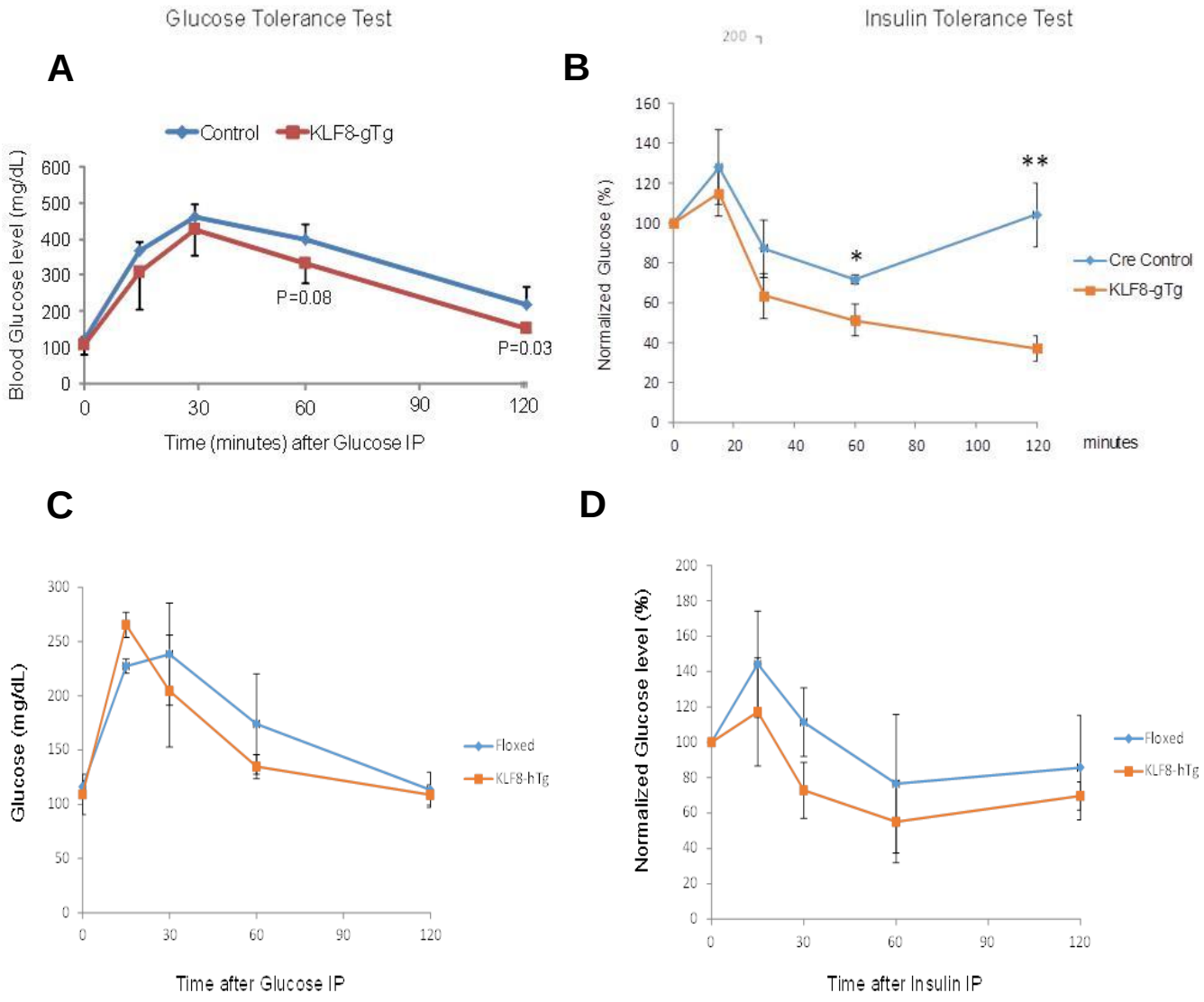

Figure 45. KLF8-gTg and KLF8-hTg mice glucose and insulin tolerance test

(A-B) KLF8-gTg mice glucose tolerance (A) and insulin tolerance (A) showed that KLF8-gTg mice have increased glucose tolerance and insulin sensitivity. (C-D) KLF8-hTg mice glucose tolerance (C) and insulin tolerance (D) showed similar trend but was not significant.

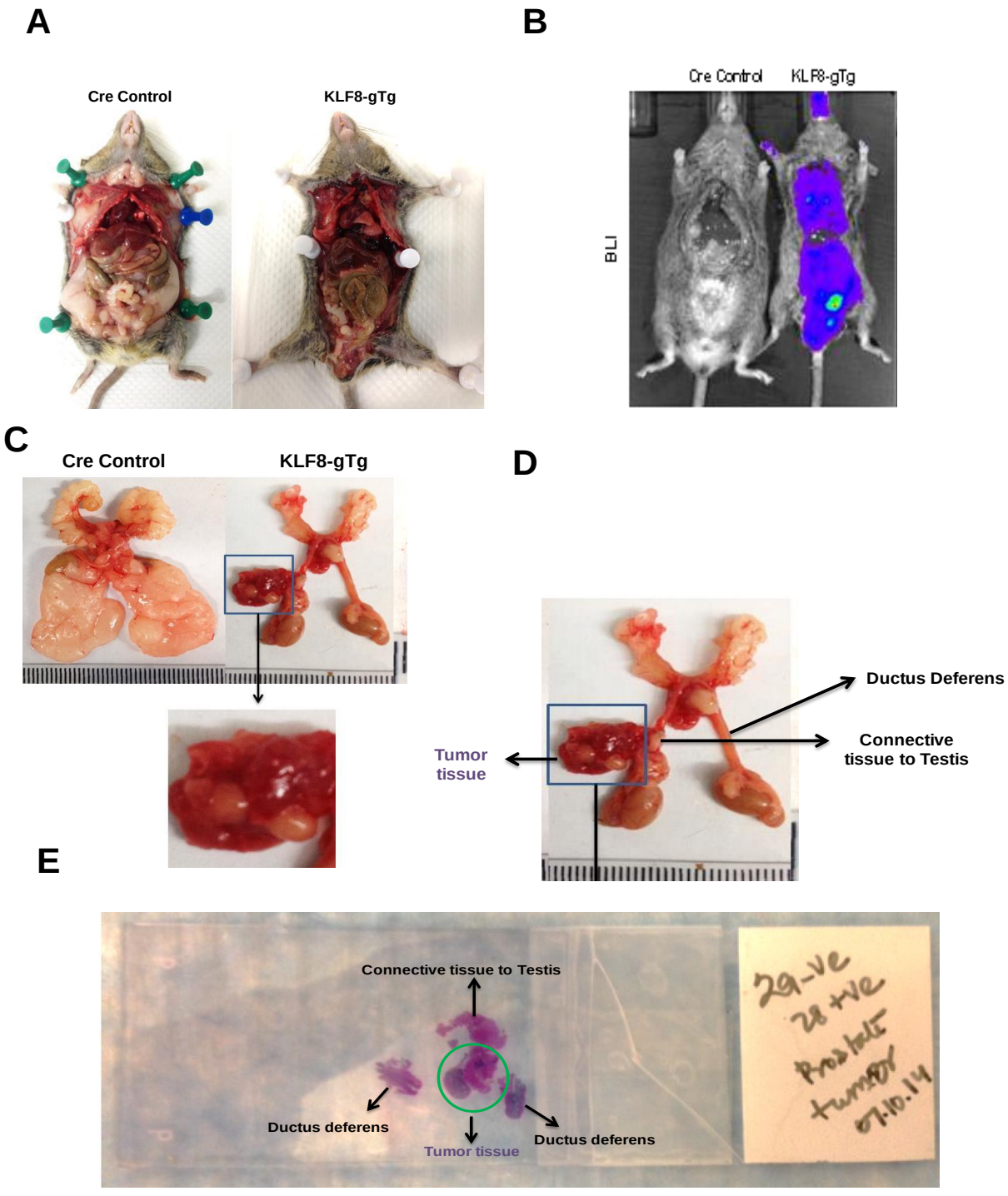

Figure 46. KLF8-gTg mice developed testicular tumor

(A-B) KLF8-gTg mice developed testicular tumor which was positive for BLI signal. (C-D) Tumor was found to be attached with ductus deferens. (E) H&E staining shows neoplasia in the potential tumor tissue.

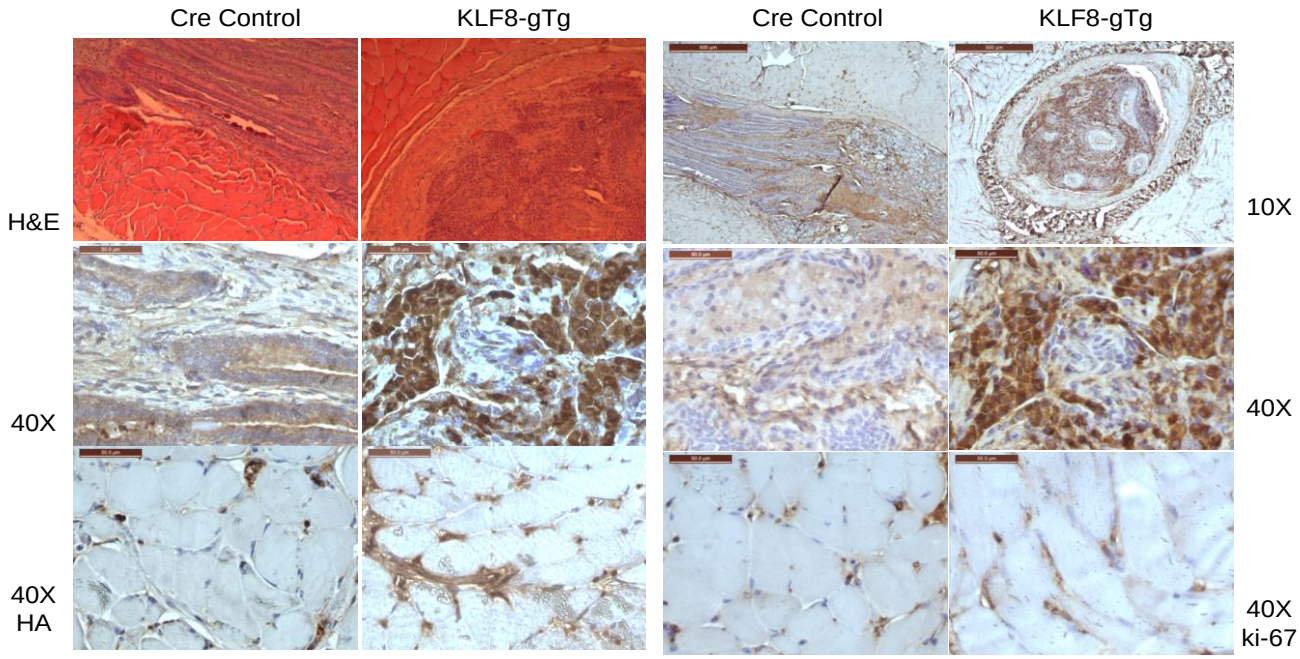

Figure 47. KLF8-gTg mouse testicular tumor was positive for ki-67 staining

We confirmed HA-KLF8 expression in KLF8-gTg mice testicular tumor tissue. Most of the cells in this tumor-like tissue were highly proliferative which was confirmed by positive ki-67 staining (Right panel).

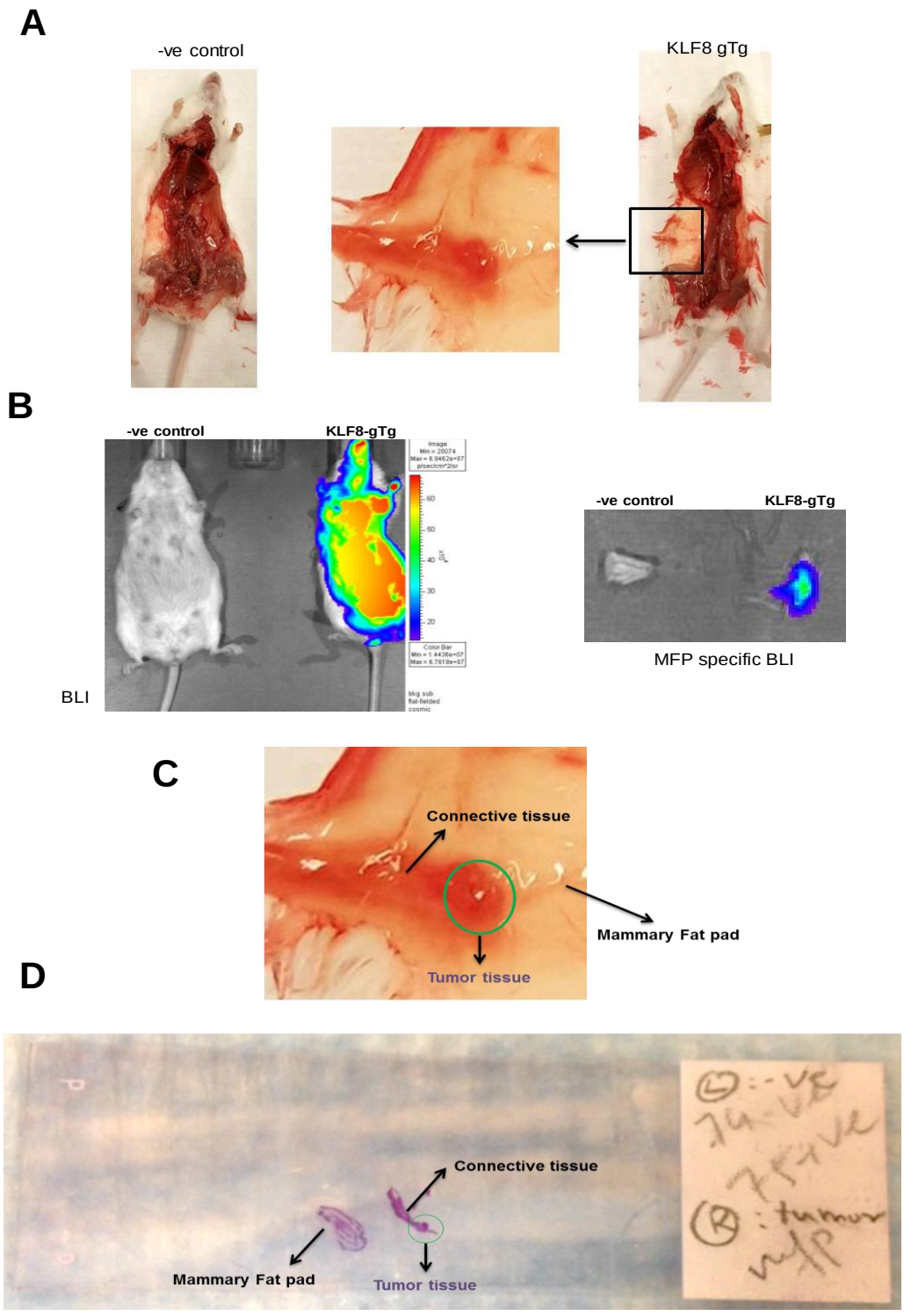

Figure 48. KLF8-gTg mice developed testicular tumor

(A-B) FVB background KLF8-gTg mice developed mammary tumor which was positive for BLI signal. (C) Tumor was found to be attached with mammary fat pad. (D) H&E staining shows neoplasia in the potential tumor tissue.

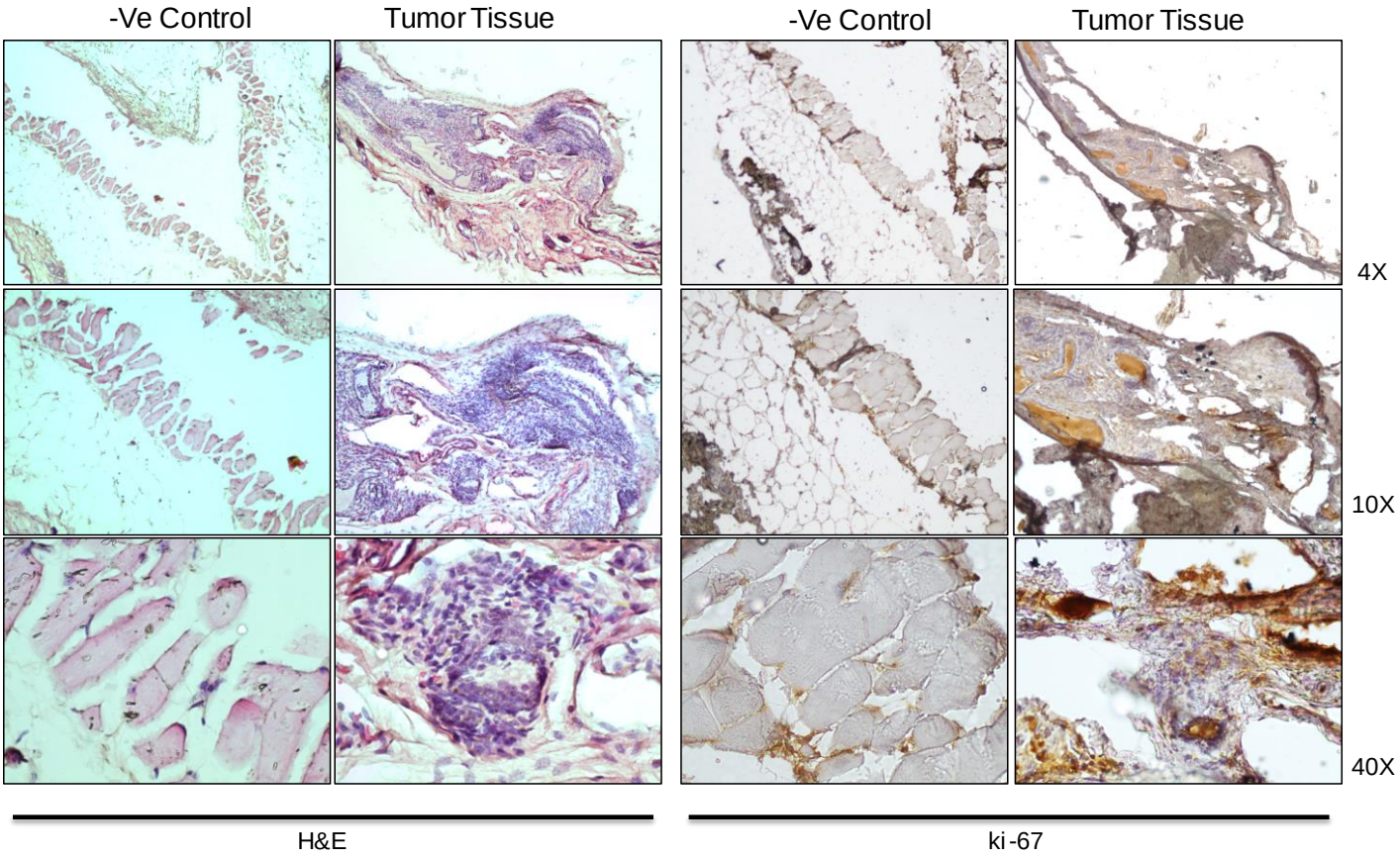

Figure 49. KLF8-gTg mouse showed mammary hyperplasia

We confirmed accumulation of cells by increase in nuclear staining by H&E. Most of the cells in this tumor-like tissue were highly proliferative which was confirmed by positive ki-67 staining (Right panel).

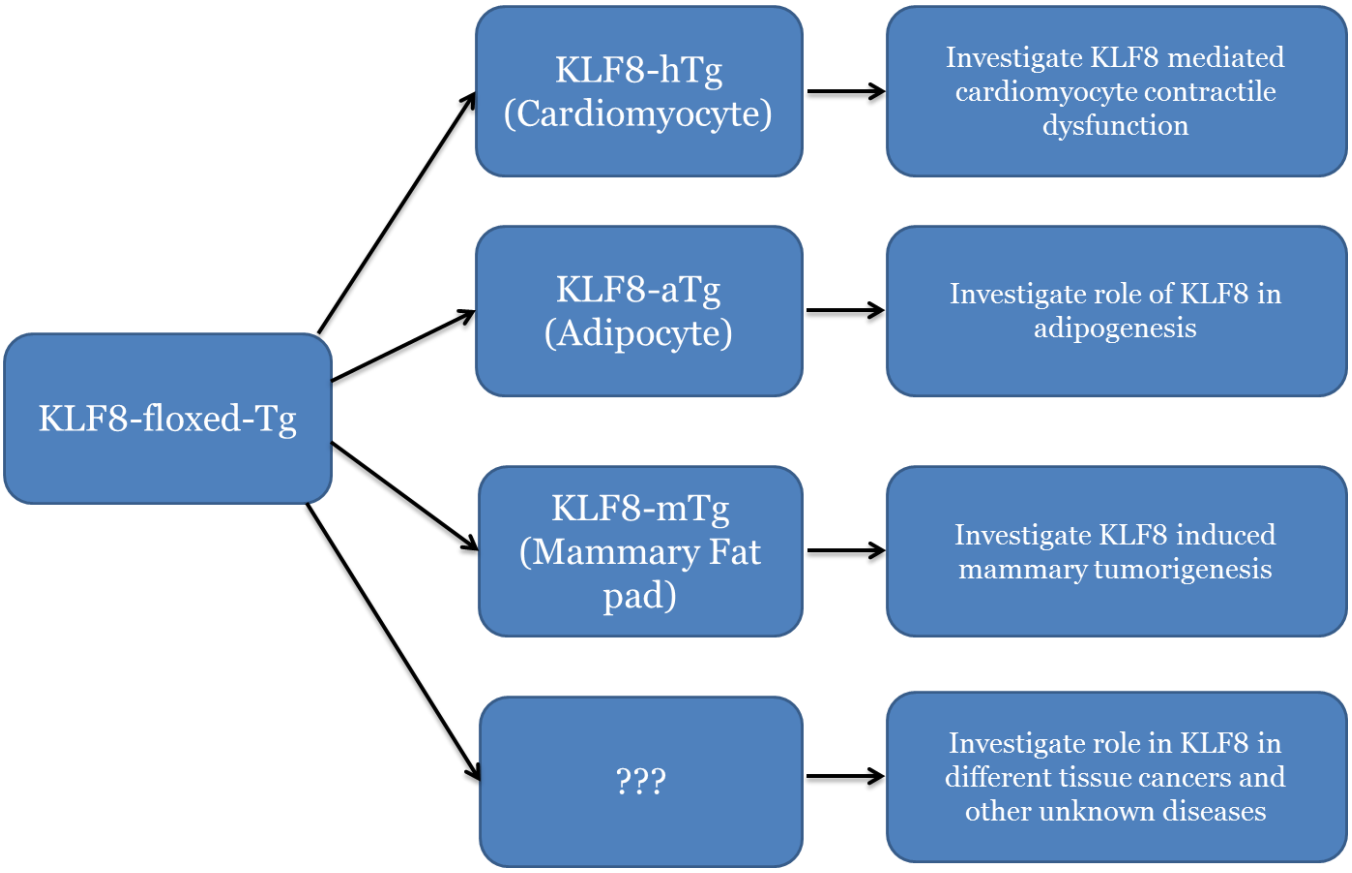

Figure 50. Future Prospective

APPENDIX A: PUBLICATIONS

1. Satadru K. Lahiri, Heng Lu, Debarati Mukherjee, Lin Yu and Jihe Zhao. ERK2 Phosphorylates Kruppel-like Factor 8 Protein at Serine 48 to Maintain Its Stability. Am J Cancer Res 2016;6(5):910-923

2. Lahiri SK, Zhao J. Krüppel-like factor 8 emerges as an important regulator of cancer. Am J Transl Res. 2012;4(3):357-63. (2012)

3. Debarati Mukherjee, Heng Lu, Lin Yu, Satadru K. Lahiri, Tianshu Li, and Jihe Zhao. 2015. Krüppel-like factor 8 activates the transcription of C-X-C cytokine receptor type 4 to promote breast cancer cell invasion, transendothelial migration and metastasis. Oncotarget. 2016 Mar 14. doi: 10.18632/oncotarget.8083. [Epub ahead of print]

4. Tianshu Li, Heng Lu, Debarati Mukherjee, Satadru K. Lahiri, Chao Shen, Lin Yu and Jihe Zhao. Identification of epidermal growth factor receptor and its inhibitory microRNA141 as novel targets of Krüppel-like factor 8 in breast cancer. Oncotarget. Aug 28;6(25):21428-42. (2015)

5. Lu H, Hu L, Yu L, Wang X, Urvalek AM, Li T, Shen C, Mukherjee D, Lahiri SK, Wason MS, Zhao J. KLF8 and FAK cooperatively enrich the active MMP14 on the cell surface required for the metastatic progression of breast cancer. Oncogene. May 29;33(22):2909-17 (2014)

6. Li T, Lu H, Shen C, Lahiri SK, Wason MS, Mukherjee D, Yu L, Zhao J. Identification of epithelial stromal interaction 1 as a novel effector downstream of Krüppel like factor 8 in breast cancer invasion and metastasis. Oncogene. 2014 Sep 25;33(39):4746-55. (2014)

7. Lu H, Hu L, Li T, Lahiri S, Shen C, Wason MS, Mukherjee D, Xie H, Yu L, Zhao J. A novel role of Kruppel-like factor 8 in DNA repairs in breast cancer cells. J Biol Chem. 2012 Dec1;287(52):43720-9. doi: 10.1074/jbc.M112.418053. Epub 2012 Oct 26. PMID: 23105099. (2012)

APPENDIX B: PROTOCOLS

Floxed-KLF8 mice genotyping:

- 23 positive mice were received in the transgenic mice facility and left in quarantine for 5 weeks. 478 (0730) mouse was found dead in the transgenic facility, so we are left with 22 mice. After they are declared clean, 1-2 cm of tail from each mouse was snapped.
- Before cutting tail, we tried bio-fluorescent imaging at the vivarium to see the expression of RFP and GFP, but due to high background it was not clearly identified. Nude mice were used as a negative control. The tails were observed for RFP expression under fluorescent microscope.
- All tails are homogenized separately in two set of experiments (12 and 10 at a time) using liquid nitrogen by individual mortar/pestles to avoid cross contamination. The homogenized tissue was divided into two tubes, one for RNA and other for protein.
- 125 ul of 1.5X sample buffer was added to one part of the homogenized tissue and denatured at 95 c for 10 mins and stored in 4c (later in -80c)
- 700 ul of Trizol reagent added to the other part of tissue to extract RNA. This trizol added sample can be stored in -80c for long time. Quiagen RNA extraction was used to get total RNA from tissue. Nude mice tail was used also for RNA and protein. RNA was eluted with 40 ul buffer and quantified with nanodrop.
- These RNA was reverse transcribed using oligodT primers and invitrogen superscript cDNA synthesis kit and both RNA and cDNA was stored in -80C.

- We used four primers
  - RFP RT primer: (194 bp)

    GTC ATC ACC GAG TTC ATG CG,RFP-RT-F,Satadru,25N,,,DSL

    ACC TTG GAG CCG TAC TGG AA,RFP-RT-R,Satadru,25N,,,DSL
  - GFP RT primer: (165bp)

    TGA ACT TCA AGA TCC GCC ACA,eGFP-RT-F,Satadru,25N,,,DSL

    TTC TCG TTG GGG TCT TTG CT,eGFP-RT-R,Satadru,25N,,,DSL
  - HuKLF8 primer: (156 bp)

    CTT TTG GCT AGT GAT TTC AG

    AAC AGT AGG AAT GTT TGC TG
  - Hu GAPDH primer: (305 bp)

    AAC GGG AAG CTC ACT GGC ATG

    TCC ACC ACC CTG TTG CTG TAG

- Rabbit anti RFP antibody (ab34771) ----- 1:2000 in PBST
- Mouse anti GFP (B-2) antibody (sc9996) ----- 1:1000 in PBST
- Mouse anti-HA antibody ---------- 1:3000 in PBST
- Mouse anti-b actin antibody -------- 1:3000 in PBST

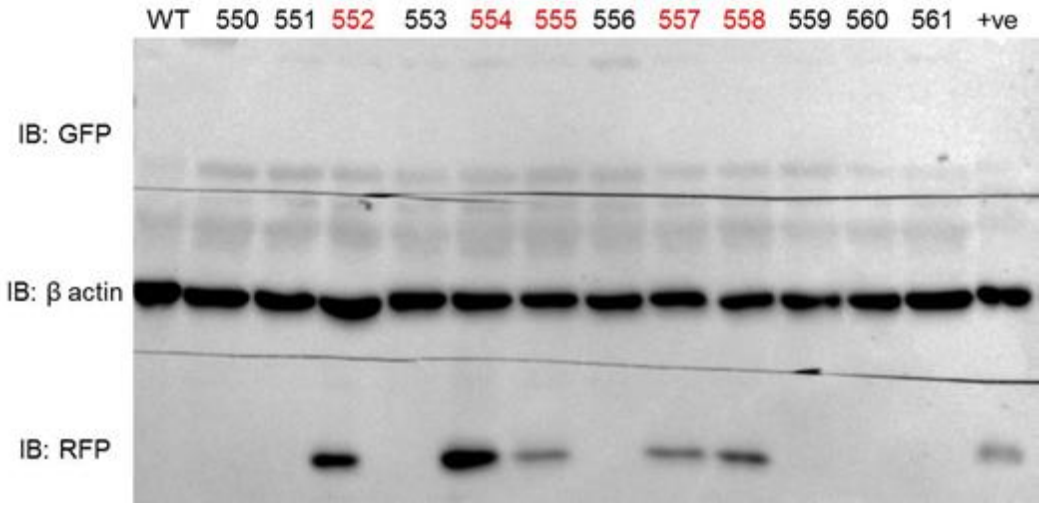

Figure 51. Floxed-KLF8 mice genotyping (western blot with RFP) (Red shows positive founder mice)

KLF8-gTg mice genotyping

- Tail Snip of offspring from B65 Tg-Floxed-KLF8 X FVb-Cre mice.
- Collect genomic DNA, RNA and Protein.
- Genomic DNA PCR with transgene and loxP specific primer.
- Western Blot with GFP, RFP, HA, B-actin
- RT PCR was done with GFP, RFP, HA, GAPDH for the positive mice only
- We got total 50 pups from different breeding pairs from our first experiment.
- Genomic DNA genotyping is shown below.

FVB-Floxed mice or B65-floxed mice are crossed with FVB-EIIA-Cre mice. As EIIA-Cre mice are homozygous; the offspring includes **KLF8-gTg and Cre control mice**. After tail snips are collected, genomic DNA is extracted by 'dirty prep' and PCR is done with pTg-K8 primers to check for the presence of KLF8 transgene. As the Cre mice are homozygous, all the offspring mice will carry Cre transgene and thus we don't have to check presence of Cre transgene. The mice with both KLF8 and Cre transgene are KLF8-gTg mice and the mice with only Cre transgene are Cre control mice. The primer pairs used to genotype KLF8-gTg mice are –

pTg-K8-F (5'-TTC GGC TTC TGG CGT GTG ACC-3')

PTg-K8-R (5'-TGG CAT CCA GGA GTG TTG GAG-3')

The pTg-K8 forward and reverse primer will give rise to an amplification of 450 bp after Cre recombination.

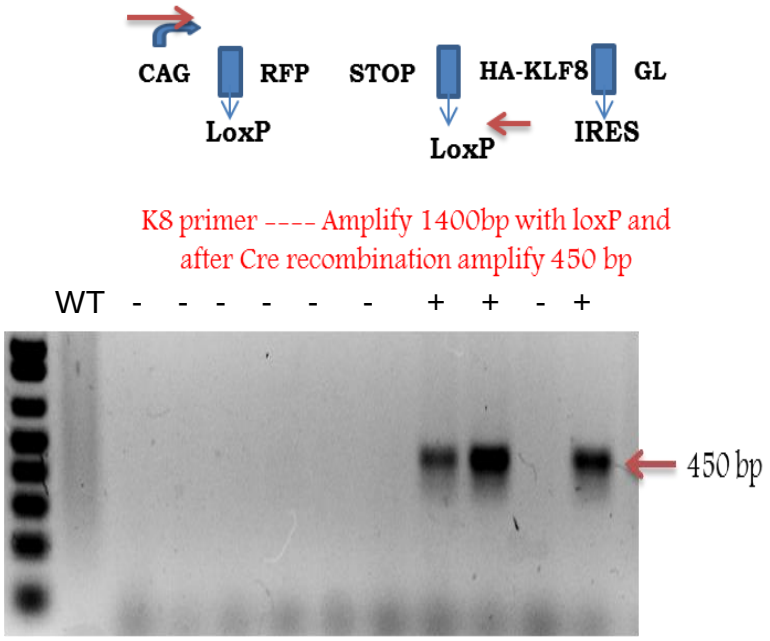

Figure 52. KLF8-gTg mice genomic DNA PCR for genotyping

KLF8-hTg mice genotyping

FVB-Floxed mice are crossed with B6-Myh6-Cre mice. B6-Myh6-Cre mice are heterozygous which leads to four type of offspring including mixed strain KLF8-hTg, Floxed control, Cre control and WT control mice. As we are detecting the genotype from tail snip DNA, we have to investigate presence of both KLF8 transgene and Cre transgene. Mice with both of them will be KLF8-hTg. Mice with only KLF8 transgene will be our floxed control. Mice with only Cre transgene will be our Cre control and mice without any of these two transgenes will be our WT control. As in tail DNA the Cre won't express, keeping the floxed transgene intact, we checked for presence of RFP as indicator of KLF8 transgene.

For presence of KLF8 transgene ---

- ✓ RFP-RT-F 5'-GTC ATC ACC GAG TTC ATG CG-3'
- ✓ RFP-RT-R 5'-ACC TTG GAG CCG TAC TGG AA- 3'

These primer pair will detect 200 bp amplification and positive will indicate presence of KLF8 transgene.

For presence of Cre transgene –

- ✓ oIMR1084 - F - GCG GTC TGG CAG TAA AAA CTA TC
- ✓ oIMR1085 - R - GTG AAA CAG CAT TGC TGT CAC TT

These primer pair will detect 100 bp amplification and positive will indicate presence of Cre transgene.

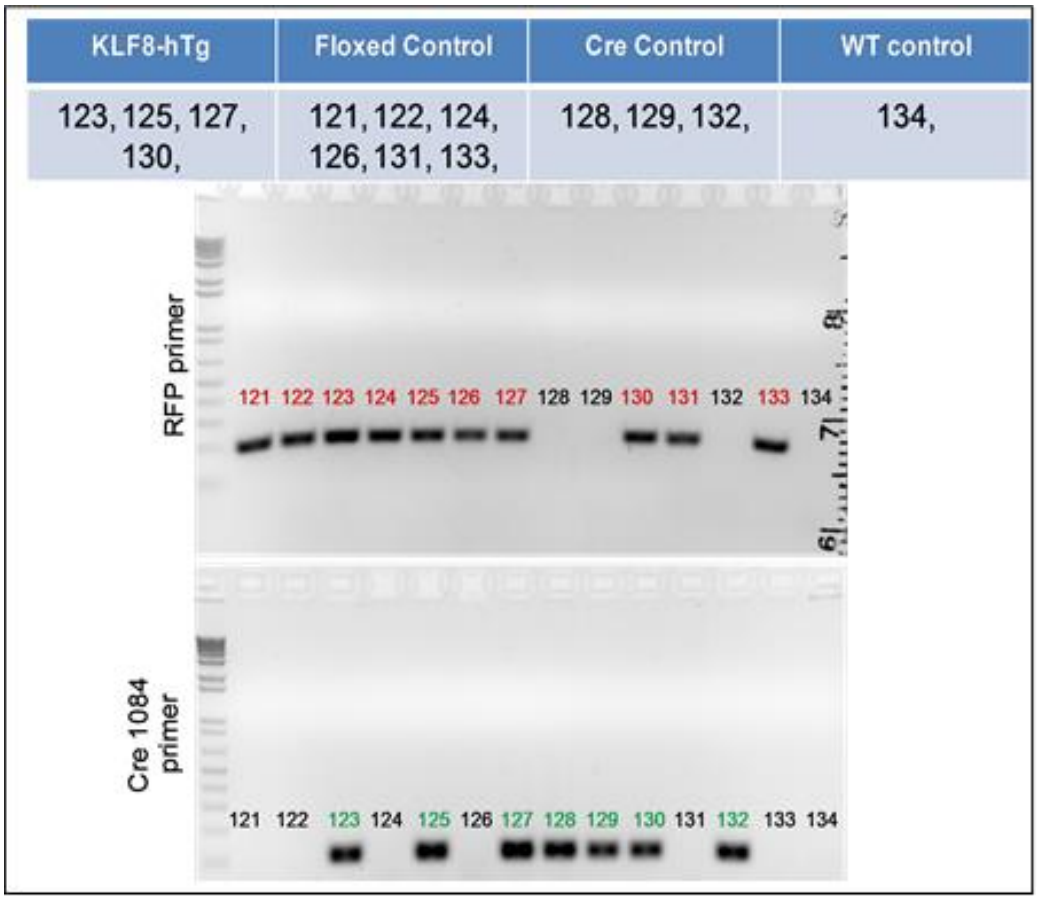

Figure 53. KLF8-hTg mice genomic DNA PCR for genotyping

Ultrasound Echocardiograph and hemodynamic analysis

Materials

1. Vevo 3100 Imaging Platform with MX550D transducer
2. Aquasonic clear ultrasound gel

3. Signagel electrode gel

4. Aquagel lubricating gel

5. Hair shaving cream

6. ddH_20 and paper towel cut into small square pieces.
7. Sterilized cotton buds.
8. Tape to restrain the mouse.
9. PV-15 spray to wipe the bench after the procedure.

10. PI spray to clean the image platform.

Procedures

Starting up the Vevo 3100 machine:

- The Visual Sonics VEVO 3100 echocardiography machine is turned on first along with the oxygen generator to ensure the oxygen supply.
    - Starting Up and Shutting down the System before you power up the Vevo 3100 Imaging System, ensure that the AC power cord is plugged into the wall outlet using the proper plug, and that the main power switch on the back (red circled in left image) of the bottom of the system base is turned ON. The power button (red circled on the right image) is then turned on to start the computer.

Figure 54. Vevo 3100 ultrasound

- The ultrasound gel warmer is turned on before to pre-warm the gel. The heart rate monitor is also turned on. Mouse handling pad is warmed and maintained in 37c throughout the procedure.

Preparation of the mice

- Mice are anesthetized with isoflurane (1.5-2%). The isoflurane chamber as shown below has two outlets; one going into the imaging platform and other going into mouse anesthesia chamber. This outlet lines have regulatory switch on them. It is turned on when the switch is parallel to the line and turned off when it is rotated to vertical position. The isoflurane level can be regulated by the nob (red arrow on isoflurane chamber image). Make sure the oxygen level (black arrow) is between 1-2.

Figure 55. Isoflurane chamber

- First the mouse of interest is put into anesthesia chamber after turning outlet to this chamber on. After 3-4 minutes the mouse can be transferred to the image platform.

Figure 56. Mouse anesthesia chamber

- Before transferring the mouse to the imaging platform, the isoflurane outlet to the platform is turned on and outlet to the chamber is turned off. Make sure both the outlet is not turned off at the same time which may harm the machine. The anesthetized mouse is then secured to the imaging platform in supine position with its nose covered by a cone with constant supply of 1-2% isoflurane to maintain anesthesia.

- Mouse paws are secured to the electrode pads with conductive gel (SIGNAGEL® Electrode Gel – Parkers Laboratories) and tape to assess ECG. A rectal probe is

inserted into mouse anus with Aquagel lubricating gel to overall ensure 37c body temperature and respiration rate for physiological assessment during imaging.

- Depilatory (hair shaving) crème is applied on the mouse chest and upper abdomen area for couple of minutes. All hair in those areas is removed by sterilized cotton buds and further cleaned with water soaked paper towels to remove any trace of remaining hair.

Ultrasound echocardiograph Imaging:

- Pre-warmed ultrasound gel (Aquasonic clear ultrasound gel – parker Laboratories) is applied on the mouse chest and cotton buds are used to get rid of the bubbles. MX550D transducer (ultrasound probe) of the Visual Sonics VEVO 3100 echocardiography machine is moved gently on the mouse chest with gentle pressure to find the long axis view of LV.

- Before starting to take image, Log in, or use the Guest button. Choose an application from the transducer panel (cardiology for mouse).

- After selecting the application; start a new study by selecting “new study”. Series comes under a study. For example “KLF8-hTg 1 month” is a study and under that individual mouse will come as individual series. You can change the Study or

Series name, or add information to the Study or Series by going to the Study Browser.

- VEVO 3100 machine is used to record both B mode and M mode images of the left ventricle in long axis region and then the probe is rotated right side around 90^{o} to obtain the parasternal short axis view of LV. The M mode images are used for measurements analysis. The first image must be inverted selecting the 'left' button on the screen to always get the apex of the heart on your left hand side. The transducer has a notch on one of its side. The notch is denoted by a blue dot on the screen which helps to identify the direction of the image.

- Refine your image using the various control panel controls such as Image Depth, Gain and Orientation.

- Tap Freeze to stop the data acquisition. This mode will save a snapshot of the current view.

- Tap Save Clip to save the clip in the buffer. Save clip will save the time frame video which is required for analysis later on.

- Slide the "Slide to Scan" control to resume the data acquisition.

- Continue imaging and use Freeze and Save Clip as required. You can also save during scanning using Save Clip.

- Tap the Current Series navigation button to view all your saved images for the current series. You can also see these images in the Study Browser.

- After B-mode image is captured, start M mode imaging. In M mode, you have to place the line on the heart (the widest width) and press start on the screen and save the image with save clip and freeze.

- Overall, first capture both B mode and M mode images for the long axis view of heart and then move the transducer 90 degree on the right side to get short axis view. Capture B mode and M mode images of short axis of heart. Both axis M mode images are analyzed later to investigate cardiac function.

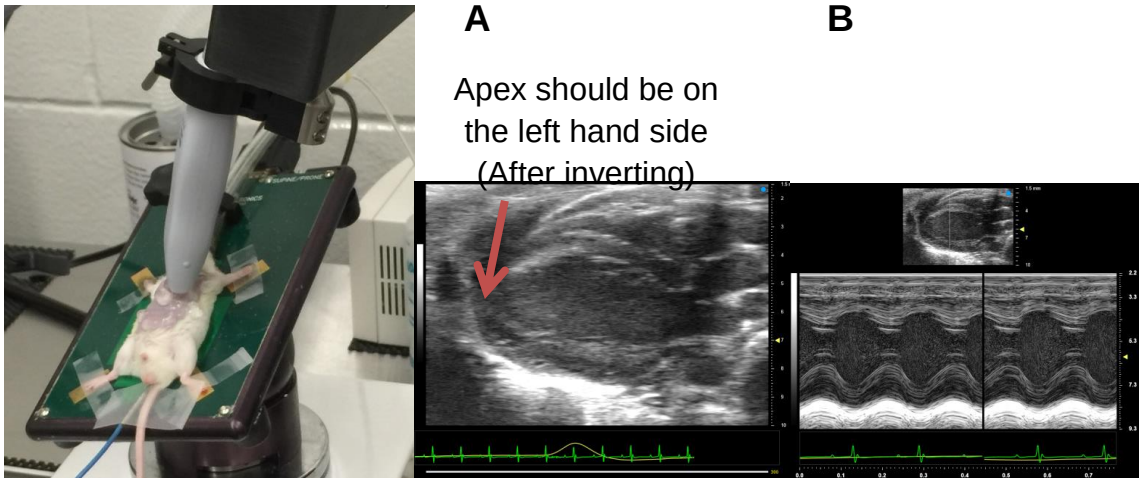

Figure 57. Long axis imaging; B mode (A) and M mode (B)

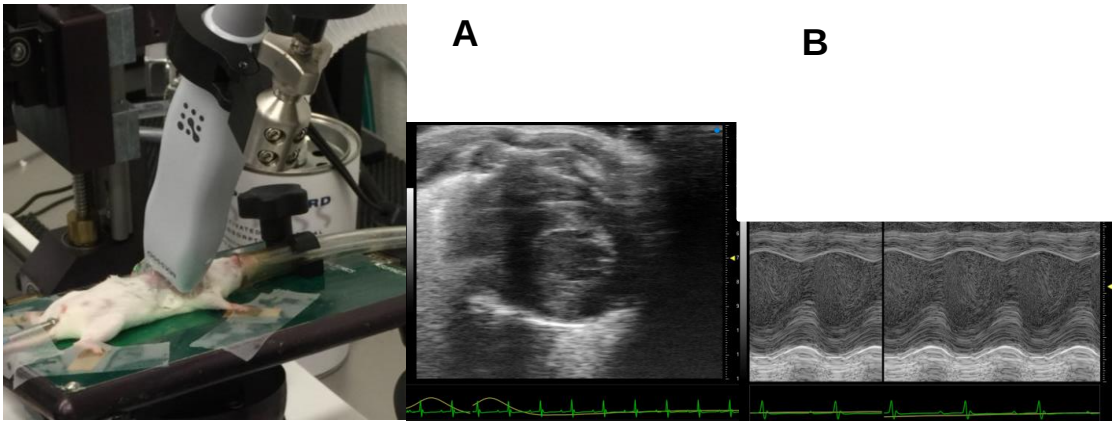

Figure 58. Short axis Imaging; B mode (A) and M mode (B)

- After recording all the images, the mouse is cleaned with a sterilized wipe soaked with water and returned to its cage. The cage is kept on a heating pad to help the mouse regain consciousness. The mouse is monitored following few days to ensure no side effects of this procedure.

- To copy the acquired date, tap the Export button from the Study Browser. Here, you can: Export To Vevo LAB to export your whole study for further analysis by vevo software (upstairs) and/or export to other file types to export clips, images, and other file formats. Shut down the machine after the procedures by pressing the top right button mentioned before and finally turn off the main power button on the back of the machine.

- Clean the transducer with a normal wipe and put it back the 3100 machine. Clean the image platform with PI spray. Turn off the oxygen generator,

isoflurane, gel warmer and heart rate monitor. Clean the imaging station with PI spray. Clean everything else with accel wipes or PV-15 spray.

Bio-Luminescent Imaging (BLI)

Materials

1. Xenogen IVIS 50 imaging instrument.
2. D-Luciferin (30mg/ml stock_ dilution method is described in the procedure)
3. Syringe
4. Mouse opthalmic ointment

5. Hair shaving cream (Nair) and sterilized cotton buds

Procedures

Preparation of D-luciferin stock

D-Luciferin is light sensitive and kept in -20C for long term storage. 30 mg/ml D-Luciferin stock is prepared beforehand and stored in -20C after aliquoting into small tubes. To prepare this working stock, D-Luciferin (gold biotechnology) is thawed at room temperature and dissolved in DPBS to a final concentration of 30 mg/mL (0.3gm of D-luciferin in 10 ml of PBS). After completely dissolving the substrate (1-2hrs in room temperature), the D-luciferin solution is sterilized through 0.22 µm filter and aliquoted into small tubes to prevent freeze-thaw cycles. Always wrap the d-luciferin tubes with aluminum foil during preparation and storage to protect from light. Before imaging, take out required amount of D-luciferin (30mg/ml) and thaw on ice approximately for 1 hr.

Starting up the IVIS 50

1. The IVIS 50 instrument is always turned on. There are two gas buttons (as showed in the pic below with two arrows). Turn both of them on first and start the oxygen generator (wait for green light to be stable).

Figure 59. Xenoxen IVIS 50

2. The computer associated with IVIS50 is also always turned on. First start the Living Image® 2.5 software program from the desktop. A system control panel will appear in the lower right corner of the monitor.

3. Click the Initialize IVIS system button in the camera control panel. After initialization, the Temperature Status box in the center of the panel should be green, indicating that the CCD camera is adequately cooled.

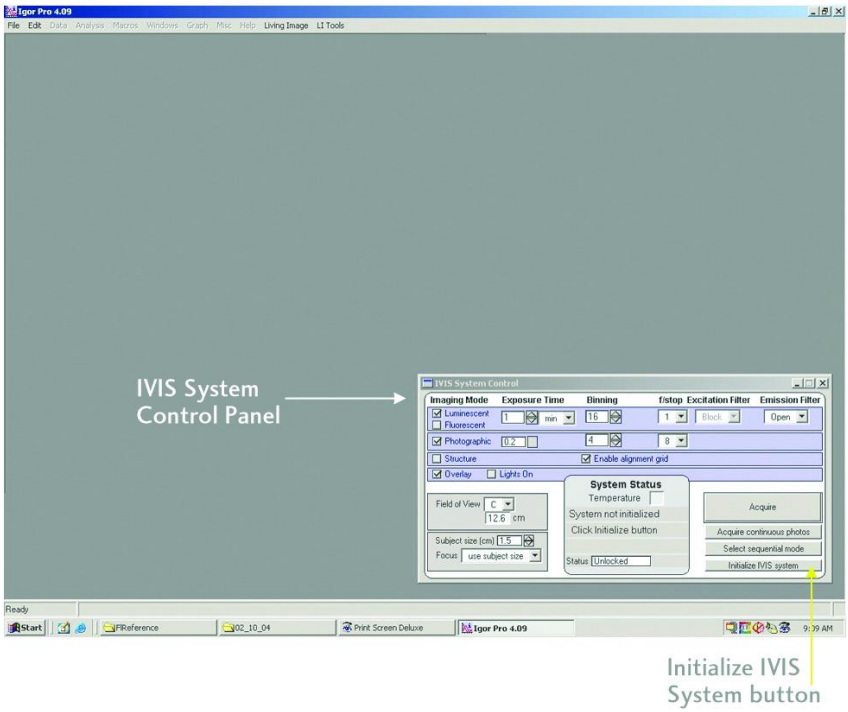

Figure 60. IVIS 50 software startup

Preparation of mice:

1. There are two flip switches on the anesthesia controller; one of them (the right most one_5 in the image) controls oxygen and isoflurane flow to the anesthesia chamber and the other one (the middle_4 in the image) controls flow towards the IVIS machine. It is in 'On' position when flipped up (parallel to the floor) and in 'Close' position when flipped down (Perpendicular to the floor). Avoid switching on the 'Evacuation switch' (1 in the image) on the left hand side of the panel as it can kill the mice during imaging. Control oxygen and isoflurane flow by the middle and right switch as desired. Also make sure the oxygen level for the anesthesia chamber is around 2 and for the IVIS chamber is

around 1. It can be increased and decreased by turning the nob associated with the level indicator.

2. The mice were anaesthetized using isoflurane (1.5-2%). The mouse of interest is kept in the anesthesia chamber first. Make sure that the regulator to anesthesia chamber (no 5) is turned on and regulator to IVIS (switch 4) is in off position. 3 mice can be anesthetized together. After putting the mice in the anesthesia chamber, D-luciferin is filled in syringe for IP injection.

Evacuation pump (never use)

1. Gas turn on/ turn off switch
2. Isoflurane regulator
3. Isoflurane and oxygen outflow regulator to IVIS chamber
4. Isoflurane and oxygen outflow regulator to anesthesia chamber (Both these regulator are shown in turned off position in this image. It is turned on when parallel to the floor.
5. Anesthesia chamber

Figure 61. Isoflurane chamber

3. Mice were then injected intraperitoneally with D-Luciferin in phosphate buffer (150 mg/kg mouse weight = (5 * Body weight) ul of 30mg/ml D-luciferin stock) and kept in the

anesthesia chamber for 8-10 minutes to let the substrate circulate throughout the mouse body. Mice hair is removed from the area of interest during this time (similarly as in ultrasound procedure).

4. After 10 minutes, apply ophthalmic ointment ointment to the mouse eyes to protect them from UV light during imaging.

Imaging

1. Turn on the isoflurane regulator to IVIS (switch 4 in the image) and turn off the regulator to anesthesia chamber. Place the mouse to be imaged in the center of the stage in the imaging chamber. Close the door. Make sure that the mouse nose is inside the anesthesia cone. Avoid switching on the ‘Evacuation switch’ on the left hand side of the panel as it can kill the mice during imaging.

2. Check the Overlay box in the control panel and set the Exposure Time desired for the luminescent image. We use 2-3 minutes for this luminescent imaging. Also make sure that the photographic image is also checked to get the overlay image.

3. Click the Acquire button on the control panel.

4. After the exposure is complete, the overlaid image is displayed. Edit the information in the Change Information window and click ‘Done’.

5. Similarly capture the fluorescence image by selecting fluorescence and photographic image capture method. We use 1 min for this image. For RFP imaging, select DSRed in both excitation and emission channels and for GFP imaging select GFP. Fluorescence imaging in IVIS 50 is not that reliable.

6. After all the required image is captured, save the images by clicking ‘Save Graphics’ from ‘File’. It will have options to save the image as JPEG or TIF format. Save it in desired format (mostly JPEG) to the desired location. A message will prompt asking if you want to save the data when you try to close the image after saving it in JPEG format. Click ‘Yes’ and save the file for later analysis. You can also save by choosing Save Living Image Data under the Living Image menu item to save the displayed data.

7. Keep the mice on heat pad to regain consciousness and monitor regularly for any detrimental effect.

8. Clean the anesthesia chamber and IVIS machine with Accel wipes. Turn off the oxygen pump and wait for few minutes before turning off the gas buttons to close positions. Flip down the anesthesia control buttons.

9. Close the Living image software. It will take 5 minutes to close. Leave the machine and computer on and return the mouse to room 146.

10. Fill the isoflurane to the bottom of the triangle mark in the isoflurane chamber.

APPENDIX C: IACUC PERMISSIONS

University of Central Florida

Office of Research & Commercialization

2/19/2014

Dr. Jihe Zhao
Burnett School of Biomedical Sciences
Lake Nona
6900 Lake Nona Blvd. BSS 313
Orlando, FL 32827

Subject: Institutional Animal Care and Use Committee (IACUC) Protocol Submission

Dear Dr. Jihe Zhao:

This letter is to inform you that your following animal protocol was re-approved by the IACUC. The IACUC Animal Use Renewal Form is attached for your records.

Animal Project #:	12-17
Title:	Novel Translation Research Models for Breast and Ovarian Cancers
First Approval Date:	3/16/2012

Please be advised that IACUC approvals are limited to one year maximum. Should there be any technical or administrative changes to the approved protocol, they must be submitted in writing to the IACUC for approval. Changes should not be initiated until written IACUC approval is received. Adverse events should be reported to the IACUC as they occur. Furthermore, should there be a need to extend this protocol, a renewal must be submitted for approval at least three months prior to the anniversary date of the most recent approval. If the protocol is over three years old, it must be rewritten and submitted for IACUC review.

Should you have any questions, please do not hesitate to call me at (407) 882-1164.

Please accept our best wishes for the success of your endeavors.

Best Regards,

Cristina Caamaño
Assistant Director

Copies: Facility Manager (when applicable.)

12201 Research Parkway • Suite 501 • Orlando, FL 32826-3246 • 407-823-3778 • Fax 407-823-3299

THE UNIVERSITY OF CENTRAL FLORIDA
INSTITUTIONAL ANIMAL CARE and USE COMMITTEE (IACUC)
Re-Approval to Use Animals

Dear Dr. Jihe Zhao,

Your application for IACUC Re-Approval has been reviewed and appproved by the UCF IACUC Committee Reviewers.

Approval Date: 2/17/2014

Title: Novel Translation Research Models for Breast and Ovarian Cancers

Department: Burnett School of Biomedical Sciences

Animal Project #: 12-17

Expiration: 3/16/2015

You may purchase and use animals according to the provisions outlined in the above referenced animal project. This project will expire as indicated above. You will be notified 2-3 months prior to your expriation date regarding your need to file another renewal.

Christopher Parkinson, Ph.D.
IACUC Chair

Approved ✓ Renewed ✓

UNIVERSITY OF CENTRAL FLORIDA
RESEARCH & COMMERCIALIZATION

6/4/2015

Dr. Jibe Zhao
Burnett School of Biomedical Sciences
Lake Nona
6900 Lake Nona Blvd. BSS 313
Orlando, FL 32827

Subject: Institutional Animal Care and Use Committee (IACUC) Protocol Submission

Dear Dr. Jibe Zhao:

This letter is to inform you that your following animal protocol was approved by the IACUC. The IACUC Use Approval Form is attached for your records.

Animal Project #:	15-27
Title:	Transcriptional Control for Myocardial Function, Systemic Metabolism and Energy Homeostasis
First Approval Date:	6/4/2015

Please be advised that IACUC approvals are limited to one year maximum. Should there be any technical or administrative changes to the approved protocol, they must be submitted in writing to the IACUC for approval. Changes should not be initiated until written IACUC approval is received. Adverse events should be reported to the IACUC as they occur. Furthermore, should there be a need to extend this protocol, a renewal must be submitted for approval at least three months prior to the anniversary date of the most recent approval. If the protocol is over three years old, it must be rewritten and submitted for IACUC review.

Should you have any questions, please do not hesitate to call the office of Animal Welfare at (407) 882-1164

Please accept our best wishes for the success of your endeavors.

Best Regards,

Cristina Casmallo

Cristina Casmallo
Associate Director, Research Program Services
Office of Research and Commercialization

Copies: Appropriate Facility Manager (when applicable)

12201 Research Parkway • Suite 501 • Orlando, FL 32826-3246 • 407-823-3778 • Fax 823-3299

THE UNIVERSITY OF CENTRAL FLORIDA
INSTITUTIONAL ANIMAL CARE and USE COMMITTEE (IACUC)
Approval to Use Animals

Dear Dr. Jihe Zhao,

Your application for IACUC Approval has been reviewed and approved by the UCF IACUC Reviewers.

Approval Date:	6/4/2015
Title:	Transcriptional Control for Myocardial Function, Systemic Metabolism and Energy Homeostasis
Department:	Burnett School of Biomedical Sciences
Animal Project #:	15-27
Expiration:	6/3/2016

You may purchase and use animals according to the provisions outlined in the above referenced animal project.

Christopher Parkinson, Ph.D.
IACUC Chair

Contact: Cristina Casarallo, Associate Director, Research Program Services Email: ccasarano@ucf.edu
Phone: (407) 882-1164 Fax: (407) 823-3299

APPENDIX D: COPYRIGHT PERMISSIONS

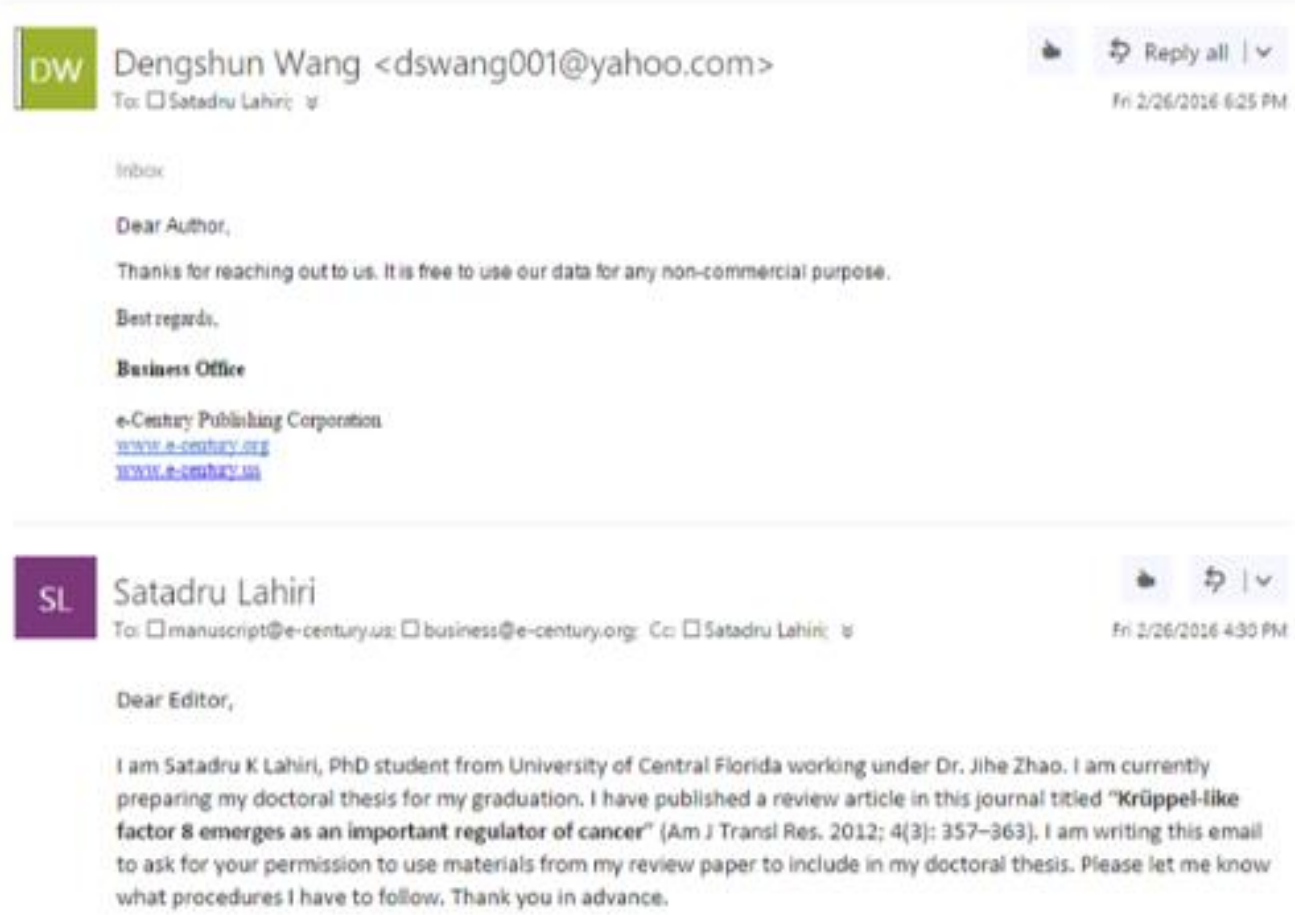

DW

Dengshun Wang <dswang001@yahoo.com>

To: ☐ Satadru Lahiri

Reply all

Fri 2/26/2016 6:25 PM

Inbox

Dear Author,

Thanks for reaching out to us. It is free to use our data for any non-commercial purpose.

Best regards,

Business Office

e-Century Publishing Corporation

www.e-century.org

www.e-century.us

SL

Satadru Lahiri

To: ☐ manuscript@e-century.us; ☐ business@e-century.org; Cc: ☐ Satadru Lahiri

Fri 2/26/2016 4:30 PM

Dear Editor,

I am Satadru K Lahiri, PhD student from University of Central Florida working under Dr. Jihe Zhao. I am currently preparing my doctoral thesis for my graduation. I have published a review article in this journal titled "**Krüppel-like factor 8 emerges as an important regulator of cancer**" (Am J Transl Res. 2012; 4(3): 357–363). I am writing this email to ask for your permission to use materials from my review paper to include in my doctoral thesis. Please let me know what procedures I have to follow. Thank you in advance.

For figure 1

http://www.ajcr.us/Instructions.html

For Chapter 2

Chapter 3 is unpublished work by Satadru K Lahiri.

REFERENCES

1. Tetreault, M.P., Y. Yang, and J.P. Katz, Kruppel-like factors in cancer. Nat Rev Cancer, 2013. 13(10): p. 701-13.

2. Lahiri, S.K. and J. Zhao, Kruppel-like factor 8 emerges as an important regulator of cancer. Am J Transl Res, 2012. 4(3): p. 357-63.

3. Lossi, A.M., et al., Abnormal expression of the KLF8 (ZNF741) gene in a female patient with an X;autosome translocation t(X;21)(p11.2;q22.3) and non-syndromic mental retardation. J Med Genet, 2002. 39(2): p. 113-7.

4. Wang, X., et al., KLF8 promotes human breast cancer cell invasion and metastasis by transcriptional activation of MMP9. Oncogene, 2011. 30(16): p. 1901-11.

5. Wang, X., et al., Kruppel-like factor 8 induces epithelial to mesenchymal transition and epithelial cell invasion. Cancer Res, 2007. 67(15): p. 7184-93.

6. Yan, Q., et al., KLF8 promotes tumorigenesis, invasion and metastasis of colorectal cancer cells by transcriptional activation of FHL2. Oncotarget, 2015. 6(28): p. 25402-17.

7. Zhao, J., et al., Identification of transcription factor KLF8 as a downstream target of focal adhesion kinase in its regulation of cyclin D1 and cell cycle progression. Mol Cell, 2003. 11(6): p. 1503-15.

8. Li, T., et al., Identification of epithelial stromal interaction 1 as a novel effector downstream of Kruppel-like factor 8 in breast cancer invasion and metastasis. Oncogene, 2014. 33(39): p. 4746-55.

9. Lu, H., et al., KLF8 and FAK cooperatively enrich the active MMP14 on the cell surface required for the metastatic progression of breast cancer. Oncogene, 2014. 33(22): p. 2909-17.

10. Li, T., et al., Identification of epidermal growth factor receptor and its inhibitory microRNA141 as novel targets of Kruppel-like factor 8 in breast cancer. Oncotarget, 2015. 6(25): p. 21428-42.

11. Zhang, P., et al., A functional screen for Kruppel-like factors that regulate the human gamma-globin gene through the CACCC promoter element. Blood Cells Mol Dis, 2005. 35(2): p. 227-35.

12. van Vliet, J., J. Turner, and M. Crossley, Human Kruppel-like factor 8: a CACCC-box binding protein that associates with CtBP and represses transcription. Nucleic Acids Res, 2000. 28(9): p. 1955-62.

13. Eaton, S.A., et al., A network of Kruppel-like Factors (Klfs). Klf8 is repressed by Klf3 and activated by Klf1 in vivo. J Biol Chem, 2008. 283(40): p. 26937-47.

14. Urvalek, A.M., et al., KLF8 recruits the p300 and PCAF co-activators to its amino terminal activation domain to activate transcription. Cell Cycle, 2010. 9(3): p. 601-11.

15. Mehta, T.S., et al., A unique sequence in the N-terminal regulatory region controls the nuclear localization of KLF8 by cooperating with the C-terminal zinc-fingers. Cell Res, 2009. 19(9): p. 1098-109.

16. Lu, H., et al., A novel role of Kruppel-like factor 8 in DNA repair in breast cancer cells. J Biol Chem, 2012. 287(52): p. 43720-9.

17. Lu, H., et al., Identification of poly (ADP-ribose) polymerase-1 (PARP-1) as a novel Kruppel-like factor 8-interacting and -regulating protein. J Biol Chem, 2011. 286(23): p. 20335-44.

18. Beltrao, P., et al., Systematic functional prioritization of protein posttranslational modifications. Cell, 2012. 150(2): p. 413-25.

19. Wei, H., et al., Sumoylation delimits KLF8 transcriptional activity associated with the cell cycle regulation. J Biol Chem, 2006. 281(24): p. 16664-71.

20. Urvalek, A.M., et al., Regulation of the oncoprotein KLF8 by a switch between acetylation and sumoylation. Am J Transl Res, 2011. 3(2): p. 121-32.

21. Wang, X., et al., Activation of KLF8 transcription by focal adhesion kinase in human ovarian epithelial and cancer cells. J Biol Chem, 2008. 283(20): p. 13934-42.

22. Yang, T., et al., Kruppel-like factor 8 is a new Wnt/beta-catenin signaling target gene and regulator in hepatocellular carcinoma. PLoS One, 2012. 7(6): p. e39668.

23. Wang, X. and J. Zhao, KLF8 transcription factor participates in oncogenic transformation. Oncogene, 2007. 26(3): p. 456-61.

24. De Craene, B. and G. Berx, Regulatory networks defining EMT during cancer initiation and progression. Nat Rev Cancer, 2013. 13(2): p. 97-110.

25. Wang, X., et al., Kruppel-like factor 8 promotes tumorigenic mammary stem cell induction by targeting miR-146a. Am J Cancer Res, 2013. 3(4): p. 356-73.

26. Fu, W.J., et al., Small interference RNA targeting Kruppel-like factor 8 inhibits the renal carcinoma 786-0 cells growth in vitro and in vivo. J Cancer Res Clin Oncol, 2010. 136(8): p. 1255-65.

27. Zhang, H., et al., Kruppel-like factor 8 contributes to hypoxia-induced MDR in gastric cancer cells. Cancer Sci, 2014. 105(9): p. 1109-15.

28. Cox, B.D., et al., New concepts regarding focal adhesion kinase promotion of cell migration and proliferation. J Cell Biochem, 2006. 99(1): p. 35-52.

29. Liu, L., et al., Lentivirus-delivered Kruppel-like factor 8 small interfering RNA inhibits gastric cancer cell growth in vitro and in vivo. Tumour Biol, 2012. 33(1): p. 53-61.

30. Chen, G., et al., Lentivirus-mediated gene silencing of KLF8 reduced the proliferation and invasion of gastric cancer cells. Mol Biol Rep, 2012. 39(10): p. 9809-15.

31. Zhang, H., et al., KLF8 involves in TGF-beta-induced EMT and promotes invasion and migration in gastric cancer cells. J Cancer Res Clin Oncol, 2013. 139(6): p. 1033-42.

32. Wang, W.F., et al., Kruppel-like factor 8 overexpression is correlated with angiogenesis and poor prognosis in gastric cancer. World J Gastroenterol, 2013. 19(27): p. 4309-15.

33. Li, J.C., et al., Up-regulation of Kruppel-like factor 8 promotes tumor invasion and indicates poor prognosis for hepatocellular carcinoma. Gastroenterology, 2010. 139(6): p. 2146-2157 e12.

34. Wan, W., et al., Small interfering RNA targeting Kruppel-like factor 8 inhibits U251 glioblastoma cell growth by inducing apoptosis. Mol Med Rep, 2012. 5(2): p. 347-50.

35. Schnell, O., et al., Kruppel-like factor 8 (KLF8) is expressed in gliomas of different WHO grades and is essential for tumor cell proliferation. PLoS One, 2012. 7(1): p. e30429.

36. He, H.J., et al., Kruppel-like factor 8 is a novel androgen receptor co-activator in human prostate cancer. Acta Pharmacol Sin, 2013. 34(2): p. 282-8.

37. Shi, X., et al., Suppression of KLF8 induces cell differentiation and sensitizes colorectal cancer to 5-fluorouracil. Oncol Rep, 2015. 34(3): p. 1221-30.

38. Shi, H., et al., MiR-135a inhibits migration and invasion and regulates EMT-related marker genes by targeting KLF8 in lung cancer cells. Biochem Biophys Res Commun, 2015. 465(1): p. 125-30.

39. Liang, K., et al., KLF8 is required for bladder cancer cell proliferation and migration. Biotechnol Appl Biochem, 2015. 62(5): p. 628-33.

40. Bin, Z., et al., Downregulation of KLF8 expression by shRNA induces inhibition of cell proliferation in CAL27 human oral cancer cells. Med Oral Patol Oral Cir Bucal, 2013. 18(4): p. e591-6.

41. Wei, Y., et al., Krupel-like factor 8 is a potential prognostic factor for pancreatic cancer. Chin Med J (Engl), 2014. 127(5): p. 856-9.

42. Lin, F., et al., KLF8 knockdown suppresses proliferation and invasion in human osteosarcoma cells. Mol Med Rep, 2014. 9(5): p. 1613-7.

43. Wang, J., et al., Small hairpin RNA-mediated Kruppel-like factor 8 gene knockdown inhibits invasion of nasopharyngeal carcinoma. Oncol Lett, 2015. 9(6): p. 2515-2519.

44. Yang, Z., et al., Downregulated Kruppel-like factor 8 is involved in decreased trophoblast invasion under hypoxia-reoxygenation conditions. Reprod Sci, 2014. 21(1): p. 72-81.

45. Yang, Z.M., et al., [Expression of KLF-8 and MMP-9 in placentas and their relationship with the pathogenesis of preeclampsia]. Zhonghua Fu Chan Ke Za Zhi, 2013. 48(10): p. 755-8.

46. Tsai, M.Y., et al., Modulation of p53 and met expression by Kruppel-like factor 8 regulates zebrafish cerebellar development. Dev Neurobiol, 2015. 75(9): p. 908-26.

47. Yi, R., et al., Kruppel-like factor 8 ameliorates Alzheimer's disease by activating beta-catenin. J Mol Neurosci, 2014. 52(2): p. 231-41.

48. Lee, H., et al., Kruppel-like factor KLF8 plays a critical role in adipocyte differentiation. PLoS One, 2012. 7(12): p. e52474.

49. Bedell, M.A., et al., Mouse models of human disease. Part II: recent progress and future directions. Genes Dev, 1997. 11(1): p. 11-43.

50. Bedell, M.A., N.A. Jenkins, and N.G. Copeland, Mouse models of human disease. Part I: techniques and resources for genetic analysis in mice. Genes Dev, 1997. 11(1): p. 1-10.

51. Eppig, J.T., et al., The Mouse Genome Database (MGD): facilitating mouse as a model for human biology and disease. Nucleic Acids Res, 2015. 43(Database issue): p. D726-36.

52. Jaenisch, R. and B. Mintz, Simian virus 40 DNA sequences in DNA of healthy adult mice derived from preimplantation blastocysts injected with viral DNA. Proc Natl Acad Sci U S A, 1974. 71(4): p. 1250-4.

53. Jaenisch, R., Infection of mouse blastocysts with SV40 DNA: normal development of the infected embryos and persistence of SV40-specific DNA sequences in the adult animals. Cold Spring Harb Symp Quant Biol, 1975. 39 Pt 1: p. 375-80.

54. Hanahan, D., E.F. Wagner, and R.D. Palmiter, The origins of oncomice: a history of the first transgenic mice genetically engineered to develop cancer. Genes Dev, 2007. 21(18): p. 2258-70.

55. Avila, M.D., J.P. Morgan, and X. Yan, Genetically modified mouse models used for studying the role of the AT2 receptor in cardiac hypertrophy and heart failure. J Biomed Biotechnol, 2011. 2011: p. 141039.

56. Politi, K. and W. Pao, How genetically engineered mouse tumor models provide insights into human cancers. J Clin Oncol, 2011. 29(16): p. 2273-81.

57. Doyle, A., et al., The construction of transgenic and gene knockout/knockin mouse models of human disease. Transgenic Res, 2012. 21(2): p. 327-49.

58. Nguyen, D. and T. Xu, The expanding role of mouse genetics for understanding human biology and disease. Dis Model Mech, 2008. 1(1): p. 56-66.

59. Becher, O.J. and E.C. Holland, Genetically engineered models have advantages over xenografts for preclinical studies. Cancer Res, 2006. 66(7): p. 3355-8, discussion 3358-9.

60. Richmond, A. and Y. Su, Mouse xenograft models vs GEM models for human cancer therapeutics. Dis Model Mech, 2008. 1(2-3): p. 78-82.

61. Walrath, J.C., et al., Genetically engineered mouse models in cancer research. Adv Cancer Res, 2010. 106: p. 113-64.

62. Frese, K.K. and D.A. Tuveson, Maximizing mouse cancer models. Nat Rev Cancer, 2007. 7(9): p. 645-58.

63. Smith, H.W. and W.J. Muller, Transgenic mouse models--a seminal breakthrough in oncogene research. Cold Spring Harb Protoc, 2013. 2013(12): p. 1099-108.

64. Turan, S., et al., Recombinase-mediated cassette exchange (RMCE): traditional concepts and current challenges. J Mol Biol, 2011. 407(2): p. 193-221.

65. Sauer, B., Functional expression of the cre-lox site-specific recombination system in the yeast Saccharomyces cerevisiae. Mol Cell Biol, 1987. 7(6): p. 2087-96.

66. Sauer, B. and N. Henderson, Site-specific DNA recombination in mammalian cells by the Cre recombinase of bacteriophage P1. Proc Natl Acad Sci U S A, 1988. 85(14): p. 5166-70.

67. Orban, P.C., D. Chui, and J.D. Marth, Tissue- and site-specific DNA recombination in transgenic mice. Proc Natl Acad Sci U S A, 1992. 89(15): p. 6861-5.

68. Weissman, T.A., et al., Generation and imaging of Brainbow mice. Cold Spring Harb Protoc, 2011. 2011(7): p. 851-6.

69. Feil, R., et al., Ligand-activated site-specific recombination in mice. Proc Natl Acad Sci U S A, 1996. 93(20): p. 10887-90.

70. Whiteside, T.L., The tumor microenvironment and its role in promoting tumor growth. Oncogene, 2008. 27(45): p. 5904-12.

71. Chen, F., et al., New horizons in tumor microenvironment biology: challenges and opportunities. BMC Med, 2015. 13: p. 45.

72. D'Cruz, C.M., et al., c-MYC induces mammary tumorigenesis by means of a preferred pathway involving spontaneous Kras2 mutations. Nat Med, 2001. 7(2): p. 235-9.

73. Jamerson, M.H., M.D. Johnson, and R.B. Dickson, Of mice and Myc: c-Myc and mammary tumorigenesis. J Mammary Gland Biol Neoplasia, 2004. 9(1): p. 27-37.

74. Sinn, E., et al., Coexpression of MMTV/v-Ha-ras and MMTV/c-myc genes in transgenic mice: synergistic action of oncogenes in vivo. Cell, 1987. 49(4): p. 465-75.

75. Stewart, T.A., P.K. Pattengale, and P. Leder, Spontaneous mammary adenocarcinomas in transgenic mice that carry and express MTV/myc fusion genes. Cell, 1984. 38(3): p. 627-37.

76. You, M., et al., Activation of the Ki-ras protooncogene in spontaneously occurring and chemically induced lung tumors of the strain A mouse. Proc Natl Acad Sci U S A, 1989. 86(9): p. 3070-4.

77. Muller, W.J., et al., Single-step induction of mammary adenocarcinoma in transgenic mice bearing the activated c-neu oncogene. Cell, 1988. 54(1): p. 105-15.

78. Miyazaki, J., et al., Expression vector system based on the chicken beta-actin promoter directs efficient production of interleukin-5. Gene, 1989. 79(2): p. 269-77.

79. Niwa, H., K. Yamamura, and J. Miyazaki, Efficient selection for high-expression transfectants with a novel eukaryotic vector. Gene, 1991. 108(2): p. 193-9.

80. Alexopoulou, A.N., J.R. Couchman, and J.R. Whiteford, The CMV early enhancer/chicken beta actin (CAG) promoter can be used to drive transgene expression during the differentiation of murine embryonic stem cells into vascular progenitors. BMC Cell Biol, 2008. 9: p. 2.

81. Gu, H., et al., Deletion of a DNA polymerase beta gene segment in T cells using cell type-specific gene targeting. Science, 1994. 265(5168): p. 103-6.

82. Weissman, T.A. and Y.A. Pan, Brainbow: new resources and emerging biological applications for multicolor genetic labeling and analysis. Genetics, 2015. 199(2): p. 293-306.

83. Lee, G. and I. Saito, Role of nucleotide sequences of loxP spacer region in Cre-mediated recombination. Gene, 1998. 216(1): p. 55-65.

84. Agah, R., et al., Gene recombination in postmitotic cells. Targeted expression of Cre recombinase provokes cardiac-restricted, site-specific rearrangement in adult ventricular muscle in vivo. J Clin Invest, 1997. 100(1): p. 169-79.

85. Lakso, M., et al., Efficient in vivo manipulation of mouse genomic sequences at the zygote stage. Proc Natl Acad Sci U S A, 1996. 93(12): p. 5860-5.

86. Eguchi, J., et al., Transcriptional control of adipose lipid handling by IRF4. Cell Metab, 2011. 13(3): p. 249-59.

87. Wagner, K.U., et al., Cre-mediated gene deletion in the mammary gland. Nucleic Acids Res, 1997. 25(21): p. 4323-30.

88. Wexler, R.K., et al., Cardiomyopathy: an overview. Am Fam Physician, 2009. 79(9): p. 778-84.

89. Lloyd-Jones, D.M., et al., Lifetime risk for developing congestive heart failure: the Framingham Heart Study. Circulation, 2002. 106(24): p. 3068-72.

90. Bleumink, G.S., et al., Quantifying the heart failure epidemic: prevalence, incidence rate, lifetime risk and prognosis of heart failure The Rotterdam Study. Eur Heart J, 2004. 25(18): p. 1614-9.

91. Huffman, M.D., et al., Lifetime risk for heart failure among white and black Americans: cardiovascular lifetime risk pooling project. J Am Coll Cardiol, 2013. 61(14): p. 1510-7.

92. Maron, B.J., et al., Contemporary definitions and classification of the cardiomyopathies: an American Heart Association Scientific Statement from the

Council on Clinical Cardiology, Heart Failure and Transplantation Committee; Quality of Care and Outcomes Research and Functional Genomics and Translational Biology Interdisciplinary Working Groups; and Council on Epidemiology and Prevention. Circulation, 2006. 113(14): p. 1807-16.

93. Report of the WHO/ISFC task force on the definition and classification of cardiomyopathies. Br Heart J, 1980. 44(6): p. 672-3.

94. Elliott, P., et al., Classification of the cardiomyopathies: a position statement from the European Society Of Cardiology Working Group on Myocardial and Pericardial Diseases. Eur Heart J, 2008. 29(2): p. 270-6.

95. Sisakian, H., Cardiomyopathies: Evolution of pathogenesis concepts and potential for new therapies. World J Cardiol, 2014. 6(6): p. 478-94.

96. McCartan, C., et al., Cardiomyopathy classification: ongoing debate in the genomics era. Biochem Res Int, 2012. 2012: p. 796926.

97. Luk, A., et al., Dilated cardiomyopathy: a review. J Clin Pathol, 2009. 62(3): p. 219-25.

98. Pacheco, O.E., J.E. Novoa, and R.A. Cox, Dilated cardiomyopathy: a clinical review of patients evaluated at a tertiary care center in Puerto Rico. P R Health Sci J, 1995. 14(4): p. 269-73.

99. Aurigemma, G.P., M.R. Zile, and W.H. Gaasch, Contractile behavior of the left ventricle in diastolic heart failure: with emphasis on regional systolic function. Circulation, 2006. 113(2): p. 296-304.

100. Boffa, G.M., et al., Ischemic cardiomyopathy: lack of clinical applicability of the WHO/ISFC classification of cardiomyopathies. Ital Heart J, 2001. 2(10): p. 778-81.

101. Momiyama, Y., H. Mitamura, and M. Kimura, ECG characteristics of dilated cardiomyopathy. J Electrocardiol, 1994. 27(4): p. 323-8.

102. Silva Marques, J. and F.J. Pinto, Clinical use of multimodality imaging in the assessment of dilated cardiomyopathy. Heart, 2015. 101(7): p. 565-72.

103. Tei, C., et al., New index of combined systolic and diastolic myocardial performance: a simple and reproducible measure of cardiac function--a study in normals and dilated cardiomyopathy. J Cardiol, 1995. 26(6): p. 357-66.

104. Rihal, C.S., et al., Systolic and diastolic dysfunction in patients with clinical diagnosis of dilated cardiomyopathy. Relation to symptoms and prognosis. Circulation, 1994. 90(6): p. 2772-9.

105. Wood, M.J. and M.H. Picard, Utility of echocardiography in the evaluation of individuals with cardiomyopathy. Heart, 2004. 90(6): p. 707-12.

106. Ross, J., Jr., Dilated cardiomyopathy: concepts derived from gene deficient and transgenic animal models. Circ J, 2002. 66(3): p. 219-24.

107. Ku, L., et al., Cardiology patient page. Familial dilated cardiomyopathy. Circulation, 2003. 108(17): p. e118-21.

108. McNally, E.M., J.R. Golbus, and M.J. Puckelwartz, Genetic mutations and mechanisms in dilated cardiomyopathy. J Clin Invest, 2013. 123(1): p. 19-26.

109. Hazebroek, M., R. Dennert, and S. Heymans, Idiopathic dilated cardiomyopathy: possible triggers and treatment strategies. Neth Heart J, 2012. 20(7-8): p. 332-5.

110. Givertz, M.M., Cardiology patient page: peripartum cardiomyopathy. Circulation, 2013. 127(20): p. e622-6.

111. Piano, M.R., Alcoholic cardiomyopathy: incidence, clinical characteristics, and pathophysiology. Chest, 2002. 121(5): p. 1638-50.

112. Rangel, I., et al., Toxic dilated cardiomyopathy: recognizing a potentially reversible disease. Arq Bras Cardiol, 2014. 102(4): p. e37.

113. Ellis, E.R. and M.E. Josephson, Heart failure and tachycardia-induced cardiomyopathy. Curr Heart Fail Rep, 2013. 10(4): p. 296-306.

114. Masci, P.G., et al., Myocardial fibrosis as a key determinant of left ventricular remodeling in idiopathic dilated cardiomyopathy: a contrast-enhanced cardiovascular magnetic study. Circ Cardiovasc Imaging, 2013. 6(5): p. 790-9.

115. Agapitos, E., et al., The myocardial fibrosis in patients with dilated cardiomyopathy. The application of image analysis in the myocardial biopsies. Gen Diagn Pathol, 1996. 141(5-6): p. 305-11.

116. Wilson, A.J., et al., Cardiomyocyte growth and sarcomerogenesis at the intercalated disc. Cell Mol Life Sci, 2014. 71(1): p. 165-81.

117. Hershberger, R.E., D.J. Hedges, and A. Morales, Dilated cardiomyopathy: the complexity of a diverse genetic architecture. Nat Rev Cardiol, 2013. 10(9): p. 531-47.

118. Morales, A. and R.E. Hershberger, Genetic evaluation of dilated cardiomyopathy. Curr Cardiol Rep, 2013. 15(7): p. 375.

119. Hershberger, R.E. and J.D. Siegfried, Update 2011: clinical and genetic issues in familial dilated cardiomyopathy. J Am Coll Cardiol, 2011. 57(16): p. 1641-9.

120. Burkett, E.L. and R.E. Hershberger, Clinical and genetic issues in familial dilated cardiomyopathy. J Am Coll Cardiol, 2005. 45(7): p. 969-81.

121. Kamisago, M., et al., Mutations in sarcomere protein genes as a cause of dilated cardiomyopathy. N Engl J Med, 2000. 343(23): p. 1688-96.

122. Moller, D.V., et al., The role of sarcomere gene mutations in patients with idiopathic dilated cardiomyopathy. Eur J Hum Genet, 2009. 17(10): p. 1241-9.

123. Dellefave, L. and E.M. McNally, Sarcomere mutations in cardiomyopathy, noncompaction, and the developing heart. Circulation, 2008. 117(22): p. 2847-9.

124. Arimura, T., et al., Dilated cardiomyopathy-associated BAG3 mutations impair Z-disc assembly and enhance sensitivity to apoptosis in cardiomyocytes. Hum Mutat, 2011. 32(12): p. 1481-91.

125. Parvari, R. and A. Levitas, The mutations associated with dilated cardiomyopathy. Biochem Res Int, 2012. 2012: p. 639250.

126. Olson, T.M., et al., Actin mutations in dilated cardiomyopathy, a heritable form of heart failure. Science, 1998. 280(5364): p. 750-2.

127. Li, D., et al., Desmin mutation responsible for idiopathic dilated cardiomyopathy. Circulation, 1999. 100(5): p. 461-4.

128. Barresi, R., et al., Disruption of heart sarcoglycan complex and severe cardiomyopathy caused by beta sarcoglycan mutations. J Med Genet, 2000. 37(2): p. 102-7.

129. Villard, E., et al., Mutation screening in dilated cardiomyopathy: prominent role of the beta myosin heavy chain gene. Eur Heart J, 2005. 26(8): p. 794-803.

130. Murphy, R.T., et al., Novel mutation in cardiac troponin I in recessive idiopathic dilated cardiomyopathy. Lancet, 2004. 363(9406): p. 371-2.

131. Lakdawala, N.K., et al., Familial dilated cardiomyopathy caused by an alpha-tropomyosin mutation: the distinctive natural history of sarcomeric dilated cardiomyopathy. J Am Coll Cardiol, 2010. 55(4): p. 320-9.

132. Olson, T.M., et al., Metavinculin mutations alter actin interaction in dilated cardiomyopathy. Circulation, 2002. 105(4): p. 431-7.

133. McConnell, B.K., et al., Dilated cardiomyopathy in homozygous myosin-binding protein-C mutant mice. J Clin Invest, 1999. 104(12): p. 1771.

134. Mohapatra, B., et al., Mutations in the muscle LIM protein and alpha-actinin-2 genes in dilated cardiomyopathy and endocardial fibroelastosis. Mol Genet Metab, 2003. 80(1-2): p. 207-15.

135. Carniel, E., et al., Alpha-myosin heavy chain: a sarcomeric gene associated with dilated and hypertrophic phenotypes of cardiomyopathy. Circulation, 2005. 112(1): p. 54-9.

136. Bienengraeber, M., et al., ABCC9 mutations identified in human dilated cardiomyopathy disrupt catalytic KATP channel gating. Nat Genet, 2004. 36(4): p. 382-7.

137. Brodsky, G.L., et al., Lamin A/C gene mutation associated with dilated cardiomyopathy with variable skeletal muscle involvement. Circulation, 2000. 101(5): p. 473-6.

138. Schmitt, J.P., et al., Dilated cardiomyopathy and heart failure caused by a mutation in phospholamban. Science, 2003. 299(5611): p. 1410-3.

139. Zheng, M., et al., Cardiac-specific ablation of Cypher leads to a severe form of dilated cardiomyopathy with premature death. Hum Mol Genet, 2009. 18(4): p. 701-13.

140. Verhaert, D., et al., Cardiac involvement in patients with muscular dystrophies: magnetic resonance imaging phenotype and genotypic considerations. Circ Cardiovasc Imaging, 2011. 4(1): p. 67-76.

141. Tigen, K. and C. Cevik, beta-blockers in the treatment of dilated cardiomyopathy: which is the best? Curr Pharm Des, 2010. 16(26): p. 2866-71.

142. Pitt, B., et al., The effect of spironolactone on morbidity and mortality in patients with severe heart failure. Randomized Aldactone Evaluation Study Investigators. N Engl J Med, 1999. 341(10): p. 709-17.

143. Maron, B.J., Hypertrophic cardiomyopathy: a systematic review. JAMA, 2002. 287(10): p. 1308-20.

144. Maron, B.J., et al., Hypertrophic cardiomyopathy: present and future, with translation into contemporary cardiovascular medicine. J Am Coll Cardiol, 2014. 64(1): p. 83-99.

145. Houston, B.A. and G.R. Stevens, Hypertrophic cardiomyopathy: a review. Clin Med Insights Cardiol, 2014. 8(Suppl 1): p. 53-65.

146. Maron, B.J. and M.S. Maron, Hypertrophic cardiomyopathy. Lancet, 2013. 381(9862): p. 242-55.

147. Seidman, C.E. and J.G. Seidman, Identifying sarcomere gene mutations in hypertrophic cardiomyopathy: a personal history. Circ Res, 2011. 108(6): p. 743-50.

148. Maron, B.J., M.S. Maron, and C. Semsarian, Genetics of hypertrophic cardiomyopathy after 20 years: clinical perspectives. J Am Coll Cardiol, 2012. 60(8): p. 705-15.

149. Hensley, N., et al., Hypertrophic cardiomyopathy: a review. Anesth Analg, 2015. 120(3): p. 554-69.

150. Caleshu, C., et al., Furthering the link between the sarcomere and primary cardiomyopathies: restrictive cardiomyopathy associated with multiple mutations in genes previously associated with hypertrophic or dilated cardiomyopathy. Am J Med Genet A, 2011. 155A(9): p. 2229-35.

151. Kushwaha, S.S., J.T. Fallon, and V. Fuster, Restrictive cardiomyopathy. N Engl J Med, 1997. 336(4): p. 267-76.

152. Mogensen, J. and E. Arbustini, Restrictive cardiomyopathy. Curr Opin Cardiol, 2009. 24(3): p. 214-20.

153. Klauke, B., et al., De novo desmin-mutation N116S is associated with arrhythmogenic right ventricular cardiomyopathy. Hum Mol Genet, 2010. 19(23): p. 4595-607.

154. Cox, M.G., et al., Arrhythmogenic right ventricular dysplasia/cardiomyopathy: pathogenic desmosome mutations in index-patients predict outcome of family screening: Dutch arrhythmogenic right ventricular dysplasia/cardiomyopathy genotype-phenotype follow-up study. Circulation, 2011. 123(23): p. 2690-700.

155. Lu, H., et al., Transformation of human ovarian surface epithelial cells by Kruppel-like factor 8. Oncogene, 2014. 33(1): p. 10-8.

156. Zhao, J.H., H. Reiske, and J.L. Guan, Regulation of the cell cycle by focal adhesion kinase. J Cell Biol, 1998. 143(7): p. 1997-2008.

157. Seger, R., et al., Overexpression of mitogen-activated protein kinase kinase (MAPKK) and its mutants in NIH 3T3 cells. Evidence that MAPKK involvement in cellular proliferation is regulated by phosphorylation of serine residues in its kinase subdomains VII and VIII. J Biol Chem, 1994. 269(41): p. 25699-709.

158. Brady, D.C., et al., Copper is required for oncogenic BRAF signalling and tumorigenesis. Nature, 2014. 509(7501): p. 492-6.

159. Levin-Salomon, V., et al., Isolation of intrinsically active (MEK-independent) variants of the ERK family of mitogen-activated protein (MAP) kinases. J Biol Chem, 2008. 283(50): p. 34500-10.

160. Chu, Y., et al., The mitogen-activated protein kinase phosphatases PAC1, MKP-1, and MKP-2 have unique substrate specificities and reduced activity in vivo toward the ERK2 sevenmaker mutation. J Biol Chem, 1996. 271(11): p. 6497-501.

161. Zhao, J., R. Pestell, and J.L. Guan, Transcriptional activation of cyclin D1 promoter by FAK contributes to cell cycle progression. Mol Biol Cell, 2001. 12(12): p. 4066-77.

162. Zhao, J., C. Zheng, and J. Guan, Pyk2 and FAK differentially regulate progression of the cell cycle. J Cell Sci, 2000. 113 (Pt 17): p. 3063-72.

163. Patel, S., et al., Tissue-specific role of glycogen synthase kinase 3beta in glucose homeostasis and insulin action. Mol Cell Biol, 2008. 28(20): p. 6314-28.

164. Wegener, A.D. and L.R. Jones, Phosphorylation-induced mobility shift in phospholamban in sodium dodecyl sulfate-polyacrylamide gels. Evidence for a protein structure consisting of multiple identical phosphorylatable subunits. J Biol Chem, 1984. 259(3): p. 1834-41.

165. Wolf, A., et al., Insulin signaling via Akt2 switches plakophilin 1 function from stabilizing cell adhesion to promoting cell proliferation. J Cell Sci, 2013. 126(Pt 8): p. 1832-44.

166. Huyer, G., et al., Mechanism of inhibition of protein-tyrosine phosphatases by vanadate and pervanadate. J Biol Chem, 1997. 272(2): p. 843-51.

167. Leger, J., et al., Conversion of serine to aspartate imitates phosphorylation-induced changes in the structure and function of microtubule-associated protein tau. J Biol Chem, 1997. 272(13): p. 8441-6.

168. Hao, M., et al., Mutation of phosphoserine 389 affects p53 function in vivo. J Biol Chem, 1996. 271(46): p. 29380-5.

169. Aaron, J.A. and D.W. Christianson, Trinuclear Metal Clusters in Catalysis by Terpenoid Synthases. Pure Appl Chem, 2010. 82(8): p. 1585-1597.

170. Sorenson, C.M. and N. Sheibani, Focal adhesion kinase, paxillin, and bcl-2: analysis of expression, phosphorylation, and association during morphogenesis. Dev Dyn, 1999. 215(4): p. 371-82.

171. Blom, N., S. Gammeltoft, and S. Brunak, Sequence and structure-based prediction of eukaryotic protein phosphorylation sites. J Mol Biol, 1999. 294(5): p. 1351-62.

172. Sears, R., et al., Multiple Ras-dependent phosphorylation pathways regulate Myc protein stability. Genes Dev, 2000. 14(19): p. 2501-14.

173. Marampon, F., C. Ciccarelli, and B.M. Zani, Down-regulation of c-Myc following MEK/ERK inhibition halts the expression of malignant phenotype in rhabdomyosarcoma and in non muscle-derived human tumors. Mol Cancer, 2006. 5: p. 31.

174. Zhang, Z. and C.T. Teng, Phosphorylation of Kruppel-like factor 5 (KLF5/IKLF) at the CBP interaction region enhances its transactivation function. Nucleic Acids Res, 2003. 31(8): p. 2196-208.

175. Dewi, V., et al., Phosphorylation of Kruppel-like factor 3 (KLF3/BKLF) and C-terminal binding protein 2 (CtBP2) by homeodomain-interacting protein kinase 2 (HIPK2) modulates KLF3 DNA binding and activity. J Biol Chem, 2015. 290(13): p. 8591-605.

176. Yeo, J.C., et al., Klf2 is an essential factor that sustains ground state pluripotency. Cell Stem Cell, 2014. 14(6): p. 864-72.

177. Okamoto, Y. and S. Shikano, Phosphorylation-dependent C-terminal binding of 14-3-3 proteins promotes cell surface expression of HIV co-receptor GPR15. J Biol Chem, 2011. 286(9): p. 7171-81.

178. Nasu-Nishimura, Y., et al., Identification of an endoplasmic reticulum-retention motif in an intracellular loop of the kainate receptor subunit KA2. J Neurosci, 2006. 26(26): p. 7014-21.

179. Remenyi, A., M.C. Good, and W.A. Lim, Docking interactions in protein kinase and phosphatase networks. Curr Opin Struct Biol, 2006. 16(6): p. 676-85.

180. Schutze, M.P., P.A. Peterson, and M.R. Jackson, An N-terminal double-arginine motif maintains type II membrane proteins in the endoplasmic reticulum. EMBO J, 1994. 13(7): p. 1696-705.

181. Zerangue, N., et al., Analysis of endoplasmic reticulum trafficking signals by combinatorial screening in mammalian cells. Proc Natl Acad Sci U S A, 2001. 98(5): p. 2431-6.

182. Gassmann, M., et al., The RXR-type endoplasmic reticulum-retention/retrieval signal of GABAB1 requires distant spacing from the membrane to function. Mol Pharmacol, 2005. 68(1): p. 137-44.

183. Shikano, S. and M. Li, Membrane receptor trafficking: evidence of proximal and distal zones conferred by two independent endoplasmic reticulum localization signals. Proc Natl Acad Sci U S A, 2003. 100(10): p. 5783-8.

184. Borders, C.L., Jr., et al., A structural role for arginine in proteins: multiple hydrogen bonds to backbone carbonyl oxygens. Protein Sci, 1994. 3(4): p. 541-8.

185. Garcia, A., et al., New insights in protein phosphorylation: a signature for protein phosphatase 1 interacting proteins. C R Biol, 2004. 327(2): p. 93-7.

186. Lewit-Bentley, A. and S. Rety, EF-hand calcium-binding proteins. Curr Opin Struct Biol, 2000. 10(6): p. 637-43.

187. Mohanta, T.K., et al., Genome-Wide Identification of Calcium Dependent Protein Kinase Gene Family in Plant Lineage Shows Presence of Novel D-x-D and D-E-L Motifs in EF-Hand Domain. Front Plant Sci, 2015. 6: p. 1146.

188. Sindreu, C.B., Z.S. Scheiner, and D.R. Storm, Ca2+ -stimulated adenylyl cyclases regulate ERK-dependent activation of MSK1 during fear conditioning. Neuron, 2007. 53(1): p. 79-89.

189. Zhao, J., KLF8: so different in ovarian and breast cancer. Oncoscience, 2014. 1(4): p. 248-249.

190. Yi, X., et al., KLF8 knockdown triggered growth inhibition and induced cell phase arrest in human pancreatic cancer cells. Gene, 2016. 585(1): p. 22-7.

191. Jaenisch, R., Transgenic animals. Science, 1988. 240(4858): p. 1468-74.

192. Funnell, A.P., et al., Generation of mice deficient in both KLF3/BKLF and KLF8 reveals a genetic interaction and a role for these factors in embryonic globin gene silencing. Mol Cell Biol, 2013. 33(15): p. 2976-87.

193. Szczesna-Cordary, D., et al., Cardiomyopathies: classification, clinical characterization, and functional phenotypes. Biochem Res Int, 2012. 2012: p. 870942.

194. Hershberger, R.E., A. Morales, and J.D. Siegfried, Clinical and genetic issues in dilated cardiomyopathy: a review for genetics professionals. Genet Med, 2010. 12(11): p. 655-67.

195. Dec, G.W. and V. Fuster, Idiopathic dilated cardiomyopathy. N Engl J Med, 1994. 331(23): p. 1564-75.

196. Spodick, D.H., Restrictive cardiomyopathy. N Engl J Med, 1997. 336(26): p. 1917; author reply 1917-8.

197. Shah, P.M., Hypertrophic cardiomyopathy and diastolic dysfunction. J Am Coll Cardiol, 2003. 42(2): p. 286-7.

198. Russell, B., et al., Mechanical stress-induced sarcomere assembly for cardiac muscle growth in length and width. J Mol Cell Cardiol, 2010. 48(5): p. 817-23.

199. Mukherjee, D., et al., Kruppel-like factor 8 activates the transcription of C-X-C cytokine receptor type 4 to promote breast cancer cell invasion, transendothelial migration and metastasis. Oncotarget, 2016.

200. Yoshida, T., et al., Kruppel-like factor 4 protein regulates isoproterenol-induced cardiac hypertrophy by modulating myocardin expression and activity. J Biol Chem, 2014. 289(38): p. 26107-18.

201. Haldar, S.M., et al., Klf15 deficiency is a molecular link between heart failure and aortic aneurysm formation. Sci Transl Med, 2010. 2(26): p. 26ra26.

202. Leenders, J.J., et al., Regulation of cardiac gene expression by KLF15, a repressor of myocardin activity. J Biol Chem, 2010. 285(35): p. 27449-56.

203. Zhang, Y., et al., Kruppel-like factor 4 transcriptionally regulates TGF-beta1 and contributes to cardiac myofibroblast differentiation. PLoS One, 2013. 8(4): p. e63424.

204. Federmann, M. and O.M. Hess, Differentiation between systolic and diastolic dysfunction. Eur Heart J, 1994. 15 Suppl D: p. 2-6.

205. Little, W.C. and R.J. Applegate, Congestive heart failure: systolic and diastolic function. J Cardiothorac Vasc Anesth, 1993. 7(4 Suppl 2): p. 2-5.

206. Xu, J., et al., Myocyte enhancer factors 2A and 2C induce dilated cardiomyopathy in transgenic mice. J Biol Chem, 2006. 281(14): p. 9152-62.

207. Lee, D., et al., Calreticulin induces dilated cardiomyopathy. PLoS One, 2013. 8(2): p. e56387.

208. Herman, D.S., et al., Truncations of titin causing dilated cardiomyopathy. N Engl J Med, 2012. 366(7): p. 619-28.

209. Andersson, K.B., et al., Moderate heart dysfunction in mice with inducible cardiomyocyte-specific excision of the Serca2 gene. J Mol Cell Cardiol, 2009. 47(2): p. 180-7.

210. Kho, C., et al., SUMO1-dependent modulation of SERCA2a in heart failure. Nature, 2011. 477(7366): p. 601-5.

211. Stephanou, A., Activated STAT-1 pathway in the myocardium as a novel therapeutic target in ischaemia/reperfusion injury. Eur Cytokine Netw, 2002. 13(4): p. 401-3.

212. Ng, D.C., et al., Activation of signal transducer and activator of transcription (STAT) pathways in failing human hearts. Cardiovasc Res, 2003. 57(2): p. 333-46.

213. Wu, L., et al., Induction of high STAT1 expression in transgenic mice with LQTS and heart failure. Biochem Biophys Res Commun, 2007. 358(2): p. 449-54.

214. Stephanou, A., et al., Ischemia-induced STAT-1 expression and activation play a critical role in cardiomyocyte apoptosis. J Biol Chem, 2000. 275(14): p. 10002-8.

215. Knight, R.A., T.M. Scarabelli, and A. Stephanou, STAT transcription in the ischemic heart. JAKSTAT, 2012. 1(2): p. 111-7.

216. McCormick, J., et al., STAT1 deficiency in the heart protects against myocardial infarction by enhancing autophagy. J Cell Mol Med, 2012. 16(2): p. 386-93.

217. Merkle, S., et al., A role for caspase-1 in heart failure. Circ Res, 2007. 100(5): p. 645-53.

218. Prescimone, T., et al., Caspase-1 transcripts in failing human heart after mechanical unloading. Cardiovasc Pathol, 2015. 24(1): p. 11-8.

219. Wencker, D., et al., A mechanistic role for cardiac myocyte apoptosis in heart failure. J Clin Invest, 2003. 111(10): p. 1497-504.

220. Chiong, M., et al., Cardiomyocyte death: mechanisms and translational implications. Cell Death Dis, 2011. 2: p. e244.

221. Kang, P.M. and S. Izumo, Apoptosis and heart failure: A critical review of the literature. Circ Res, 2000. 86(11): p. 1107-13.

222. Basu, P., et al., KLF2 is essential for primitive erythropoiesis and regulates the human and murine embryonic beta-like globin genes in vivo. Blood, 2005. 106(7): p. 2566-71.

223. Kuo, C.T., et al., The LKLF transcription factor is required for normal tunica media formation and blood vessel stabilization during murine embryogenesis. Genes Dev, 1997. 11(22): p. 2996-3006.

224. Carlson, C.M., et al., Kruppel-like factor 2 regulates thymocyte and T-cell migration. Nature, 2006. 442(7100): p. 299-302.

225. Kuo, C.T., M.L. Veselits, and J.M. Leiden, LKLF: A transcriptional regulator of single-positive T cell quiescence and survival. Science, 1997. 277(5334): p. 1986-90.

226. Wani, M.A., S.E. Wert, and J.B. Lingrel, Lung Kruppel-like factor, a zinc finger transcription factor, is essential for normal lung development. J Biol Chem, 1999. 274(30): p. 21180-5.

227. Wu, J., et al., The KLF2 transcription factor does not affect the formation of preadipocytes but inhibits their differentiation into adipocytes. Biochemistry, 2005. 44(33): p. 11098-105.

228. Shaked, I. and K. Ley, Protective role for myeloid specific KLF2 in atherosclerosis. Circ Res, 2012. 110(10): p. 1266.

229. Lingrel, J.B., et al., Myeloid-specific Kruppel-like factor 2 inactivation increases macrophage and neutrophil adhesion and promotes atherosclerosis. Circ Res, 2012. 110(10): p. 1294-302.

230. Sue, N., et al., Targeted disruption of the basic Kruppel-like factor gene (Klf3) reveals a role in adipogenesis. Mol Cell Biol, 2008. 28(12): p. 3967-78.

231. Takahashi, K., et al., Induction of pluripotent stem cells from adult human fibroblasts by defined factors. Cell, 2007. 131(5): p. 861-72.

232. Foster, K.W., et al., Induction of KLF4 in basal keratinocytes blocks the proliferation-differentiation switch and initiates squamous epithelial dysplasia. Oncogene, 2005. 24(9): p. 1491-500.

233. Segre, J.A., C. Bauer, and E. Fuchs, Klf4 is a transcription factor required for establishing the barrier function of the skin. Nat Genet, 1999. 22(4): p. 356-60.

234. Katz, J.P., et al., The zinc-finger transcription factor Klf4 is required for terminal differentiation of goblet cells in the colon. Development, 2002. 129(11): p. 2619-28.

235. Li, J., et al., Expression of Kruppel-like factor KLF4 in mouse hair follicle stem cells contributes to cutaneous wound healing. PLoS One, 2012. 7(6): p. e39663.

236. Zhou, G., et al., Endothelial Kruppel-like factor 4 protects against atherothrombosis in mice. J Clin Invest, 2012. 122(12): p. 4727-31.

237. Shindo, T., et al., Kruppel-like zinc-finger transcription factor KLF5/BTEB2 is a target for angiotensin II signaling and an essential regulator of cardiovascular remodeling. Nat Med, 2002. 8(8): p. 856-63.

238. Takeda, N., et al., Cardiac fibroblasts are essential for the adaptive response of the murine heart to pressure overload. J Clin Invest, 2010. 120(1): p. 254-65.

239. Wan, H., et al., Kruppel-like factor 5 is required for perinatal lung morphogenesis and function. Development, 2008. 135(15): p. 2563-72.

240. Oishi, Y., et al., Kruppel-like transcription factor KLF5 is a key regulator of adipocyte differentiation. Cell Metab, 2005. 1(1): p. 27-39.

241. Rajamannan, N.M., et al., TGFbeta inducible early gene-1 (TIEG1) and cardiac hypertrophy: Discovery and characterization of a novel signaling pathway. J Cell Biochem, 2007. 100(2): p. 315-25.

242. Bae, C.J., et al., Phthalic anhydride-induced skin inflammation is augmented in KLF10-deficient mice. J Dermatol Sci, 2013. 71(3): p. 221-4.

243. Zheng, Y., Y. Kong, and F. Li, Kruppel-like transcription factor 11 (KLF11) overexpression inhibits cardiac hypertrophy and fibrosis in mice. Biochem Biophys Res Commun, 2013.

244. Grunewald, M., et al., Mechanistic role for a novel glucocorticoid-KLF11 (TIEG2) protein pathway in stress-induced monoamine oxidase A expression. J Biol Chem, 2012. 287(29): p. 24195-206.

245. Nagare, T., et al., Overexpression of KLF15 transcription factor in adipocytes of mice results in down-regulation of SCD1 protein expression in adipocytes and consequent enhancement of glucose-induced insulin secretion. J Biol Chem, 2011. 286(43): p. 37458-69.

246. Horie, T., et al., MicroRNA-133 regulates the expression of GLUT4 by targeting KLF15 and is involved in metabolic control in cardiac myocytes. Biochem Biophys Res Commun, 2009. 389(2): p. 315-20.

247. Gray, S., et al., The Kruppel-like factor KLF15 regulates the insulin-sensitive glucose transporter GLUT4. J Biol Chem, 2002. 277(37): p. 34322-8.

248. Fisch, S., et al., Kruppel-like factor 15 is a regulator of cardiomyocyte hypertrophy. Proc Natl Acad Sci U S A, 2007. 104(17): p. 7074-9.

249. Takashima, M., et al., Role of KLF15 in regulation of hepatic gluconeogenesis and metformin action. Diabetes, 2010. 59(7): p. 1608-15.

250. Gray, S., et al., Regulation of gluconeogenesis by Kruppel-like factor 15. Cell Metab, 2007. 5(4): p. 305-12.

251. Prosdocimo, D.A., et al., Kruppel-like factor 15 is a critical regulator of cardiac lipid metabolism. J Biol Chem, 2014.

252. Sergeeva, I.A. and V.M. Christoffels, Regulation of expression of atrial and brain natriuretic peptide, biomarkers for heart development and disease. Biochim Biophys Acta, 2013. 1832(12): p. 2403-13.

253. Houweling, A.C., et al., Expression and regulation of the atrial natriuretic factor encoding gene Nppa during development and disease. Cardiovasc Res, 2005. 67(4): p. 583-93.

254. Dai, B., et al., STAT1/3 and ERK1/2 synergistically regulate cardiac fibrosis induced by high glucose. Cell Physiol Biochem, 2013. 32(4): p. 960-71.

255. Mir, S.A., et al., Inhibition of signal transducer and activator of transcription 3 (STAT3) attenuates interleukin-6 (IL-6)-induced collagen synthesis and resultant hypertrophy in rat heart. J Biol Chem, 2012. 287(4): p. 2666-77.

256. Garcia-Honrubia, A., et al., Clinical implications of nonsarcomeric gene polymorphisms in hypertrophic cardiomyopathy. Eur J Clin Invest, 2016. 46(2): p. 123-9.

257. Volz, H.C., et al., S100A8/A9 aggravates post-ischemic heart failure through activation of RAGE-dependent NF-kappaB signaling. Basic Res Cardiol, 2012. 107(2): p. 250.

258. Matteo, R.G. and C.S. Moravec, Immunolocalization of annexins IV, V and VI in the failing and non-failing human heart. Cardiovasc Res, 2000. 45(4): p. 961-70.